


**Brasenose College**
**University of Oxford**



# SUBSTRATE METABOLISM AND CARDIOMYOGENIC DIFFERENTIATION OF CARDIAC PROGENITOR CELLS

**KHADIJEH PAKZAD**

Cardiac Metabolism Research Group
Department of Physiology, Anatomy and Genetics

**Submitted for the degree of Doctor of Philosophy**
**Michaelmas Term 2015**

**Supervisors:**
**Prof. Carolyn Carr**
**Prof. Kieran Clarke**
**Dr Angela Russel**

# Acknowledgment

First and foremost, I would like to extend my deepest appreciation and thanks to my supervisors, Prof. Carolyn Carr, Prof. Kieran Clarke, and Dr. Angela Russell.

I am grateful to Prof. Kieran Clarke for her tremendous support, patience and trust in me to carry out this project. I would like to thank her for giving me a golden opportunity to work towards a DPhil in her laboratory.

I am very much indebted to Prof. Carolyn Carr as I would not have been able to complete this long and demanding journey towards the DPhil without her guidance. Many thanks for her countless hours of reflecting, reading, encouraging, and most of all, the patience throughout the entire process.

There are some people whose contributions to time and effort I would like to acknowledge Dr. Mary Board, Dr. Filippo Perbellini, Arne Bruyneel, Dr. Lisa Heather, Dr. Tamara Sirey, Andrew Bassett Wilfried Haerty, Dr. Alan Wainman, Nigel Rust, Mark Howard, and Daniel Heaton for contributing their expertise and work to the realization of partly of this research.

Thanks also to all the researchers, students and staff in the CMRG including Vanessa, Jun Jie, Suat-Cheng, Lien-Cheng, Sophia, Heba, Damian, Jack, Lucy, Lydia, Lucia, Brianna, Mike, Lawrie, Emma, Vicky, Yvonne, and Nicola who were extremely helpful throughout the entire period to complete my research.

I could not think of a better family, than mine, my parents Dara Pakzad and Mehrangiz Noorie, sisters: Azarmidokht, Mansoureh, Rouhangiz, and Fatemeh; brothers: Mohammad-Reza and Hamid-Rreza; relatives and friends for the support, encouragement and help throughout this period.

Finally, I dedicate this thesis to the most important person in my life who has loved, supported, encouraged, cheered, and belief in me from which I benefit every day in doing this DPhil: my sister Mansoureh Pakzad and her family Ghasem, Babak and Mehrnoosh.

# Abstract

Despite being resident in the heart, which derives most its energy needs from the oxidation of fatty acids, cardiac stem/progenitor cells are assumed to be glycolytic. Therefore, the transition of these non-contractile progenitor cells into beating cardiomyocytes necessitates an obligatory transformation of the metabolic infrastructure with mitochondrial network expansion and a distinctive switch from glycolysis to oxidative phosphorylation. However, expansion of progenitor cells in culture may impair their ability to upregulate fatty acid metabolism and increase mitochondrial function. Therefore, the main objective of this project was to determine, for the first time, substrate and energy metabolism in cardiac stem/progenitor cells before, during and after cardiomyogenic differentiation. Control passage two cardiosphere-derived cells (P2-CDCs), created through culture on fibronectin/poly-D-lysine (FN/PDL) or collagen IV/hanging drops (ColIV/HD), have been shown to derive most of their energy needs from glycolysis with elevated lactate efflux. However, after 3-weeks of treatment with 5-Azacytidine (5-Aza) and ascorbic acid (AA), differentiated cells started to upregulate fatty acid oxidation and significantly reduced glycolytic flux and lactate production. Therefore, different metabolic mediators were used to stimulate fatty acid oxidation in differentiated cells. Various media with or without synthetic small molecule(s) were tested to optimize differentiation capacity and to stimulate aerobic oxidative phosphorylation in P2-CDCs. WY-14643+TGFβ supplemented medium was able to induce cardiomyogenic differentiation of P2-CDCs into mature, differentiated myocytes. The differentiated cells showed a significant increase in expression of both cardiac-specific genes and proteins, calcium handling genes as well as transforming glycolytic metabolism into more efficiently producing higher energy system, fatty acid, and carbohydrate oxidation in addition to glycolysis, suggesting they may be forming ventricular myocytes.

# Table of Contents


**CHAPTER 1 INTRODUCTION ..... 1**

1.1 MYOCARDIAL INFARCTION (MI) ..... 2

1.2 CURRENT DRUG AND INTERVENTIONAL THERAPIES ..... 4

1.3 STEM CELL THERAPY FOR MYOCARDIAL INFARCTION ..... 4

*1.3.1 Embryonic Stem Cells ..... 4*

*1.3.2 Induced pluripotent stem cells ..... 5*

*1.3.3 Adult stem cells ..... 6*

1.3.3.1 Bone marrow-derived stem cells ..... 6

1.3.3.2 Mesenchymal stem cells ..... 7

1.3.3.3 Endothelial progenitor cells ..... 7

1.3.3.4 Skeletal myoblast ..... 8

1.3.3.5 Very small-embryonic like cells ..... 8

1.3.3.6 Endogenous cardiac stem cells ..... 9

1.3.3.6.1 Cardiac side population (SP) ..... 9

1.3.3.6.2 Stem cell antigen-1$^{+}$ cells (Sca-1$^{+}$) ..... 10

1.3.3.6.3 c-Kit+ cells ..... 10

1.3.3.6.4 Islet-1 cells ..... 11

1.3.3.6.5 Epicardial-derived stem cells ..... 12

1.3.3.6.6 Cardiosphere and cardiosphere-derived cells ..... 13

1.4 CARDIAC STEM/PROGENITOR CELL ISOLATION AND EXPANSION ..... 13

1.5 CARDIOMYOGENIC DIFFERENTIATION OF CARDIAC PROGENITOR CELLS ..... 14

1.6 METABOLISM ..... 17

*1.6.1 Adult cardiac metabolism ..... 17*

*1.6.2 Proliferating stem/progenitor cell metabolism ..... 20*

1.7 THESIS AIMS ..... 22

**CHAPTER 2 GENERAL METHODS ..... 23**

2.1 ANIMALS ..... 24

2.2 ISOLATION AND EXPANSION OF CARDIAC STEM CELLS (CSCS) ..... 24
*2.2.1 Explant culture* ..... *24*
*2.2.2 Harvesting Explant Derived Cells (EDCs)* ..... *25*
*2.2.3 Cardiosphere (CSps) culture* ..... *25*
*2.2.4 Cardiosphere-derived cell (CDC) expansion* ..... *25*
2.3 CELL COUNTING ..... 26
2.4 PROLIFERATION ASSAY ..... 26
2.5 CELL CYTOTOXICITY ASSAY ..... 26
2.6 CARDIOMYOGENIC DIFFERENTIATION ASSAYS ..... 27
*2.6.1 DMSO Conditioned Medium* ..... *27*
*2.6.2 5-Azacytidine Conditioned Medium* ..... *27*
*2.6.3 Transforming Growth Factor-β (TGF β) Conditioned Medium in a combination with or without small molecule(s)* ..... *28*
1. WY-14643 (PPARα agonist 1): ..... 28
2. CP-775146 (PPARα agonist 2): ..... 28
3. Sodium Dichloroacetate: ..... 28
4. Sodium Butyrate: ..... 28
5. 4-compounds: ..... 28
6. Baseline (control 1): ..... 28
7. 5-Aza+TGFβ (control 2): ..... 28
8. TGFβ (control 3): ..... 29
2.7 REAL-TIME QUANTITATIVE REVERSE-TRANSCRIPTION POLYMERASE CHAIN REACTION (QRT-PCR) ..... 29
*2.7.1 Primer design and optimization* ..... *29*
*2.7.2 Primer efficiency test* ..... *29*
*2.7.3 RNA extraction and DNase treatment* ..... *30*
*2.7.4 Reverse transcription (complementary DNA synthesis)* ..... *30*
*2.7.5 Quantitative real time PCR* ..... *30*
*2.7.6 qRT-PCR Data Analysis* ..... *31*
2.8 FLOW CYTOMETRY ..... 31

*2.8.1 Antibody incubation, acquisition and analysis* ..... *31*

2.9 IMMUNOCYTOCHEMISTRY ..... 32

*2.9.1 Culture of CDCs on cover slips* ..... *32*

*2.9.2 Mitochondria staining* ..... *32*

*2.9.3 Cell Fixation, permeabilization and blocking* ..... *33*

*2.9.4 Primary antibody incubation, secondary antibody labelling, DAPI staining and mounting* ..... *33*

*2.9.5 Confocal Microscopy* ..... *33*

2.10 WESTERN BLOTTING ..... 34

*2.10.1 Tissue lysate preparation* ..... *34*

*2.10.2 Cell lysate preparation* ..... *34*

*2.10.3 Protein Assay* ..... *34*

*2.10.4 Polyacrylamide gel electrophoresis and protein transfer* ..... *35*

*2.10.5 Immunoblotting detection and band quantification* ..... *35*

2.11 DETERMINATION OF LACTATE EFFLUX ..... 36

2.12 DETERMINATION OF GLYCOLYTIC FLUX ..... 36

2.13 MULTIWELL $^{14}CO_2$-CAPTURE ASSAY FOR EVALUATION OF SUBSTRATE OXIDATION RATE OF CELLS IN CULTURE ..... 37

*2.13.1 Experimental procedure of $^{14}CO_2$-capture assay* ..... *38*

2.14 CALCULATION OF ATP YIELD ..... 39

2.15 STATISTICS ..... 39

**..... 40**

**CHAPTER 3 COMPARISON OF REGENERATIVE POTENTIAL OF DIFFERENT CARDIOSPHERE-DERIVED CELL LINES FROM RAT HEART ..... 41**

3.1 ABSTRACT ..... 42

3.2 INTRODUCTION ..... 43

3.3. METHODS ..... 45

*3.3.1 Overview of designed study* ..... *45*

*3.3.2 Isolation, and expansion of CS-derived cells* ..... *46*

*3.3.3 Quantification of CDC Yield* ..... *46*

*3.3.4 Quantification of P2-CDC proliferation* ..... *46*

*3.3.5 Real-time quantitative RT-PCR* ..... *46*

*3.3.6 Flow cytometry analysis* ..... *47*

*3.3.7 Confocal imaging* ..... *47*

*3.3.8 Cardiomyogenic differentiation of cardiosphere-derived cells* ..... *47*

*3.3.9 Statistics* ..... *47*

..... 49

3.4 RESULTS ..... 50

*3.4.1 Isolation and expansion of cardiosphere-derived cells* ..... *50*

3.4.1.1 Explant-derived cells ..... 50

3.4.1.2 Cardiosphere formation ..... 50

3.4.1.3 Cardiosphere-derived cells ..... 50

*3.4.2 Quantification of CSC isolation and expansion* ..... *54*

*3.4.3 Quantification of P2-CDC proliferation* ..... *55*

*3.4.4 Phenotypic characterization of cardiosphere-derived cells* ..... *56*

3.4.4.1 Phenotype characterization of P2-CDCs using flow cytometry analysis ..... 56

*3.4.5 Characterization of cardiomyogenic differentiated P2-CDCs* ..... *60*

3.4.5.1 Genotype characterization of cardiomyogenic differentiated P2-CDCs using qRT-PCR ..... 60

3.4.5.2 Phenotype characterization of cardiomyogenic differentiated P2-CDCs using flow cytometry ..... 66

3.4.5.3 Phenotype characterization of cardiomyogenic differentiated P2-CDCs using immunocytochemistry. . 68

3.5 DISCUSSION ..... 71

*3.5.1 ColIV/HD technique yielded more CDCs compared to FN/PDL* ..... *71*

*3.5.2 P2-CDCs are a heterogeneous cell population containing both stemness and committed cells towards cardiac lineage* ..... *72*

*3.5.3 Confluent P2-CDCs cultured on FN and treated with 5-Aza were differentiated into immature cardiomyocytes cells* ..... *72*

*3.5.4 Confluency induces terminal differentiation* ..... *74*

*3.5.5 ColIV base culture induces proliferation but FN induces cardiac differentiation* ..... *74*

3.6 CONCLUSION ..... 76

**CHAPTER 4 SUBSTRATE UTILIZATION OF CARDIAC PROGENITOR CELLS CULTURED ON FIBRONECTIN OR COLLAGEN IV BEFORE AND AFTER CARDIOMYOGENIC DIFFERENTIATION ..... 77**

4.1 ABSTRACT ..... 78

4.2 INTRODUCTION ..... 79

4.3 METHODS ..... 82

*4.3.1 Overview of designed study ..... 82*

*4.3.2 Isolation, expansion, and differentiation of CSCs ..... 83*

*4.3.3 Real-time quantitative RT-PCR ..... 83*

*4.3.4 Western blotting assay ..... 84*

*4.3.5 Determination of Lactate efflux ..... 84*

*4.3.6 Determination of glycolytic flux ..... 84*

*4.3.7 Determination of substrates oxidation rates ..... 84*

*4.3.8 Calculation of ATP production ..... 85*

*4.3.9 Confocal imaging ..... 85*

4.4 RESULTS ..... 86

*4.4.1 Glucose metabolism ..... 86*

4.4.1.1 Glycolytic flux in control and treated P2-CDCs ..... 86

4.4.1.2 Lactate efflux in control and treated P2-CDCs ..... 88

*4.4.2 Substrate oxidative metabolism in control and treated P2-CDCs ..... 90*

*4.4.3 Main source of Adenosine Triphosphate (ATP) production in control and treated P2-CDCs ..... 93*

*4.4.4 Molecular profile of metabolic pathways ..... 95*

4.4.4.1 Molecular profile of glucose metabolism in control and treated P2-CDCs ..... 95

4.4.4.2 Molecular profile of fatty acid oxidation ..... 95

4.4.4.3 Protein expression changes ..... 98

4.4.4.4 Confocal imaging of Mitochondria ..... 101

4.5 DISCUSSION ..... 103

4.6 CONCLUSION ..... 110

**CHAPTER 5 CARDIOMYOGENIC DIFFERENTIATION OF CARDIAC PROGENITOR CELLS BY METABOLIC MANIPULATION USING SMALL MOLECULES ..... 111**

5.1 ABSTRACT ..... 112
5.2 INTRODUCTION ..... 113
5.3 METHODS ..... 116
*5.3.1 Overview of designed study ..... 116*
*5.3.2 Isolation, and expansion of cardiosphere-derived cells ..... 117*
*5.3.3 Cytotoxicity tests ..... 117*
*5.3.4 Cardiomyogenic differentiation of P2-CDCs ..... 117*
*5.3.5 Real-time quantitative RT-PCR ..... 119*
*5.3.6 Determination of glycolytic flux ..... 119*
*5.3.7 Determination of substrates oxidation rates ..... 119*
*5.3.8 Calculation of ATP production ..... 119*
*5.3.9 Western blot ..... 120*
*5.3.10 Confocal imaging ..... 120*
5.4 RESULTS ..... 121
*5.4.1 Cell viability and cytotoxicity ..... 121*
*5.4.2 Morphological differences ..... 123*
*5.4.3 In Vitro Cellular Metabolism ..... 127*
5.4.3.1 Glycolytic flux ..... 127
5.4.3.2 Oxidative metabolism ..... 129
5.4.3.3 Adenosine triphosphate (ATP) production in both glycolysis and oxidative metabolism ..... 132
*5.4.4 Molecular profile of cardiomyogenic differentiated P2-CDCs ..... 134*
5.4.4.1 Molecular profile of cardiomyocyte markers ..... 134
5.4.4.2 Molecular profile of smooth muscle cell markers ..... 136
5.4.4.3 Molecular profile of endothelial cell markers ..... 137
5.4.4.4 Molecular profile of calcium handling genes ..... 139
5.4.4.5 Molecular profile of glucose metabolism ..... 140
5.4.4.6 Molecular profile of fatty acid transporters ..... 142
5.4.4.7 Molecular profile of fatty acid metabolism ..... 143
*5.4.5 Molecular profile of proteins involve in metabolic pathways ..... 144*
5.4.5.1 Molecular profile of protein expression of glucose metabolism ..... 145

5.4.5.2 Molecular profile of mitochondrial and fatty acid transport proteins ..... 147

*5.4.6 Immunophenotypic characterisation of WY-14643+TGFβ treated cells ..... 149*

5.5 Discussion ..... 158

5.6 Conclusion ..... 163

**CHAPTER 6 GENERAL DISCUSSION ..... 164**

General Discussion ..... 165

**APPENDIXES ..... 192**

Appendix 1 - Medium compositions ..... 193

Appendix 2 - Synthetic small molecules and concentrations ..... 195

Appendix 3 - Designed 20 primer sequences ..... 196

Appendix 4 - Primary secondary antibodies used for flow cytometry ..... 199

Appendix 5 - Primary and secondary antibodies used for immunocytochemistry ..... 200

Appendix 6 - Fluorochromes and corresponding laser used for confocal microscopy ..... 201

Appendix 7 – Buffer Compositions ..... 202

Appendix 8 - Primary and secondary antibodies used for immunoblotting ..... 203

# Abbreviation

| | |
|---|---|
| α-KGDH | Alpha-ketoglutarate dehydrogenase |
| AA | Ascorbic acid |
| Actb | Beta-actin |
| ACADM | Acyl-Coenzyme A dehydrogenase |
| ADP | Adenosine diphosphate |
| ANOVA | Analysis of variance |
| ATP | Adenosine triphosphate |
| ADMSCs | Adipose-derived Mesenchymal Stem Cells |
| 5-aza | 5-Azacytidine |
| B2M | β2 microglobulin |
| BMI | Body mass index |
| BMSC | Bone marrow stem cell |
| BM-MSC | Bone marrow mesenchymal stem cells |
| BSA | Bovine serum albumin |
| CADUCEUS | CArdiosphere-Derived aUtologous Stem Cells to reverse ventricUlar dysfunction |
| CD | Cluster of differentiation protein |
| CD45 | Lymphocyte common antigen |
| CD90 | Thy-1 cell surface antigen |
| CD105 | Endoglin |
| CDCs | Cardiosphere-derived cells |
| cDNA | Complementary deoxyribonucleic acid |
| CISY | Citrate synthase |
| $CO_2$ | Carbon dioxide |
| ColIV/HD | Collagen IV/hanging drops |
| CM | Cardiac myocytes |
| CPT | Carnitine palmitoyltransferase |
| CXCR-4 | CXC chemokine receptor 4 |
| DNA | deoxyribonucleic acid |
| DNMT | DNA methyltransferase |
| CEM | Complete explant medium |
| CGM | Cardiosphere growth medium |
| c-kit | Stem cell factor cytokine receptor |
| CDM-1 | Cardiomyocyte differentiation medium 1 |
| CDM-2 | Cardiomyocyte differentiation medium 2 |
| CPC | Cardiac progenitor cells |
| CSC | Cardiac stem cells |
| CSp | Cardiosphere |
| cTnnT2 | Cardiac troponin T2 |
| CVD | Cardiovascular disease |
| DMEM | Dulbecco's modified Eagle medium |
| DMSO | Dimethyl sulfoxide |
| dNTP | Deoxyribonucleotide triphosphate |
| ECM | Extracellular matrix |

| | |
|---|---|
| EDC | Explant-derived cells |
| ECS | Endothelial cells |
| EPCs | Endothelial progenitor cells |
| ESCs | Embryonic stem cells |
| ETC | Electron transport chain |
| FABP | Fatty acid binding protein |
| FAK | Focal adhesion kinase |
| FBS | Fetal bovine serum |
| FFA | Free fatty acids |
| FN/PDL | Fibronectin/poly-D-lysine |
| Gata4 | Gata binding protein 4 |
| GLUT1 | Glucose transporter 1 |
| GLUT4 | Glucose transporter 4 |
| HDAC | Histone deacetylase |
| HF | Heart failure |
| HSC | Hematopoietic stem cells |
| ICM | Inner cell mass |
| IGF-1 | Insulin-like growth factor-1 |
| IMDM | Iscove's modified Dulbecco's medium |
| iPSCs | Induced pluripotent stem cells |
| Klf-4 | Kruppel-like factor 4 |
| Lin | lineage |
| LN | Laminin |
| LV | Left ventricular |
| MAPK 1/2 | Mitogen-activated protein kinase 1/2 |
| MCD | Malonyl-CoA decarboxylase |
| MCAD | Medium-chain Acyl-CoA dehydrogenase |
| MCAT | Malonyl CoA-acyl carrier protein transacylase |
| MI | Myocardial infarction |
| MSC | Mesenchymal stem cells |
| MyHC | Myosin Heavy Chain |
| Nkx 2.5 | Homeobox protein NKX2-5 |
| $O_2$ | Oxygen |
| Oct-04 | Octamer-binding transcription factor 4 |
| OXPHOS | Oxidative phosphorylations |
| P | Passage |
| PBS | Phosphate buffered saline |
| PC | Progenitor cells |
| PDH | Pyruvate dehydrogenase |
| PDK2 | Pyruvate dehydrogenase kinase-2 |
| PDK4 | Pyruvate dehydrogenase kinase-4 |
| PDL | Poly-D-Lysine |
| PLN | Phospholamban |
| PPAR | Peroxisome proliferator-activated receptor |
| qRT-PCR | Quantitative (real-time) reverse transcriptase PCR |
| RNA | Ribonucleic acid |

| | |
|---|---|
| Sca-1 | Stem cell antigen-1 |
| SCIPIO | Cardiac Stem Cell Infusion in Patients with Ischemic Cardiomyopathy |
| SD | Standard deviation |
| SEM | Standard error of mean |
| SMs | Skeletal myoblasts |
| SP | Side population |
| Sox-2 | Sex determining region Y-box 2 |
| TCA | Tricarboxylic acid cycle |
| Tel | Telomere |
| TERT | Telomerase reverse transcriptase |
| TGF-ß | Transforming growth factor beta |
| TSC | Totipotent stem cells |
| UCP | Uncoupling protein |
| VEGF | Vascular endothelial growth factor |
| VSELs | Very small-embryonic-like cells |
| VSM | Vascular smooth muscle |
| WHO | World Health Organisation |

# Chapter 1

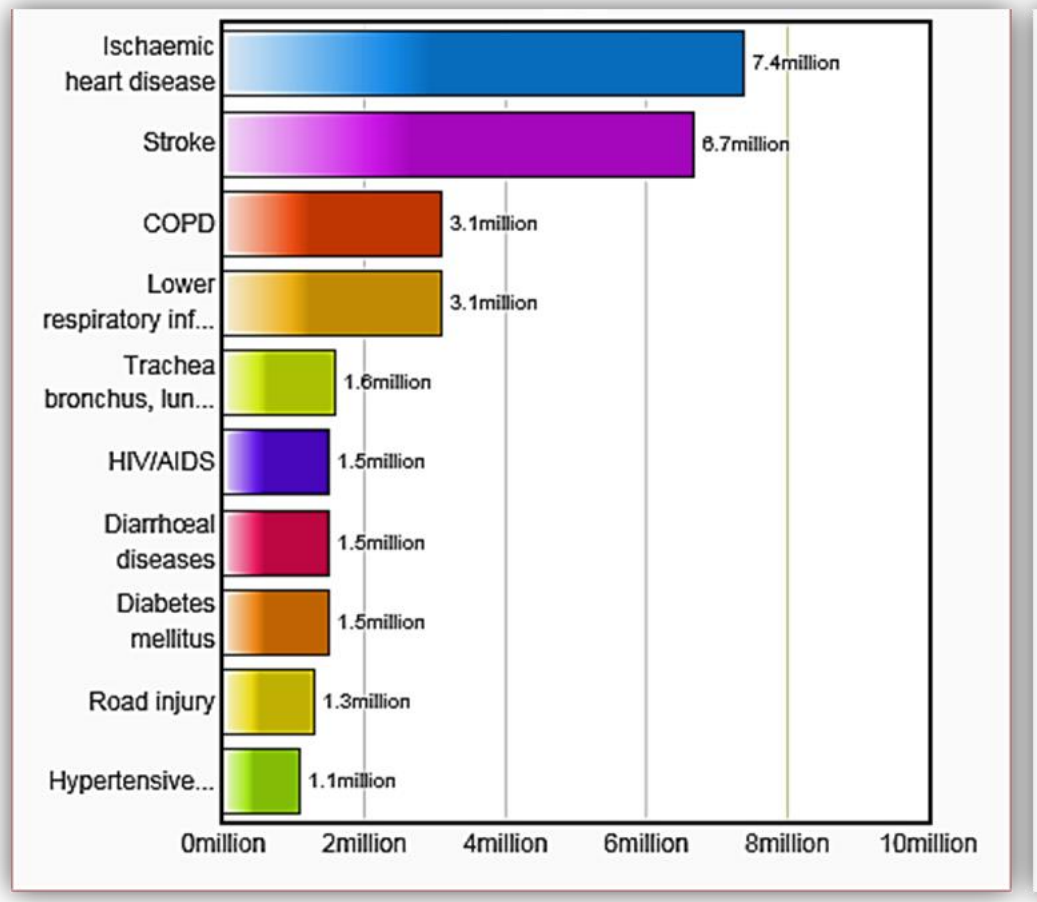
## INTRODUCTION

## 1.1 Myocardial Infarction (MI)

Myocardial infarction (MI) and its progression to heart failure, remains a major cause of death and disability in both developing and non-developing countries, with cardiovascular diseases being the leading cause of deaths, as shown by a report published in 2012 by the World Health Organisation (WHO) (Figure 1.1)[1]. According to the WHO, from 56 million worldwide deaths in total, cardiovascular diseases killed 17.5 million (31.3%) people, of these 7.4 million died of ischaemic heart disease (13.2%) and 6.7 million from stroke (11.9%) (Figure 1.1 A and B)[1]. The incidence of heart failure after MI was reported as high as 82% in 27 different studies [2], since current drugs and interventional therapies cannot control the progression of MI to final stage heart failure, leaving heart transplantation as an alternative solution for patients[3-5].

MI is caused by occlusion of a coronary artery, following rupture of a vulnerable atherosclerotic plaque, releasing a collection of lipids, macrophages, monocytes and neutrophils [6]. This initiates intracellular signaling and neurohormonal activation, which localizes the inflammatory response, resulting in ischemia, a shortage of blood supply and glucose for cellular metabolism, followed by cell necrosis and apoptosis[7, 8]. After MI, loss of cardiomyocyte mass and fibro-tissue hyperplasia leads to adverse left ventricular remodeling including dilation, hypertrophy, the formation of a collagen scar, and irreversible heart failure, defined as the inability of the heart to pump sufficient blood flow to meet the needs of the body[9, 10].

**A.**




**B.**

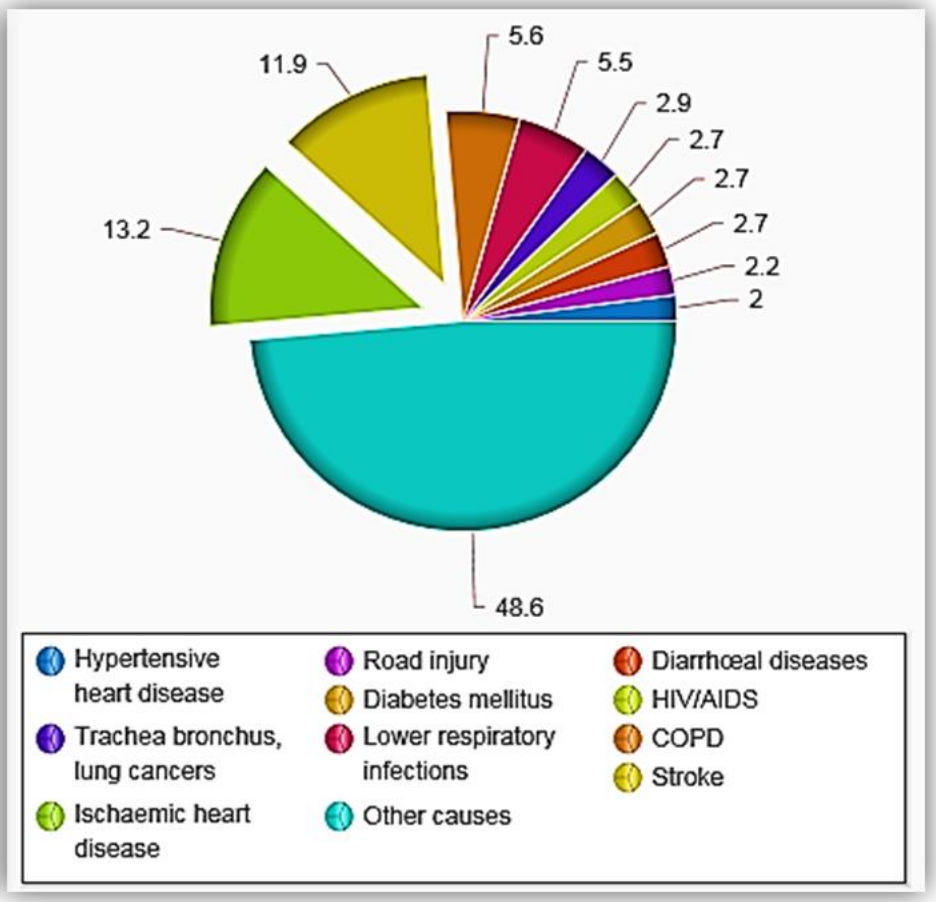



***Figure 1.1 The ten leading causes of worldwide death on 2012.*** *The numbers (A.) and the percentage (B.) of major causes of worldwide deaths on 2012 showed cardiovascular diseases are number one cause of death throughout the world (adapted from WHO, Fact Sheet Nº 310)*[1].

## 1.2 Current Drug and interventional therapies

Current drugs including diuretics, digitalis, beta-blockers, and angiotensin-converting enzyme (ACE) inhibitors; and interventional therapies such as thrombolytic agents, primary balloon angioplasty or stenting, pacemakers, coronary perfusion, and coronary artery bypass surgery are not able to prevent the progression of heart diseases to final stage heart failure, leaving heart transplantation as the only option for patients[3-5]. However, a limited number of hearts are available for transplantation, and the risks associated with surgery including immunogenic response and transplant rejection has led to the demand for an alternative therapy for heart failure and novel treatment methods for MI. Currently, the most promising treatment option that is appearing on the horizon is stem cell transplantation therapy for the repair of damaged myocardium.

## 1.3 Stem Cell therapy for myocardial infarction

A stem cell is an undifferentiated cell of a multicellular organism possessing two properties. First, the capacity for long-term self-renewal without senescence, and second, pluripotency, the ability to differentiate into one or more specific cell types[11]. There are three types of stem cells including embryonic stem cells (ESCs), induced pluripotent stem cells (iPS), and adult stem cells.

### 1.3.1 Embryonic Stem Cells

Embryonic stem (ES) cells, which originate from the inner cell mass of the blastocyst, are capable of perpetual self-renewal while maintaining an undifferentiated phenotype with normal karyotype [11-13] as well as holding the capacity to differentiate into all cells of the three germ layers (ectoderm, endoderm, and mesoderm)[14]. Human ES cells were first isolated in 1998[15, 16], when murine ES cells were already described for more than a decade[17, 18]. Since then, ES cells have attracted significant interest as a potential cell source for regenerative medicine due to their pluripotent capability and proliferation potential. *In vitro* studies using specific culture conditions and genetic modification have shown that human ES cells have the potential to differentiate into various cell types including endothelial cells[19], neurons and neural precursor cells[20], pancreatic progenitor cells[21, 22] and

cardiomyocytes[23]. *In vivo* studies on ES cells have been shown to improve cardiac function in rodents through differentiation within the donor myocardium, contributing to a stable improvement in contractile function and ventricular remodelling in the infarcted heart[24, 25]. Nevertheless, the pluripotent characteristic of ES cells results in a high risk of teratoma formation after administration[26]. Furthermore, ES cells are allogeneic, which can provoke an immunogenic response in the recipient body[27]. Moreover, problems with ethical issues, as ES cells can only be obtained by destroying an embryo [28], cause ES cell transplantation to remain problematic and restrict their clinical application.

### 1.3.2 Induced pluripotent stem cells

Induced pluripotent stem cells (iPSCs) are generated from adult cells by *ex vivo* nuclear reprogramming to become embryonic-like stem cells, through ectopic expression of stemness-related pluripotent genes Oct4, Sox2, Klf-4 and c-Myc[29, 30]. Mouse iPSCs were first reported in 2006[30], and human iPSCs were reported in 2007[29]. So far, iPSCs have been made from adult liver, stomach, skin, blood, prostate, mesenchymal and urinary tract cells[31]. Unlike ES cells, iPSCs are derived from an autologous source. Hence, they do not act as an allogeneic cell source, and they avoid the ethical dilemmas of ES cells[32]. iPS cells can be differentiated into spontaneously contracting cardiomyocytes[33, 34], providing an alternative cell source for myocardial infarction therapy. However, there remain concerns for clinical application of iPS cells because their generation employs viruses and oncogenes, which are associated with the risk of tumorigenesis. Extended culture of iPSCs has been linked to duplication of oncogenic genes[35], and around 20% of iPS cell-derived mice developed tumours[36]. Furthermore, iPSCs showed significant reprogramming variability, including retaining epigenetic imprinting associated with their tissue type of origin, which results in restricted terminal differentiation into other cell types[37-39]. Collectively, iPSCs are potent cells for therapy, however, continued the study of a wide variety of iPSCs and their ES cell counterparts are needed to understand the full range of epigenomic variability and to potentially identify factors that enable complete reprogramming of iPSCs to occur [37, 40].

## 1.3.3 Adult stem cells

Adult stem cells known as somatic stem cells are undifferentiated cells found among differentiated cells throughout the body after development. These cells exist in microenvironments known as niches[41], where cells are protected from apoptosis, differentiation stimuli and excessive stem cell division that could lead to tumour formation[42]. Somatic stem cells are able to self-renew and differentiate to yield some or all of the major specialized cell types of the tissue or organ where they are found to replenish dying cells and regenerate damaged tissues[43]. Somatic stem cells have been shown to be multipotent and able to transdifferentiate into developmentally unrelated cells[44, 45]. Multiple somatic stem cell sources have been used for myocardial infarction therapy including bone marrow stem cells, endothelial progenitor cells, mesenchymal stem cell, skeletal myoblasts and endogenous cardiac stem cells.

### 1.3.3.1 Bone marrow-derived stem cells

Bone marrow cells (BMCs) consist of a complex variety of cells that generate blood cells, bone, cartilage, fat, fibrous connective tissues and a diverse multipotent stem and progenitor cell population[46-48]. In 2001, BM cells were first used for a treatment of cardiovascular disease by injecting c-Kit$^{+}$ Lin$^{-}$ BMCs into the injured myocardium, where they transdifferentiated into cardiomyocytes, smooth muscle, endothelial cells and improved cardiac function[49, 50], igniting a lot of interest for their application in cardiac regenerative therapy. Hitherto, 41 randomised controlled trials (RCTs) of BMC therapy for the heart have been carried out across the world[51]. Nevertheless, a recent meta-analysis study, as well as most clinical trials, showed a small beneficial effect or no sufficient evidence for an effect of BMC therapy for patients with acute myocardial infarction[51-54]. It is now thought that integrating BMCs into the infarcted myocardium may improve cardiac function mainly by promoting angiogenesis, cell survival, or by other paracrine effects[55-57]. Therefore, this intervention remains unproven and needs further adequately powered trials[51].

### 1.3.3.2 Mesenchymal stem cells

Mesenchymal stem cells (MSCs) are self-renewing fibroblast-like plastic-adherent cells, initially isolated from bone marrow, but then found in virtually all post-natal organs and tissues[58]. They are positive for CD105, CD90, and CD74, but negative for CD45, CD34, CD14, CD79, CD19, and HLA-DR. MSCs are multipotent and capable of differentiating rapidly into osteoblasts, chondrocytes and adipocytes[59] as well as transdifferentiating into other cell types including cardiomyocytes[60], neural[61], and lung cells[62]. MSC therapy using either autologous or allogeneic cells has been shown to improve cardiac ejection fraction, left ventricular (LV) remodelling, and reduced scar formation of the infarcted heart[63-66] without causing an immunogenic response[67]. Hence, MSCs have proved to be a suitable cell source for allogeneic transplantation, as was demonstrated in the POSEIDON trial where autologous and allogeneic MSCs were tested on 30 patients and showed no association with adverse immune responses[68]. Furthermore, phase I and II clinical trials have shown that MSCs improved regional contractility and reverse remodelling. Nevertheless, due to their limited cardiomyogenic differentiation potential, pre-specification of MSCs with a cardiogenic cocktail[69] was tested in the C-CURE trial, where the patients showed a reduction of scar size and improvement of cardiac function and better tolerance to exercise and quality of life[70]. However, there are other studies which have reported contradictory results[71].

### 1.3.3.3 Endothelial progenitor cells

Endothelial progenitor cells (EPCs) are multiple cell types with different cell markers that have the capacity to migrate, proliferate, and differentiate into mature endothelial cells (ECs)[72]. EPCs are VEGFR-2, CD34, CD133, KDR-expressing cells that uptake AC-LDL and can be isolated from adult bone marrow, peripheral circulating blood or umbilical cord blood, and human liposuction materials[73-75]. EPCs have been shown to transdifferentiate into endothelial cells, smooth muscle cells and cardiomyocytes in vivo[76], and increased capillary density, prevented cardiomyocyte apoptosis, reduced remodelling and left ventricular scarring and improved heart function in the rat[77-79]. Nevertheless, EPCs are found to be rare in circulating blood[80] and showed reduced capacity for

neovascularization when isolated from patients with cardiovascular risk factors[81]. In addition, there are still controversies about whether the improvement in cardiac function observed following EPC transplantation resulted from an indirect effect of angiogenesis induced by EPCs[82] or direct regeneration and differentiation of EPCs into cardiomyocytes[76].

#### 1.3.3.4 Skeletal myoblast

Skeletal myoblasts (SMs) or satellite cells are small mononuclear progenitor cells with virtually no cytoplasm found in mature skeletal muscle[83]. They are precursors to skeletal muscle cells, and their activation leads to their proliferation to give rise to satellite cells or differentiation into myoblast, skeletal muscle cells[84-86]. Satellite cells can be isolated from a muscle biopsy sample and expanded *in vitro*, providing an autologous cell source for transplantation[87]. Autologous SMs were the first cells used for transplantation in ischemic heart patients with severe post-infarction left ventricular dysfunction[88, 89]. Although the preliminary data from the trial reported the feasibility and safety of autologous SMs transplantation in ischemic hearts, there was little evidence of trans-differentiation of SMs into cardiomyocytes[87, 90]. Furthermore, SM transplantation has been shown to lead to arrhythmias, requiring further cell enhancement techniques to reduce the arrhythmias[91, 92] for the phase II PERCUTANEO clinical studies[93].

#### 1.3.3.5 Very small embryonic-like cells

Very small embryonic-like stem cells (VSELs) are a rare (~0.02%) homogeneous population of CXCR-4$^{+}$ Sca-1$^{+}$ CD45$^{-}$ cells expressing pluripotent stem cell markers such as SSEA-1, Oct-4, Nanog, and Rex-1[94, 95]. VSELs were initially isolated from murine bone marrow[94], followed by isolation from other organs such as brain, kidneys, muscles and pancreas[96]. However, a recent study showed that VSELs are epiblast-derived stem cells that are deposited early during gastrulation (organogenesis) and survive into adulthood[97, 98]. VSELs are very small, ~2-4 µm, and can differentiate into all three germ layer lineages. Hence, *in vitro* differentiation of VSELs revealed their

ability to give rise to cardiomyocytes, neuronal, and pancreatic cells[94]. Furthermore, studies have shown transplantation of VSELs improved left ventricular function in an infarcted animal model[99]. Nevertheless, the low level of VSELs and their oncogenic risk could be hurdles for translation to the clinic.

### 1.3.3.6 Endogenous cardiac stem cells

Discovery of endogenous cardiac stem cells, which can replenish the cardiomyocyte population and regenerate coronary vessels[100, 101], has challenged the notion of the adult heart as a terminally differentiated organ without self-renewal potential. To date cardiac stem cells have been isolated from adult mammalian heart including mouse, rat, human, dog, and pig[100, 102-110] using surface markers, transcription factors, the side population (SP) dye efflux phenotype[108, 111], the re-activation of epicardial markers denoting their development, and growth in tissue culture as cardiospheres [106] or as colony-forming units[112].

#### 1.3.3.6.1 Cardiac side population (SP)

The first stem cell isolated from the adult heart was in 2002 based on the ability of efflux Hoechst 33342 dye, yielding a putative progenitor side population (SP) cell with stem-like cell activity[113]. The unique dye efflux ability is mediated by the ATP-binding cassette (ABC) transporter (Abcg2) which is then used as an identity marker for SP cells[114]. Abgc2 expression is involved in survival, migration and tubule formation of endothelial cells after MI, as an increased number of Abcg2 expressing cells have been found in the border zone after MI[114]. Furthermore, cardiac SP cells have been shown to be able to migrate, and differentiate into the cardiomyocyte lineage both *in vitro* when cocultured with primary cardiomyocytes and *in vivo* when injected in the rat[115], with the greatest potential for cardiomyogenic differentiation being restricted to cells co-expressing stem cell antigen-1 (SP/Sca-$1^{+}$)[108]. Nevertheless, the low quantity of SP cells, 1% of the total cell number in the adult heart, and the low frequency of their colony forming unit (1 colony per 50,000 cells plated)[113] makes it very difficult to translate into the clinical trial.

#### 1.3.3.6.2 Stem cell antigen-1$^+$ cells (Sca-1$^+$)

Although a human orthologue of stem cell antigen 1 (Sca-1$^+$) cells has yet to be identified[116], mouse Sca-1$^+$ cells have been isolated from the resident population of cardiac progenitor cells expressing neither cardiac structural genes nor *Nkx2.5*[102]. These cells have demonstrated promising properties for cardiac repair such as a high level of telomerase reverse transcriptase (TERT)[102], a reverse transcriptase that synthesizes telomere repeats on the telomere ends at the tips of chromosomes during each cell division[117, 118]. In various types of stem cells, telomerase functions to ensure long-term self-renewal capacity via maintenance of telomere length[119, 120]. Therefore, corresponding to the expression of TERT, Sca-1$^+$ cells have been found to associate with self-renewal potential[102]. Furthermore, intravenously administered Sca-1$^+$ cells after ischemia-reperfusion demonstrated homing to the injured myocardium[102], increased the left ventricular ejection fraction and induced myocardial neovascularization and modest cardiomyocyte regeneration[121]. A recent study has shown that Sca1$^+$ SP cells are clonogenic, self-renewing cardiac progenitor cells[122]. Moreover, the clonal progeny of single Sca1$^+$ SP cells showed trilineage potential differentiating into cardiomyocytes, endothelial and smooth muscle cells after cardiac grafting, augmenting cardiac function[122]. However, as with SP cells, Sca-1$^+$ cells are found in the heart at a very low number (~0.3%)[123], and also the lingering mystery of its human orthologue remains to be elucidated[116].

#### 1.3.3.6.3 c-Kit+ cells

The receptor tyrosine kinase c-Kit or CD117 found in 1986[124] is expressed highly on hematopoietic stem cells (HSCs), multipotent progenitors (MPPs) and common myeloid progenitors (CMPs) and in several non-hematopoietic tissues[125]. Binding of the ligand, stem cell factor (SCF)[126], to c-Kit causes phosphorylation and activates signal transduction molecules and propagates the signal in the cell, which plays a role in cell survival, proliferation and differentiation[127]. In 2003, a distinct resident population of cardiac stem cells expressing c-Kit but without haematopoietic lineage markers (c-Kit$^+$ Lin$^-$) was reported for the first time[100], which challenged the accepted paradigm that heart is a post-mitotic organ[128, 129]. These c-kit$^+$ Lin$^-$ cells were self-renewing, clonogenic, multipotent, and could

differentiate into cardiomyocytes, smooth muscle cells, and endothelial cells[100]. Furthermore, some of these cells expressed transcription factors Nkx2.5, GATA4, and MEF2, indicating that they were at the early stage of cardiac myogenic differentiation and were committed to the cardiac lineage[100]. Moreover, although the quantity of c-kit$^+$ Lin$^-$ cells are as low as one cell per 10,000 myocytes, they can be expanded *in vitro* for up to 40 passages without altering the cell phenotype[130]. In addition, intracoronary administration of c-kit$^+$ Lin$^-$ cells into 30-day old infarcted rat hearts has been shown to improve left ventricular ejection fraction, reduce fibrosis in the non-infarcted region, increase viable myocardium in the infarcted region, and activate the endogenous cardiac stem cells[131]. The aforementioned finding led to a clinical trial, Cardiac Stem Cell Infusion in Patients with Ischemic Cardiomyopathy (SCIPIO)[132]. Despite global studies on c-Kit as cardiac stem cells, there is growing debate about these cells since March 2014, when a relevant study has been retracted[133, 134] and raised concerns about the integrity of the SCIPIO report[132].

**1.3.3.6.4 Islet-1 cells**

Islet-1(Isl1) is a transcription factor (TF) of the LIM-homeodomain family, which was first identified in 1990, in the β-cells of the pancreas as an enhancer of the insulin gene[135]. In 2003, Isl1 became popular in the field of cardiovascular research after the discovery of severe cardiac malformation in Isl1 deficient mice, which were completely missing the outflow tract, right ventricle, and much of the atria[136]. Isl1$^+$ cells have been identified as a residue of the migrating secondary heart field (SHF) cells[137] and can be isolated from murine embryonic and neonatal hearts[138, 139] and murine or human embryonic stem cells[139, 140]. *In vitro* and *in vivo* studies have shown that Isl1$^+$ cells generate diverse multipotent cardiovascular cell lineages. They do not only differentiate into three major cell types in the heart (cardiac, smooth muscle, and endothelial cells), but also contribute to the formation of the sinoatrial node (SAN), the atrioventricular node (AVN), and smooth muscle cells of coronary arteries[138, 141-143]. Isl1$^+$ cells were considered as a different subset of cardiac progenitor cells (CPCs) from Sca-1$^+$ and c-Kit$^+$ cells[138]. However, recent findings have

shown that embryonic and foetal Isl1$^+$ cells in human hearts are also positive for c-Kit[144]. Taken all together, Isl1$^+$ cells have only been isolated from very young animals and human specimens, and the number of Isl1$^+$ cells dramatically reduce over the first few weeks after birth[138, 142], which limits their clinical potential.

#### 1.3.3.6.5 Epicardial-derived stem cells

The adult myocardium is enveloped by a layer of epithelial cells known as the epicardium. They play an important role during embryogenesis in the formation of the coronary vasculature. These cells synthesise and secrete a dense layer of extracellular matrix that resides between them and the myocardium in the subepicardial space. A subset of these cells delaminate from the epicardium and migrate into the subepicardium, and generate a population of epicardially derived cells (EPDCs), after a process called epithelial-to-mesenchymal transition (EMT)[145]. During cardiac development, the epicardium is a source of multipotent mesenchymal cells, which gives rise to endothelial and smooth muscle cells in coronary vessels and also to cardiomyocytes[146]. In the adult Zebrafish heart, EPDCs have been shown to play a role in heart repair after tissue damage [147] where, after injury, epicardial cells undergo EMT, migrate into the wound, and participate in myocardial regeneration and blood vessel formation[147]. EPDCs have been identified in adult human[148] and mouse[149] epicardium, and murine EPDCs can differentiate into endothelial cells[149]. Furthermore, quiescent EPDCs can be activated using a naturally occurring protein called thymosin beta 4 (Tβ4)[150]. Tβ4 brings the EPDCs out of dormancy and induces them to become mature cardiomyocytes[150]. In mice infused with Tβ4, the cardiac progenitor stem cells were activated and migrated from the epicardium to the site of damage and became mature cardiomyocytes[150]. Moreover, activated adult mouse EPDCs express the key embryonic epicardial gene, Willm's tumor 1 (Wt1), which ultimately contributes to *de novo* cardiomyocyte formation in the injured mouse heart[151]. EPDC-derived cardiomyocytes were structurally and functionally integrated with resident muscle and gave significant improvement in functional parameters, including increased ejection fraction, reduced end-diastolic/systolic volumes and reduced scar volume[151]. Stimulation of EPDCs to give rise to *de novo* cardiomyocytes has emerged as a new resident-cell based therapy for heart disease.

#### 1.3.3.6.6 Cardiosphere and cardiosphere-derived cells

Cardiac stem cells have been isolated from human and murine hearts and expanded as cardiospheres[106]. These cardiosphere cells have been shown to be clonogenic and to express cardiac stem cell markers, c-Kit, and Sca-1 and the endothelial progenitor cell marker, CD34[106]. Cardiosphere cells have been shown to be able to spontaneously differentiate into contracting cardiomyocytes, confirming that these cells possess cardiomyogenic potential[106]. *In vitro* expansions of cardiospheres were obtained to provide sufficient cardiosphere-derived cells (CDCs) for transplantation[152]. Transplantation of cardiospheres and CDCs in infarcted rodent hearts leads to myocardial regeneration and functional improvement of the hearts[106, 152]. This led to the clinical trial of CDCs in the CADUCEUS trial[153, 154], which showed that by six months, no patients had died, developed cardiac tumours, or experienced major adverse cardiac events (MACE) and showed increased viable heart mass and regional contractility and wall thickening[154]. However, there were no changes in end-systolic volume and left ventricle ejection fraction between groups[154]. Nevertheless, it showed that intracoronary infusion of autologous CDCs after myocardial infarction is safe and that could lead to the phase II study. Furthermore, a direct comparison of several stem cell types (CDCs, BM-MNs, BM-MSCs, and AD-MSCs) revealed the superiority of CDCs which exhibited a balanced profile of paracrine factor production and the greatest functional benefit in experimental MI[155].

## 1.4 Cardiac stem/progenitor cell isolation and expansion

Soon after the recognition of cardiac stem cells in the adult heart[100], different approaches have been used to isolate CSCs from heart tissue. First CSCs were isolated from adult hearts, based on their ability to efflux Hoechst dye, obtaining a putative progenitor side population (SP) cell with stem-like cell activity[113]. In addition, CSCs have been isolated based on a specific single cell marker like c-Kit[100] or Sca-1[102]. These methods can generate a homogenous cell population with a fairly low level of CSCs, with only 1% of SP cells[113] and one c-kit$^+$ cell in every $10^4$ cardiomyocytes[123], that requires substantial in vitro expansion to generate sufficient cell numbers for therapy[100, 113].

Messina and co-workers developed a method to isolate and culture cardiac stem cells from mouse and human heart tissue explants and expand them as cardiospheres (CSps)[106]. These CSps were clonogenic and expressed stem and endothelial progenitor cell antigens/markers (c-kit, Sca-1, and CD34). The CSps were expanded to obtain sufficient CSp-derived cells (CDCs) for transplantation[152]. Both CSps and CDCs from heart tissue explant cultured *in vitro*, are able to differentiate into myocardial cells when injected into the infarcted mouse heart *in vivo*[106, 152].

Although the adult heart contains stem cells that are able to partially repair the heart following a MI or throughout the progression of heart failure[100], however, endogenous cardiac stem cells (CSCs) are limited in quantity[113, 123, 130] and may decrease and lose their functional capacity with increased age[156, 157]. Thus, it is essential to isolate and expand the CSCs *in vitro t*o generate sufficient cells for transplantation. Preliminary work done by Tan described two approaches to the isolation and rapid expansion of cardiac stem cells (CSCs) in a short time period without compromising the quality of the cells in terms of stemness and function. The first technique was cell expansion on FN with CSps formation on poly-D-lysine (PDL). The second was cell expansion on ColIV with CSps formation in hanging drops with higher c-kit$^+$ cells (up to 11%) compared to PDL (3%). Therefore, an introduction of appropriate extracellular matrix (ECM) molecules within *in vitro* culture would certainly enhance cell isolation and expansion.

## 1.5 Cardiomyogenic differentiation of cardiac progenitor cells

Most studies on stem cell transplantation therapy on myocardially infarcted animal models as well as human clinical trials (e.g. CADUCEUS and SCIPIO) have focused on the use of undifferentiated stem cells (e.g. CDCs and c-Kit$^+$ cells). However, there is a strong possibility that *in vitro* cardiomyogenic differentiation of stem cells prior to transplantation would result in higher engraftment efficiency, enhanced myocardial regeneration, and recovery of heart function[158]. Furthermore, this may reduce the possibility of spontaneous differentiation of stem cells into undesired lineages and reduce the risk of teratoma formation.

Various strategies and approaches have been tested to develop an efficient protocol for directing *in vitro* cardiomyogenic differentiation of stem cells. Initially, the co-culture with the adult or neonatal cardiomyocytes was the most effective protocol to differentiate progenitor cells[159-162] and cardiac progenitor cells, such as cardiac $Isl1^+$ and SP cells into cardiomyocytes[114, 138]. Furthermore, rat CDCs were found to differentiate into spontaneously beating cardiac myocytes when co-cultured with neonatal rat cardiomyocytes[163]. It is possible that the cardiomyocyte co-culture effects on differentiation are mediated by transforming growth factor-beta (TGF-β), which is secreted by both adult and neonatal cardiomyocytes[164] and is also involved in cardiac differentiation of ESCs[165, 166] and human cardiomyocyte progenitor cells (hCMPCs) with up to 100% efficiency of differentiation[167]. Furthermore, TGF-β secretion by cardiomyocytes induces expression of contractile protein genes, which are up-regulated in hypertrophy[168] and maintain the beating rate of cells[169]. Furthermore, in many cell types, TGF-β increases expression of extracellular matrix proteins including fibronectin; collagen I, III, V, VI; proteoglycans; tenascin; osteonectin; osteopontin, and thrombospondin as well as upregulating integrin receptors for collagen, fibronectin, laminin and vitronectin[170, 171]. Moreover, TGF-β in cardiac fibroblast cells increases expression of collagen[172] and decreases expression of collagenase and transin in both stimulated cardiomyocytes and cardiac fibroblasts[164, 171].

In the clinical scenario, however, it would not be practical to induce differentiation of progenitor cells into cardiomyocytes through co-culture with either allogeneic or xenogeneic cell sources due to the major limitations of this technique as the two distinct cell population may cause pathogen transmission (e.g. viruses) and the difficulty of separating the co-cultured cell populations[158]. Therefore, Goumans et al[167] and Smits et al[173], have shown that cardiomyogenic differentiation of human cardiac progenitor cells was strongly enhanced by the addition of TGF-β. The phosphorylation of Smad2 mediated by TGFβ in human cardiomyocyte progenitor cells, causes earlier expression of contractile proteins, higher number of $\alpha$-actinin$^+$ cells, and more beating areas per dish. Nevertheless, recent studies in our laboratory showed that cardiomyogenic differentiation

of murine CDCs using the protocol with TGFβ did not induce the cardiac progenitor cells into fully functional beating cardiac myocyte cells (Filippo Perbellini, DPhil thesis).

Furthermore, *in vitro* studies have shown that 5-Aza can successfully induce several different types of cells to undergo differentiation into cardiomyocytes including Sca-1$^{+}$ CDCs[174], human umbilical cord-derived MSCs[175], adult human bone marrow MSCs[176, 177], murine bone marrow stromal cells[178], and primary and immortalized porcine MSCs[179]. Nevertheless, it has been reported that 5-Aza is insufficient for the cardiogenic induction of the adipose-derived stem cells (ASCs)[180]. 5-azacytidine is a hypomethylating agent, used to treat myelodysplastic syndrome (MDS)[181], and acts by incorporating into the genome of proliferating cells during DNA synthesis and trapping DNA methyltransferase (DNMTs), which targets them for degradation, resulting in hypomethylation of the genome[182].

Moreover, *in vitro* studies showed that dimethyl sulfoxide (DMSO) could induce other cell types to differentiate into cardiomyocytes. DMSO, which is a potent solvent for water-insoluble compounds and hydrogen-bond disrupter[183], has been found to be a histone deacetylase (HDAC) inhibitor[184] and to cause terminal differentiation of murine erythroleukemia cells[185]. Cell differentiation begins with modification of gene expression, regulated by acetylation of histones. Removal of the acetyl groups from histones by HDAC down-regulates expression of genes that cause cells to differentiate. Thus using HDAC inhibitors like DMSO causes deacetylation of histone and subsequent cell differentiation[186, 187]. DMSO-induced biochemical mediators of Wnt signaling by decreased phosphorylation and increased levels of β-catenin[188]. Furthermore, DMSO enhanced P19 cell differentiation into cardiomyocytes[189, 190]. DMSO has been shown to inhibit c-myc expression[191] and arrest cell cycle progression, thus affecting cell proliferation in different cell types[192].

Hitherto, the majority of studies of cardiomyogenic differentiation have focused on differentiation using chemicals, cytokines and growth factors. However, there has been a limited study of the metabolism of undifferentiated and differentiated CDCs, which may provide insights to inform

strategies for their culture and their direct differentiation into cardiomyocytes, and also a therapeutic window for pharmacological manipulation.

## 1.6 Metabolism

Metabolism plays an essential role in dictating whether a cell proliferates, differentiates or remains quiescent. Hence, different metabolic requirements exist at different stages during development including embryos, early pluripotent stem cells, tissue-resident adult stem cells, transient amplifying tissue progenitors and finally mature adult tissues.

### 1.6.1 Adult cardiac metabolism

The heart beats around 100,000 times per day. In order to maintain continual contractile activity, the heart requires a constant source of energy, supplied in the form of adenosine triphosphate (ATP). The human heart must synthesize approximately 30 kg of ATP per day[193, 194] generated almost entirely via mitochondrial oxidative phosphorylation (OXPHOS)[195]. The heart is a metabolic omnivore, capable of metabolizing a range of different exogenous substrates, mainly lipids (free fatty acids) and carbohydrates (glucose and lactate) as well as circulating ketone bodies, pyruvate and amino acids to satisfy its energy demands[196-199] (Figure 1.2). The substrates are broken down into the 2-carbon compound acetyl-CoA, which feeds into the mitochondrial Krebs cycle, generating $NADH+H^+$ and $FADH_2$. These reducing equivalents donate electrons that are shuttled between complexes I to IV of the respiratory electron transport chain (ETC) in the inner mitochondrial membrane. The electrons are accepted by an oxygen molecule at complex IV of the ETC, producing H2O as a by-product. Simultaneously, complexes I, III, and IV of the ETC use the energy released in this redox reaction to pump protons into the mitochondrial intermembrane space, generating an electrochemical gradient across the inner membrane. This gradient is the driving force for the phosphorylation of adenosine diphosphate (ADP) to ATP by facilitating the re-entry of protons into the mitochondrial matrix via the by the $F_1F_0$ ATP synthase[195, 200, 201] (Figure 1.2).

Since contractile activity and ATP synthesis are tightly coupled to the supply of oxygen and the rate of OXPHOS, the heart is highly selective in its fuel utilization. The heart is able to switch its substrate preference, and the relative contribution of the different substrates for energy production, largely determined by their availability, coronary blood flow, oxygen supply, hormone levels and cardiac workload[202, 203]. Palmitate yields more ATP than glucose, glutamine, pyruvate or acetoacetate[194]. Therefore, the healthy heart preferentially uses fatty acids as a fuel source yielding 106 ATP molecules per palmitate molecule oxidized, compared with 31 from glucose, 15 from lactate, 12.5 from pyruvate, and 20 from acetoacetate (Table 1.1)[194].

***Table 1.1 Comparative energy yields of various fuels per molecule fully oxidized***

| **Molecule** | **ATP Yield per molecule** |
|---|---|
| **Glucose** | **31** |
| **Glutamine** | **20** |
| **Palmitate** | **106** |
| **Pyruvate** | **12.5** |
| **Acetoacetate** | **20** |

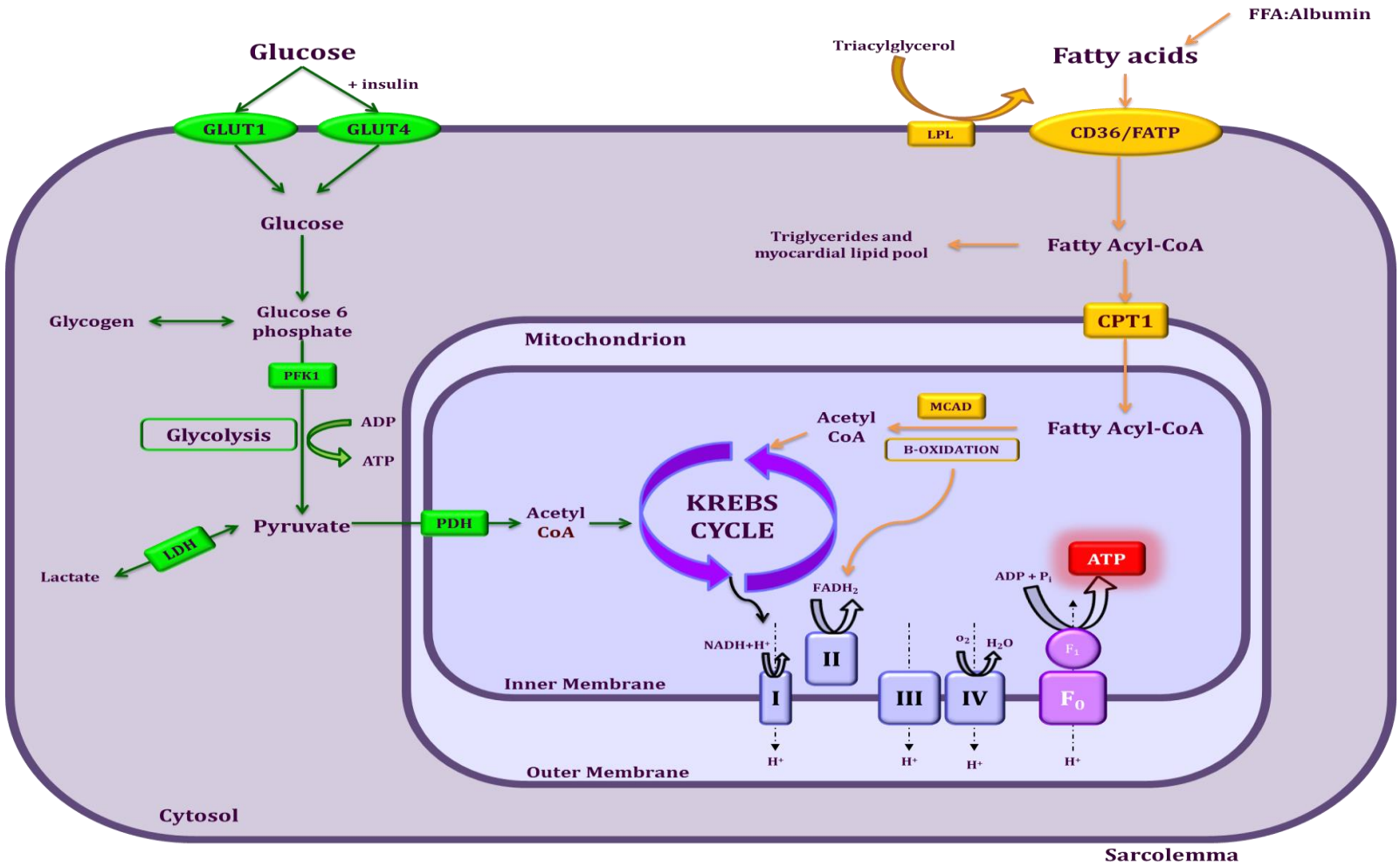



**Figure 1.2: Major energy producing pathways in the heart.** The respiratory chain consists of four complexes (I-IV). NADH derived from glycolysis, the Krebs cycle and fatty acid oxidation is oxidised by complex I, and $FADH_2$ is oxidised at complex II. Electrons are transferred through the electron transport chain to the final acceptor O2. The free energy available from the electron transfer is used to pump out $H^+$ and generate an electrochemical gradient across the inner mitochondrial membrane. This gradient is the driving force for ATP synthesis by the $F_1F_0$ ATP synthase.

### 1.6.2 Proliferating stem/progenitor cell metabolism

In proliferating stem/progenitor cells, rapid cellular growth is supported by aerobic glycolysis linked to the Krebs cycle and oxidative phosphorylation[204]. According to Otto Warburg, in comparison to normal cells, proliferating tumour cells undergo aerobic glycolysis, a phenomenon known as the Warburg effect[205]. Although these proliferating cells require ATP, even under the non-hypoxic condition they metabolise tenfold more glucose to lactate in a given time in comparison to normal cells[205, 206] without any sign of oxidative impairments[207]. Hence, glycolysis outpaces the maximal velocity of pyruvate oxidation, so that cells eliminate the excess pyruvate into lactate[208]. The glycolytic rate in proliferating cells is high enough to produce abundant ATP from abundant extracellular glucose, which can exceed the ATP produced from OXPHOS[209-211]. Furthermore, in aerobic glycolysis, the Krebs cycle is still active, and both together provide intermediates needed for biosynthetic pathways such as ribose sugars for nucleotides, glycerol and citrate (to generate building blocks for fatty acid synthesis), nonessential amino acids, and NADPH (through the oxidative pentose phosphate pathway)[208].

During embryogenesis, in the pluripotent inner cell mass (ICM), there is a sharp increase in net growth and glycolytic metabolism. During which, initially, glucose uptake increases as the embryo upregulates the expression of the glucose transporters (GLUT1 and GLUT3)[212], followed by an increase in glycolytic flux and synthesis of lactate[213]. The pluripotent inner cell mass, like embryonic totipotent stem cells (TSCs) and ESCs[214], possesses low mitochondrial mass and immature mitochondrial morphology[204]. This was predicted to be due to the high level of pyruvate dehydrogenase kinase 1 and 3 (PDK1 and PDK3), which inhibit pyruvate dehydrogenase (PDH) and mitochondrial pyruvate oxidation[215].

Cardiomyogenic transformation of ESCs occurs early in embryogenesis, as the heart forms first to sustain nutrient and oxygen delivery[216, 217]. Therefore, the transition of ESCs, which require little energy, into beating cardiomyocytes necessitates a change in energetic infrastructure capable of supporting the metabolic demands of increased electromechanical activity[218, 219]. The generation of

ESC-derived functional and energetically competent cardiomyocytes is promising for the development of regenerative therapy for heart disease[220, 221]. Nevertheless, the metabolic and energetic requirements of cardiogenic reprogramming are partially understood, which limits the exploitation of the regenerative potential of stem/progenitor cell therapy.

## 1.7 Thesis aims

Following from above, the main objective of this thesis was to determine, for the first time, substrate and energy metabolism in cardiac stem/progenitor cells before, during and after cardiomyogenic differentiation. Specifically, the aims were to:

I. Isolate EDCs and expand CDCs from 5-weeks old rat heart using both the published (FN/PDL) protocol and optimized (ColIV/HD) protocols.

II. Characterize CDCs created by both published and optimized protocols.

III. Induce cardiomyogenic differentiation of CDCs created by both protocols using either 5-Aza or DMSO.

IV. Characterize the expression profile of induced cardiomyogenic differentiated CDCs created by current and optimized protocols.

V. Determine the rates of the various pathways involved in energy metabolism of control and 3-weeks 5-Aza treated P2-CDCs using $^{3}H$- or $^{14}C$-radiolabeled substrates.

VI. Determine the source and rate of ATP production in control and 3-weeks 5-Aza treated P2-CDCs.

VII. Induce cardiomyogenic differentiation of cardiac progenitor cells using 5-Aza in combination with ascorbic acid (AA) and TGFβ to induce differentiation; with the addition of synthetic small molecule(s) to induce and upregulate fatty acid metabolism.

VIII. Assess the metabolic pathways and distinguish the glycolysis and mitochondrial oxidation levels.

IX. Assess the molecular profile of gene and protein expression levels.

# Chapter 2

## GENERAL METHODS

## 2.1 Animals

This study used 5-weeks old wild type Sprague Dawley (SD) rats. The SD rats were obtained from a commercial breeder (Harlan, Oxon, UK) and kept under controlled conditions of temperature, light, and humidity, with ad libitum access to water and chow. At the end of each experiment, rats were anaesthetised with sodium pentobarbital (270 mg/kg body weight, IP; Euthatal, Merial, UK) to allow tissue removal. Body and the heart weights were routinely recorded. All the procedures involved in this study were reviewed and approved by an Institutional Animal Care and Use Committee (IACUC), and the Home Office, and conformed to the UK government regulations (Home Office License: PIL:30/2755) for the care and use of laboratory animals.

## 2.2 Isolation and expansion of cardiac stem cells (CSCs)

In this study rat atrial and apex, tissues were used to produce cardiac-derived stem cells. The protocol used was adapted by Tan et al[222] within our laboratory, from those of Smith et al. and Messina et al[106, 152]. Unless otherwise stated, all cell culture was performed at 37°C in 5% $CO_2$:21% $O_2$:74%$N_2$.

### 2.2.1 Explant culture

Adult (5 weeks) rat hearts were excised and washed twice with Dulbecco Phosphate buffered saline (DPBS, Sigma, UK) containing 100 U penicillin and 100 U streptomycin (Sigma, UK) to remove excess blood. The heart was then minced into 1 mm explant tissue fragments in trypsin (Invitrogen) and plated on 60 X 15 mm Petri dishes, which had been pre-coated with 2ml PBS containing either 1 mg/ml fibronectin (FN) (Sigma) or 10 µg/ml collagen IV (ColIV) (Sigma) and incubated at 37°C for 30 mins and 4 hours respectively. After plating the explants, 1.5 ml Complete Explant Medium (CEM) (Appendix 1) was added to each dish.

## 2.2.2 Harvesting Explant Derived Cells (EDCs)

Explant derived cells (EDCs) grew out from the explants as round, phase bright cells overlying a layer of thin fibroblast-like cells, which emerged from the edges of explants. EDCs, once confluent, were isolated with 1 ml trypsin for five mins at 37°C.

## 2.2.3 Cardiosphere (CSps) culture

EDCs either from FN or ColIV were re-suspended individually in Cardiosphere Growth Medium (CGM) (Appendix 1). Re-suspended EDCs from FN base culture were seeded in 24-well plates (Corning), which had been pre-coated with 0.5 ml DPBS (each well) containing 16.7 µg/ml poly-D-lysine (PDL) (Gibco, Invitrogen) and incubated at 37°C for at least 30 mins before use. EDCs were plated at a density of 3 X $10^4$ cells per 300 µl of CGM (each well). Spherical cell cultures, known as cardiospheres (CSps), formed from the EDCs and were harvested after four days by mechanical trituration using a pipette.

In contrast, re-suspended EDCs from ColIV base culture were plated as hanging drops (HDs). EDCs were plated at a density of 1000 cells per 25 µl of CGM (each droplet) onto non-treated 150 mm Petri dishes (Corning), which were then flipped to invert drops. After three days, Csps formed in HDs were then transferred into bacterial dishes with fresh CGM for one day.

## 2.2.4 Cardiosphere-Derived cell (CDC) expansion

Isolated CSps from both PDL and HDs were then re-suspended in CEM and plated onto FN or ColIV coated $T_{75}$ flasks respectively for expansion into cardiosphere-derived cells (CDCs). At 80-90% confluency, CDCs were passaged and split into two new FN- or ColIV-coated flasks at a concentration of 5 x $10^5$ cells/flask for further expansion. Media was refreshed every 3-4 days.

## 2.3 Cell Counting

At the end of each stage (EDCs, P1-CDCs, and P2-CDCs) when the cells were fully confluent, they were enzymatically digested and counted using a haemocytometer under an inverted light microscope (Nikon, UK). The quantity of cell number was calculated per milligram tissue biopsies that initially used to explant.

## 2.4 Proliferation assay

Cardiosphere-derived cells at passage two were seeded at different densities (250-20,000 cells) on pre-coated micro-plates (96-well plates) with either FN or ColIV. On day 1, 2, 3, 5, and 7 culture media was aspirated, and cells washed with PBS and kept at -80°C. Proliferation level was assessed using CyQUANT® Cell Proliferation Assay Kit (Molecular Probes, Invitrogen detection technologies) plus RNase treatment according to the manufacturer's instructions. In brief, frozen cells were thawed at room temperature, treated with RNase, and lysed by addition of a buffer containing the CyQUANT GR dye. Fluorescence was then measured directly using a microplate reader (FluoStar from BMG) with excitation 485 ± 10 nm and emission detection at 530 ± 12.5 nm. The linear range of the assay under these conditions is from 250 to 20,000 cells per 200 µl samples. In order to calibrate the assay for use of the same fluorometer or microplate reader at different times or on different days, a standard curve for DNA content was prepared using bacteriophage λ DNA standard according to the manufacturer's instruction.

## 2.5 Cell cytotoxicity assay

Cardiosphere-derived cells at passage two were seeded (10,000 cells/$cm^2$) onto micro-plates (96-well plates) precoated with FN-containing CEM and cultured overnight. The next day cells were treated with various small molecules (Appendix 2). Treated CDCs were subjected to cytotoxicity tests at different intervals, day-1, -3, and -7 using "LIVE / DEAD® Viability / Cytotoxicity Assay Kit" (Molecular Probes, Invitrogen detection technologies) according to the manufacturer's instructions.

The relative number of dead cells were measured with EthD-1 which can only enter dead cells, as they possess damaged membranes, where it binds to the nucleic acids producing a bright red fluorescence, which was measured using 96-well plate reader (FluoStar from BMG) at ~495 nm excitation and ~635 nm emission.

## 2.6 Cardiomyogenic differentiation assays

Approximately 20,000 CDCs/cm$^2$ for confluent and 10,000 cells/cm$^2$ for non-confluent conditions were seeded on $T_{75}$ precoated with either 1 mg/ml FN or 10 µg/ml ColIV containing CEM. After 24 hours cardiomyogenic differentiation was induced using one of the protocols below.

### 2.6.1 DMSO Conditioned Medium

Cardiomyogenic differentiation medium-1 (CDM-1) (Appendix 1) containing 1 mM dimethyl sulfoxide (DMSO) (Sigma, UK) was added to each dish. On each of the next two days, 20µl/1ml of DMSO was added directly to the wells. On day-4, the medium was changed for CDM-1 only without DMSO and refreshed every 2-3 day for 7 days. On day-7 the medium was replaced with CDM-1 containing 0.1 mM AA (Sigma, UK). The medium was refreshed every 2-3 days until day-14.

### 2.6.2 5-Azacytidine Conditioned Medium

Cardiomyogenic differentiation medium-1 (CDM-1) (Appendix 1) containing 5 µM 5-Aza (Sigma, UK) was added to each dish. On each of the next two days, 20µl/1ml of 5-Aza was added directly to the wells. On day-4, the medium was changed for CDM-1 only without 5-Aza and refreshed every 2-3 day for 7 days. On day-7 the medium was replaced with CDM-1 containing 0.1 mM AA (Sigma, UK). The medium was refreshed every 2-3 days until day-14.

### 2.6.3 Transforming Growth Factor-β (TGF β) Conditioned Medium in a combination with or without small molecule(s)

Cardiosphere-derived cells at passage 2 (20,000 / $cm^2$) created through CoIV/HD technique, were seeded on 1 mg / ml FN in 0.01% gelatin coated 6- and 12-well plates containing CEM. Once cells reached confluency, cardiomyogenic differentiation medium-2 (CDM-2) (Appendix 1) containing 5-Aza (5 µM) was added to each dish (2ml/well of a 6-well plate; 1ml/well of 12-well plate). On each of the next two days 20µl/ml of 5-Aza (5 µM) was added directly to the wells. On day-4, the medium was changed for CDM-2 only without 5-Aza and refreshed every 2-3 day for 7 days. On day-7 cells were washed with PBS and replaced with one of the following media:

1. **WY-14643 (PPARα agonist 1):** CDM-2 containing 1 ng/ml TGF-β (Peptotech, UK) and 0.1 mM AA (Sigma, UK) plus 100 µM WY-14643 (Sigma, UK).

2. **CP-775146 (PPARα agonist 2):** CDM-2 containing 1 ng/ml TGF-β (Peptotech, UK) and 0.1 mM AA (Sigma, UK) plus 10 µM CP-775146 (Sigma, UK).

3. **Sodium Dichloroacetate:** CDM-2 containing 1 ng/ml TGF-β (Peptotech, UK) and 0.1 mM AA (Sigma, UK) plus 100 µM sodium dichloroacetate (Sigma, UK).

4. **Sodium Butyrate:** CDM-2 containing 1 ng/ml TGF-β (Peptotech, UK) and 0.1 mM AA (Sigma, UK) plus 10 mM sodium butyrate (Sigma, UK).

5. **4-compounds:** CDM-2 containing 1 ng/ml TGF-β (Peptotech, UK) and 0.1 mM AA (Sigma, UK) plus 100 µM WY-14643 (Sigma, UK), 10 µM CP-775146 (Sigma, UK), 100 µM sodium dichloroacetate (Sigma, UK), and 10 mM sodium butyrate (Sigma, UK).

6. **Baseline (control 1):** P2-CDCs only without further treatment.

7. **5-Aza+TGFβ (control 2):** P2-CDCs treated with CDM-2 containing 1 ng/ml TGF-β (Peptotech, UK) and 0.1 mM AA (Sigma, UK) with initial treatment of 5-Aza.

8. **TGFβ (control 3):** P2-CDCs treated with CDM-2 containing 1 ng/ml TGF-β (Peptotech, UK) and 0.1 mM AA (Sigma, UK) from day-1 to day-30 without initial treatment with 5-Aza.

From day-7 forward the medium was refreshed every 2-3 days for the following 23 days.

## 2.7 Real-Time Quantitative Reverse-Transcription Polymerase chain reaction (qRT-PCR)

Quantitative real-time reverse transcriptase PCR (qRT-PCR) was used in this study.

### 2.7.1 Primer design and optimization

Primer pairs for chapter 3 were designed and tested by Tan[223]. Primer pairs for chapter 4 and 5 were designed based on interpretation of GeneBank or Ensemble Genome Browser, and Integrated DNA Technology (IDT) (please refer to Appendix 3 for primer sequence). Primer specificity was enhanced by designing a primer pair that flanked the exon-exon border of the gene of interest. This can avoid the primers amplifying genomic DNA that may be contained in samples. Primer specificity was confirmed by BLASTing the primer sequence against genomic databases available at NCBI. No significant homology sequence should be found, to ensure gene specific amplification rather than amplification of several transcripts with one primer pair.

### 2.7.2 Primer efficiency test

For primer efficiency test, a series of 2-fold dilutions of cDNA in DEPC treated water (Life Technologies) were prepared and amplified with the consistent concentration of primers using an AB 7500 fast RT-PCR machine. The threshold cycle (Ct) value was obtained after the PCR procedure and plotted against log cDNA dilution. Primer amplification efficiency was calculated as:

Where E is the amplification efficiency and m is the slope of the dilution curve.

$$E = \left( \frac{\exp - 1}{m - 1} \right) \times 100\%$$

### 2.7.3 RNA extraction and DNase treatment

Total RNA extraction was performed in two different ways. For single cell suspension of cultured CDCs, total RNA was extracted using the Qiagen® RNeasy Mini Kit (QIAGEN, UK) according to the manufacturer's instruction. In contrast, for differentiated CDCs that formed tissue-like structure, the total RNA was extracted using Qiagen® RNeasy Fibrous Tissue Kit (QIAGEN, UK), according to the manufacturer's instructions. DNase treatment was performed using RNase-Free DNase Set (QIAGEN, UK) to degrade any DNA present. The concentration and purity of RNA were determined by measuring the absorbance at A230, A260 and A280 using a NanoDrop® ND-1000 spectrophotometer (NanoDrop Technologies). A ratio of A260/A280 ~ 2.0 indicates that the RNA is protein-free and accepted as pure RNA. Also the ratio of a 260/230 ~ 2.0 indicated that the RNA was phenol and ethanol free.

### 2.7.4 Reverse transcription (complementary DNA synthesis)

The complementary DNA (cDNA) was synthesized from the RNA template using the AB high capacity transcriptase kit (Applied Biosystems). Every 1 µg RNA sample was reverse transcribed using 1 µl reverse transcriptase, 2 µl buffer, 0.8 µl dNTPs (10 mM each), 2 µl random primers, and topped up with RNase-free water to a total volume of 20 µl. The reaction mixture was incubated for 10 minutes at 25°C, 120 minutes at 37°C and 5 seconds at 85°C.

### 2.7.5 Quantitative real-time PCR

Real-time PCR amplification was performed using the Applied Biosystems StepOnePlus Real-Time PCR System (AB International, CA). The real-time PCR master mix was prepared by adding 5 µl AB Sybrgreen PCR master mix (AB International, CA), 0.5 µl forward primer, 0.5 µl reverse primer, 1.2 µl cDNA (15 ng) and 2.8 µl DEPC water. The total volume for each real-time PCR reaction was 10 µl. The PCR program was set up with an initial heat activation step at 95°C for 10 minutes, followed by 40 cycles of thermocycling were performed with a denaturation step at 95°C for 15 seconds; an annealing step at 60°C for 30 seconds; and an extension step at 72°C for 30 seconds.

Fluorescence was measured at the end of each extension step. After amplification, a melting curve was acquired by heating the product at 4°C/sec to 95°C, cooling it at 4°C/sec to 70°C, keeping it at 70°C for 20 seconds, and then slowly heating it at 4°C/sec to 95°C. Fluorescence was measured through the slow heating phase. Melting curves were used to determine the specificity of PCR products.

### 2.7.6 qRT-PCR Data Analysis

Various housekeeping genes were validated to ensure that the different groups had the similar level of gene expression. Relative quantification of target gene expression, which normalized to the geometric mean of the housekeeping genes β-Actin (Actb) and β-2 microglobulin (β2M) and one calibrator (the control sample), was performed using comparative Ct method (the $2^{-\Delta\Delta Ct}$ method).

## 2.8 Flow Cytometry

Treated or non-treated CDCs were used to obtain a single cell suspension. Cells were washed with PBS, trypsinized using 0.05% trypsin at 37°C for 4-5 minutes, washed with PBS, fixed with 4% paraformaldehyde (PFA) for 10 minutes at room temperature, washed with PBS, and $3 \times 10^5$ - $5 \times 10^5$ cells per sample were used for flow cytometry analysis. Unless otherwise stated, all samples were kept on ice all the time and used fluorescence-activated cell sorting (FACS) buffer (DPBS with 0.5% bovine serum albumin (BSA)) at all washing steps.

### 2.8.1 Antibody incubation, acquisition, and analysis

Cells were incubated with blocking solution (2% FBS + 2% BSA) for 30 mins to 1 hour at room temperature or 4°C overnight. Samples were then incubated with the diluted primary antibody (Appendix 4) in blocking solution for 1 hour at room temperature or 4°C for overnight. Then, samples were washed to remove the excess antibody, and incubated with the diluted secondary antibody (Appendix 4) in blocking solution for 30 minutes at room temperature and washed again in FACS buffer. After washing and centrifugation, the supernatant was discarded, and the cell pellets were re-

suspended in 300 µl FACS buffer. Unstained cells and cells stained with secondary antibody alone were used for negative thresholds. Cells were analysed using FACSCalibur flow cytometer (BD Biosciences, San Jose, CA) and each acquisition included 1 x $10^4$ events. The data were analysed using Flowing Software 2.5.1. To quantify the number of positive cells for the different markers, the threshold of the positive population for all data analysis was set at 99.9 % of the negative control cell population, as confirmed by Mr. Nigel Rust, Flow Cytometry Facility Manager, Dunn School of Pathology, University of Oxford.

## 2.9 Immunocytochemistry

### 2.9.1 Culture of CDCs on cover slips

Pre-coated 24-well plates, containing cover slips, with either 1 mg/ml FN or 10 µg/ml ColIV were seeded with P2-CDCs (3 x $10^3$/well) and cultured as control or treated with specific differentiation protocols.

### 2.9.2 Mitochondria staining

To label mitochondria, cells were stained with MitoTracker® Red CMXRos reagent (Cat. No. M7512, 5 µg / vial). Control or treated cells cultured on cover slips were washed with PBS, incubated with MitoTracker reagent (100 nM) for 20 mins at 37ºC, washed with PBS twice, fixed with PFA, stained with DAPI and visualized by confocal microscope imaging. These cell-permeant mitochondrion-selective probes contain a mildly thiol-reactive chloromethyl moiety for labelling mitochondria. The reduced version of these probes does not fluoresce until they enter an actively respiring cell, where they are oxidized to MitoTracker Red CMXRos and then sequestered in the mitochondria where it can react with thiols on proteins and peptides to form aldehyde-fixable conjugates. MitoTracker Red CMXRos appears to preferentially accumulate in mitochondria based on mitochondrial membrane potential ($\Delta\psi m$). The fluorescence will be retained in the mitochondria during cell fixation and permeabilization. The visible light absorption maximum of MitoTracker® Red CMXRos is 579 nm, and the emission maximum occurs at 599 nm.

### 2.9.3 Cell Fixation, permeabilization and blocking

The medium was aspirated and cells washed with sterile DPBS for three times. Cells were fixed by adding cold 4% PFA for 10 minutes, and then washed with washing solution (0.1% Tween 20 in PBS) three times for 5 minutes on a shaking table. For staining the intracellular markers, the fixed cells were permeabilized with PBS containing 0.1% Tween 20 and 0.1% Triton-X100 for 10 minutes at room temperature, then washed with washing solution (0.1% Tween 20 in PBS) three times for 5 minutes on a shaking table. Then cells were incubated with blocking solution (10% donkey serum in 0.1% PBS-tween) at $4^0$C for overnight.

### 2.9.4 Primary antibody incubation, secondary antibody labelling, DAPI staining and mounting

Primary antibodies were diluted in blocking solution according to the dilution factors (Appendix 5). The slides were taken out of the wells, placed on parafilm, covered with diluted primary antibody solution (~150 µl/slide) and incubated at 4˚C overnight in a humidified chamber. The cells were washed gently with washing solution (0.1% Tween 20 in PBS), three times for 5 minutes. An appropriate secondary antibody solution (Appendix 5) was added on top of each slide and incubated at room temperature for an hour. Nuclei were stained by covering each slide with 20 mg/ml DAPI solution for 5 minutes at room temperature and protected from light. Cover slips were mounted on top of a drop of Vectashield mounting medium (Vector Laboratories, UK).

### 2.9.5 Confocal Microscopy

All immune-labelled samples were scanned using an Inverted Olympus FV1000 confocal system. The laser power was kept to a minimum, and the image contrast was optimized by adjusting the gain. The pinhole was set to ~1 to minimize background signal. Scanning was performed in 4-bit multi-track scan mode, and a 512 x 512-pixel image was generated. Type of lasers and filters used are listed in (Appendix 6) and all images were processed using Olympus Viewer software.

## 2.10 Western Blotting

Whole heart and cell lysates were used in this study. A general description of the technique is outlined below, with variation for the specific proteins supplied in Appendix 1.

### 2.10.1 Tissue lysate preparation

Frozen clamped hearts were crushed using a pestle, mortar, and liquid nitrogen. Approximately 30 mg of powdered frozen tissue was added to 300 µl of lysis buffer (Appendix 7) and homogenized using a Polytron homogenizer for 30 seconds. The lysates were boiled at 95°C for 5 minutes and centrifuged at 7267g for 5 min at 4°C; the supernatant was saved. An aliquot of each sample was removed for determination of protein concentration (BCA protein assay kit, Perbio, UK). To the remaining supernatant, 5% β-mercaptoethanol (v/v) was added, followed by boiling for 5 min and storage at -80°C.

### 2.10.2 Cell lysate preparation

Control and treated P2-CDCs were washed twice with PBS. Approximately 17µl/1cm$^2$ lysis buffer (Appendix 7) was added to cell culturing dishes and cells were scraped from wells into 1.5 ml Eppendorf and immediately frozen in liquid nitrogen. Cells in lysis buffer were homogenised, boiled at 95°C for 5 minutes, centrifuged at 7267g for 5 min at 4°C, and the supernatant was saved. An aliquot of each sample was removed for determination of protein concentration (BCA protein assay kit, Perbio, UK). To the remaining supernatant, 5% β-mercaptoethanol (v/v) was added, followed by boiling for 5 min and storage at -80°C.

### 2.10.3 Protein Assay

Known concentrations of bovine serum albumin (BSA) protein standards were prepared and compared with a dilution of 5 µl tissue or cell lysates in 95 µl ddH2O. Standards and samples were put onto a 96 multiwell plate (25 µl/well) in duplicate along with 200 µl of working solutions (BCA

protein assay solutions, Thermo Scientific) before incubation for 30 minutes at 37°C. The absorbance at 550 nm was read in a plate reader and then plotted against protein concentration for the standard.

### 2.10.4 Polyacrylamide gel electrophoresis and protein transfer

Equal amounts of protein (20-40 µg) were diluted in Laemmli loading buffer (Appendix 7) and loaded onto 12.5% polyacrylamide gels. Gels were run at 120 V for approximately 2 hours. All samples were run in duplicate with Rainbow marker (Fermentas) loaded into the first lane. A piece of Immobilon-P membrane (Millipore, UK) and two pieces of extra thick chromatography paper (BioRad, UK) were cut to the same size of the gel. These were soaked with the gel for 30 min in sodium dodecyl sulphate (SDS) transfer buffer (Appendix 7), layered onto the semi-dry transfer apparatus (BioRad, UK) and transferred at 0.07 A per gel for 1 hour. The membranes were stained with Ponceau S, a sodium salt of a diazo dye of a light red colour (Sigma, UK), to determine successful protein transfer and even protein loading. Blots were washed in TBS-Tween (Appendix 7) and blocked in 5% (w/v) dried milk in TBS-Tween (25 ml per blot) for at least 1 hour at room temperature.

### 2.10.5 Immunoblotting detection and band quantification

The membrane was washed for 1 hour in TBS-Tween, with the solution changed every 15 minutes. The specific primary antibody (Appendix 8) was diluted in 5% (w/v) dried milk in TBS-Tween (12 ml per blot), and incubated on the membrane at 4°C overnight. The membranes were then washed for 2 hours in TBS-Tween, with the solution changed every 15 minutes. The appropriate horseradish peroxidase-conjugated secondary antibody (Appendix 8) was diluted in 5% (w/v) dried milk in TBS-Tween (12 ml per blot), and incubated on the membrane for 1 hour at room temperature. Membranes were washed for a further hour in TBS-Tween, with the solution changed every 15 minutes. The membrane was covered in enhanced chemiluminescence (ECL) detection solution (Amersham, UK) and sandwiched between sheets of acetate. Membranes were exposed to X-ray film and developed using a Compact X4 automatic X-ray film processor (X-ograph Imaging system, UK). Protein bands were quantified using Un-Scan-It, Version 6.1 (Silk Scientific, USA).

## 2.11 Determination of Lactate Efflux

The lactate level was determined using ABX Pentra 400 Chemistry Analyser (Horiba Ltd. USA), an automated analyser for in vitro diagnostic of a wide range of chemical compounds. To run this assay, cell culture medium was collected after the experiment and ran through ABX Pentra with lactate reagent (A11A01721, Horiba Ltd.). This reagent bound to the lactate molecules present in the medium and fluoresced. The analyser detected the signal and analysed the concentration of lactate.

## 2.12 Determination of Glycolytic flux

Glycolysis was measured as the production of $^{3}H_2O$ from 5-$^{3}$H-glucose, which occurs during the step catalysed by enolase. P2-CDCs (20,000 / cm$^2$) were seeded on pre-coated 6-well plates coated with either FN or ColIV, as appropriate, and containing CEM. After overnight incubation where the control cells were attached or at the end of differentiation procedure, cells were given 10 ml of control or cardiomyogenic differentiation medium, which contained around 25 mM glucose, and a trace of D[5-$^{3}$H]-glucose (1.48 MBq/mmol) (Amersham, Bucks, UK). The glycolytic rates were determined by collecting 0.6 ml of aliquots of culture medium at different intervals including 0-, 1-, 4-, 6-, 8-, 24-, 48-, and 72-hours. Glycolytic rates were determined in culture medium aliquots, as the conversion of $^{3}$H-glucose to $^{3}H_2O$. $^{3}H_2O$ was separated from $^{3}$H-glucose using a Dowex anion exchange column (Sigma, UK) (Figure 2.1). For each aliquot sample, glycolytic rates were calculated using the equations:

$$\text{Total glycolytic flux per sample } (\mu\text{mol. Sample } well^{-1}/\text{min}) = \frac{[\![Sample\ cpm - Sample\ time\ 0\ cpm]\!] \times CEM\ volume\ (ml)}{\frac{[Specific\ Activity.ml^{-1} - Sample\ time\ 0\ cpm]}{Glucose\ (mM)}} / \text{Time (min)}$$

$$\text{Total glycolytic flux per mg protein concentration } (\mu\text{mol. mgpc}^{-1}/\text{min}) = \frac{\text{Total glycolytic flux } (\mu\text{mol.Sample well}^{-1})}{\text{Protein concentration (mg)}}$$

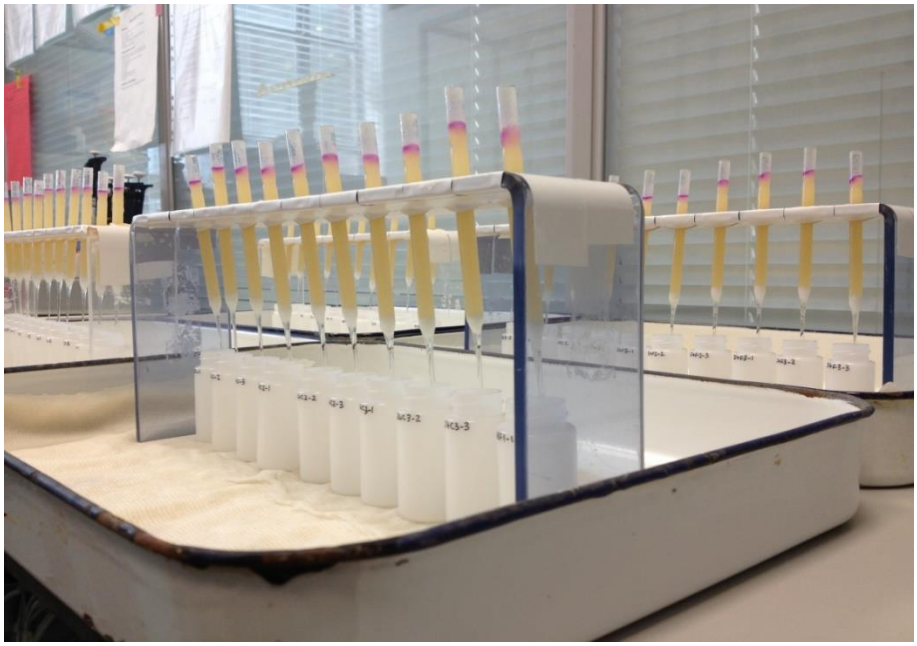


**Figure 2.1 Dowex resin ion exchange glass columns.** Sample medium that was taken from control and 5-Aza treated P2-CDCs that have had supplied with [5-$^{3}$H]glucose, were run through the prepared dowex resin ion exchange glass columns, where the [5-$^{3}$H]glucose is separated from $^{3}H_2O$, a product from enolase step, during glycolysis pathway.

## 2.13 Multiwell $^{14}CO_2$-capture assay for evaluation of substrate oxidation rate of cells in culture

Based on Collins method[224] with some modification, control and treated CDCs in a 6-well plate were incubated for 4 hours in the presence of a single radiolabelled substrate (with addition of unlabelled substrates where indicated): 10 mM glucose-containing 21 MBq/mmol D-U-$^{14}$C-glucose; 5 mM pyruvate-containing 0.35 MBq/mmol 1-$^{14}$C-pyruvate; 10 mM acetoacetate-containing 0.185 MBq/mmol 3-$^{14}$C-acetoacetate; 2 mM glutamine-containing 1.2 MBq/mmol U-$^{14}$C-glutamine; and 2 mM palmitate-containing 10.27 Mβq/mmol 1-$^{14}$C-palmitate in DMEM (containing no pyruvate, glucose or glutamine) in a total volume of 1 ml/well. Evolved $^{14}CO_2$ was trapped and measured by the method of Collins et al. 1998[224] (Figure 2.2A), except that, after addition of perchloric acid to the wells, plates were gently agitated for 60 minutes to release dissolved $^{14}CO_2$. The radioactivity of filter papers containing trapped $^{14}CO_2$ were measured using a scintillation counter.

## 2.13.1 Experimental procedure of $^{14}CO_2$-capture assay

Cultured cells were washed with substrate-free DMEM (Gibco, A14430-01) containing 10 mM HEPES. Then, 1 ml of substrate-free DMEM base supplemented with 4% bovine serum albumin BSA, Sigma) and one of the substrates doped with a trace of the corresponding $^{14}C$- substrate ($^{14}C$-Glucose, $^{14}C$-Glutamine, $^{14}C$-Pyruvate, $^{14}C$-Palmitate, and $^{14}C$-Acetoacetate) was added per well, except for control wells to which the media containing the un-doped substrate was added. A gasket (Hobbycraft Glue Gun Pad, UK), the size of the 6-well plate, with a 5 mm hole, created using a standard hole-punch at sites corresponding to the centre of each well, was placed over the culture plate, to allow free passage of $^{14}CO_2$ without allowing significant $^{14}CO_2$ leakage (Figure 2.2B). Then, a prepared 6-well plate containing filter paper soaked with 100 µl 40% KOH, with a 5 mm hole in the centre of each well and the bottom of the plate sealed with an adhesive sheet, was inverted and placed over the rubber gasket and culture plate (Figure 2.2B). Therefore, each well of the culture plate was aligned with a hole in the rubber gasket and a KOH-saturated filter, thus, forming a small $^{14}CO_2$-capture chamber. The assembly was placed in an apparatus (designed with the help of departmental workshop), which applied weight over the assembly in a firm position, assuring the gasket seal was airtight, preventing $^{14}CO_2$ leakage (Figure 2.2C). The details of each substrate and its concentration have been provided at each figure legend in the result sections. For each filtered sample, the oxidation rate was calculated using below equation:

$$\text{Total Substrate Oxidation}\left(\mu\text{Mol/Min/mg}\right) = \frac{\left(\frac{\mu\text{M Substrate in Standard}}{\text{Standard DPM1}}\right) \times \left(\frac{\text{Sample DPM1} - \textit{Blank DPM}}{\text{Total incubation time (minutes)}}\right)}{\text{Protein Concentration (mg/ml)}}$$

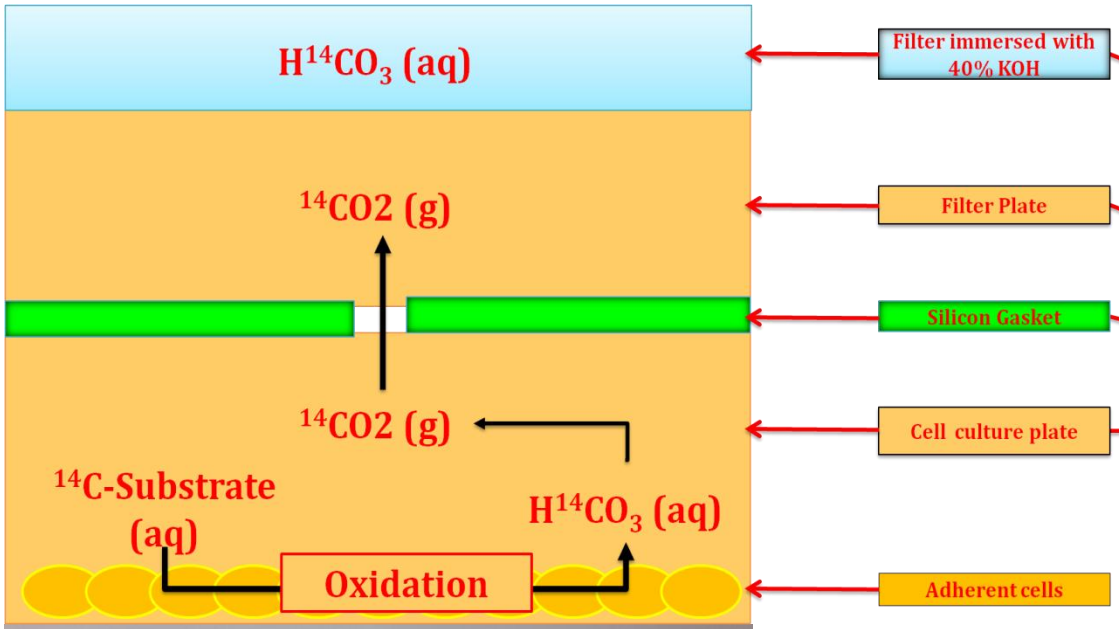
## 2.14 Calculation of ATP yield

ATP-yields were calculated from the following values, assuming full oxidation of each substrate: glycolysis, 2 mol ATP/mol glucose; glucose oxidation, 31 mol ATP/mol glucose; pyruvate oxidation, 12.5 mol ATP/mol pyruvate; acetoacetate oxidation, 20 mol ATP/mol acetoacetate; glutamine oxidation, 20 mol ATP/mol glutamine; palmitate oxidation, 106 mol ATP/mol palmitate.

## 2.15 Statistics

Data are presented as mean ± SEM. Data were subjected to ANOVA (GraphPad Prism v6.o.1) and if a significant difference ($p<0.05$) was detected, further analysis by t-test (for comparison of each group with a single control) was performed.

**A.**




**B.**



**C.**

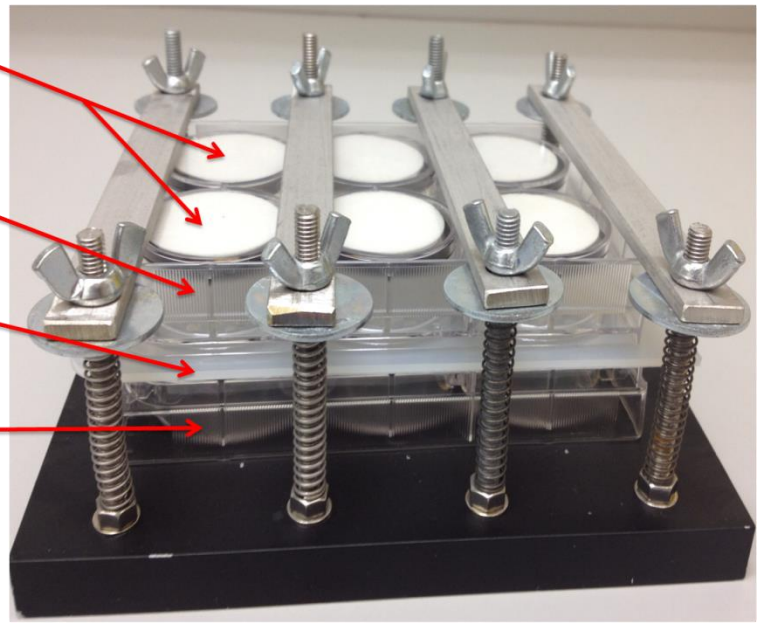


**Figure 2.2. The substrate oxidation appliance**. **(A)** The principles of $^{14}CO_2$ trapping system. **(B)** Different parts of $^{14}CO_2$ trapping appliance including filter papers (**I**), soaked with 40% KOH, placed in filter plate (**II**) and supported with black O-rings; silicon gasket (**III**), which placed at the top of cell culture plate (**IV**), containing adherent cells (**V**). **(C)** The appliance after assembly of different parts in **(B)**.

# Chapter 3

## Comparison of Regenerative Potential of Different Cardiosphere-Derived Cell Lines from Rat Heart

## 3.1 Abstract

Preliminary work done by Dr. Jun Jie Tan described two approaches to the isolation and rapid expansion of cardiac stem cells (CSCs) in a short time period without compromising the quality of the cells in terms of stemness and function[222]. The first technique was cell expansion on fibronectin (FN) with cardiosphere (CSp) formation on poly-D-lysine (PDL). The second was cell expansion on collagen IV (ColIV) with CSp formation in hanging drops (HD), which resulted in increased c-kit$^+$ cells (up to 11%) compared to culture on PDL (3%). The work in this chapter was to isolate and expand CSCs using both approaches, characterize both cell lines, and assess whether or not the changes in the culture protocol affected the differentiation potential of CSCs towards functional cardiomyocytes. Quantification of cell isolation and proliferation assay revealed a higher cell number and increased proliferation of passage 2 CSp-derived cells (P2-CDCs) cultured on ColIV relative to FN baseline. Also, flow cytometry analysis showed P2-CDCs cultured on FN or ColIV expressed both the stemness markers such as Oct4, Nanog, CD90 and c-kit; and cardiac specific proteins including Nkx2.5, cTnnT2, cMHC, and Titin; and endothelial cell marker vWF. This suggested that a population of P2-CDCs were already committed towards cardiac lineage phenotype. For cardiomyocyte differentiation, several different conditions were tested using confluent or non-confluent cell densities and treatment with 5-Azacytidine (5-Aza) or dimethyl sulfoxide (DMSO). The qRT-PCR analysis confirmed that P2-CDCs cultured on FN with higher cell density, and treated with 5-Aza, were able to acquire a cardiac phenotype, increasing gene expression of cardiac troponin-T2 (cTnnT2), and peroxisome proliferator-activated receptor alpha (PPARα), a major regulator of lipid metabolism, compared to the other conditions. Flow cytometry analysis and confocal microscopy supported this conclusion with increasing cardiac-specific proteins such as cTnnT2, MHC, and Titin.

## 3.2 Introduction

It has been 12 years since the discovery of resident CSCs[225] that questioned the dogma of the heart being considered as a terminally differentiated organ with a very low intrinsic renewal capacity[129]. Although the adult heart contains stem cells that are able to partially repair the heart following a MI or throughout the progression of heart failure[100], endogenous CSCs are limited in quantity[123] and may decrease and lose their functional capacity with increased age[156, 157]. Thus, it is essential to isolate and expand the CSCs *in vitro t*o generate sufficient viable progenitor cells for transplantation.

Shortly after the recognition of cardiac stem cells in the adult heart[100], different approaches were used to isolate CSCs from heart tissue. First CSCs were isolated from adult heart, based on their ability to efflux Hoechst dye, generating a putative progenitor side population (SP) cell with stem-like cell activity[113]. In addition, CSCs have been isolated based on a specific single cell marker like c-kit[100] or Sca-1[102]. Although these methods can generate a homogenous cell population, the quantity of cells obtained are at a fairly low level, with SP cells being only 1% of the total cell number[113], one c-kit$^{+}$ cell in every 10,000 cardiomyocytes and 1% Sca1 (of the total cell number)[123]. Therefore, they required substantial *in vitro* expansion to generate sufficient cell numbers for therapy[100, 113].

Messina and co-workers developed a method to isolate and culture cardiac stem cells from mouse and human heart tissue explants and expand them as CSps[106]. These CSps were clonogenic and expressed stem and endothelial progenitor cell antigens/markers (c-kit, Sca-1, and CD34)[106]. The CSps were expanded to obtain sufficient CDCs for transplantation[152]. Both CSps and CDCs from heart tissue explant cultured *in vitro*, were able to differentiate into myocardial cells when injected into the infarcted mouse heart *in vivo*[106, 152].

Direct comparison of different stem cell types/subpopulations have shown that CDCs have a balanced profile of paracrine factor production and provide the most functional benefit in experimental myocardial infarction suggesting CDCs are a promising candidate for cell therapy[155]. To allow early administration of CDCs to patients, isolation and expansion of CDCs must be performed in the shortest time possible. In addition, the therapeutic effect of CDCs may be limited

by the low level of cardiac stem cell numbers (~ 3% c-kit) when using the currently published protocol for CSC isolation and expansion.

To overcome these two hurdles, preliminary studies from our laboratory by Dr. JJ Tan confirmed that creating CSps in the form of HDs generated a higher level of c-kit positive cells (~9%) relative to the current protocol (~3%), of CSps formation on PDL coated plates[106, 152]. In addition, instead of using FN substrate to coat plates, using ColIV coated plates, was found to enhance explant-derived cells (EDCs) migration and CDC proliferation as well as generating even more c-kit$^+$ cells (~11%)[226].

The aims of this study were to:

I. Isolate EDCs and expand CDCs from adult rat heart using both the published protocol and optimised protocol from our laboratory[106, 152, 227].

II. Characterize CDCs created by both protocols.

III. Induce cardiomyogenic differentiation of CDCs created by both protocols.

IV. Characterize the expression profile of induced cardiomyogenic differentiated CDCs created by current and optimised protocols.

## 3.3. Methods

### 3.3.1 Overview of designed study

The study design described in this chapter is illustrated in a schematic flow diagram (Figure 3.1), which described specific experimental methodologies.

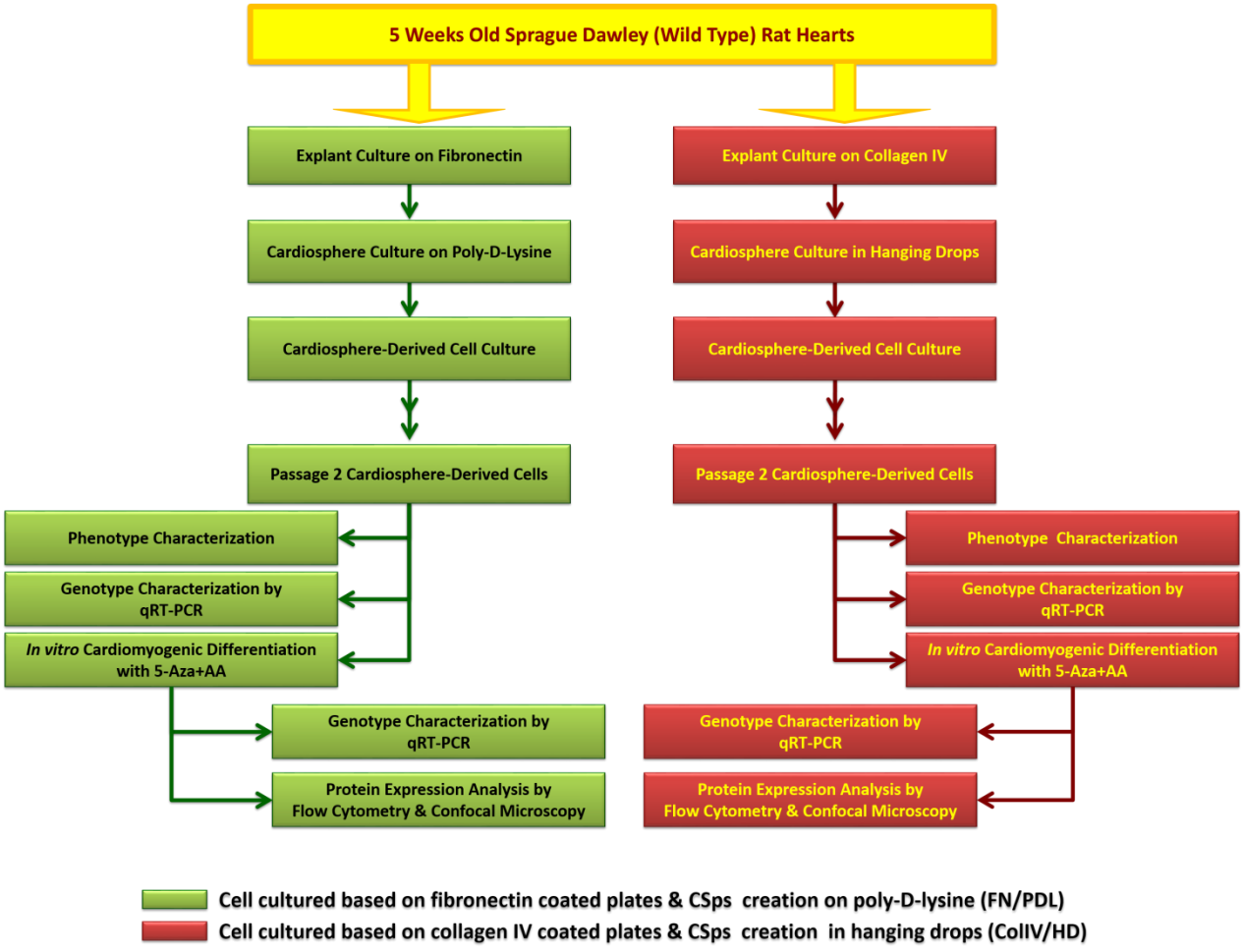



***Figure 3.1 Flow diagram showing an overview of study design to compare the two different types of cardiosphere-derived cells (CDCs) created in two distinct protocols.***

### 3.3.2 Isolation, and expansion of CS-derived cells

Methods are described in Chapter 2. Briefly, five weeks old SD rat heart explanted on either FN or ColIV coated dishes containing CEM, EDCs were harvested, resuspended in CGM, and plated into pre-coated plates with PDL or as HDs respectively. Then CSps were mechanically harvested by pipetting and seeded on FN or ColIV coated dishes and cultured until passage 2. All experiments in this chapter used CDCs at passage 2 (P2) unless otherwise stated.

### 3.3.3 Quantification of CDC Yield

Cardiac stem/progenitor cells at EDCs, P1-CDCs, and P2-CDCs from both FN/PDL and ColIV/HD at three different harvests were enzymatically digested, counted and normalized to the mg tissue explants.

### 3.3.4 Quantification of P2-CDC proliferation

P2-CDCs were seeded at different densities (250-20,000 cells) on pre-coated micro-plates (96-well plates) with either FN or ColIV. Cells were cultured and frozen at -80°C on day-1, -2, -3, -5, and -7. Proliferation level was assessed using CyQUANT® Cell Proliferation Assay Kit plus RNase treatment. Fluorescence was measured directly using a microplate reader. In order to calibrate the assay for the utilisation of the same microplate reader at different times, a standard curve for DNA content was prepared using bacteriophage λ DNA standard.

### 3.3.5 Real-time quantitative RT-PCR

Real-time quantitative reverse transcriptase polymerase chain reaction (qRT-PCR) was used to determine the expression of the cardiac stem cell marker, c-kit; mesenchymal stem cell marker, CD90; cardiac-specific protein, cTnnT2; and metabolic, Glut1 and PPARα, genes in control and treated P2-CDCs. All qRT-PCR data were normalized to Actb and B2M as the reference genes.

### 3.3.6 Flow cytometry analysis

Treated or non-treated CDCs were used to obtain a single cell suspension. Cells were washed with PBS, trypsinized using 0.05% trypsin at 37°C for 4-5 minutes, washed with PBS, fixed with 4% PFA (10 minutes at room temperature), washed with PBS, and $3 \times 10^5$ - $5 \times 10^5$ cells per sample were used for flow cytometry analysis. Unless otherwise stated, all samples were kept on ice all the time and used FACS buffer (DPBS with 0.5% BSA) at all washing steps.

### 3.3.7 Confocal imaging

Cultured and differentiated CDCs on cover slips were fixed with 4% PFA, immuno-labelled with primary antibodies, then secondary antibodies for cardiac-specific markers (cTnnT2, MHC, Titin) and scanned using an Inverted Olympus FV1000 Confocal system.

### 3.3.8 Cardiomyogenic differentiation of cardiosphere-derived cells

Cardiomyogenic differentiation of CSCs was performed by culturing P2-CDCs on FN or ColIV coated plates containing cardiomyogenic differentiation medium-1 (CDM-1), treating with 5-Aza or DMSO for 3-days, followed by treating with ascorbic acid (AA) for a total 7 or 14 days (Figures 3.2 and 3.3).

### 3.3.9 Statistics

Data are presented as mean ± SEM. Data was subjected to ANOVA (GraphPad Prism v6.o.1) and if a significant difference ($p<0.05$) was detected, further analysis by t-test (for comparison of each group with a single control) was performed.

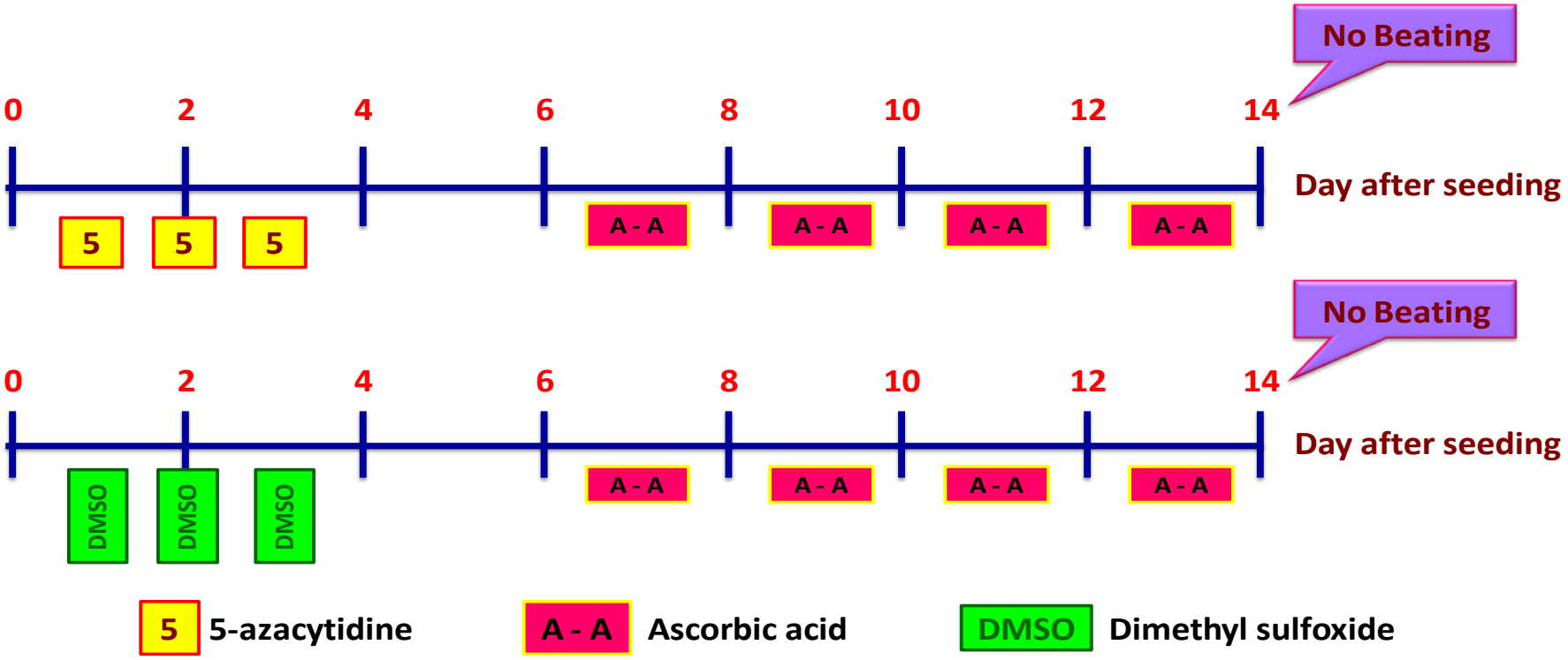



***Figure 3.2 Timeline of the differentiation procedure***. *The blue line indicates the number of days after plating cells. For the first three consecutive days 5 µM 5-Aza,* ***(A)*** *(yellow boxes), or 1 mM DMSO,* ***(B)*** *(green boxes), is added to the culture medium, CDM-1, for the three, followed by standard CDM-1 for further 3 days. From day seven forward until day-14, cells were supplied with CDM-1 containing 0.1 µM ascorbic acid (pink boxes), added every two days, and refreshed the medium every 2-3 days.*

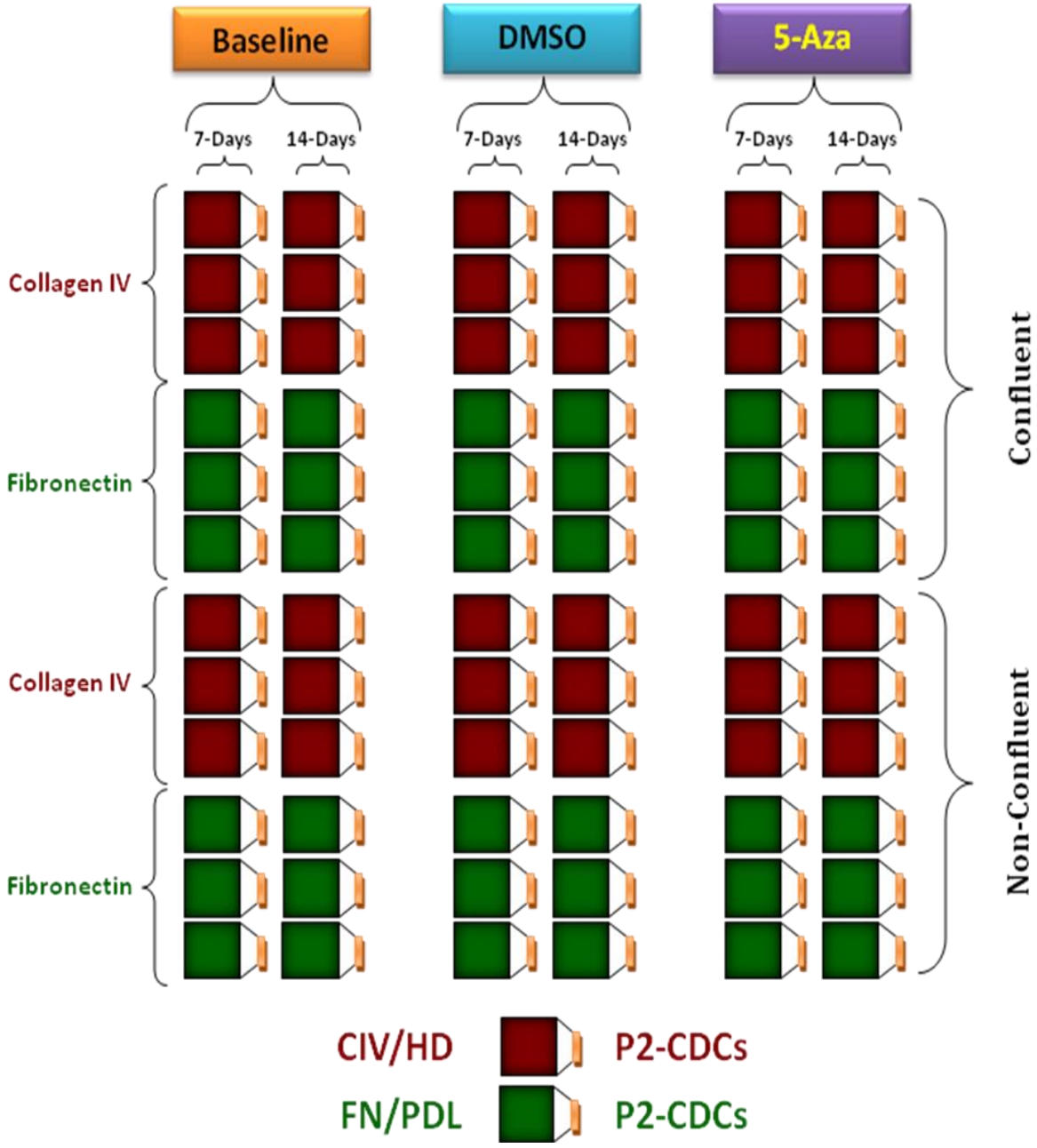



***Figure 3.3 Schematic diagram of cardiomyogenic differentiation of CDCs.*** *P2-CDCs from both FN/PDL and ColIV /HD were seeded on T75 flasks precoated with FN or ColIV respectively at low ($10^4$/10cm$^2$), and high ($10^5$/10cm$^2$) cell densities, treated with either 5µM 5-Aza or 1 mM DMSO, and cultured for either 7 or 14 days. Abbreviations: ColIV: Collagen IV, DMSO: Dimethyl sulfoxide, FN: Fibronectin, P2-CDCs: Passage 2-Cardiosphere-Derived Cells, 5-Aza: 5-Azacytidine, 7-D: 7 days, 14-D: 14 days.*

# 3.4 Results

## 3.4.1 Isolation and expansion of cardiosphere-derived cells

### 3.4.1.1 Explant-derived cells

The atria and apex of 5-weeks old SD rat hearts were explanted into either FN or ColIV coated dishes containing CEM (Appendix 1). Explants adhered well to the FN or ColIV and generated a layer of thin, flat stromal-like cells after 3-4 days. Round phase bright cells were observed growing out from the explants and migrating over the fibroblast cell layer after four days (Figure 3.4A & 3.5A). These cells are termed explant-derived cells (EDCs) and can be harvested up to 3 times with an interval of 9-14 days between each harvest. One rat heart (atrium and apex) can generate approximately 2 $x10^4$ and 4 x $10^4$ EDCs per mg tissue when cultured on FN and ColIV respectively (Figure 3.6).

### 3.4.1.2 Cardiosphere formation

Explant derived cells (EDCs) were allowed to grow in either PDL coated 24-well plates (Figures 3.4B) or as hanging drops (HD) (Figures 3.5B) in CGM (Appendix 1). Adherent cells on PDL and in HD gradually self-assembled into clusters, termed cardiospheres (CSps), (Figures 3.4C-D and 3.5C-D). CSps formed after three days of incubation on PDL (Figure 3.4E), but within 24 hr in hanging drops (Figure 3.5D). Approximately 400 CSps were obtained from each well of a 24-well plate (3626 ± 238 CSps/heart with an average size of 50-100 µm) and 1-2 CSps per HD (2346 ± 403 CSps/heart with an average size of 100-150 µm) after four days of incubation (Figures 3.4F & 3.5F).

### 3.4.1.3 Cardiosphere-Derived cells

The CSps from both treatments, PDL and HD, could easily be isolated by pipetting and expanded by culturing into a FN and CIV coated flask respectively containing CEM (Appendix 1). CDCs were formed after 3-4 days of incubation and reached 80-90% confluency within 5 to 7 days (Figures 3.4G & 3.5G). The cells were subsequently passaged in the ratio 1:2 for further expansion up to passage 2 (Figures 3.4H & 3.5H). At the end of passage 2 (P2) of three harvests, the total number of CDCs

produced in FN and ColIV based substrates were approximately $0.6 \pm 0.08 \times 10^5$ and $4.5 \pm 1.8 \times 10^5$ of CDCs per mg tissue respectively (Figure 3.6).

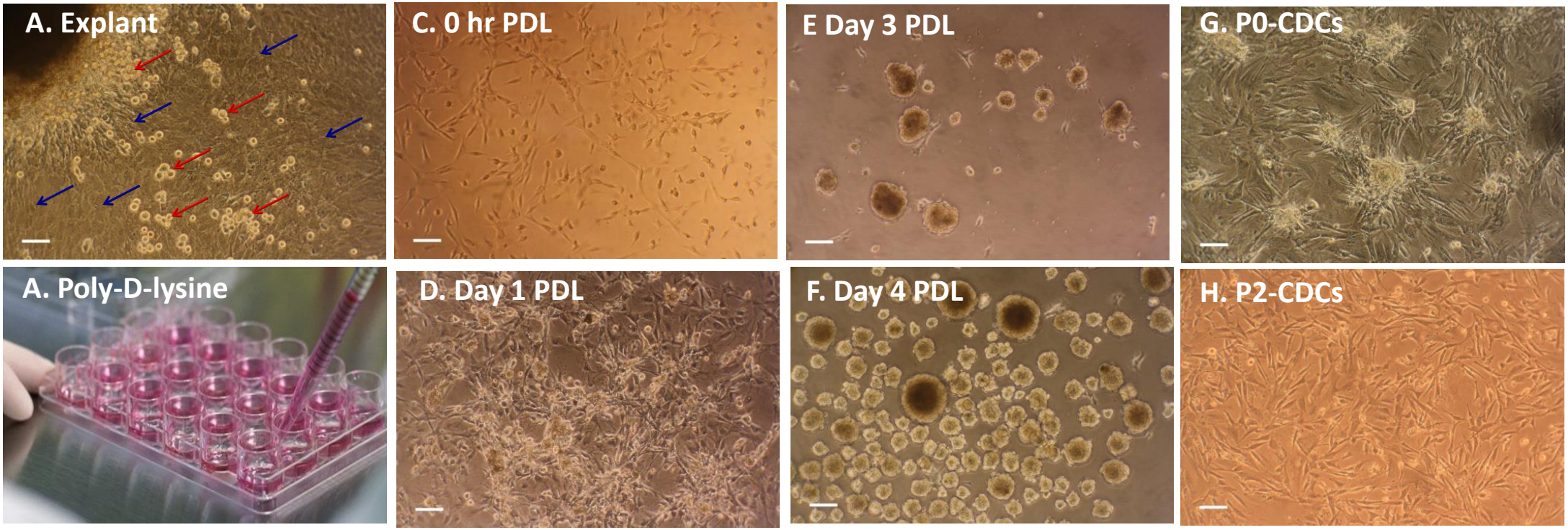



***Figure 3.4 Representative micrographs of cardiac stem cell isolation by explant culture on fibronectin and cardiosphere formation on poly-D-lysine. A.*** *Heart tissue was minced into pieces and explanted on fibronectin-coated Petri dishes with CEM. Phase bright cells (red arrows) on top of the stromal-like cells (blue arrows) were confluent by 9-14 days.* ***B.*** *EDCs were seeded on poly-D-lysine precoated 24-well plates with CGM and cultured for four days (**C-F**); C. Cardiospheres at 0-hr;* ***D.*** *24-hr;* ***E.*** *3-days; and* ***F.*** *4-days.* ***G.*** *&* ***H.*** *CDCs were obtained by culturing cardiospheres on fibronectin-coated flasks (G = P0-CDCs & H = P2-CDCs). Abbreviations: CDCs: Cardiosphere-Derived Cells; CEM: Complete Explant Medium; CGM: Cardiosphere Growth Medium; EDCs: Explant-Derived Cells; P0: passage zero; P2: passage two; PDL: Poly-D-Lysine. Scale bar 100 µm.*

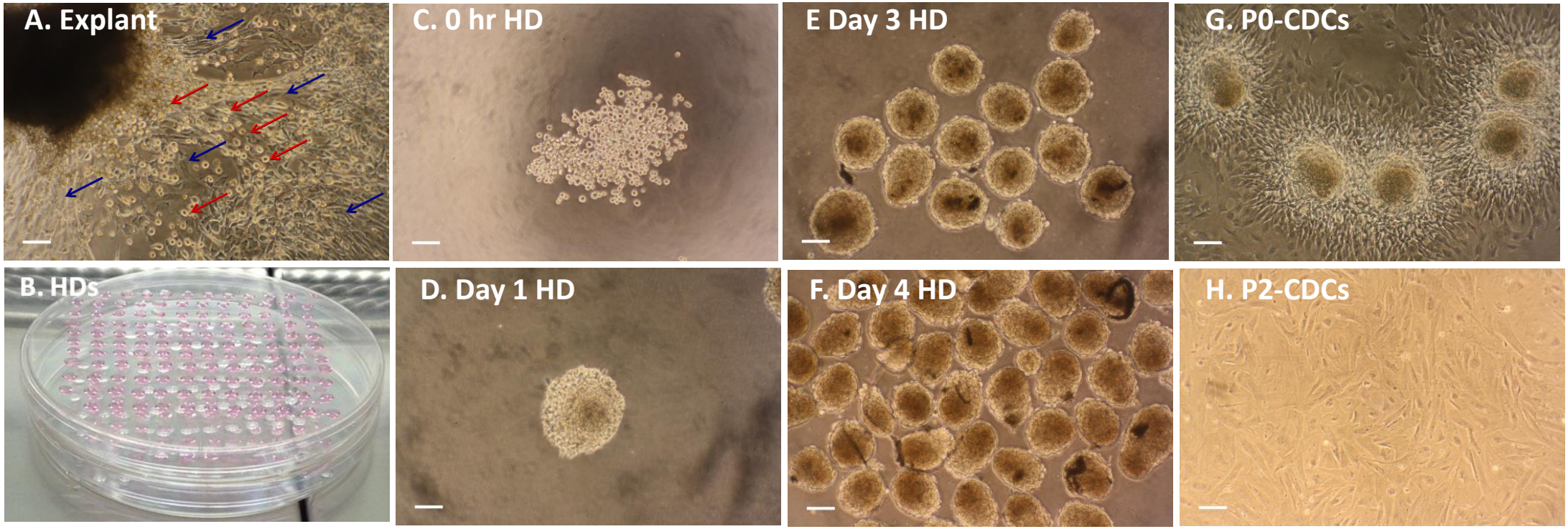



***Figure 3.5 Representative micrographs of cardiac stem cell isolation by explant culture on ColIV and cardiosphere formation in hanging drops. A.*** *Heart tissue was minced into pieces and explanted on ColIV-coated Petri dishes with CEM. Phase bright cells (red arrows) on top of the stromal-like cells (blue arrows) were confluent by 9-14 days.* ***B.*** *EDCs suspended in CGM were placed on bacterial dishes as hanging drops, cultured for 3-days (**C**-**E**), transferred into a new bacterial dishes with fresh CGM and cultured for one day,* ***C.*** *Cardiospheres at 0-hr;* ***D.*** *24-hr;* ***E.*** *3-days; and* ***F.*** *4-days.* ***G.*** *&* ***H.*** *CDCs were obtained by culturing cardiospheres on collagen IV-coated flasks (G = P0-CDCs & H = P2-CDCs). Abbreviations: CDCs: Cardiosphere-Derived Cells; CEM: Complete Explant Medium; CGM: Cardiosphere Growth Medium; EDCs: Explant-Derived Cells; P0: passage zero; P2: passage two; ColIV: Collagen IV. Scale bar 100 µm.*

## 3.4.2 Quantification of CSC isolation and expansion

In order to compare cell isolation and expansion between the CDCs created using the FN/PDL or ColIV/HD techniques, cells at each stage (EDCs, P1-CDCs, and P2-CDCs), from three harvests with three biological replicates were enzymatically digested and counted using a haemocytometer. The cell numbers were normalized to the weight of explanted tissue (Figure 3.6). In comparison to the FN/PDL, ColIV/HD culture technique yielded a significantly higher cell number at P2 ($4.5 \pm 1.8 \times 10^5$ vs. $0.6 \pm 0.08 \times 10^5$) per milligram tissue biopsies.

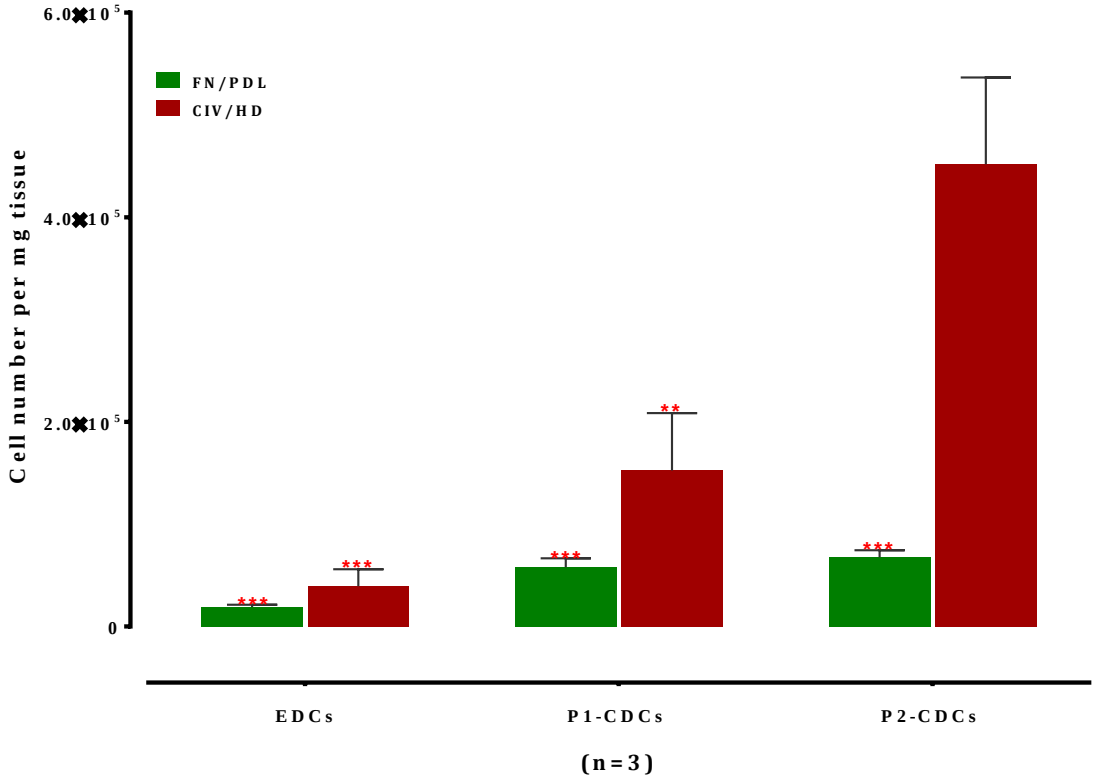



***Figure 3.6 Comparison of cell yield between the FN/PDL and ColIV/HD culture techniques.*** *Heart tissue specimens were weighed and cultured on either FN or ColIV. EDCs were harvested three times and expanded through CSp formation until passage 2. At each stage including EDCs, P1-CDC, and P2-CDC, cells were enzymatically digested and counted using a haemocytometer. The cell numbers were normalized to the weight of tissue biopsies that initially used to explant. Abbreviations: CDCs: Cardiosphere-Derived Cells; ColIV/HD: collagen IV/hanging drop; CSp: Cardiosphere; EDCs: Explant-Derived Cells; FN/PDL: fibronectin/Poly-D-lysine; P1: Passage one; P2: Passage two. Data are presented as mean ± SEM (n=3). ***P < 0.0004, **P < 0.003 vs. ColIV/HD P2-CDCs.*

### 3.4.3 Quantification of P2-CDC proliferation

The proliferation of CDCs at passage 2 created through FN/PDL (Figures 3.3) and ColIV/HD (Figures 3.4) techniques was assessed using the CyQUANT® Cell Proliferation Assay Kit (Figure 3.7). P2-CDCs created through ColIV/HD method had a significantly higher proliferation rate at day 5 (418 ± 57 *vs.* 159 ±31) and day-7 (592 ± 31 *vs.* 204 ± 42) in comparison to CDCs in FN/PDL technique with the p-value less than 0.0001 (Figure 3.7).

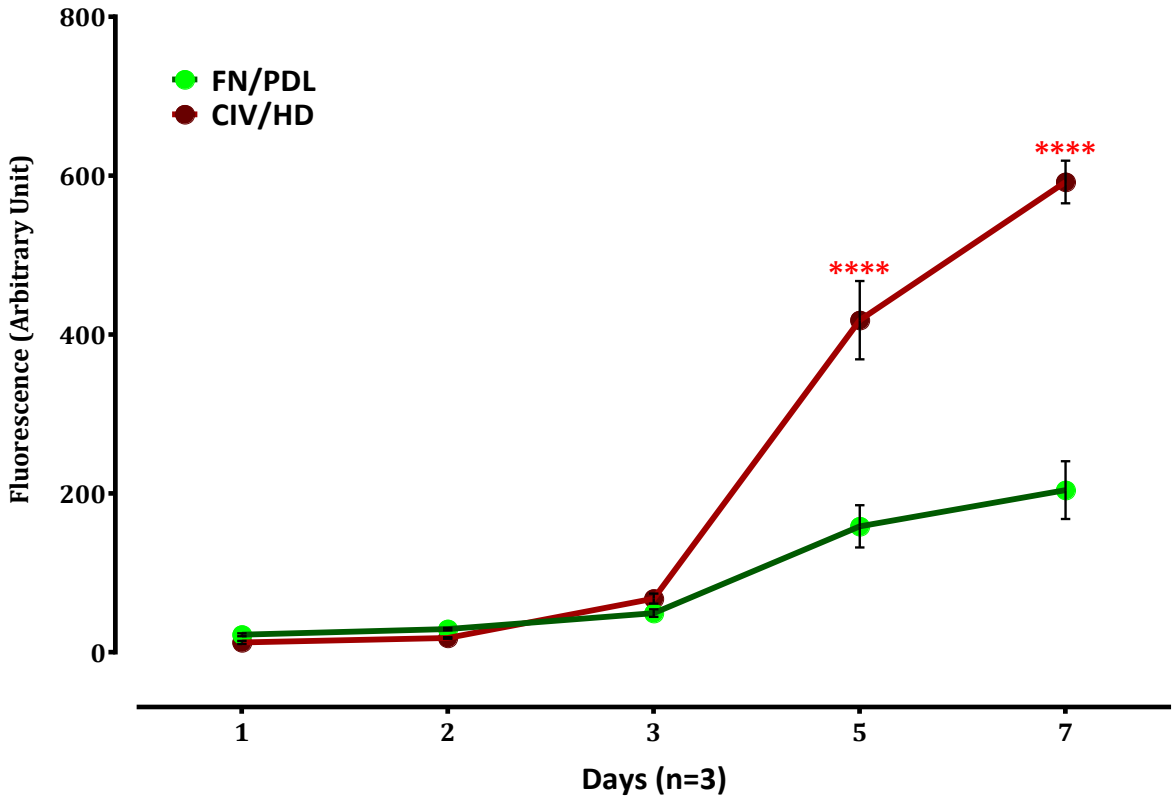



***Figure 3.7 Quantitation of CDCs using the CyQUANT® Cell Proliferation Assay Kit.*** *P2-CDCs were seeded (250 cells/well) on pre-coated microplates with either FN or ColIV. Cells were cultured at different intervals (day1, 2, 3, 5, and 7), then freeze at -80°C, treated with RNase, added CyQUANT, and measured fluorescence of DNA content using a microplate reader with excitation 485 ± 10 nm and emission detection at 530 ± 12.5 nm. DNA content was normalized to λDNA standard curve. Abbreviations: P2-CDCs: passage 2 Cardiosphere-Derived Cells; ColIV: collagen IV; FN: fibronectin. Data are presented as mean ± SEM (n=4).* **** *p< 0.0001 vs. FN.*

## 3.4.4 Phenotypic characterization of cardiosphere-derived cells

The phenotype of P2-CDC created through FN/PDL and ColIV/HD techniques was characterized using flow cytometry to identify and quantify the cell surface and intracellular markers.

### 3.4.4.1 Phenotype characterization of P2-CDCs using flow cytometry analysis

Flow cytometry analysis of P2-CDCs created through both FN/PDL and ColIV/HD techniques revealed that both cell types expressed stem cell marker, Oct4 (FN= 1.9 ± 0.3% *vs.* ColIV= 10.3 ± 4.5%; p = 0.01); Nanog (FN= 24 ± 1.2% *vs.* ColIV= 47 ± 7.4%; p = 0.0008); mesenchymal stem cell marker, and CD90, (FN= 43.5 ± 0.2% *vs.* ColIV= 23.9 ± 0.2%; p < 0.0001); (Figure 3.8). However, c-kit expression was detected (FN= 0.2 ± 0.01% *vs.* ColIV= 0.3 ± 0.01%; p < 0.0001) at a very low level (Figure 3.8). In addition, P2-CDCs created through both FN/PDL and ColIV/HD techniques expressed the early cardiac transcription factor, Nkx-2.5 (FN= 7.2 ± 0.3% *vs.* ColIV= 4.1 ± 0.8%, p = 0.01); and low levels of cardiac-specific proteins, cTnnT2 (FN= 5.4 ± 0.2% *vs.* ColIV= 2.2 ± 0.2%, p < 0.0001); cMHC (FN= 3.3 ± 0.3% *vs.* ColIV= 2.2 ± 0.1%, p = 0.0009 ); and Titin (FN= 1 ± 0.07% *vs.* ColIV= 0.4 ± 0.05%, p < 0.0001); and endothelial cell marker, von willebrand factor, vwf (FN= 3.5 ± 0.3% *vs.* ColIV= 1.5 ± 0.2%, p = 0.0001) (Figure 3.9).

In some cases, there was a clear shift in the fluorescence intensity peak that was not necessarily reflected in the quantification. For instance, in Oct4 and Nanog expression (Figure 3.8), there were a substantial number of cells with a fluorescence intensity that was higher than that of most, but not all, of the negative controls. These were not included within the quantification (as they fell below the gate set at 99.9% of negative control) but may have expressed a low level of Oct4 or Nanog. This is of particular relevance here, where there was a high signal in the negative control from non-specific binding or autofluorescence which may have masked a low level of expression of, for example, c-kit, titin and vwf (Figures 3.8 and 3.9). Non-specific binding differs from cell to cell population and may depend on cell physiology. For example, DNA contains Flavins, which are excited by the 488nm laser, the more open the structure of the DNA (i.e. Cells using the DNA for transcription) the more

they give autofluorescence, which broad spectrum emission. Therefore, when DNA condensed (i.e. in Lymphocytes) the less autofluorescence we see.

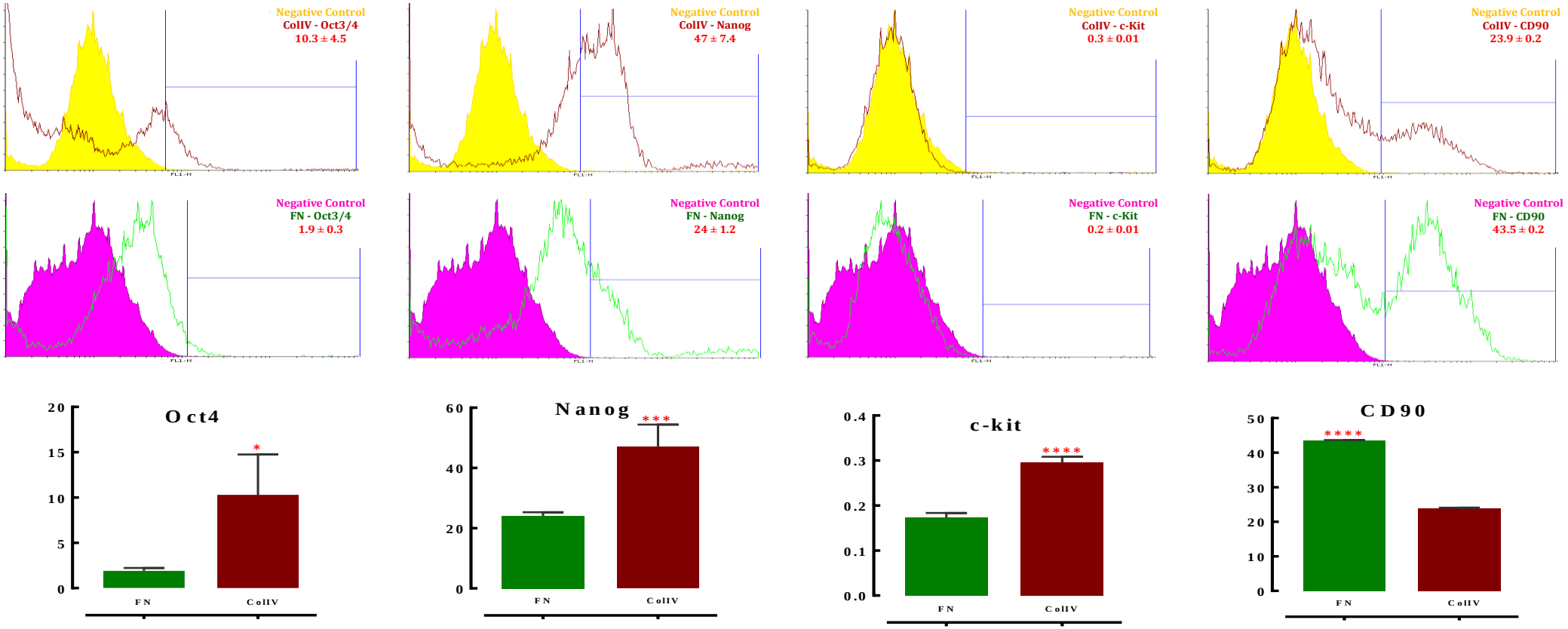



***Figure 3.8 Flow cytometry analysis of cardiosphere-derived cells for phenotype characterization.*** *The expression of Oct4, Nanog, c-kit and CD90 on P2-CDCs including those created through FN/PDL and ColIV/HD was analysed using flow cytometry and shown as a percentage of positive cells. The results revealed the presence of* ***(A)*** *stem cell marker, Oct4;* ***(B)*** *pluripotent stem cell marker, Nanog;* ***(C)*** *c-kit and* ***(D)*** *mesenchymal stem cell marker, CD90.* ***(a)*** *Histogram plots for P2-CDCs on collagen IV (dark red lines) with their negative controls (yellow).* ***(b)*** *Histogram plots for P2-CDCs on FN (lime green lines) with their negative controls (magenta).* ***(c)*** *Chart representation of the percentage of expression level. Abbreviations: P2-CDCs: Passage 2 Cardiosphere-Derived Cells, FN: Fibronectin, ColIV: Collagen IV. Data are presented as mean ± SEM (n=3) and performed one-way ANOVA with Tukey post hoc test. *: $p < 0.01$; ***: $p < 0.004$; ****: $p < 0.0001$.*

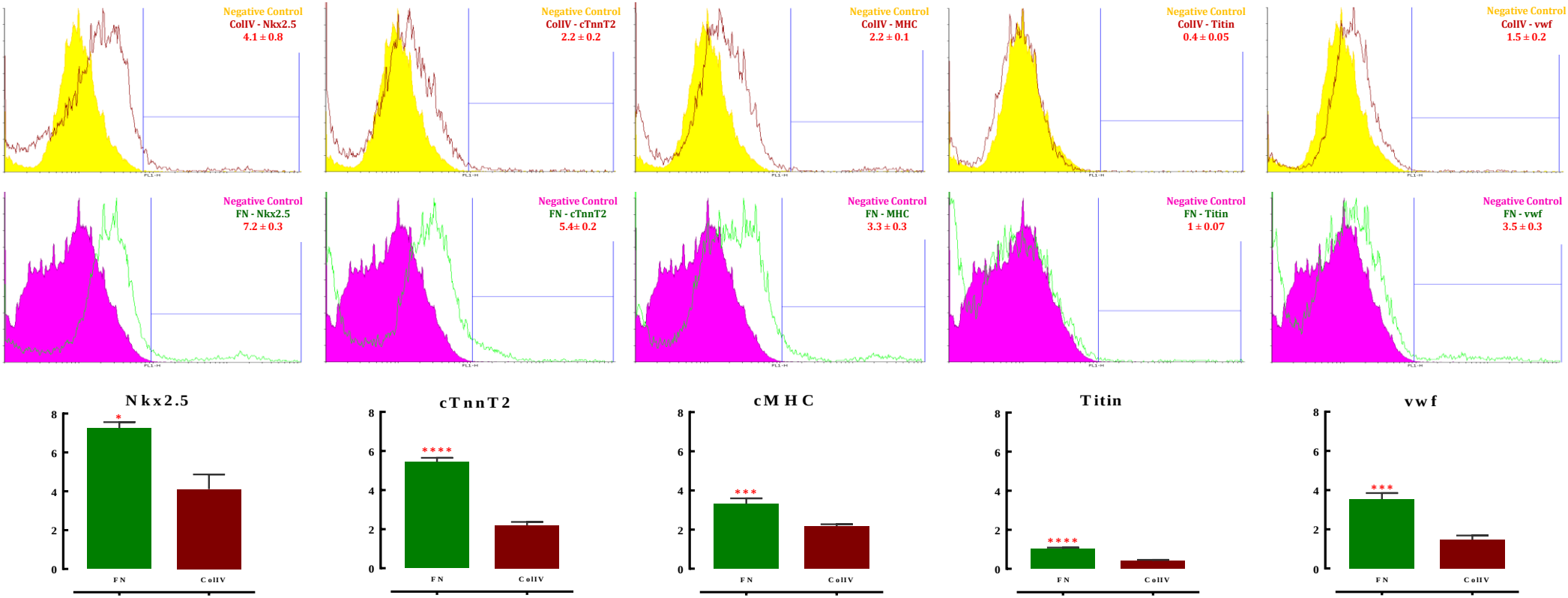



***Figure 3.9 Flow cytometry analysis of cardiosphere-derived cells for phenotype characterization.*** *The expression of Nkx2.5, cTnnT2, cMHC, titin and vwf on P2-CDCs including those created through FN/PDL and ColIV/HD was analysed using flow cytometry and shown as a percentage of positive cells. The results revealed the presence of* ***(A)*** *early cardiac-specific transcription factor, NKx2.5; cardiac-specific markers including* ***(B)*** *Cardiac-Troponin T2 (cTnnT2);* ***(C)*** *cardiac myosin heavy chain, cMHC;* ***(D)*** *Titin;* ***(E)*** *and endothelial specific marker, von Willebrand factor, vwf.* ***(a)*** *Histogram plots for P2-CDCs on collagen IV (dark red lines) with their negative controls (yellow).* ***(b)*** *Histogram plots for P2-CDCs on FN (lime green lines) with their negative controls (magenta).* ***(c)*** *Graph representation of percentage of expression level. Abbreviations: P2-CDCs: Passage 2 Cardiosphere-Derived Cells, FN: Fibronectin, ColIV: Collagen IV. Data are presented as mean ± SEM (n=3) and performed one-way ANOVA with Tukey post hoc test. ***: $p < 0.004$; ****: $p < 0.0001$.*

## 3.4.5 Characterization of cardiomyogenic differentiated P2-CDCs

Genotype and phenotype characterization of cardiomyogenic differentiation of P2-CDCs, created through FN/PDL and ColIV/HD techniques, were assessed using qRT-PCR, flow cytometry and immunocytochemistry in order to identify, quantify and localize genes and proteins specific to the cardiomyocytes.

### 3.4.5.1 Genotype characterization of cardiomyogenic differentiated P2-CDCs using qRT-PCR

To assess whether or not the changes in the culture protocols of the CDC through the FN/PDL and ColIV/HD techniques affected the differentiation potential of these cells into functional beating myocardiocytes, several different conditions were designed (Figures 3.2 – 3.3). Therefore, P2-CDCs created through both FN/PDL and ColIV/HD techniques were seeded on FN or ColIV coated plates at low ($10^3/cm^2$) or high cell densities ($10^4/cm^2$), treated for 3 days with CDM-1 (Appendix 1) containing either 5-Aza (5µM) or DMSO (1mM), then treated with CDM-1 only until day 7. From day 7 onward, cultures were treated with CDM-1 containing AA (0.1 µM) until day 14 (Figures 3.2 – 3.3). Results from qRT-PCR showed that, relative to the baseline, in most conditions P2-CDCs were successfully induced towards the cardiomyocyte phenotype (Figures 3.10 – 3.14). However, the extent of differentiation differed between the different conditions with some conditions found to be the most favourable for cardiac differentiation than others; including P2-CDCs created through FN/PDL technique instead of ColIV/HD, higher cell density over low cell density, and treating with 5-Aza compared to DMSO for total duration of 14 days in relative to 7 days (Figures 3.10 – 3.14).

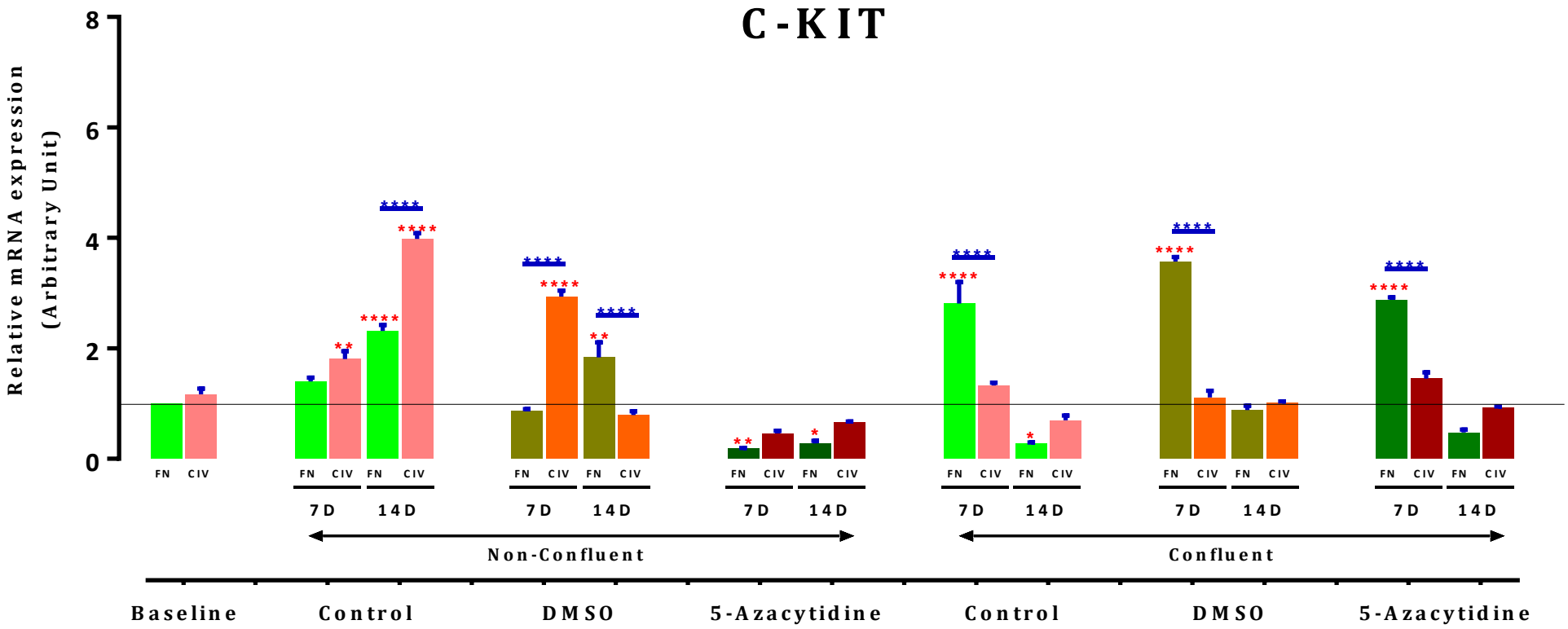



***Figure 3.10 The relative mRNA expression of c-kit using qRT-PCR.*** *Passage 2 CDCs created through FN/PDL and ColIV/HD were seeded on FN or ColIV coated flasks containing CDM-1 with low ($10^3$ cells/cm$^2$) and high ($10^4$ cells/cm$^2$) cell densities. Cells were treated with either 5-Aza (5µM) or DMSO (1 mM), alongside with non-treated P2-CDCs cultured in CEM as controls for total 7- and 14-days. The mRNA expression was normalized to Actb and β2M as reference genes and P2-CDCs from FN/PDL technique was used as a calibrator. Abbreviations: CDM: Cardiomyocytes Differentiation Medium; CEM: Complete Explant Medium; ColIV/HD: Collagen IV/Hanging Drop; FN/PDL: Fibronectin/Poly-D-Lysine; P2-CDCs: Passage 2-Cardiosphere-Derived Cells. Data are presented as mean ± SEM (n=3) and were analysed using a two-way ANOVA with Tukey post hoc test.* ****(Red stars)****: All conditions vs. FN Baseline;* ****(blue stars)****: FN vs. ColIV; *: $p < 0.01$; **: $p < 0.001$; ***: $p < 0.004$; ****: $p < 0.0001$.*

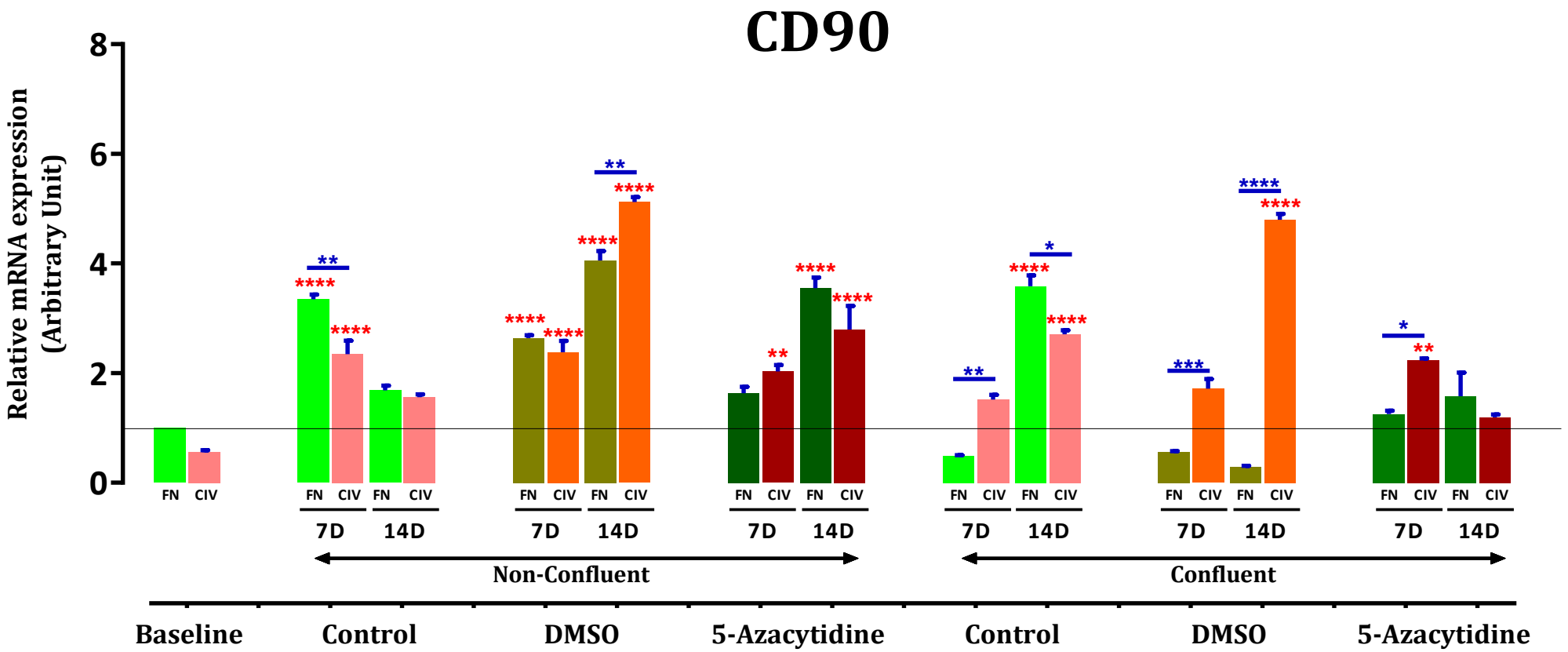



***Figure 3.11 The relative mRNA expression of CD90 using qRT-PCR.*** *Passage 2 CDCs created through FN/PDL and ColIV/HD were seeded on FN or ColIV coated flasks containing CDM-1 with low ($10^3$ cells/cm$^2$) and high ($10^4$ cells/cm$^2$) cell densities. Cells were treated with either 5-Aza (5µM) or DMSO (1 mM), alongside with non-treated P2-CDCs cultured in CEM as controls for total 7- and 14-days. The mRNA expression was normalized to Actb and β2M as reference genes and P2-CDCs from FN/PDL technique was used as a calibrator. Abbreviations: CDM: Cardiomyocyte Differentiation Medium; CEM: Complete Explant Medium; ColIV/HD: Collagen IV/Hanging Drop; FN/PDL: Fibronectin/Poly-D-Lysine; P2-CDCs: Passage 2-Cardiosphere-Derived Cells. Data are presented as mean ± SEM (n=3) and were analysed using a two-way ANOVA with Tukey post hoc test.* ****(Red stars)****: All conditions vs. FN Baseline;* ****(blue stars)****: FN vs. ColIV; *: p < 0.01; **: p < 0.001; ***: p < 0.004; ****: p < 0.0001.*

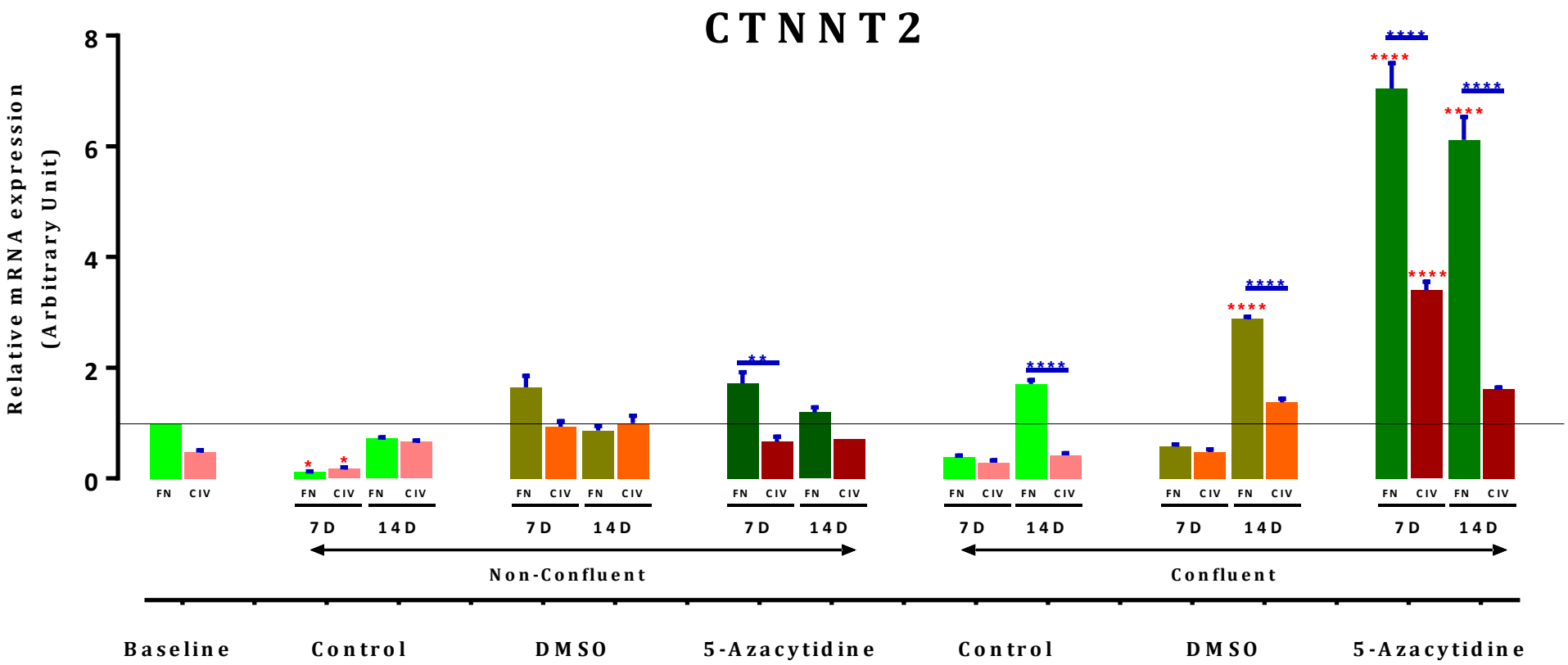



***Figure 3.12 The relative mRNA expression of cTnnT2 using qRT-PCR.*** *Passage 2 CDCs created through FN/PDL and ColIV/HD were seeded on FN or ColIV coated flasks containing CDM-1 with low ($10^3$ cells/cm$^2$) and high ($10^4$ cells/cm$^2$) cell densities. Cells were treated with either 5-Aza (5µM) or DMSO (1 mM), alongside with non-treated P2-CDCs cultured in CEM as controls for total 7- and 14-days. The mRNA expression was normalized to Actb and β2M as reference genes and P2-CDCs from FN/PDL technique was used as a calibrator. Abbreviations: CDM: Cardiomyocyte Differentiation Medium; CEM: Complete Explant Medium; ColIV/HD: Collagen IV/Hanging Drop; FN/PDL: Fibronectin/Poly-D-Lysine; P2-CDCs: Passage 2-Cardiosphere-Derived Cells. Data are presented as mean ± SEM (n=3) and were analysed using a two-way ANOVA with Tukey post hoc test.* ****(Red stars)****: All conditions vs. FN Baseline;* ****(blue stars)****: FN vs. ColIV; *: p < 0.01; **: p < 0.001; ***: p < 0.004; ****: p < 0.0001.*

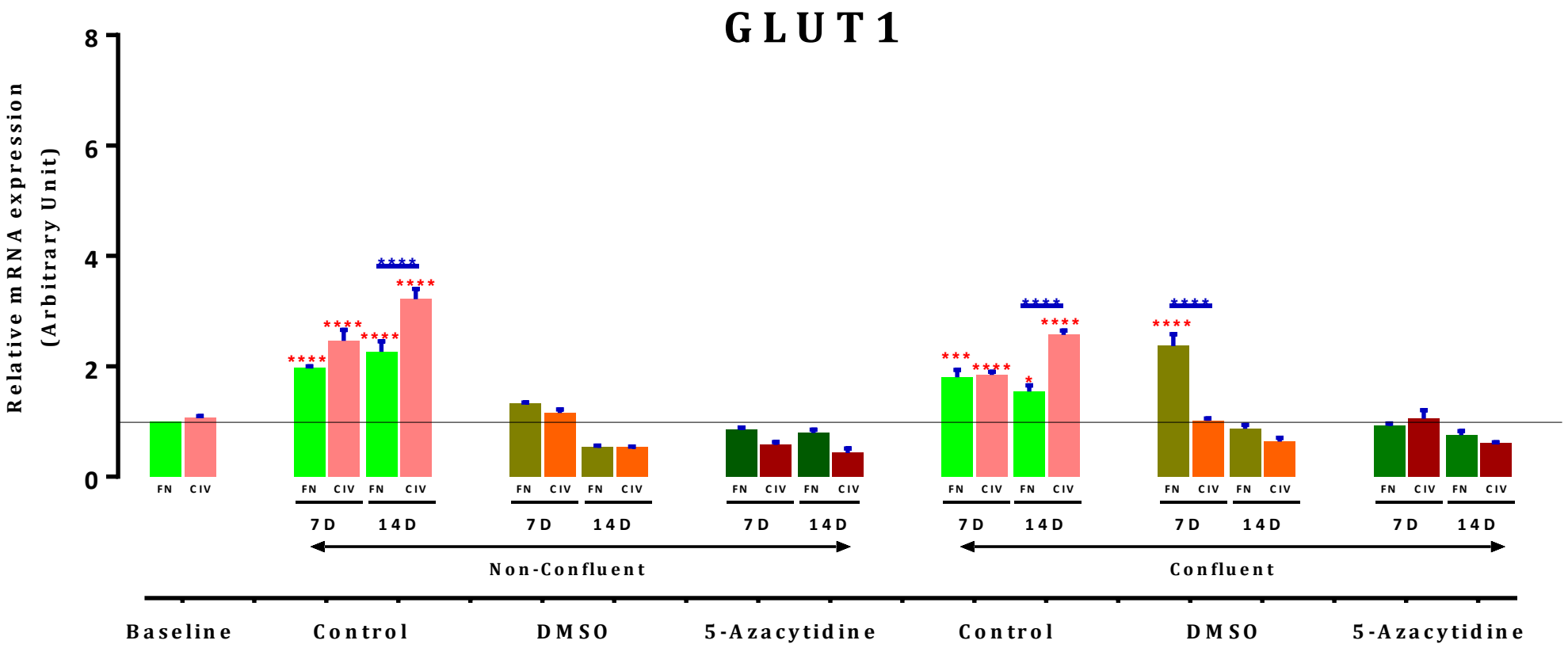



***Figure 3.13 The relative mRNA expression of Glut1 using qRT-PCR.*** *Passage 2 CDCs created through FN/PDL and ColIV/HD were seeded on FN or ColIV coated flasks containing CDM-1 with low ($10^3$ cells/cm$^2$) and high ($10^4$ cells/cm$^2$) cell densities. Cells were treated with either 5-Aza (5µM) or DMSO (1 mM), alongside with non-treated P2-CDCs cultured in CEM as controls for total 7- and 14-days. The mRNA expression was normalized to Actb and β2M as reference genes and P2-CDCs from FN/PDL technique was used as a calibrator. Abbreviations: CDM: Cardiomyocyte Differentiation Medium; CEM: Complete Explant Medium; ColIV/HD: Collagen IV/Hanging Drop; FN/PDL: Fibronectin/Poly-D-Lysine; P2-CDCs: Passage 2-Cardiosphere-Derived Cells. Data are presented as mean ± SEM (n=3) and were analysed using a two-way ANOVA with Tukey post hoc test.* ****(Red stars)****: All conditions vs. FN Baseline;* ****(blue stars)****: FN vs. ColIV; *: p < 0.01; **: p < 0.001; ***: p < 0.004; ****: p < 0.0001.*

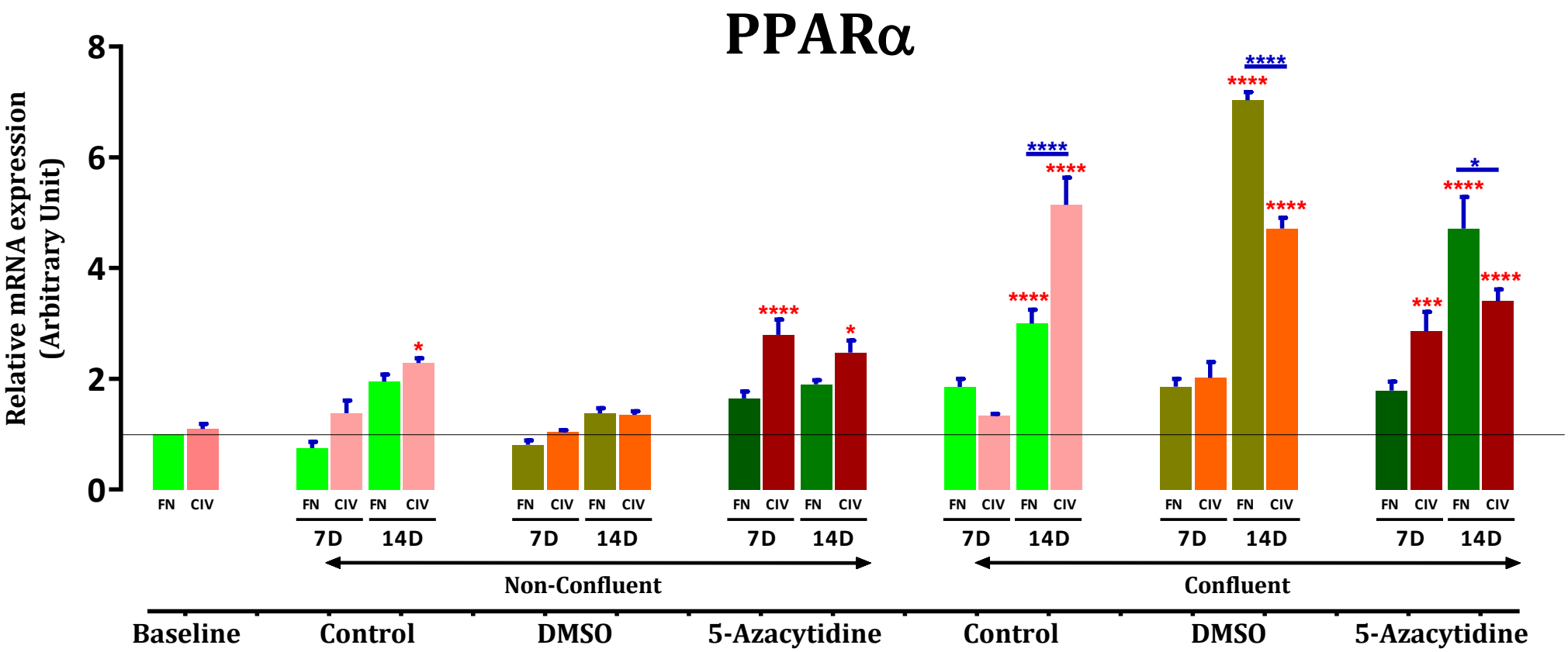



***Figure 3.14 The relative mRNA expression of PPARα using qRT-PCR.*** *Passage 2 CDCs created through FN/PDL and ColIV/HD were seeded on FN or ColIV coated flasks containing CDM-1 with low ($10^3$ cells/cm$^2$) and high ($10^4$ cells/cm$^2$) cell densities. Cells were treated with either 5-Aza (5µM) or DMSO (1 mM), alongside with non-treated P2-CDCs cultured in CEM as controls for total 7- and 14-days. The mRNA expression was normalized to Actb and β2M as reference genes and P2-CDCs from FN/PDL technique was used as a calibrator. Abbreviations: CDM: Cardiomyocyte Differentiation Medium; CEM: Complete Explant Medium; ColIV/HD: Collagen IV/Hanging Drop; FN/PDL: Fibronectin/Poly-D-Lysine; P2-CDCs: Passage 2-Cardiosphere-Derived Cells. Data are presented as mean ± SEM (n=3) and were analysed using a two-way ANOVA with Tukey post hoc test.* ****(Red stars)****: All conditions vs. FN Baseline;* ****(blue stars)****: FN vs. ColIV; *: p < 0.01; **: p < 0.001; ***: p < 0.004; ****: p < 0.0001.*

### 3.4.5.2 Phenotype characterization of cardiomyogenic differentiated P2-CDCs using flow cytometry

To support qRT-PCR, flow cytometry analysis was carried out on 5-Aza treated P2-CDCs, seeded with high cell density ($10^4$ cells/10 $cm^2$) and cultured for 14 days. The results showed no significant differences in mesenchymal stem cell marker, CD90 (FN= 29.2 ± 1.3% *vs.* ColIV= 28.3 ± 5.3%, p = 0.88) (Figure 3.15A) and early cardiac-specific transcription factor, Nkx-2.5, in between the FN or ColIV-based cell differentiation (FN= 46.3 ± 12.2% *vs.* ColIV= 62.2 ± 4.8%, p = 0.2) (Figure 3.15B). Nevertheless, there were significant differences in cardiac-specific cell markers, cTnnT2 (FN= 54.5 ± 2% *vs.* ColIV= 25.5 ± 1.8%, p < 0.0001) (Figure 3.15C); cMHC (FN= 63.1 ± 1.9% *vs.* ColIV= 9.5 ± 1.3%, p < 0.0001) (Figure 3.15D); and Titin (FN= 28.3 ± 2.4% *vs.* ColIV= 5.5 ± 1.5%, p = 0.0001) (Figure 3.15E); endothelial cell marker, von willebrand factor, and vwf (FN= 56.1 ± 1.1% *vs.* ColIV= 33.4 ± 2.2, p < 0.0001) (Figure 3.15F).

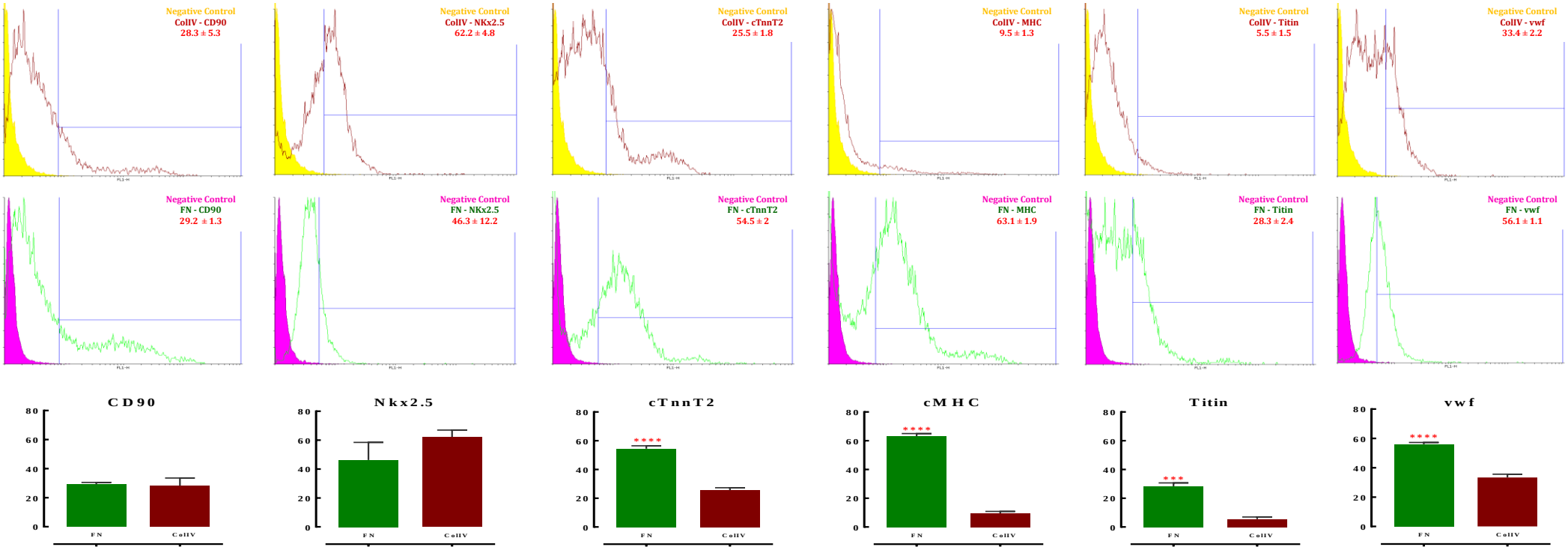



***Figure 3.15 Flow cytometry analysis of cardiomyogenic differentiation of P2-CDCs using 5-azacytidine.*** *The expression of CD90, Nkx-2.5, cTnnT2, cMHC, titin, and vwf on 5-Aza treated P2-CDCs created through FN/PDL, or ColIV/HD was analysed using flow cytometry and shown as a percentage of positive cells. The results revealed the presence of* ***(A)*** *mesenchymal stem cell marker, CD90;* ***(B)*** *early cardiac-specific transcription factor, NKx2.5;* ***(C)*** *Cardiac-Troponin T2;* ***(D)*** *cardiac myosin heavy chain, cMHC;* ***(E)*** *cardiac-specific marker, Titin;* ***(F)*** *and endothelial specific marker, von Willebrand factor, vwf.* ***(a)*** *Histogram plots for P2-CDCs on collagen IV (dark red lines) with their negative controls (yellow).* ***(b)*** *Histogram plots for P2-CDCs on FN (lime green lines) with their negative controls (magenta).* ***(c)*** *Graph representation of the percentage of expression level. Abbreviations: P2-CDCs: Passage 2 Cardiosphere-Derived Cells, FN: Fibronectin, ColIV: Collagen IV. Data are presented as mean ± SEM (n=3) and performed one-way ANOVA with Tukey post hoc test. ***: $p < 0.004$; ****: $p < 0.0001$*

### 3.4.5.3 Phenotype characterization of cardiomyogenic differentiated P2-CDCs using immunocytochemistry.

Flow cytometry analysis validated the qRT-PCR analysis and showed that confluent P2-CDCs cultured on FN and treated with 5-Aza and AA for total 14 days, started commitment into the cardiac lineage. Further support using immunocytochemistry analysis, was performed to localize cardiac specific proteins in these cells including cardiac troponin T2 (cTnnT2), cardiac troponin I (cTnnI), myosin heavy chain (MHC), alpha sarcomeric actin (α-SA) and titin (Figure 3.17A-F) alongside with negative controls (Figure 3.16A-C).

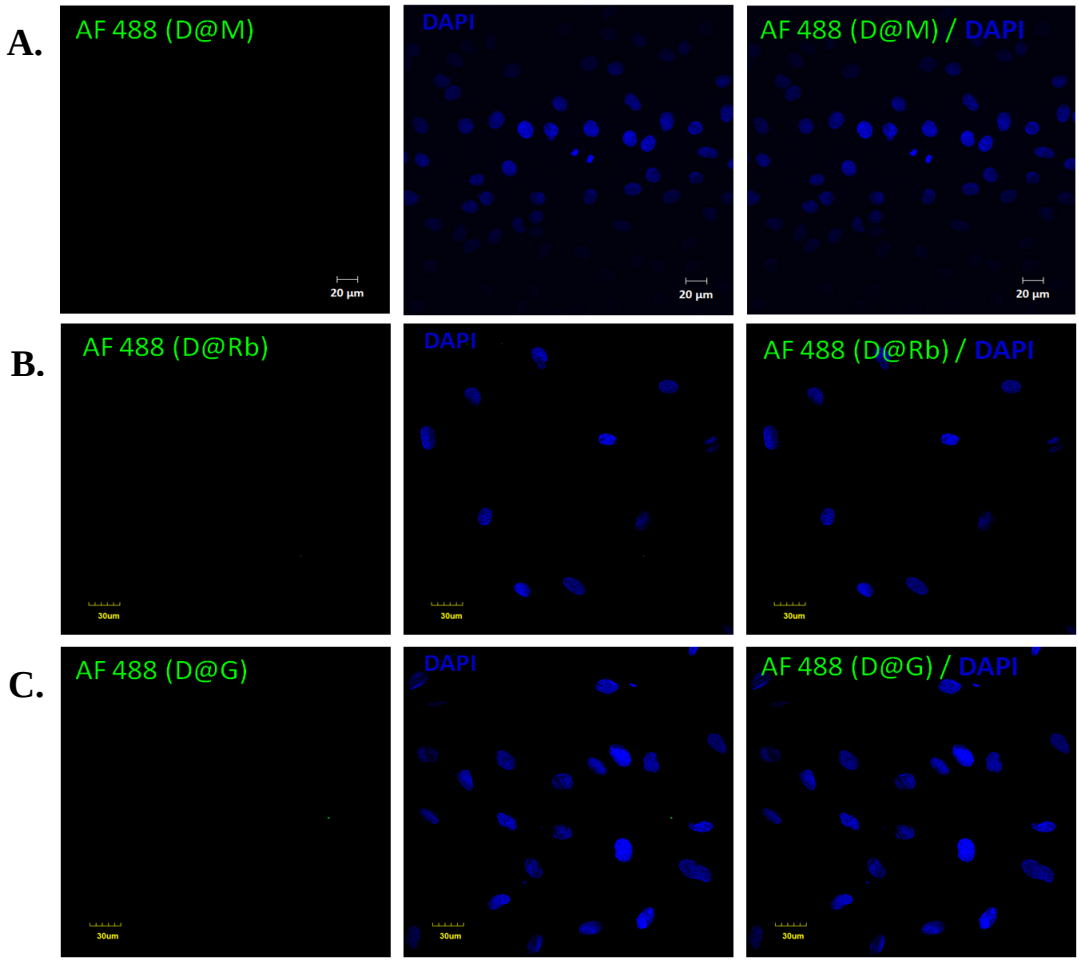



***Figure 3.16 Representative confocal images of negative controls.*** *Cardiosphere-derived cells generated from fibronectin-based cell culture technique were grown and treated with 5-Aza for two weeks, fixed with PFA, blocked and stained with secondary antibodies only,* ***A.*** *Alexa Fluor 488 Donkey anti-Mouse (D@M),* ***B.*** *Alexa Fluor 488 Donkey anti-Rabbit (D@Rb),* ***C.*** *Alexa Fluor 488 Donkey anti-Goat (D@G) and DAPI. Nuclei were stained with DAPI (blue). Abbreviations: CDCs: Cardiosphere-Derived Cells, DAPI: 4', 6-diamidino-2-phenylindole. Scale bar 20 and 30 µm.*

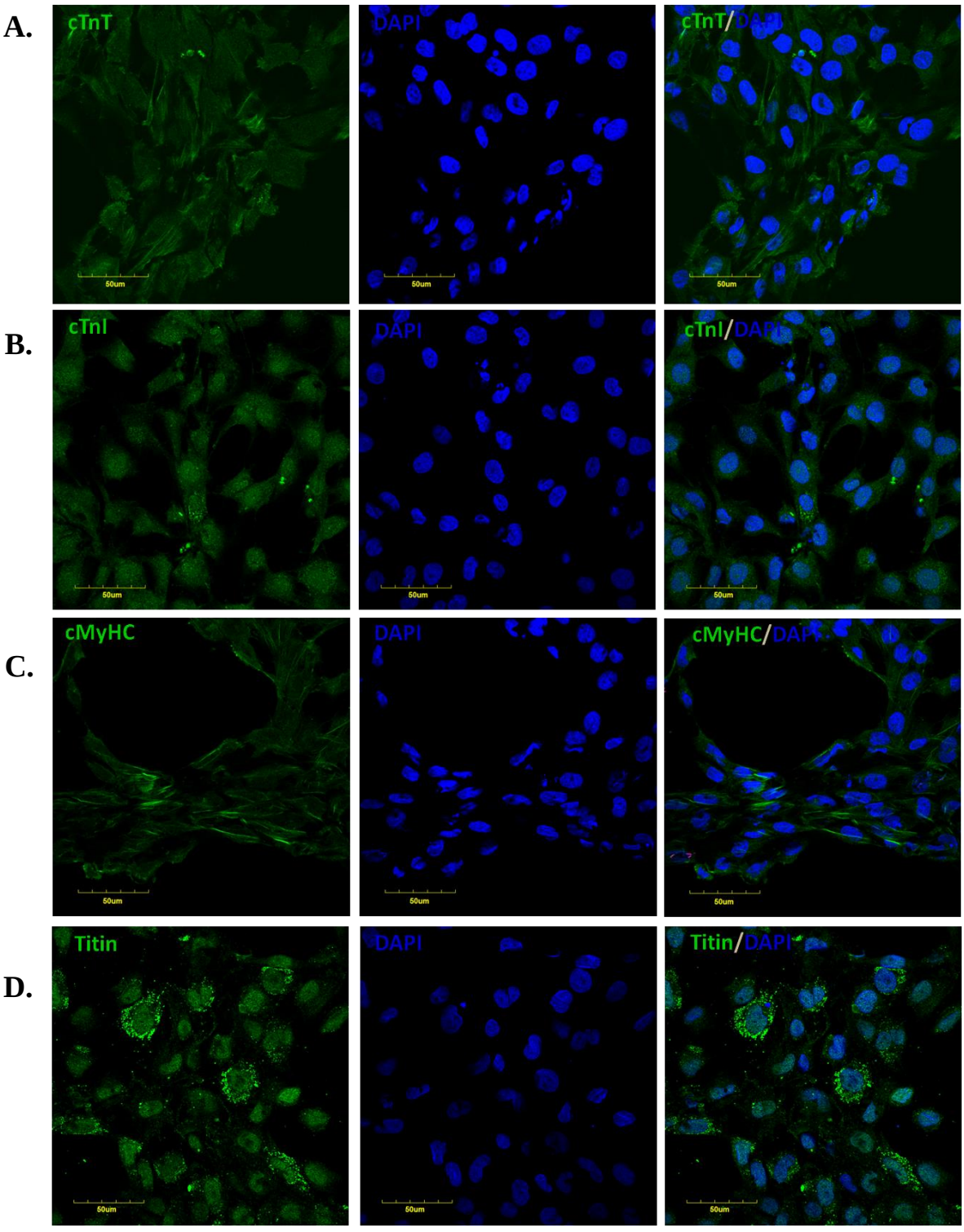
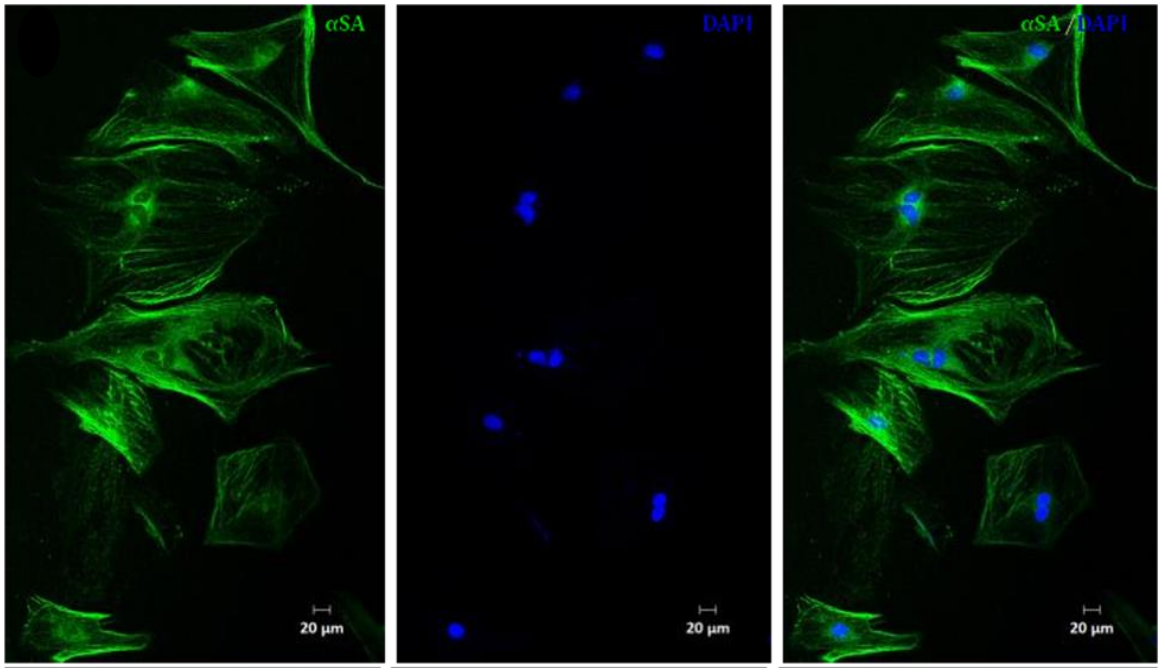
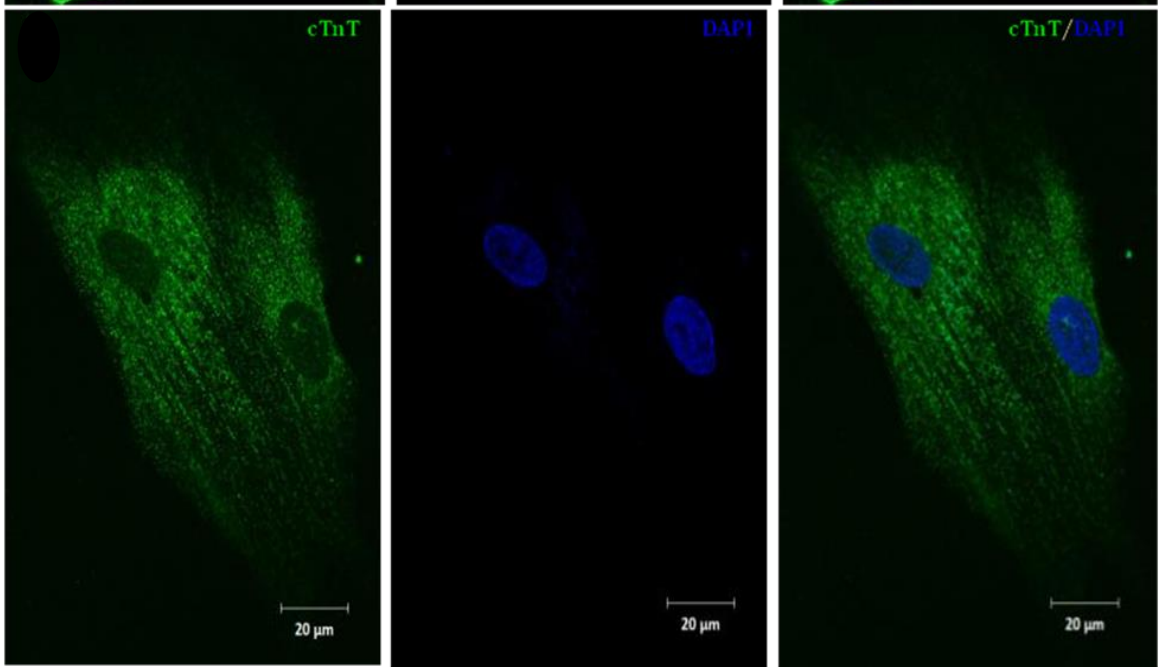



***Figure 3.17 Immunophenotyping of rat 5-Aza treated P2-CDC on fibronectin.*** *Representative confocal images of immunostained 5-Aza treated CDCs showed the expression of cardiac-specific cell markers including* ***A.*** *cardiac troponin T, (cTnT, Green),* ***B.*** *and* ***F.*** *cardiac troponin I (cTnI),* ***C.*** *cardiac myosin heavy chain (cMyHC) and* ***D.*** *cardiac Tintin* ***E.*** *Alpha-Sarcomeric Actin (αSA). Nuclei were stained with DAPI (blue). Abbreviations: CDCs: Cardiosphere-Derived Cells; DAPI: 4', 6-diamidino-2-phenylindole. Scale bar 50 µm or 20 µm as indicated.*

**E.**


αSA
20 μm
DAPI
20 μm
αSA/DAPI
20 μm

**F.**


cTnT
20 μm
DAPI
20 μm
cTnT/DAPI
20 μm

## 3.5 Discussion

The aims of the work described in this chapter were *ex vivo* isolation, expansion, characterization and cardiomyogenic differentiation of endogenous cardiac stem/progenitor cells using both current published and optimised culture techniques and to assess whether or not the changes in the culture protocol affected the potential cardiomyogenic differentiation of these CSCs.

### 3.5.1 ColIV/HD technique yielded more CDCs compared to FN/PDL

The identification of endogenous cardiac stem/progenitor cells has raised interest in these cells for treating myocardial infarction[100]. Isolation based on a single cell marker gives a homogenous CSC population from heart tissue[100, 102, 113] with very low cell yield, which requires time-consuming *ex vivo* expansion to generate sufficient cell numbers for therapy, and that may compromise stem cell properties[100, 113, 228].

In this study, we used explant culture technique using either FN or ColIV substrates, followed by stem/progenitor cell isolation and enrichment through the generation of CSps either on PDL-coated plates or HDs, which were a practical way to obtain sufficient cells in a short time period. In the currently published protocol, 1.7 ± 0.4 million CDCs were produced from 21.0 ± 1.9 mg specimens within 60 days[152]. In contrast, here, only the atria and apex of adult rat hearts (FN = 165.33 mg; ColIV= 168.67 mg) were used and yielding significantly higher CDCs number at passage 2 (FN = 10.95 ± 2 and ColIV= 118.590 ± 62 million P2-CDCs within 46 ± 5 days, from a total of 3 harvests with n=3). Cells created through the ColIV/HD yielded more cells due to their higher level of proliferation rate at passage 2 relative to FN/PDL culture technique. ColIV-mediated signalling has been shown to induce proliferation through intracellular signalling molecules in active forms of focal adhesion kinase (FAK) and mitogen-activated protein kinase 1/2 (MAPK 1/2)[229].

### 3.5.2 P2-CDCs are a heterogeneous cell population containing both stemness and committed cells towards cardiac lineage

Studies have suggested that murine CSps and CDCs are not a source of stem cells as they are mainly composed of cardiac fibroblasts and $CD45^+$ hematopoietic cells[230]. Nevertheless, similar to other studies[106, 152] here in this study we have shown that P2-CDCs created through both protocols expressed stemness markers Oct4, Nanog, and CD90, although at a low level. In comparison to the preliminary data from Dr. JJ Tan with 3% c-$Kit^+$ cells in FN/PDL and 11% in ColIV/HD culture technique from explants of neonatal rat heart (1-3 days old), here we obtained fewer c-$Kit^+$ cells both in FN/PDL (0.2708 ± 0.044%; 4.2 fold less) and in ColIV/HD (0.2307 ± 0.004; 47 fold less) using adult rat heart (over 5-weeks old). This could be due to several different reasons. Tan measured c-kit level in cells isolated from neonatal rat heart that would be expected to have more stem cells compared to those from adult rat heart, as progenitors in the adult heart may decrease and lose their functional capacity with increased age[156, 157]. Furthermore, the percentage of c-$Kit^+$ cells may vary between individuals, for example in human CDCs c-Kit expression varies widely (0.3% to 7.2%; > 20 fold) from patient to patient[231]. Nevertheless, similar to Tan's study, we observed that P2-CDCs have express fairly low level of cardiac transcription factor, Nkx-2.5, and cardiac-specific proteins, cTnnT2, Titin, cMHC, and endothelial cell marker, vwf, which suggests that P2-CDCs are a heterogeneous cell population containing both stemness and committed cells towards cardiac lineage.

### 3.5.3 Confluent P2-CDCs cultured on FN and treated with 5-Aza were differentiated into immature cardiomyocytes cells

Despite studies that have suggested that murine CSps and CDCs have no cardiomyogenic potential[230], other studies have suggested that both 5-Aza and DMSO individually can induce several different cell types including CSCs to undergo differentiation into cardiomyocytes[174-183, 185, 186, 188-192, 232-234]. Here in this study, we used a protocol that induced P2-CDCs to start commitment into immaturely differentiated myocytes, with downregulation of the stem cell marker, CD90 both in

confluent and non-confluent cell density, especially after 14 days on FN and ColIV compared to control. In addition, differentiation of CDCs was associated with increased expression of the cardiac specific gene, cTnnT2, which increased in most differentiated CDCs, particularly with highly significant 50 fold changes in confluent CDCs cultured on FN and treated with 5-Aza. In addition, results showed over 7-fold increased expression of PPARα, which plays a critical role in mitochondrial fatty acid β-oxidation (FAO), in confluent CDCs treated with either DMSO or 5-Aza, especially at 2-weeks, with decreased expression of the glucose transporter, Glut1. Furthermore, differentiation was supported by immunocytochemistry, which detected the cardiac specific proteins cTnnT2, cTnnI, titin, cMHC, and αSA.

*In vitro* studies have shown that 5-Aza can successfully induce several different types of cells to undergo differentiation into cardiomyocytes including Sca-1$^+$ CDCs[174], human umbilical cord-derived MSCs [175], adult human bone marrow MSCs[176, 177], murine bone marrow stromal cells[178], and primary and immortalized porcine MSCs[179]. Nevertheless, it has been reported that 5-Aza is insufficient for the cardiogenic induction of the adipose-derived stem cells (ASCs)[180].

5-Aza as a cardiomyogenic stimulus has been widely studied, and some details of underlying mechanisms have been reported at the level of DNA methylation and protein expression. A study showed that 5-Aza treatment could cause both losses of DNA methylation and alterations in target genes bound by modified histones. They found that most changes in gene expression after 5-Aza treatment were from genes whose promoter regions were not silenced by DNA methylation or repressive histones, but rather from genes that reside in active chromatin[233]. Ye *et al.* performed a proteomic analysis of the biochemical processes related to the effect of 5-Aza on porcine bone marrow MSCs and found up-regulation in the expression of proteins involved in cell proliferation and differentiation including cardiac alpha tropomyosin[232].

In addition, *in vitro* studies showed that DMSO could cause other cell types to differentiate into cardiomyocytes. One has shown that DMSO-induced biochemical mediators of Wnt signalling by decreased phosphorylation and increased levels of β-catenin[188]. Another study revealed that DMSO

and/or Cardiogenol C enhanced P19 cell differentiation into cardiomyocytes[189]. In addition, SRC kinase family inhibitor PP2 inhibited proliferation of P19 cells and, together with DMSO, induced cardiac differentiation of this cell type[190]. DMSO has been shown to inhibit c-myc expression[191] and arrest cell cycle progression, thus affecting cell proliferation in different cell types[192].

DMSO is a hydrogen-bond disrupter[183] and found to be a histone deacetylase (HDAC) inhibitor[235] in a study designed to understand why DMSO caused terminal differentiation of murine erythroleukemia cells[185]. Cell differentiation begins with modification of gene expression, regulated by acetylation of histones. Removal of the acetyl groups from histones by HDAC down-regulates expression of genes that cause cells to differentiate. Thus using HDAC inhibitors causes deacetylation of histone and subsequent cell differentiation[186, 187].

### 3.5.4 Confluency induces terminal differentiation

Several studies have suggested that cell confluence strongly influenced commitment to terminal differentiation by a dramatic loss of proliferation and expression of early differentiation markers[236, 237]. One study has demonstrated that *in vitro* confluence culture of human epidermal keratinocytes resulted in a loss of clonogenicity, irreversibly arrested growth, and initiated expression of the suprabasal keratins K1 and K10, early differentiation markers. In addition, studies on skeletal muscle myoblasts have suggested that close cell contacts in the confluent state of high seeding culture induced myoblast differentiation and permanently ablated proliferation[236]. Likewise, here in this study, we observed that confluent culture of P2-CDCs on either FN or ColIV, treated with either DMSO or 5-Aza, induced early cardiac specification lineage by increasing the expression of cTnnT2 and PPARα and decreasing the expression of c-kit and GLUT1.

### 3.5.5 ColIV base culture induces proliferation, but FN induces cardiac differentiation

Stem cell fate is regulated through signals from the microenvironment including extracellular matrix (ECM), which tethers stem cells[238, 239] and sequesters and modulates the local concentration of

secreted factors presented inside the stem cell niche[240-243]. Cardiac ECM consists principally of 3D interstitial collagens, type I and III, to which other matrix components such as FN and laminin (LN) are attached, and mediates key functions such as healing and remodelling[244] by surrounding and supporting myocardial constitutive cells including: CMs, vascular smooth muscle cells (SMCs), cardiac fibroblasts, and endothelial cells (ECs). CMs, SMCs, and ECs produce the LN, while FN is synthesized by CM, fibroblasts and SMCs[245]. mRNA expression of the heart revealed that collagen I and III are relatively highly expressed, while FN, LN, and collagen IV are at intermediate levels[246].

ECM components vary over the time in the developing heart and by location (epicardium, endocardium, and myocardium). In early development particularly in the myocardium, FN and collagen I are at the highest level at E12.5, and then lower after birth, at day-2 post-natal (P2). In contrast, ColIV is low at (E12.5) and increased later in development (P2)[246]. Although ECM and their signalling pathway(s) in embryonic stem cell development is well studied and characterized, their key function in adult stem/progenitor cell maintenance and differentiation into specific lineages is poorly understood. Here in this study, we used two different ECM molecules, FN and ColIV, in order to find out which of them had the greater influence on the specification of adult cardiac stem/progenitor cells towards the cardiomyocyte lineage. Hence, we characterised and compared the isolated, expanded and 5-Aza, or DMSO treated P2-CDCs on either FN or ColIV.

Several studies have suggested that 2D culture of different stem/progenitor cells on ColIV substrate maintains the stemness markers, with an even higher level of markers in 3D culture[229, 247-253]. Likewise, studies have suggested that ColIV-mediated signalling is involved in rat progenitor Leydig cell (PLC) proliferation during day 14-21 post-natal life, through intracellular signalling via active forms of focal adhesion kinase (FAK) and mitogen-activated protein kinase 1/2 (MAPK 1/2)[229]. Here in this study, the results from quantification of cell number and proliferation assay have revealed that CDCs cultured on ColIV produced substantially more cells and significantly higher proliferation rate relative to CDCs cultured on FN.

The results from qRT-PCR and immunocytochemistry revealed that cells cultured on FN and treated with 5-Aza or DMSO had initiated differentiation towards the cardiac lineage at both gene and protein level, although without reaching a beating phenotype. This immature differentiation could be through the FN-integrin signalling pathways as recent studies have revealed that human ESCs (hESCs) differentiated to cardiomyocytes on 70:30 FN:LN with greater efficiency (~60%-70%) compared with gelatin (~50%-60%)[252]. This effect was proved to be due to the integrin-mediated activation of MEK/ERK-induced differentiation and by significant increases in FN and LN receptors, integrin-β5 and -β4 (ITGB5 and ITGB4) respectively[252, 254, 255].

## 3.6 Conclusion

Isolated endogenous cardiac progenitor cells, cultured using both FN/PDL and ColIV/HD techniques, are heterogeneous as they express both stemness and early cardiac-specific markers. Furthermore, cells produced using the ColIV/HD technique yielded significantly higher CDC numbers compare to the FN/PDL due to a substantially greater level of proliferation than P2-CDCS on FN. However, direct comparison of CDC differentiation under 24 different conditions, revealed that treatment of confluent P2-CDCs on FN with 5-Aza+AA for two weeks, was the most efficient protocol for cardiomyogenic differentiation. This was supported by down-regulation of stem cell markers, c-kit and CD90; and up-regulating the cardiac specific gene, cTnnT2, and proteins including cTnnT2, cTnnI, cMHC, titin and α-SA.

# Chapter 4

## Substrate Utilization of Cardiac Progenitor Cells Cultured on Fibronectin or Collagen IV Before and After Cardiomyogenic Differentiation

# 4.1 Abstract

Despite being resident in the heart, which derives most its energy needs from the oxidation of fatty acids[256], cardiac stem/progenitor cells are assumed to be glycolytic. The main objective of the work described in this chapter was to determine, for the first time, substrate and energy metabolism in cardiac stem/progenitor cells before and after cardiomyogenic differentiation. Therefore, control and 5-Aza differentiated P2-CDCs, cultured on either FN/PDL or ColIV/HD were assessed for glycolytic flux and oxidative metabolism using $^{3}$H- and $^{14}$C-labelled substrates respectively. The results from glycolytic flux revealed that the rate of glycolysis was considerably higher in control P2-CDCs cultured on ColIV compared to cells on FN. Relative to the controls, the glycolytic rate was significantly reduced in 5-Aza treated P2-CDCs on FN or ColIV. This was supported by elevated lactate efflux in control P2-CDCs on ColIV compared to FN control, with a significantly reduced lactate efflux from 5-Aza treated cells on FN and ColIV. Furthermore, glucose oxidation was increased in 5-Aza treated CDCs on FN compared to the controls and ColIV 5-Aza treated cells. Relative to the FN control and 5-Aza treated cells, glutamine oxidation was higher in control P2-CDCs on ColIV but reduced in 5-Aza treated cells. Similarly, palmitate oxidation increased in FN 5-Aza treated CDCs compared to the control cells on FN and ColIV, and 5-Aza treated cells on ColIV. Pyruvate oxidation was high in FN control cells but decreased in FN 5-Aza treated CDCs, whereas control cells on ColIV had low pyruvate oxidation level, which increased when cells were treated with 5-Aza. Moreover, in comparison to other tested substrates, acetoacetate demonstrated the highest level of oxidation in both control and 5-Aza treated cells cultured on either FN or ColIV. In summary, this study, for the first time, has measured substrate utilisation in control and 5-Aza treated P2-CDCs, and calculated ATP production which revealed that the highest level of energy production occurred through oxidation of acetoacetate, followed by pyruvate and palmitate, with lower ATP production from glycolysis and glucose and glutamine oxidation.

## 4.2 Introduction

Organ function is affected by physiological, pathological and pharmacological alterations in energetic substrate metabolism[214, 257, 258]. Hence, manipulation of tissue-specific substrate metabolism as a potential therapeutic intervention is an attractive approach to treat illnesses including ischemic heart disease. Similarly, the transition of heart stem/progenitor cells, which mainly use glycolysis for their energy needs, into beating cardiomyocytes, which mainly use oxidative phosphorylation, requires a change in the energetic infrastructure of metabolism from glycolysis to oxidative phosphorylation[214, 257]. Therefore, precise measurement of metabolic parameters is a fundamental key when assessing pathway utilisation. There are a number of experimental techniques available to measure energy metabolism *in vivo* and *in vitro* including the use of radioactive isotopic tracers like $^{14}C$- or $^{3}H$-radiolabelled substrates[198, 259-264]. These allow direct measurement of flux through the various energy-yielding pathways such as glycolysis, glucose oxidation, fatty acid oxidation and the associated rate of ATP production in the cells in tissue culture or the perfused heart.

The heart has an ability to use mainly lipids (free fatty acids) and carbohydrates (glucose and lactate) as well as circulating ketone bodies, pyruvate, and amino acids[198]. In contrast, non-contractile adult stem/progenitor cells, which reside in the heart, are assumed to derive most of their energy from glycolysis. Two of the by-products of oxidation and glycolytic pathways are carbon dioxide and water respectively. When the fatty acid or glucose substrates in the cell culture medium or heart perfusate are labelled appropriately with $^{14}C$ or $^{3}H$, it is possible to measure the $^{14}CO_2$ or $^{3}H_2O$ produced. Therefore, with the knowledge of the specific activity of the radiolabelled substrate used, it is feasible to quantitate the rate of flux through the particular pathway(s) using radioisotopes labelled at specific carbons or hydrogens on the different energy substrates[259].

To quantify glycolytic flux, [5-$^{3}H$] glucose can be added to the cell culture medium or heart perfusate. At the enolase step of glycolysis, this $^{3}H$ is released as $^{3}H_2O$ (Figure 4.1). Through a collection of timed culture medium or perfusate samples and separation of $^{3}H_2O$ from [$^{3}H$] glucose, it is possible to directly measure glycolysis in *in vitro* cultured cells or a perfused heart. Similarly, collection of

$^{3}H_2O$ from culture medium or perfusate containing [9,10-$^{3}$H] palmitate can be used to measure rates of palmitate oxidation.

Throughout the oxidation of substrates like glucose or palmitate, cultured cells or perfused heart release carbon dioxide produced during the passage of Acetyl-CoA (derived from glucose or palmitate) through the tricarboxylic acid (TCA) cycle. A quantitative collection of $^{14}CO_2$ produced from cells or heart supplied with $^{14}$C-radiolabelled substrates, allows direct measurement of substrate oxidation (Figure 4.1).

Therefore, the objectives of this study were to assess the source and rate of ATP production in the endogenous cardiac stem/progenitor cells before and after cardiomyogenic differentiation.

The aims of this study were to:

- Determine the rates of the various pathways involved in energy metabolism of control and 3-weeks 5-Aza treated P2-CDCs using $^{3}$H- and $^{14}$C-radiolabeled substrates.
- Determine the source and rate of ATP production in control and 3-weeks 5-Aza treated P2-CDCs.

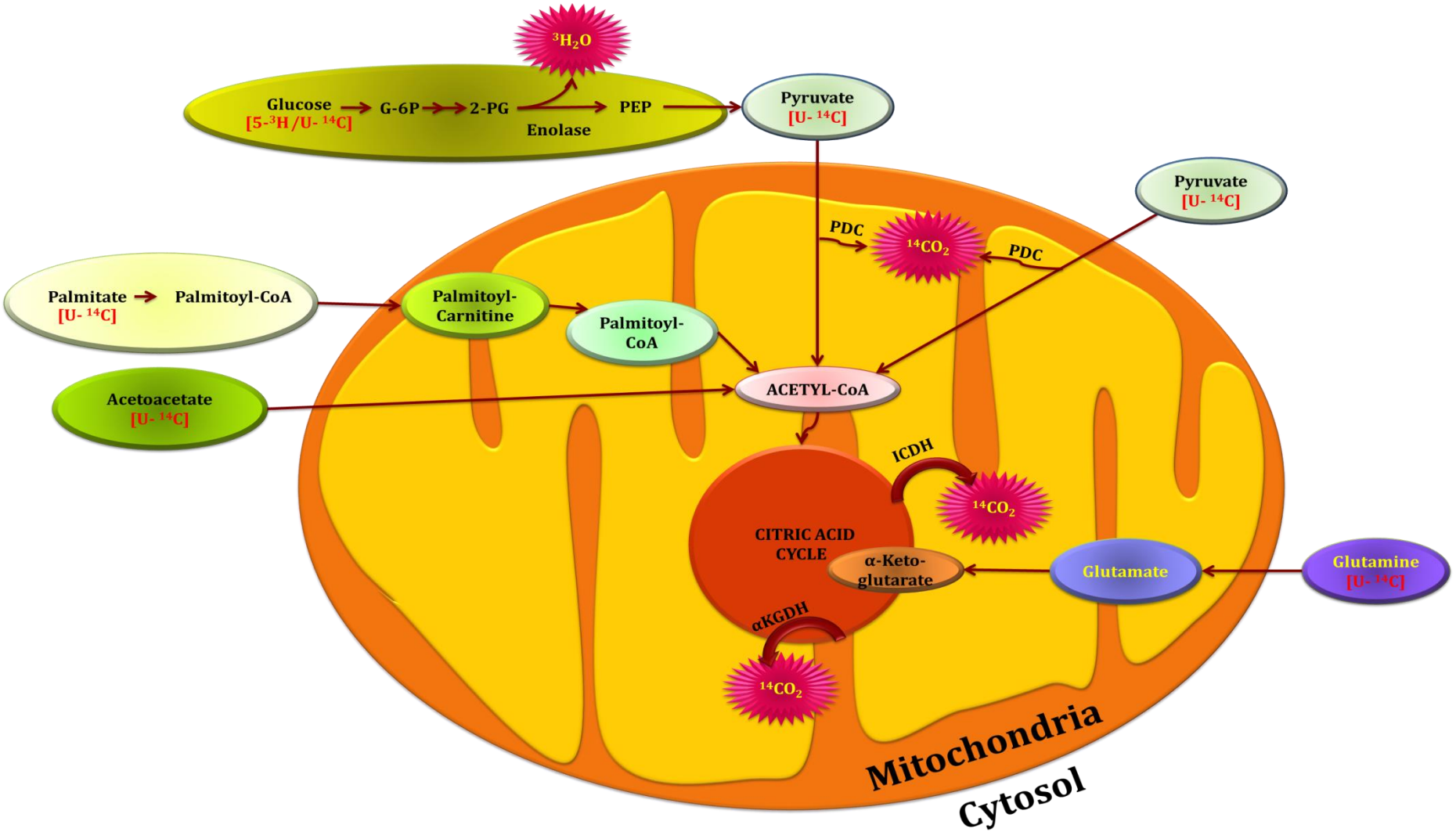



***Figure 4.1 Fate of [5-$^3$H]- and [U-$^{14}$C]-radiolabelled glucose, or [U-$^{14}$C]-radiolabelled glutamine, palmitate, pyruvate, and acetoacetate in cellular metabolism.***

## 4.3 Methods

### *4.3.1* Overview of designed study

The study design described in this chapter is illustrated in a schematic flow diagram (Figure 4.2), which described specific experimental methodologies.




***Figure 4.2 Flow diagram showing an overview of study design to assess the metabolic pathways involved in control and 5-Aza treated P2-CDCs.***

## 4.3.2 Isolation, expansion, and differentiation of CSCs

Methods are described in Chapter 2 (See section 2.2). Briefly, tissue from five weeks old SD rat hearts was explanted on either FN or CIV coated dishes containing CEM, EDCs were harvested, resuspended in CGM, and plated into pre-coated plates with PDL or as HD respectively. Then CSps were mechanically harvested, seeded on FN or CIV coated dishes and cultured until passage two when they were treated with 5-Aza and AA for 3-weeks (Figure 4.3). All experiments in this chapter used P2-CDCs as control and 3-weeks 5-Aza treated P2-CDCs as cardiomyogenic differentiated cells unless otherwise stated.

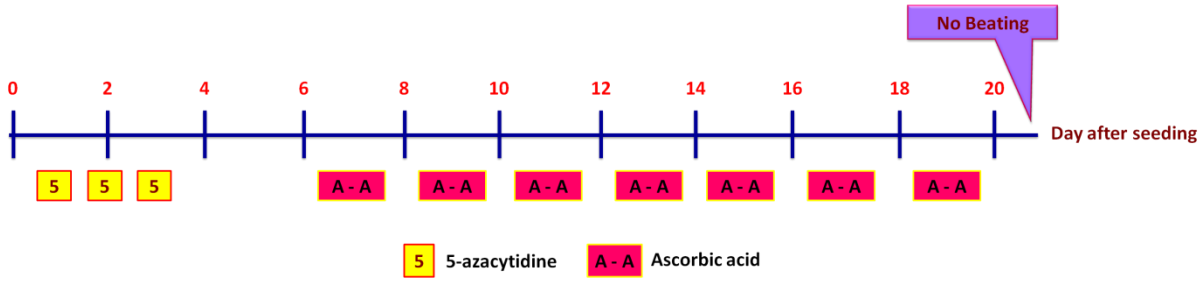



***Figure 4.3 Timeline of the differentiation procedure***. *The blue line indicates the number of days after plating. For the first three consecutive days, 5µM 5-Aza (yellow boxes) is added to the culture medium, CDM-1, followed by normal CDM-1 for further three days. From day seven forward until day-21, cells were supplied with CDM-1 and 0.1 µM ascorbic acid (pink boxes), which is added every two days*. Abbreviation: CDM-1: cardiomyogenic differentiation medium-1.

## 4.3.3 Real-time quantitative RT-PCR

Real-time quantitative reverse transcriptase polymerase chain reaction (qRT-PCR) was used to determine the expression of genes involved in glucose metabolism including GLUT1, GLUT4, PDK1, and PDK4; fatty acid transporter genes such as CD36 and CPT1B; and fatty acid metabolism like PPARα, MCAD and ACADM in control and 5-Aza treated P2-CDCs. All qRT-PCR data were normalised to Actb and B2M as the reference genes and P2-CDCs as the calibrator.

### 4.3.4 Western blotting assay

Cell culture samples were lysed and frozen in liquid nitrogen. The levels of proteins involved in glucose metabolism including GLUT1, GLUT4, PDK1, and PDK4; mitochondrial proteins, αKGDH, and CISY; fatty acid transporter, CD36; and fatty acid metabolism MCAD and UCP3 were measured by Western blotting (See section 2.10).

### 4.3.5 Determination of Lactate efflux

To determine the level of lactate production, cell culture medium of control and 5-Aza treated cells were collected at different intervals (8-, 24-, 48-, and 72-hours) and lactate levels measured using an ABX Pentra 400 Chemistry Analyser, which detected the signal and analysed the concentration of lactate (See section 2.11).

### 4.3.6 Determination of glycolytic flux

A trace of [5-$^{3}$H] glucose (1.48 MBq/mmol) was added to the medium of control and 3-weeks 5-Aza treated P2-CDCs for 72-hours. Samples were taken at different intervals (8-, 24-, 48-, and 72-hours) and run through prepared Dowex resin ion exchange columns in order to separate $^{3}$H-glucose from $^{3}H_2O$ (Chapter 2, Figure 2.1). The radioactivity was measured using a liquid scintillation counter (See section 2.12).

### 4.3.7 Determination of substrates oxidation rates

A $^{14}CO_2$-capture technique, based on Collins method [224] with some modification with a home designed appliance (Chapter 2, Figure 2.2), was used to determine the oxidative level of different substrates in control and 5-Aza treated cells including 10 mM glucose-containing 21 MBq/mmol D-U-$^{14}$C-glucose; 5 mM pyruvate-containing 0.35 MBq/mmol 1-$^{14}$C-pyruvate; 10 mM acetoacetate-containing 0.185 MBq/mmol 3-$^{14}$C-acetoacetate; 2 mM glutamine-containing 1.2 MBq/mmol U-$^{14}$C-glutamine; and 2 mM palmitate-containing 10.27 Mβq/mmol U-$^{14}$C-palmitate (See section 2.13).

## 4.3.8 Calculation of ATP production

Adenosine triphosphate produced through the glycolysis, and oxidative pathways were calculated based on glycolytic flux and different individual substrate oxidation level (Table 4.1).

| Substrates (1 mole/substrate) | Mole of ATP/Pathway | |
|---|---|---|
| | OXPHOS | Glycolysis |
| Glucose | 31 | 2 |
| Glutamine | 20 | ------ |
| Palmitate | 106 | ------ |
| Pyruvate | 12.5 | ------ |
| Acetoacetate | 20 | ------ |

***Table 4.1 Calculation of ATP per mole of substrate.*** *The ATP produced per substrate was calculated based on their particular metabolic pathway either including glycolysis or OXPHOS.*

## 4.3.9 Confocal imaging

Methods are described in Chapter 2 (section 2.10.2). Briefly, MitoTracker probe was used to stain the mitochondria in control and 5-Aza treated P2-CDCs as well as neonatal rat heart cells and visualised by confocal microscope imaging.

# 4.4 Results

## 4.4.1 Glucose metabolism

### 4.4.1.1 Glycolytic flux in control and treated P2-CDCs

To determine the level of glycolytic flux in control and 3-weeks 5-Aza+AA treated P2-CDCs, $^{3}$H-glucose was added into the culture medium and samples collected over 72-hours. The results revealed that the rate of glycolytic flux was considerably higher in control CDCs cultured through ColIV/HD relative to the control CDCs cultured through FN/PDL after 8-hours (ColIV 0.023 ± 0.002 *vs.* FN 0.009 ± 0.003 µmol/min/mg) and 24-hours (ColIV 0.020 ± 0.002 *vs.* FN 0.006 ± 0.001 µmol/min/mg) (Figure 4.4). However, there was no significant difference in glucose consumption between 5-Aza treated CDCs on FN and ColIV at any time point during 72 hours.

Nevertheless, there was significant differences in glycolytic flux between control and 5-Aza treated cells, in that the level of glycolysis was reduced significantly in 5-Aza treated CDCs relative to their controls in both ColIV at 8- (0.008 ± 0.0007 µmol/min/mg), 24- (0.004 ± 0.0004 µmol/min/mg) and 48-hours (0.004 ± 0.0004 µmol/min/mg); and FN at 48- (0.002 ± 0.0000 µmol/min/mg) and 72-hours (0.002 ± 0.0000 µmol/min/mg) (Figure 4.4). There was no significant difference in control CDCs on FN over 8, 24, 48 and 72-hours relative to each other (Figure 4.4).

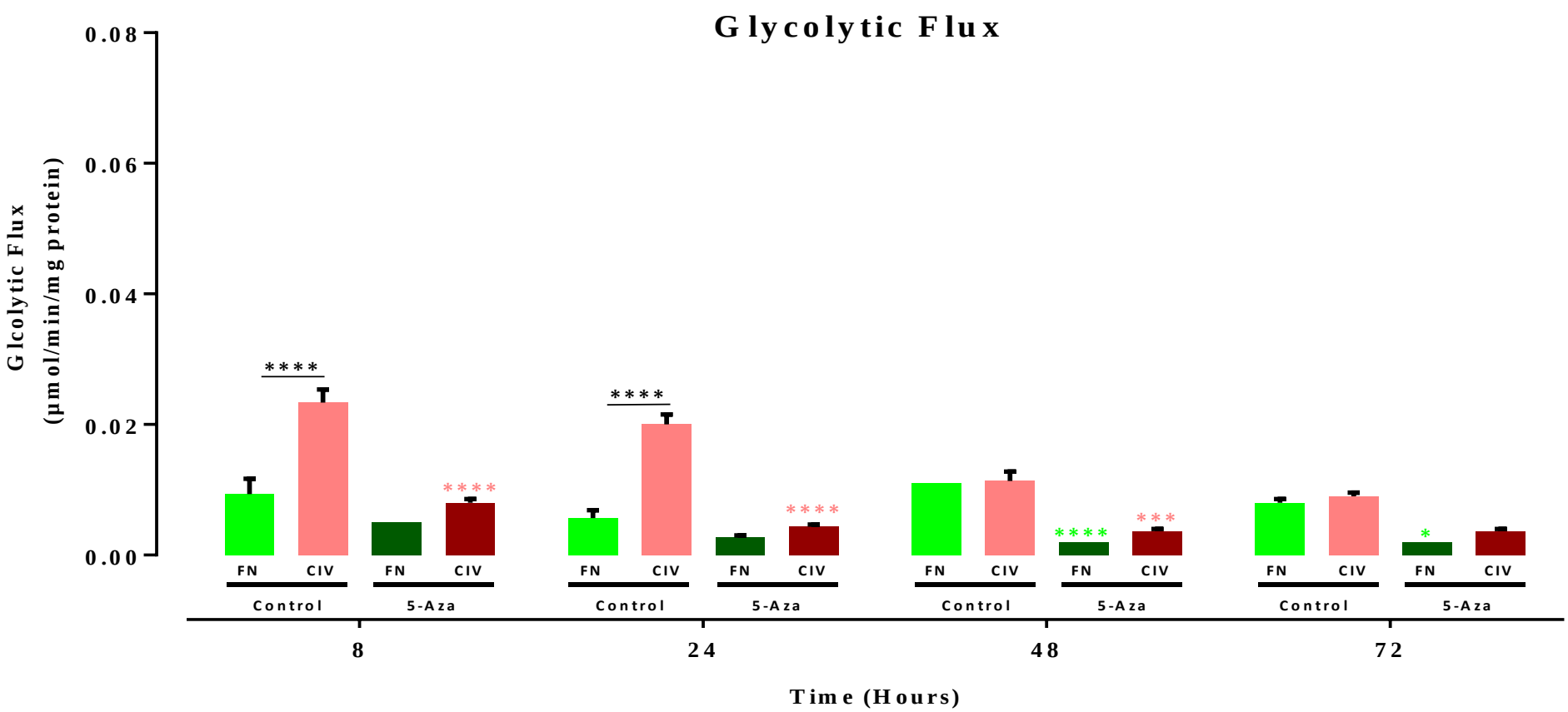



***Figure 4.4 The rate of glycolysis in control and 5-Aza treated P2-CDCs created through FN/PDL and ColIV/HD protocols.*** *The level of glycolytic flux was assessed by adding [5-$^{3}$H]glucose into the culture medium of both control and 3-weeks 5-Aza+AA treated CDCs, sample medium were collected at different intervals, 8-72 hrs, $^{3}H_2O$, glycolysis by-product, was separated from $^{3}$H-glucose using a dowex anion exchange column, followed by scintillation counting of $^{3}H_2O$ radioactivity in the eluate. Abbreviations: AA: Ascorbic Acid; ColIV/HD: Collagen IV/Hanging Drop; FN/PDL: Fibronectin/Poly-D-Lysine; P2-CDCs: Passage 2-Cardiosphere-Derived Cells, 5-Aza: 5-azacytidine. Data are presented as mean ±SEM (n=3) and assessed using a two-way ANOVA with Tukey post hoc test. Multicolour stars indicate multiple comparisons vs. control at each interval. *: $p < 0.01$; ***: $p < 0.004$; ****: $p < 0.0001$.*

#### 4.4.1.2 Lactate efflux in control and treated P2-CDCs

To support the results from glycolytic flux and to determine the level of lactate efflux, sample media were collected over 72-hours. The results revealed that there was no significant difference in lactate production between control ColIV and FN baseline P2-CDCs, at 8-, 24, and 48-hrs except at 72-hrs (FN control 0.02 ± 0.0008 vs. ColIV control 0.06 ± 0.0005 µmol/min/mg with $p = 0.0007$) (Figure 4.5). Likewise, there were no differences in lactate production by control ColIV baseline CDCs over the 72 hours. However, lactate level was decreased in control FN base CDCs at 48-hrs (0.02 ± 0.0005 µmol/min/mg) relative to 8-hrs (0.05 ± 0.005 µmol/min/mg; $p = 0.004$) and remained unaltered until 72 hours (Figure 4.5). Furthermore, lactate production from 5-Aza treated CDCs was considerably decreased in both FN (at 8-hrs: 0.01 ± 0.0006 and 24-hrs: 0.01 ± 0.0005 µmol/min/mg) and ColIV (24-hr: 0.02 ± 0.0003, 48-hrs: 0.01 ± 0.0004, and 72-hrs: 0.01 ± 0.0003 µmol/min/mg) relative to their controls at each interval with $p < 0.05$ (Figure 4.5). However, there was no significant differences in between FN and ColIV 5-Aza treated CDCs, except at 8-hrs (FN-8hrs: 0.01 ± 0.0006 vs. ColIV-8hr: 0.04 ± 0.02 with $p = 0.03$ µmol/min/mg) (Figure 4.5).

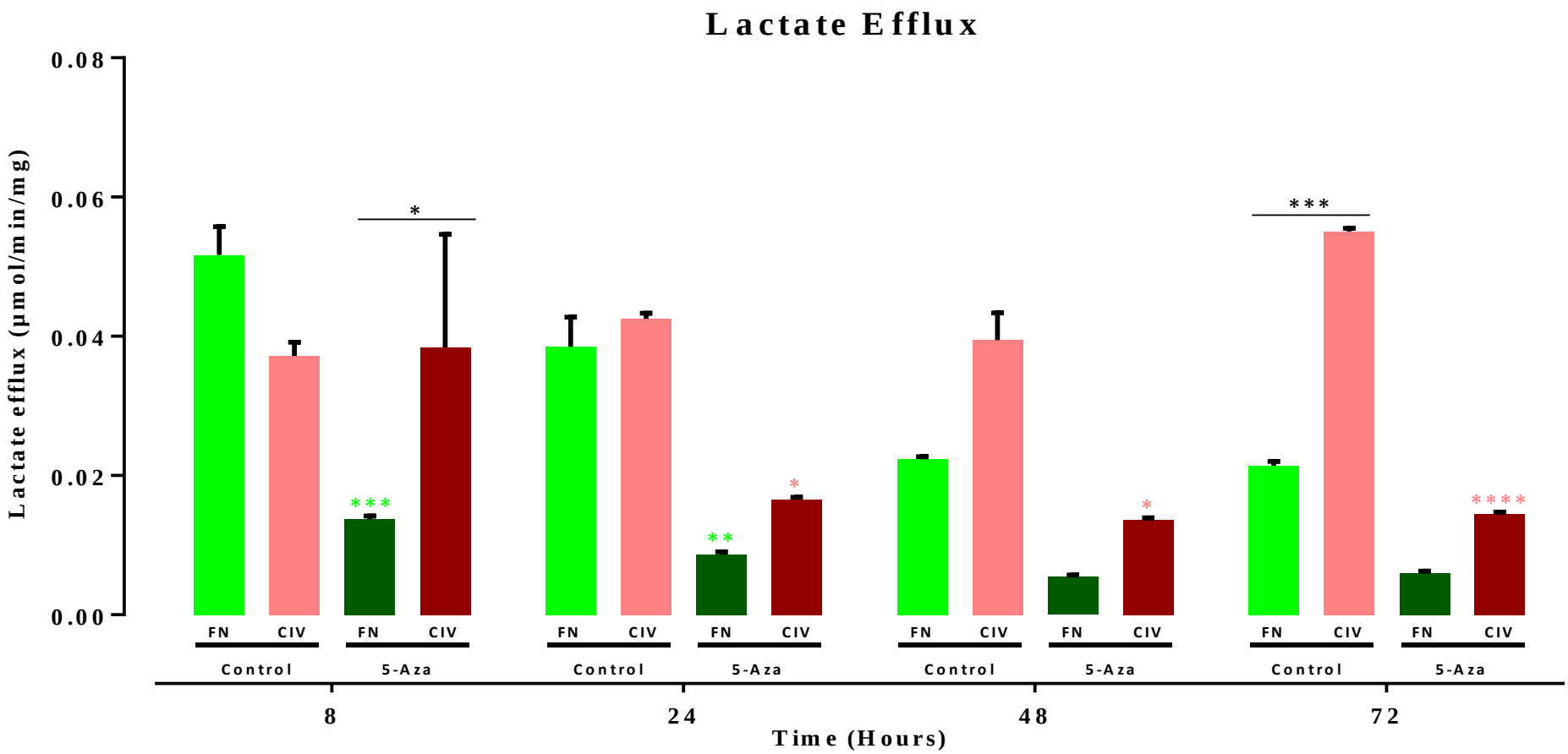



***Figure 4.5 The rate of lactate efflux in control and 5-Aza treated P2-CDCs created through FN/PDL and ColIV/HD protocols.*** *The level of lactate production was assessed by collecting sample medium from both control and 3-weeks 5-Aza+AA treated CDCs at different intervals, 8-72 hrs, followed by analysing lactate concentration in the sample medium using ABX Pentra 400. Abbreviations: AA: Ascorbic Acid;* ColIV*/HD: Collagen IV/Hanging Drop; FN/PDL: Fibronectin/Poly-D-Lysine; P2-CDCs: Passage 2-Cardiosphere-Derived Cells, 5-Aza: 5-azacytidine. Data are presented as mean ± SEM (n=3) and assessed using a two-way ANOVA with Tukey post hoc test. Multicolour stars indicate multiple comparisons vs. control at each interval. *: $p < 0.01$; **: $p < 0.001$; ***: $p < 0.004$; ****: $p < 0.0001$.*

### 4.4.2 Substrate oxidative metabolism in control and treated P2-CDCs

To determine the level of oxidative metabolism in control and 5-Aza treated CDCs, several different $^{14}C$-radiolabelled substrates were added individually into the substrate free culture medium and assessed for oxidation level using the $^{14}CO_2$ capture technique. The results from glucose oxidation in control P2-CDCs on FN and ColIV revealed that the level of oxidation was very low (FN 5.4 x $10^{-5}$ ± 6 x $10^{-6}$ *vs*. ColIV 4 x $10^{-6}$ ± 9 x $10^{-6}$ µmol/min/mg) with no major differences between the two groups (Figure 4.6). Nevertheless, glucose oxidation in 3-weeks 5-Aza+AA treated P2-CDCs was increased significantly in both FN (1 x $10^{-3}$ ± 6 x $10^{-5}$ µmol/min/mg, $p < 0.0001$) and ColIV (1 x $10^{-4}$ ± 8 x $10^{-6}$ µmol/min/mg, $p = 0.001$) relative to their controls (Figure 4.6).

Furthermore, glutamine oxidation showed that the control P2-CDCs on ColIV had the highest level of oxidation (ColIV 3 x $10^{-4}$ ± 3 x $10^{-5}$ µmol/min/mg) compared to control FN (FN 1.6 x $10^{-4}$ ± 6 x $10^{-5}$ µmol/min/mg) with $p = 0.02$, but this was reduced considerably when the cells had been treated with 5-Aza+AA for 3-weeks (1 x $10^{-4}$ ± 1 x $10^{-5}$, $p = 0.005$ µmol/min/mg) (Figure 4.6).

Moreover, palmitate oxidation revealed that control P2-CDCs on FN and ColIV had a very low level of oxidation (FN 9 x $10^{-5}$ ± 6 x $10^{-5}$ *vs*. ColIV 9 x $10^{-5}$ ± 6 x $10^{-5}$ µmol/min/mg; $p > 0.05$) (Figure 4.). The oxidation level was significantly increased in FN P2-CDCs when treated with 5-Aza+AA for 3-weeks (1 x $10^{-3}$ ± 6 x $10^{-4}$ µmol/min/mg; $p = 0.01$) relative to controls (Figure 4.6).

In addition, pyruvate and acetoacetate oxidation in both controls and 5-Aza treated cells on FN or ColIV showed a much higher rate of oxidation relative to other substrates (glucose, glutamine and palmitate) (Figure 4.6). The Pyruvate oxidation rate was significantly higher in control P2-CDCs on FN (6 x $10^{-3}$ ± 4 x $10^{-4}$ µmol/min/mg) compared to control ColIV (3 x $10^{-3}$ ± 6 x $10^{-5}$ µmol/min/mg) with $p = 0.054$. However, this was reduced significantly compared to the controls in 5-Aza+AA treated cells in FN (3 x $10^{-3}$ ± 8 x $10^{-4}$ µmol/min/mg, $p = 0.002$) but increased, compared to controls, in CIV (6 x $10^{-3}$ ± 2 x $10^{-4}$ µmol/min/mg, $p = 0.0004$) so that pyruvate oxidation in 5-Aza treated cells on ColIV was significantly higher than that in 5-Aza treated cells on FN ($p = 0.0005$; Figure 4.6). Likewise, acetoacetate oxidation level was significantly higher in FN and ColIV control P2-

CDCs (FN 2 x $10^{-2}$ ± 3 x $10^{-3}$, ColIV 2 x $10^{-2}$ ± 3 x $10^{-3}$ µmol/min/mg) (Figure 4.6). However, the oxidation level was reduced considerably in 5-Aza+AA treated P2-CDCs (FN 2 x $10^{-3}$ ± 1 x $10^{-3}$, ColIV 8 x $10^{-3}$ ± 1 x $10^{-3}$ µmol/min/mg) (Figure 4.6).

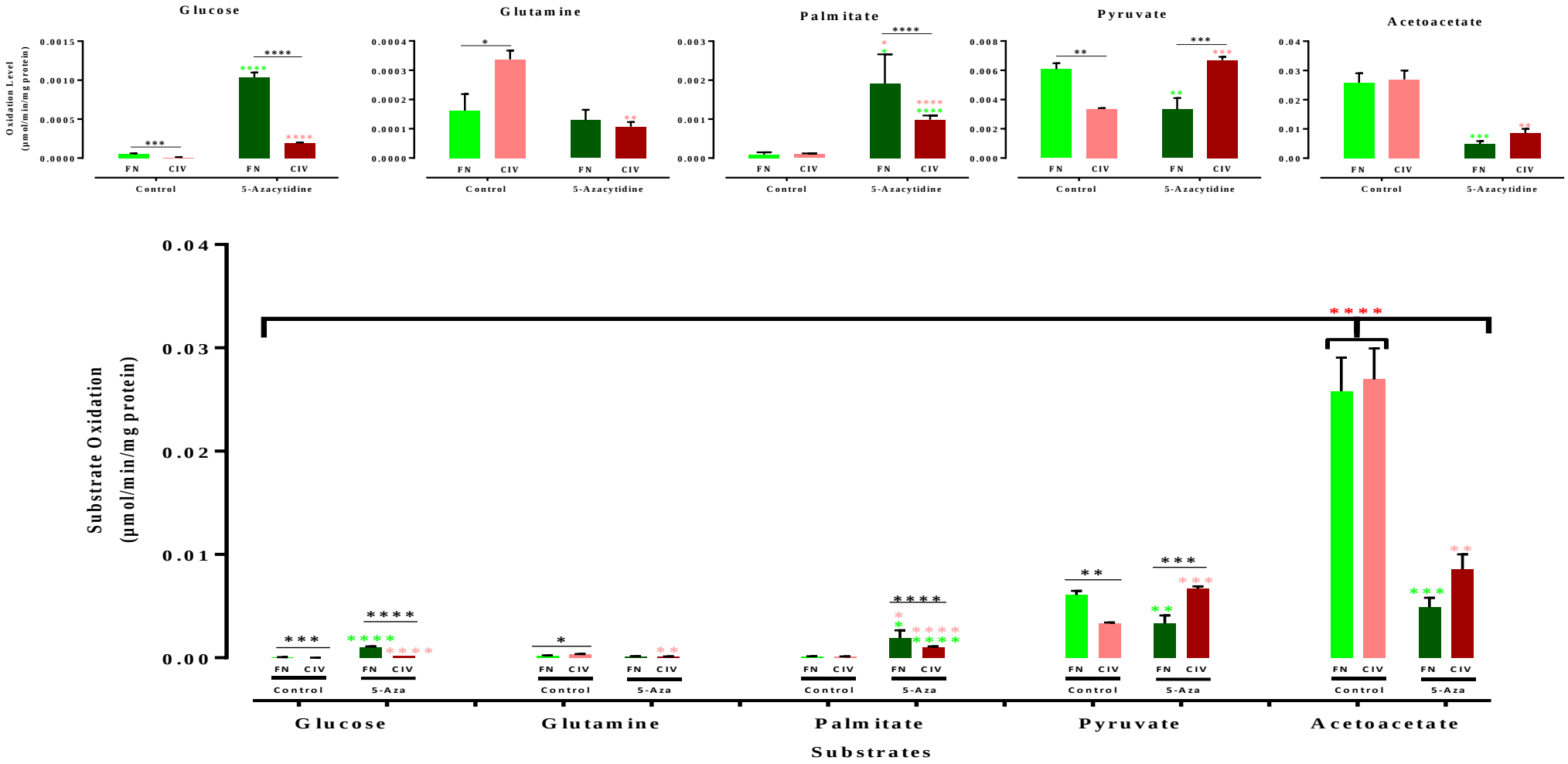



***Figure 4.6 The rate of substrate oxidative metabolism in control and cardiomyogenic differentiated P2-CSCs.*** *The level of oxidative metabolism of different substrates including $^{14}$C-glucose, $^{14}$C-glutamine, $^{14}$C-palmitate, $^{14}$C-pyruvate and $^{14}$C-acetoacetate was assessed in control and 3-weeks 5-Aza+AA treated P2-CDCs created through FN/PDL or ColIV/HD using $^{14}CO_2$ capture technique. Abbreviations: ColIV/HD: Collagen IV/Hanging Drop; FN/PDL: Fibronectin/Poly-D-Lysine; P2-CDCs: Passage 2-Cardiosphere-Derived Cells, 5-Aza: 5-Azacytidine. Data are presented as mean ± SEM (n=4) and assessed using a two-way ANOVA with Tukey post hoc test. Multicolour stars indicate multiple comparisons vs. control for each substrate. *: p < 0.05; **: p < 0.001; ***: p < 0.004; ****: p < 0.0001.*

### 4.4.3 Main source of Adenosine Triphosphate (ATP) production in control and treated P2-CDCs

Substrates can produce different levels of adenosine triphosphate (ATP) depending on the metabolic pathway, 1 mole of glucose produces 2 moles of ATP during glycolysis, but it produces 31 moles of ATP in oxidative metabolism. Moreover, during oxidative metabolism 1 mole of glutamine, pyruvate, acetoacetate, and palmitate produce 20, 12.5, 20, 106 moles of ATP, respectively. To determine the level of ATP produced in control and differentiated CDCs was determined from the data for glycolytic flux and substrate oxidation (Table 4.1).

The results from these calculations revealed that there is no significant difference in ATP production between glycolytic flux (control and 5-Aza treated), glucose oxidation (FN 5-Aza treated), palmitate (control and 5-Aza treated), and pyruvate (control and 5-Aza treated) (Figure 4.7). Nevertheless, acetoacetate oxidation produced significantly more ATP relative to the other substrates ($p < 0.0001$, Figure 4.7).

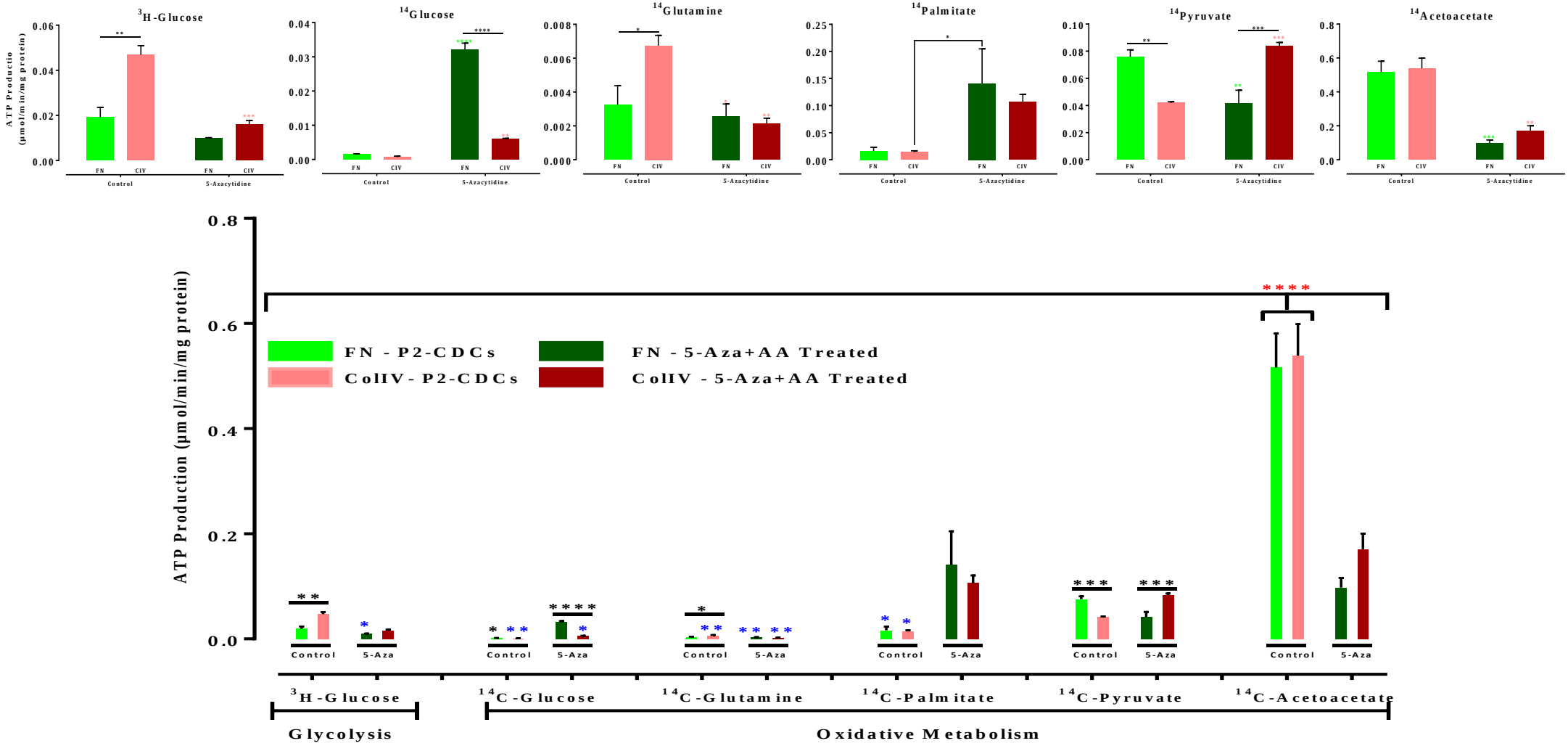



***Figure 4.7 The rate of adenosine triphosphate (ATP) production in control and 5-Aza treated P2-CDCs created through FN/PDL and ColIV/HD protocols.*** *The level of ATP production is calculated based on the level of glycolytic flux and oxidative metabolism. Abbreviations: ColIV/HD: Collagen IV/Hanging Drop; FN/PDL: Fibronectin/Poly-D-Lysine; P2-CDCs: Passage 2-Cardiosphere-Derived Cells, 5-Aza: 5 azacytidine. Data are presented as mean ± SEM (n=3) and assessed using a two-way ANOVA with Tukey post hoc test. Black star (**) vs. Palmitate-5-Aza treated cells cultured on FN; Blue stars (*) vs. Acetoacetate-5-Aza treated cells cultured on ColIV; Red stars (*): Acetoacetate-controls on FN and ColIV vs. all other conditions. *: p < 0.01; **: p < 0.001; ****: p < 0.0001.*

## 4.4.4 Molecular profile of metabolic pathways

To determine the level of mRNA expression of genes involved in glycolysis and oxidative metabolism, control, and 3-weeks 5-Aza treated P2-CDCs, were analysed using qRT-PCR.

### 4.4.4.1 Molecular profile of glucose metabolism in control and treated P2-CDCs

The level of mRNA expression of genes involved in glucose metabolism was determined by looking at the glucose transporters 1 and 4 (GLUT1 and GLUT4), pyruvate dehydrogenase kinase isozyme 1 and 4 (PDK1 and PDK4).

Fold changes in qRT-PCR results demonstrated a high level of GLUT1 expression in control P2-CDCs on ColIV compare to the control FN with $p < 0.0001$ (Figure 4.8). However, this was decreased ($p < 0.0001$) when cells had been treated with 5-Aza for three weeks (Figure 4.8). In contrast, the GLUT4 expression level was very low in controls on FN and ColIV but increased significantly after treatment with 5-Aza (Figure 4.8).

Furthermore, qRT-PCR results demonstrated that PDK1 and PDK4 mRNA expression was the same in control P2-CDCs on FN and ColIV at a very low level (Figure 4.8), but the level of expression was significantly increased in 5-Aza treated P2-CDCs on FN ($p < 0.0001$) and ColIV ($p = 0.008$) compared to the controls, with the most highly significant increase in FN 5-Aza treated cells ($p < 0.0001$) (Figure 4.8).

### 4.4.4.2 Molecular profile of fatty acid oxidation

The level of mRNA expression of genes involved in fatty acid oxidation was determined for the fatty acid transporters, CD36 and CPT1B, and fatty acid metabolism genes including peroxisome proliferator-activated receptor alpha (PPARα), malonyl-CoA-acyl carrier protein transacylase (MCAT), and Acyl-Coenzyme A dehydrogenase (ACADM).

Relative to the control P2-CDCs on FN and ColIV, the level of CD36 expression was significantly higher in 5-Aza treated cells both on FN and ColIV ($p < 0.0001$) (Figure 4.8). Likewise, CPT1B

expression was at a very low level in control P2-CDCs on FN and ColIV, whereas the level of expression was significantly increased in 5-Aza treated P2-CDCs on FN ($p < 0.0001$) and ColIV ($p = 0.04$) compared to the controls. In both cases, mRNA expression was significantly higher in FN 5-Aza treated cells compared with those on ColIV ($p < 0.0001$) (Figure 4.8).

Furthermore, qRT-PCR results for the PPARα gene revealed that the level of expression was significantly higher in 5-Aza treated P2-CDCs on FN ($p < 0.0001$) and ColIV ($p = 0.005$) relative to their controls with highest expression in differentiated cells on FN compared to ColIV with $p < 0.0001$ (Figure 4.8). Similarly, relative to the controls on FN and ColIV, MCAT expression level was significantly higher in 5-Aza treated cells cultured on FN ($p < 0.0001$) and ColIV ($p < 0.0001$), with the highest expression in differentiated cells cultured on FN compared to those cultured on ColIV ($p < 0.0001$). Likewise, ACADM mRNA expression was highest in the 5-Aza treated cells cultured on FN and ColIV relative to the controls cultured on FN and ColIV with $p < 0.0001$. Yet again, the level of ACADM expression was highest in differentiated cells cultured on FN than in those cultured on ColIV with $p = 0.0003$ (Figure 4.8).

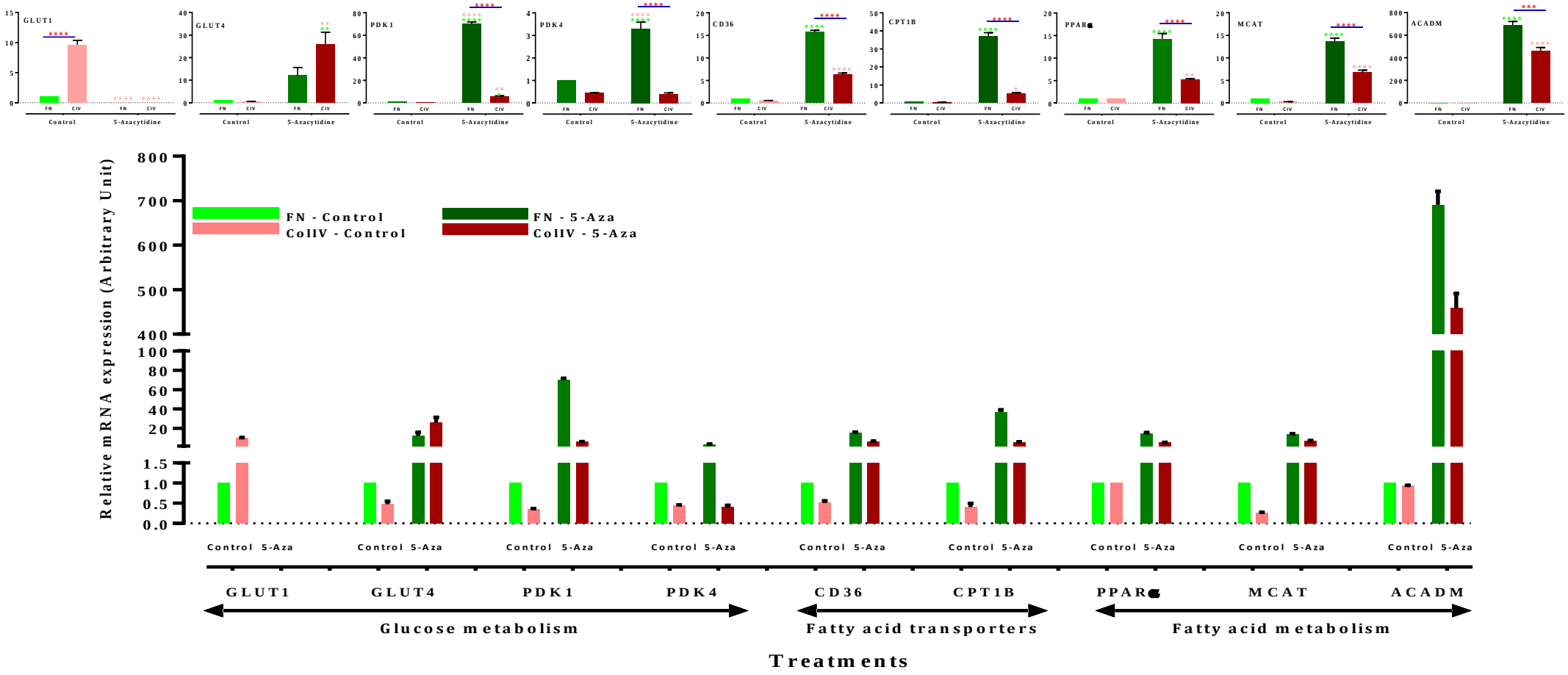



***Figure 4.8 The relative mRNA expression of genes involve in glucose and fatty acid metabolism using qRT-PCR.*** *Control and 3-weeks 5-Aza+AA treated P2-CDCs cultured on either FN or ColIV were used to assess the molecular profile of glucose metabolism including GLUT1, GLUT4, PDK1, and PDK4, fatty acid transporters including FAT/CD36, CPT1B, and fatty acid metabolism including PPARα, MCAT, and ACADM. The mRNA expression was normalized to the geometric mean of Actb and β2M as reference genes and FN control as calibrate. Abbreviations: ACADM: acyl-Coenzyme A dehydrogenase; CPT1B: carnitine palmitoyltransferase I; FAT/CD36: fatty acid translocase/cluster of differentiation 36; GLUT1: glucose transporter-1; GLUT4: glucose transporter-4; MCAT: Malonyl CoA-acyl carrier protein transacylase; PDK1: pyruvate dehydrogenase kinase, isozyme 1; and PDK4: pyruvate dehydrogenase kinase, isozyme 4; PPARα: peroxisome proliferator-activated receptor alpha; P2-CDCs: Passage 2-Cardiosphere-Derived Cells. Data are presented as mean ± SEM (n=3) and assessed using a two-way ANOVA with Tukey post hoc test. Multicolour stars indicate multiple comparisons between groups and FN and ColIV control; *: $p < 0.01$; **: $p < 0.001$; ****: $p < 0.0001$.*

### 4.4.4.3 Protein expression changes

Protein expression was assessed using Western blotting. No signal was detected for CD36, MCAD and UCP3 in any cells assayed although the signal was detected from the positive control(s) (Figure 4.9).

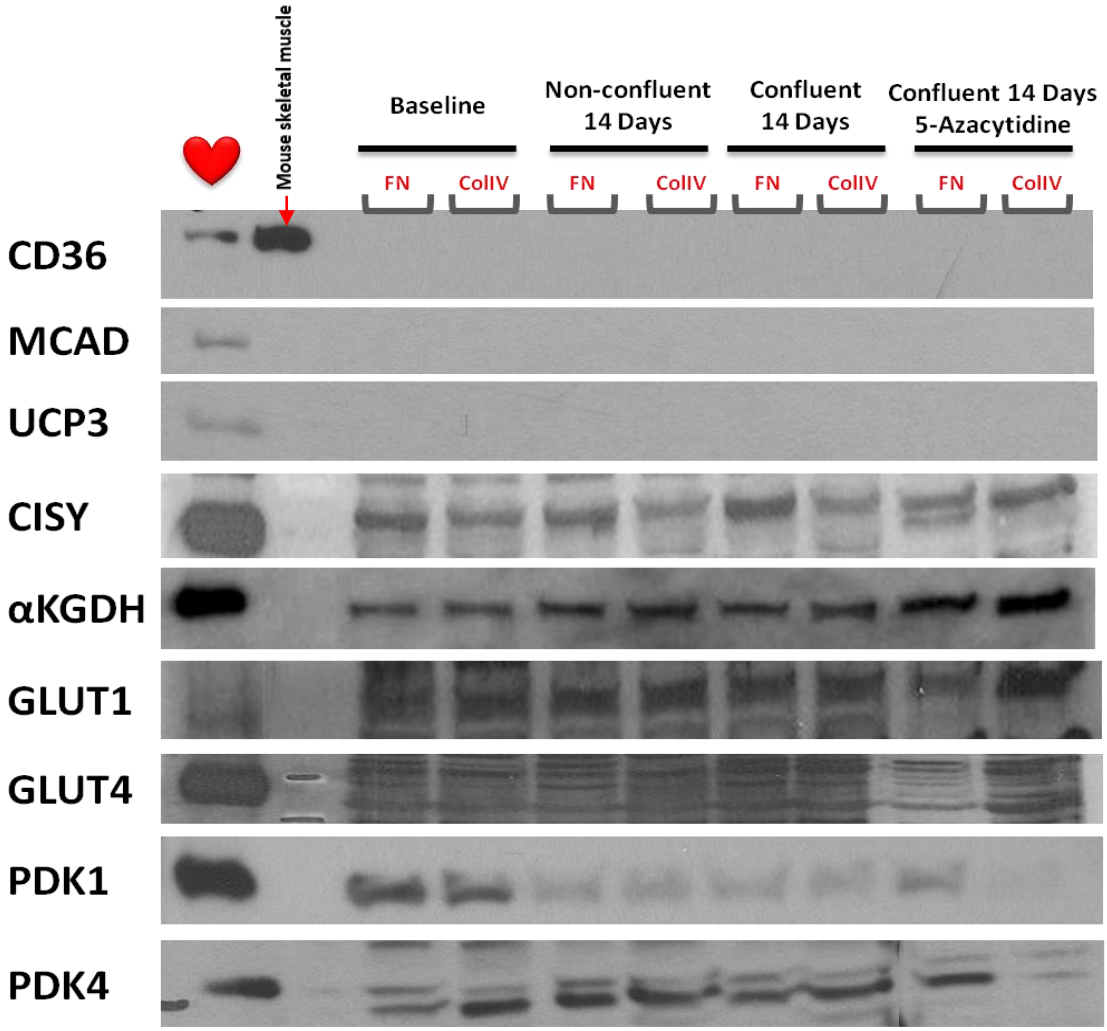



***Figure 4.9 Immunoblotting gels showing control and 5-Aza treated P2-CDCs expressed proteins involved in glucose metabolism and citric acid cycle, but not fatty acid oxidation.*** *Control and 3-weeks 5-Aza+AA treated P2-CDCs cultured on either FN or ColIV were used to assess the biochemical profile of glucose metabolism (PDK 1 and 4, Glut1 and 4), citric acid cycle (CISY and αKGDH), and fatty acid metabolism (CD36, MCAD, and UCP3). Adult rat heart lysates were used as positive controls in all gels, and mouse skeletal muscle was used for CD36 only. Abbreviations: αKGDH: alpha-Ketoglutarate Dehydrogenase; CD36: Cluster of differentiation 36; CISY: Citrate synthase; ColIV: Collagen type IV; FN: Fibronectin substrate; Glut1 and 4: Glucose transporter 1 and 4; MCAD: medium-chain acyl-CoA dehydrogenase; PDK1 and 4: Pyruvate dehydrogenase lipoamide kinase 1 and 4; UCP3: uncoupling protein 3.*

The glucose transporter (Glut) family comprises integral membrane transporter proteins found in most mammalian cells that catalyse the entry of monosaccharide sugars such as glucose into cells[265]. In this study, cells cultured on ColIV had a significantly higher level of GLUT1 protein expression in non-confluent (ColIV: 1.64 ± 0.15 vs. FN: 0.55 ± 0.10 with $p < 0.0001$), confluent (ColIV: 1.44 ± 0.11 vs. FN: 0.35 ± 0.02 with $p < 0.0001$) and 5-Aza treated (ColIV: 1.48 ± 0.09 vs. FN: 0.93 ± 0.16 with $p = 0.02$) P2-CDCs compared with those cultured on FN (Figure 4.10). In addition, differentiated cells cultured on ColIV demonstrated considerably higher level of GLUT4 protein expression (2.06 ± 0.49) compared to control cells cultured on FN (1.0 ± 0.0; $p = 0.001$) and the rest of conditions with $p < 0.0001$ including ColIV baseline (0.75 ± 0.04); non-confluent (FN: 0.72 ± 0.02 & ColIV: 0.60 ± 0.11); confluent (FN: 0.57 ± 0.08 & ColIV: 0.78 ± 0.07) and FN 5-Aza (0.67 ± 0.07) treated cells (Figure 4.10).

Furthermore, pyruvate dehydrogenase kinase 1 (PDK1) expression level was significantly higher in control cells on FN (0.42 ± 0.05) with $p < 0.0001$ compared to all other conditions including non-treated P2-CDCs, ColIV baseline (0.27 ± 0.06), non-confluent (FN: 0.11 ± 0.03 & ColIV: 0.13 ± 0.03), confluent (FN: 0.11 ± 0.02 & ColIV: 3), and 5-Aza treated P2-CDCs on FN (0.16 ± 0.03) and ColIV (0.05 ± 0.01) (Figure 4.10). Nevertheless, in 5-Aza treated P2-CDCs, FN had a considerably higher PDK1 protein level than ColIV with $p = 0.003$. The results from PDK4 protein expression revealed a high level of protein in ColIV baseline (3.54 ± 0.89) but this was significantly reduced in ColIV non-confluent (1.22 ± 0.57), ColIV confluent (0.98 ± 0.46), and ColIV 5-Aza (0.34 ± 0.13) treated P2-CDCs. In contrast, PDK4 protein level was very low in non-treated FN baseline cells (FN baseline: 1; FN non-confluent: 0.27 ± 0.13; FN confluent: 0.39 ± 0.15), but this was considerably increased after 5-Aza treatment (5.83 ± 1.13) ($p < 0.0001$, Figure 4.10).

Differentiation was increased protein levels of the mitochondrial proteins alpha-ketoglutarate dehydrogenase (αKGDH) and citrate synthase (CISY) in ColIV CDCs treated with 5-Aza but not in those differentiated on FN (Figure 4.10).

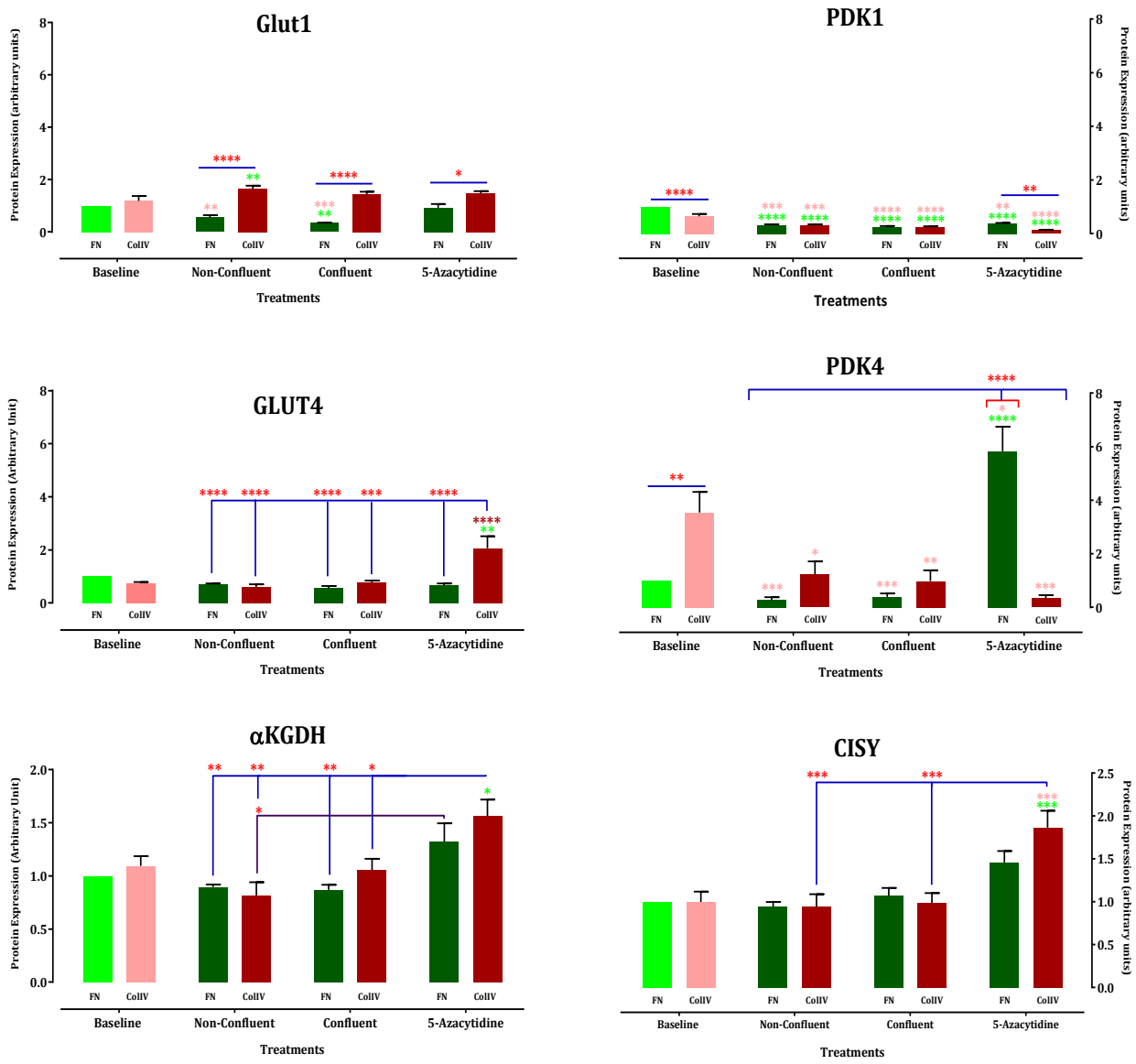



***Figure 4.10 The relative protein expression of proteins involved in glucose, citric acid cycle, and fatty acid metabolism.*** *The expression of proteins involved in glucose metabolism including GLUT1 and 4, PDK1 and 4; citric acid cycle proteins such as CISY and αKGDH were analysed by Western blotting. Abbreviations: αKGDH: alpha-Ketoglutarate Dehydrogenase; CISY: Citrate synthase; ColIV: Collagen type IV; FN: Fibronectin substrate; GLUT1 and 4: Glucose transporter 1 and 4; PDK1 and 4: Pyruvate dehydrogenase lipoamide kinase 1 and 4. Data are presented as mean ± SEM (n=3) and assessed using a two-way ANOVA with Tukey post hoc test. Multicolour stars indicate multiple comparisons between groups and FN and ColIV control; *: p < 0.01; **: p < 0.001; ***: p < 0.004; ****: p < 0.0001.*

### 4.4.4.4 Confocal imaging of Mitochondria

Mitochondrial characterization of control and 5-Aza differentiated P2-CDCs cultured on either FN or ColIV as well as neonatal rat heart cells (a gift from Prof Zaccolo's laboratory) was assessed using Mito Tracker probes (Chapter 2 section 2.10.2). Compared to the neonatal rat heart cells (Figure 4.11A-F), the control P2-CDCs cultured on either FN (Figure 4.12Aa-d) or ColIV (Figure 4.12Da-c) had decreased fluorescence intensity, corresponding to decreased mitochondrial membrane potential (Δψm) activity. Nevertheless, 5-Aza differentiated P2-CDCs cultured on FN (Figure 4.12Ba-d and 4.12Ca-d) showed higher fluorescence intensity or Δψm activity relative to those differentiated on ColIV (Figure 4.12Ea-d).

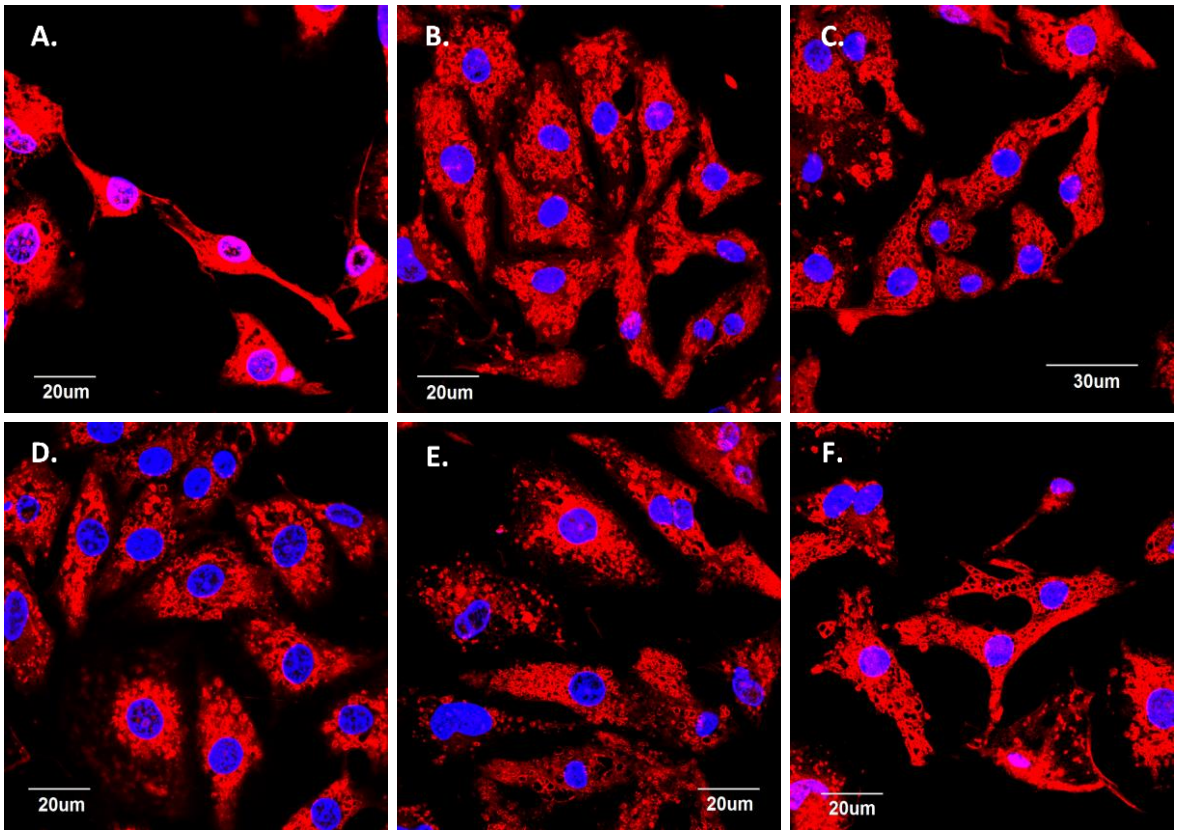



***Figure 4.11 Mitochondria membrane potential (Δψm) in neonatal rat heart cells.*** *Enzymatically isolated cells from neonatal rat heart and cultured on coverslips for 24 hours were incubated with MitoTracker® Red CMXRos reagent (100 nM) at 37°C for 20 min, fixed with PFA and visualized by confocal imaging (A-F). The visible light absorption maximum of Mito Tracker Red CMXRos is 579 nm, and the emission maximum occurs at 599 nm. Nuclei were stained with blue-fluorescent DAPI. Abbreviations: DAPI = 4', 6-diamidino-2-phenylindole. Scale bars are 20 µm and 30 µm.*

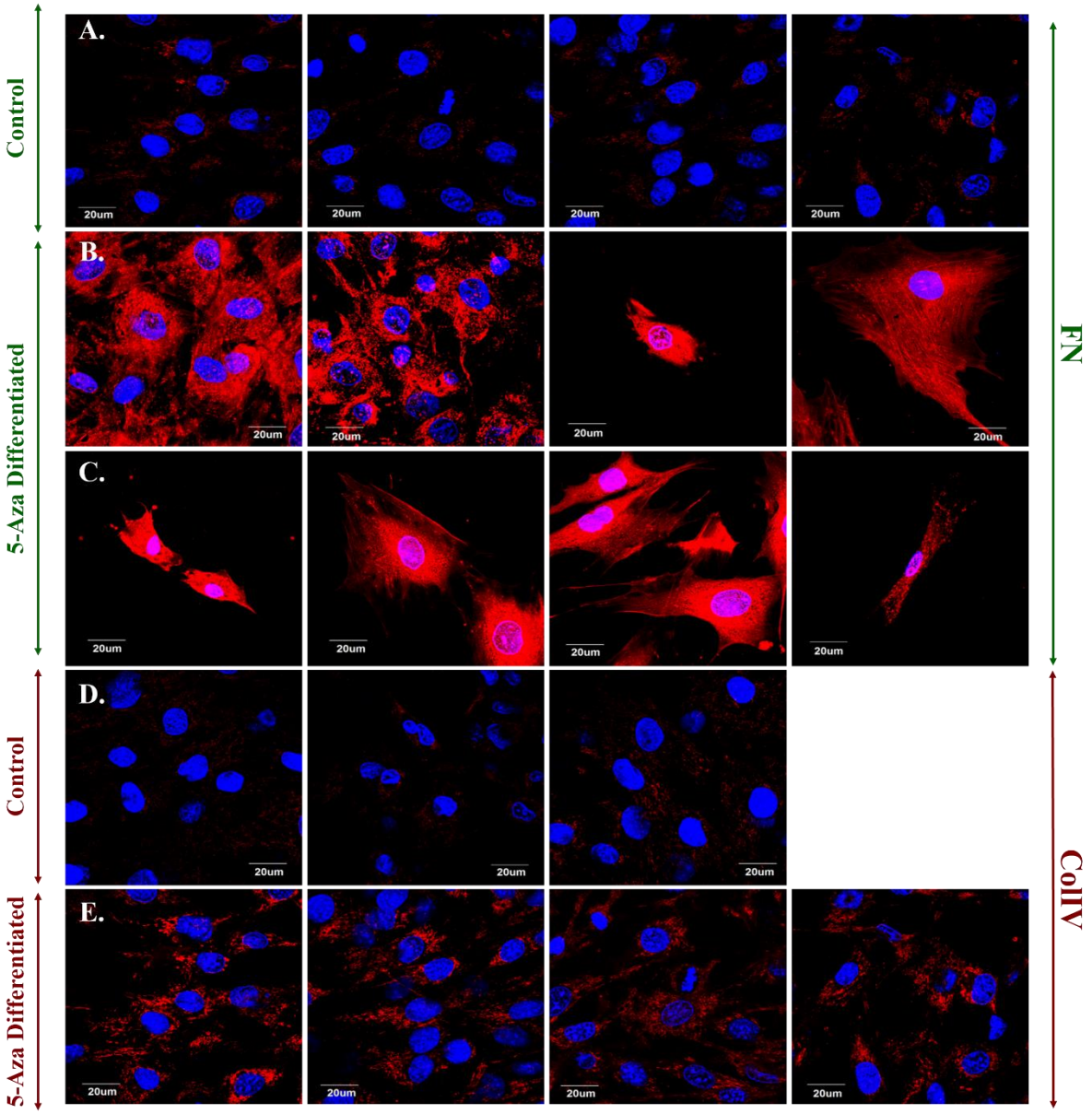



***Figure 4.12 Mitochondria membrane potential (Δψm) increased in 5-Aza+AA differentiated CDCs cultured on FN.*** *Control and 3-weeks 5-Aza+AA differentiated P2-CDCs cultured on pre-coated cover slips with either FN or ColIV were incubated with MitoTracker® Red CMXRos reagent (100 nM) at 37°C for 20 min, fixed with PFA and visualized by confocal imaging. The visible light absorption maximum of Mito Tracker Red CMXRos is 579 nm, and the emission maximum occurs at 599 nm. Nuclei were stained with blue-fluorescent DAPI. Abbreviations: AA: ascorbic acid; 5-Aza: 5-azacytidine; P2-CDCs = Passage 2 Cardiosphere-Derived Cells, DAPI = 4', 6-diamidino-2-phenylindole. Scale bars are 20 µm.*

## 4.5 Discussion

### *Principal finding*

The work in this chapter was the first to investigate *ex vivo* metabolism of isolated and expanded cardiac stem/progenitor cells, created through both FN/PDL and ColIV/HD techniques, before and after 3-weeks differentiation with 5-Azacytidine. Here we determined the rates of the various pathways involved in energy metabolism and the source of ATP production in those cells. In summary, the results revealed that the control P2-CDCs are more glycolytic, however, they start switching to more oxidative metabolism when differentiated with 5-Azacytidine for 3-weeks.

### *High glycolytic flux in control P2-CDCs cultured on ColIV but significantly reduced when differentiated with 5-Aza on FN*

The glucose transporter family (GLUT1-4) comprises an integral membrane transport protein that catalyses the entry of monosaccharide sugars such as glucose into mammalian cells[265]. Studies have shown that there is a shift in glucose transporter isoform expression during myogenic differentiation with high GLUT1 expression in myoblasts, which decreased in differentiated contracting myotubes, with a switch to the high-affinity and insulin-sensitive GLUT4 expression[266]. Here in this study GLUT1 expression was higher in non-differentiated control p2-CDCs cultured on ColIV compared with those cultured on FN but was significantly reduced in CDCs cultured on FN or ColIV after differentiation with 5-Aza. In contrast, GLUT4, which is commonly expressed in heart tissue[267], showed significantly higher expression in 5-Aza differentiation CDCs cultured on FN or ColIV in comparison to non-differentiated/control cells.

During mouse preimplantation development in pluripotent stem cells, glucose uptake rises sharply as the embryo upregulates gene expression of GLUT1 and GLUT3[204, 212] associated with increasing lactate synthesis[213]. In the current study, radiolabelled substrate uptake assays revealed that the glycolytic rate was significantly higher in control P2-CDCs cultured on ColIV of those cultured on FN. However, this level was reduced considerably in 5-Aza differentiated cells cultured on either

substrate. As expected, lactate production was significantly higher in control P2-CDCs cultured on ColIV relative to those cultured on FN and reduced significantly in 5-Aza differentiated cells cultured on FN or ColIV relative to the control cells. Nevertheless, the differentiated cells on ColIV had a significant high lactate level compared to differentiated cells on FN. Furthermore, protein analysis revealed a high level of GLUT1 in control P2-CDCs cultured on ColIV compared to those cultured on FN, and the protein level was reduced significantly in 5-Aza differentiated cells cultured on FN.

Pyruvate dehydrogenase kinases (PDK1-4) catalyse phosphorylation and inactivation of the pyruvate dehydrogenase complex (PDC)[268] and are expressed in a tissue-specific manner, with PDK1 limited to the heart muscle, PDK2 in all tissue but low in spleen and lung, PDK3 in rat testis and PDK4 in skeletal muscle and heart[269]. They are activated by ATP, NADH, and acetyl-CoA and inhibited by ADP, NAD+ and CoA-SH and pyruvate[269]. Studies showed that NADH increases the activity of PDK1 by 20%, but NADH and acetyl-CoA increased the activity by 200%. Similarly, NADH increases the activity of PDK4 by 200%[269]. These isoenzymes are traditionally upregulated in a tissue-specific manner in response to starvation and diabetes[270], and it has been shown that PDK1 is responsible for sensing simultaneous changes in intra-mitochondrial concentrations of pyruvate and ADP[269]. PDK4 contributes to the regulation of the adaptive response or long-term[271, 272] control of PDC activity[269]. In addition, quiescent adult stem cells showed expression of PDK1 and PDK4, which inhibit PDH activity and reduce OXPHOS capacity in this cells[215]. Here in this study PDK1 and PDK4 were significantly increased in 5-Aza differentiated CDCs cultured on FN compared to controls and differentiated cells on ColIV. PDK expression inhibits PDH activity, and as the glycolytic flux and lactate production level in these cells were reduced significantly and palmitate oxidation increased in the differentiated cells, this suggests a possible switch to fatty acid oxidation and/or the increased level of ATP, NADH, or Acetyl-CoA may have induced both PDK1 and 4 to be expressed and activated. Furthermore, support for protein analysis revealed that the level of PDK1 and PDK4, were increased in 5-Aza differentiated CDCs cultured on FN compared to those cultured on ColIV. This may suggest the significant reduction of pyruvate oxidation due to the PDK activity, resulting in accumulation of pyruvate. As previous results showed that the level of lactate was

reduced in these cells, it is likely that the pyruvate was converted to alanine, which may be interesting to analyse in future work.

### *Fatty acid transporter genes increased in 5-Aza differentiated CDCs on FN*

Genes involved in fatty acid transport (CD36/FAT and CPT1B) and fatty acid metabolism (PPARα, MCAT, and ACADM) were expressed at a very low level in control or non-differentiated P2-CDCs. However, the expression of these markers was increased significantly when cells were differentiated with 5-Aza especially in those cells cultured on FN compared to differentiated cells on ColIV.

The uptake of fatty acid through the sarcolemma is facilitated through the cluster of differentiation 36 (CD36), an integral cell membrane protein, which functions in long-chain fatty acid uptake to the cytosol, where the fatty acids will be activated by Acyl-CoA synthase (ACS) to form fatty Acyl-CoA derivatives. This is followed by transportation of fatty Acyl-CoA into the mitochondria facilitated by carnitine palmitoyltransferase 1B (CPT1B), which is a mitochondrial enzyme, with a pivotal role in beta-oxidation of long-chain fatty acids, shuttling long-chain fatty acids from the cytosol into the mitochondrial matrix. In the mitochondria, Acyl-CoA is oxidised via β-oxidation[273-276]. Here in this study CD36 and CPT1b mRNA expression was very low in control CDCs cultured on FN or ColIV but increased significantly in both 5-Aza differentiated CDCs especially in cells cultured on FN compared to those differentiated on ColIV.

### *Genes involved in fatty acid metabolism increased in 5-Aza differentiated CDCs on FN*

Peroxisome proliferator-activated receptors alpha (PPARα), which is a transcription factor, functions as a major regulator of lipid metabolism in the heart and some other tissues (liver, brown adipose tissue and kidney)[277]. PPARα is activated under conditions of energy deprivation, which leads to increased uptake, utilization, and catabolism of fatty acids by up-regulation of genes involved in fatty acid transport (CD36) and esterification[278-280], fatty acid mitochondrial import (CPT1)[281, 282], and mitochondrial β-oxidation (MCAD)[279, 283], as well as upregulation of uncoupling protein (UCP3)[284, 285], and regulation of glucose metabolism by upregulating PDK4[286, 287].

The current finding shows that PPARα was expressed at a very low level in control CDCs cultured on FN or ColIV. However, the expression level was increased significantly in both 5-Aza differentiated CDCs especially in cells cultured on FN compared to those differentiated on ColIV. Likewise, acyl-Coenzyme A dehydrogenase (ACADM), is essential for breaking down medium-chain fatty acids, and Malonyl CoA-acyl carrier protein transacylase (MCAT), which is part of a fatty acid synthase complex[288], were barely expressed in control CDCs cultured on FN and/or ColIV; however, their expression levels were increased significantly when differentiated with 5-Aza especially in cells cultured on FN relative to those differentiated on ColIV. However, Western blot analysis did not detect the presence of the proteins involved in fatty acid transporter (CD36) and fatty acid metabolism (MCAD & UCP3) suggesting that mRNA expression had not yet resulted in protein synthesis. However, this is highly unlikely as differentiated cells on FN or ColIV had increased fatty acid oxidation, suggesting that three may have been problems with the Western blotting of those proteins.

### *Acetoacetate was preferred substrate in control CDCs, but oxidation was reduced in differentiated CDCs*

Ketone bodies including 3-hydroxybutyrate (3HB), acetoacetate (ACA), and acetone are characterized as fuels of prolonged starvation, persisting at low levels in the blood in the fed state (<0.1 mM) but increasing up to 6 mM after a fast of approximately 24 hours in the human adult[289]. Usually, ketone bodies have been regarded as an essential fuel for neuronal tissues under these conditions. More recent reports have indicated that consumption of ketone bodies by cells, particularly neurons, may represent a way of reducing oxidative stress[290, 291]. In addition, stem cells tend to reside in an environment where there are low levels of ROS[292], which may be a strategy to aid their survival or their maintenance of the undifferentiated state. Numerous recent reports have indicated a therapeutic role for a ketogenic diet, where a high ratio of fat:carbohydrate intake stimulates ketone body production so that plasma levels may reach 6-8 mM[293]. Such reports range from neuronal protection[291, 294, 295] to more general protection against age-related damage[296, 297].

The current findings show that acetoacetate was the most favourable substrate to be taken up and oxidized by both controls and 5-Aza differentiated P2-CDCs cultured on either FN or ColIV. It may be that the control CDCs produce a high level of ROS during proliferation, glycolysis and lactate production. Hence, ACA oxidation may represent a way of reducing oxidative stress in order to aid survival, aging, and maintenance of the undifferentiated state of CDCs. In addition, recent findings in our laboratory showed that the rates of ROS generation in hMSCs were 4.5-fold lower, on a mole ROS per mole substrate oxidised basis, with an acetoacetate substrate than they are with a glucose substrate (Dr. Mary Board - Unpublished data). Oxidation of ACA was reduced in differentiated cells cultured on FN or ColIV, possibly as differentiated cells have begun to switch to fatty acid oxidation.

### *Pyruvate was 2$^{nd}$ most highly oxidized substrate in both control 5-Aza differentiated CDCs*

Pyruvate is the simplest ketone and a key intermediate in several metabolic pathways. Despite no acknowledged rationale for a preference of pyruvate usage, several studies have found evidence for pyruvate to be used as the only energy and carbon source, with a relatively low $O_2$ consumption rate, by totipotent stem cells (TSCs) as well as primordial germ cells. Oocytes and spermatocytes, use pyruvate secreted by ovarian follicle cells and lactate secreted by testicular Sertoli cells, even though the mitochondria are structurally immature in these cell types[204, 213, 298].

The current findings show that in comparison to the other substrates, pyruvate is the second fastest substrate to be taken up and oxidized by controls and 5-Aza differentiated P2-CDCs cultured on either FN or ColIV. The oxidation level was higher in control cells cultured on FN compared to those control cells on ColIV, reduced in differentiated cells on FN but increased on those differentiated on ColIV.

Control cells have a high proliferation rate and glycolytic flux. When cultured with pyruvate alone, they may use this substrate at a very high level via pyruvate carboxylase (PC) to generate oxaloacetate (OAA) for anaplerosis or gluconeogenesis for nucleotide synthesis, generating NADPH in the process. Nevertheless, in 5-Aza differentiated cells, which show a significantly lower level of

glycolysis, pyruvate would be used via pyruvate dehydrogenase (PDH) to generate Acetyl-CoA (Ac-CoA) for producing ATP, as cells are differentiating more towards cardiomyocytes.

### *Highly oxidized fatty acid, palmitate, in 5-Aza differentiated P2-CDCs on FN*

Palmitic acid or palmitate (salt and esters of palmitic acid) is the most common fatty acid found in animals, plants, and microorganisms[299]. Studies have shown that the long-chain saturated fatty acid palmitate reduces proliferation and induces BM-MSC apoptosis[300]. These effects may be due to the extracellular acidification by respiratory $CO_2$, which contributes 34% of acidification compared to acidification by lactate produced during glycolysis (66%) [301]. In contrast, palmitate had no effect on proliferation or apoptosis of rat calvarial cells (FRC). Palmitate accumulation may lead to a lipotoxic effect on osteoblast differentiation and mineralization, where an increase in fatty acid oxidation may help prevent lipotoxicity[302]. Here in this study palmitate was the third most preferred substrate to be taken up and oxidized by 5-Aza differentiated P2-CDCs cultured on either FN or ColIV, and utilization was significantly higher in differentiated cells cultured on FN. This may suggest that although 5-Aza differentiated CDCs on FN did not start to beat, they have already increased fatty acid oxidation as they differentiated toward cardiomyocytes as well as significantly reducing proliferation, glycolysis and lactate production.

### *Highly oxidized glucose in 5-Aza differentiated P2-CDCs on FN*

During the early stage of mammalian embryonic development, glucose oxidation is inhibited as pyruvate is the only substrate to be used at the pre-implantation stage[298]. Glucose oxidation is the predominant substrate at blastocyst stage onwards[204, 213]. In the healthy heart, 20-30% of energy produced is derived from the oxidation of glucose. During normal oxidative metabolism, glycolytically produced pyruvate is decarboxylated to acetyl-CoA within the mitochondria before entry into the TCA cycle for glucose oxidation[194].

The current study showed that glucose oxidation is minimal in control CDCs but increased following differentiation, particularly on FN. The results suggest that the control CDCs cultured on ColIV are still at the proliferating and undifferentiated stage as they showed minimal glucose oxidation.

However, control cells cultured on FN showed more commitment towards cardiomyogenic differentiation, as they had higher glucose oxidation relative to those on ColIV. Likewise, 3-weeks 5-Aza differentiated CDCs cultured on FN demonstrated substantially higher glucose oxidation compared to those on ColIV.

### *Highly oxidized glutamine in control P2-CDCs on ColIV but decreased when 5-Aza differentiated*

Glutamine is one of the 20 amino acids considered as a conditionally essential amino acid[303] and the most abundant free amino acid in human blood at around 500-900 μmol/l[304]. Studies have shown that glutamine plays a key role in cellular energy metabolism in proliferating cells as an additional source to glucose[305]. Further studies on cardiac progenitor cells revealed that glutamine has a role as a central regulator of metabolism, survival, and proliferation in this cells[306] and that one of the products from glutamine oxidation, α-KG, is sufficient to stimulate both cell proliferation (through mTOR) and mitochondrial activity[306]. However, the current study showed little or no glutamine oxidation in control cells or following differentiation, contrary to that which is reported for other proliferating cell types[305, 306], although control cells on ColIV did show slightly higher glutamine oxidation than those on FN or after differentiation

### *5-Aza differentiated P2-CDCs cultured on FN had increased in mitochondrial membrane potential activity*

MitoTracker® Red CMXRos reagent is one of the fluorescent mitochondrial markers, which covalently binds free sulfhydryls and may have some value in quantifying the mitochondrial membrane potential ($\Delta\psi m$) of cultured cells by the level of the intensity of fluorescence[307]. It is a lipophilic cationic compound that equilibrates across membranes in a Nernstian fashion (balances between the concentration gradient to the electric gradient), accumulating into the mitochondrial membrane matrix space in inverse proportion to the membrane potential, the more negative $\Delta\psi m$ will accumulate more dye and vice versa[308-311]. Here in this study, control stem/progenitor cells cultured on either FN or ColIV have shown less fluorescent intensity or lower mitochondrial $\Delta\psi m$.

However, when CDCs were cultured on FN and treated with 5-Aza for 3-weeks, they started to upregulate either the mitochondrial numbers or Δψm.

## 4.6 Conclusion

In summary we found that the control P2-CDCs cultured on ColIV had the highest rate of glycolysis as they demonstrated significant level of glucose uptake, higher lactate production, higher expression of GLUT1, but low expression of GLUT4, PDK1, PDK4 and fatty acid metabolism (CD36, CPT1, PPARα, MCAT, ACADM), as well as low oxidation level of glucose and palmitate, but higher oxidation in acetoacetate followed by pyruvate and glutamine. In contrast, 5-Aza differentiated cells cultured on FN demonstrated significantly reduced glycolysis by decreased glucose uptake, reduced lactate production, reduced GLUT1 expression, and increased expression of GLUT4, PDK1, PDK4 and genes involved in fatty acid metabolism (CD36, CPT1, PPARα, MCAT, ACADM), increased mitochondrial Δψm as well as high level of oxidation of acetoacetate followed by pyruvate, palmitate, and glucose. As a result, we decided to test compounds to optimise differentiation on cells cultured on ColIV but differentiated on FN, to obtain both optimum expansion and differentiation as well as using small molecules to induce mitochondrial oxidative phosphorylation.

# CHAPTER 5

# Cardiomyogenic Differentiation of Cardiac Progenitor Cells by Metabolic Manipulation using small molecules

## 5.1 Abstract

Transition from a non-contractile stem cell, which normally derives most of its energy needs from anaerobic glycolysis, into a beating cardiomyocyte, which normally derives its energy from aerobic oxidative phosphorylation of fatty acids and carbohydrates, necessitates an obligatory transformation of the metabolic infrastructure with prominent mitochondrial network expansion and a distinctive switch from glycolysis to oxidative phosphorylation. Therefore, the main objective of this project is to stimulate aerobic oxidative phosphorylation in cardiosphere-derived cells using synthetic small molecule(s) including PPARα agonists: WY-14643 and CP-775146, dichloroacetate, butyrate, and a combination of these 4-compounds. These small molecules were added into the cardiomyogenic differentiation medium of P2-CDCs for 30-days, and the samples were assessed for glycolytic flux, oxidative phosphorylation, molecular gene and protein analysis, and confocal imaging. Here, for the first time, rat P2-CDCs treated with cardiomyogenic differentiation medium containing TGFβ and PPARα agonists, WY-14643, started to slow twitch at day-26 and slow beating at day-30 and continued slow beating for three days and then stopped. The results from micrographs demonstrate striking morphological changes in all TGFβ treated P2-CDCs forming 3D tissue structures containing a large bulbous body that supported with two elongated arms to the side of Petri dishes in comparison to control and 3-weeks 5-Aza differentiated P2-CDC which stayed firmly attached to the plate as a monolayer. The results from metabolic studies revealed that the level of glycolysis was considerably reduced in P2-CDCs treated with the PPARα agonist, WY-14643, with an associated increase in oxidative metabolism of fatty acid (palmitate) and carbohydrates (glucose). Molecular analysis of genes and protein assessments showed increased expression of calcium ($Ca^{2+}$) transporter gene of sarcoplasmic reticulum, Serca2a, cardiac-specific genes including cTnnT2, MYH7 (slow twitch), and proteins like cTnnT2, titin, MHC, MLC, and CX43, as well as increased in mitochondrial membrane potential, $\Delta\psi m$ and networking.

## 5.2 Introduction

Transition from a non-contractile stem cell, which normally derives most of its energy needs from anaerobic glycolysis, into a beating cardiomyocyte, which normally derives its energy from aerobic oxidative phosphorylation (OXPHOS) of fatty acids and carbohydrates, necessitates an obligatory transformation of the metabolic infrastructure with prominent mitochondrial network expansion and a distinctive switch from glycolysis to oxidative phosphorylation[214, 312, 313]. To date, *in vitro* cardiomyogenic differentiation of a heterogeneous population of adult rat cardiac stem/progenitor cells (CDCs) has resulted in limited success. Nevertheless, cardiac differentiation takes place following CDCs transplantation[110]. Hence, *in vivo* substrate availability may affect cardiac differentiation as cells experience a dramatic shift in substrate availability from that in stem cell culture medium, which typically contains 20 mM glucose and no free fatty acids (FFA), to that in the plasma comprising ~5 mM glucose and ~ 0.5 mM FFA. For example, we have found that culture of CDCs in low glucose increased expression of PGC-1α, which regulates mitochondrial biogenesis[222].

Studies have found evidence that in the heart, activation of the transcription factor peroxisome proliferator activated receptor α (PPARα) increased expression of fatty acid transporters such as CD36 and CPT1, and oxidation enzymes like MCAD[277] (Figure 5.1). Other studies documented that butyrate can reduce proliferation and induce differentiation, through inhibition of histone deacetylases, thereby allowing transcription of differentiation genes[314]. In addition, β-oxidation of butyrate generates acetyl-CoA, allowing butyrate to replace glucose in the TCA cycle[314] (Figure 5.1). Furthermore, several studies have found evidence that dichloroacetate decreases tumour growth in vitro and in vivo by inhibiting mitochondrial pyruvate dehydrogenase kinase (PDK), which shifts pyruvate metabolism from glycolysis and lactate production to glucose oxidation in the mitochondria[269, 315, 316] (Figure 5.1). In contrast, studies have documented that metabolic conversion from mitochondrial oxidative phosphorylation (OXPHOS) to glycolysis using a small molecule cocktail enhances reprogramming of human primary somatic cells to iPSCs with exogenous

expression of only OCT4[317]. Therefore, it may be possible to manipulate metabolism of stem/progenitor cells into fully functional cardiomyocytes (Figure 5.1).

In addition to metabolism, studies have shown that addition of Transforming growth factor beta (TGFβ), a multifunctional growth factor involved in the cardiac differentiation of ESCs[165, 166], facilitates *in vitro* differentiation of human cardiomyocyte progenitor cells (hCMPC) into electrophysiologically and immunologically mature cardiomyocytes[167, 318]. Nevertheless, previous studies carried out in our laboratory demonstrated the limited success of cardiomyogenic differentiation of mouse CDCs using TGFβ[319], possibly as these cells may still metabolically rely on glycolysis instead of mitochondrial OXPHOS. Therefore, cardiomyogenic differentiation of adult cardiac stem/progenitor cells may be improved by conversion of glycolytic metabolism to mitochondrial OXPHOS via a combination of small molecule(s) and TGFβ.

Hence, the objectives of this study were to assess, for the first time, whether adult rat cardiac progenitors expanded on plastic are able to fully differentiate into beating cardiomyocytes and whether maturation can be stimulated *in vitro* by upregulating fatty acid oxidation using different synthetic small molecule(s) in combination with TGFβ.

The aims of this study were to:

- Induce cardiomyogenic differentiation of P2-CDCs using: TGFβ plus one or more of several different synthetic small molecules including PPARα agonists such as WY-14643 and CP-775146, dichloroacetate, butyrate, and a combination of these four compounds (WY-14643 + CP-775146 + dichloroacetate + butyrate) so called 4-compounds.
- Assess the metabolic pathways (glycolysis and OXPHOS).
- Evaluate the molecular profile of gene and protein expression levels.
- Confocal microscopy

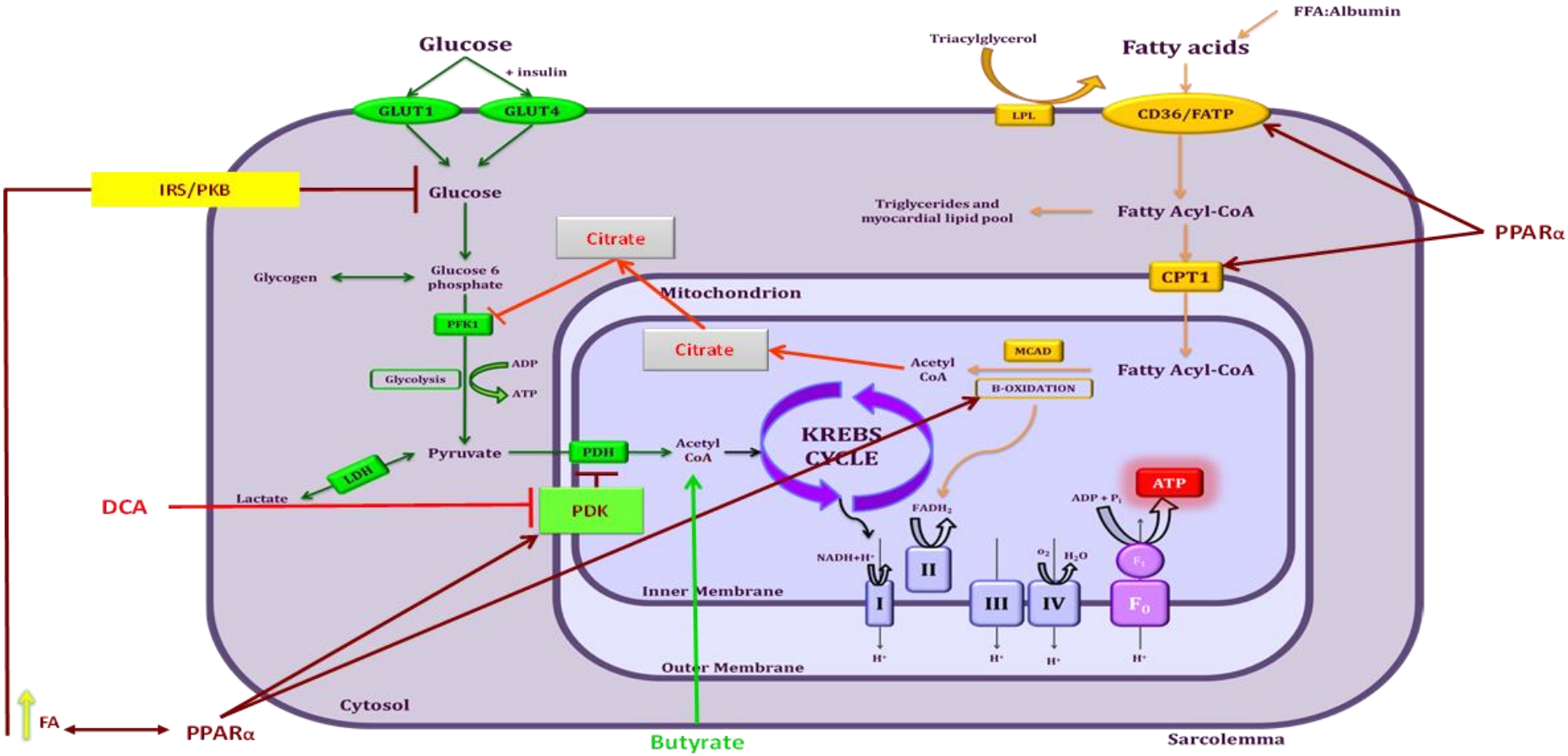



***Figure 5.1 Metabolic manipulation using small molecules.*** *Inhibition of glycolysis by fatty acids (FA) utilization, as accumulation of FA impairs insulin-mediated glucose uptake through inhibition of insulin receptor substrate (IRS) and protein kinase-B (PKB). Increased intracellular FA also activates PPAR-α expression.* ***PPAR-α*** *agonists promotes the expression of genes involved in FA oxidation by increasing CD36, CPT1, and MCAD, as well as PDK4, known to inhibit PDH and pyruvate flux.* ***Butyrate****, Increased acetyl-CoA and NADH caused by the high rate of FA oxidation activate PDK4, leading to further inactivation of PDH. Augmented acetyl-CoA also causes accumulation of citrate in the cytosol, which subsequently inhibits PFK1 and glycolysis.* **Dichloroacetate** (DCA) inhibits PDKs, which shifts pyruvate metabolism from glycolysis and lactate production to glucose oxidation in the mitochondria. *Abbreviations: CD36: Cluster of differentiation protein 36; CPT1:* carnitine palmitoyltransferase 1*; MCAD: Medium-chain acyl-coenzyme A dehydrogenase;* PDK: pyruvate dehydrogenase kinase; *PPAR-α:* peroxisome proliferator activated receptor α.

## 5.3 Methods

### 5.3.1 Overview of designed study

The study design described in this chapter is illustrated in a schematic flow diagram (Fig. 5.1), and the specific experimental methodologies are described below.




***Figure 5.2 Flow diagram of study design.*** *Flow diagram showing an overview of study conceived in this chapter to isolate and expand CSCs through ColIV/HD technique until passage 2, then differentiate P2-CDCs on fibronectin in gelatine coated plates containing CDM-1+5-Aza first, then with CDM-2+TGFβ+AA plus corresponding small molecule(s) and their downstream analysed processing. Abbreviations: AA: Ascorbic Acid; ColIV/HD: collagen type IV/Hanging Drops; CSCs: Cardiac Stem Cells; CDM-1 and -2: Cardiomyogenic Differentiation Medium-1 and -2; FN: fibronectin; TGFβ: Transforming growth factor beta.*

### 5.3.2 Isolation, and expansion of cardiosphere-derived cells

Methods are described in Chapter 2 (See section 2.2). Briefly, P2-CDCs created through ColIV/HD technique were seeded on 1 mg/ml FN/0.1% gelatine coated dishes for further differentiation protocols using different synthetic compound(s) (Figure 5.2).

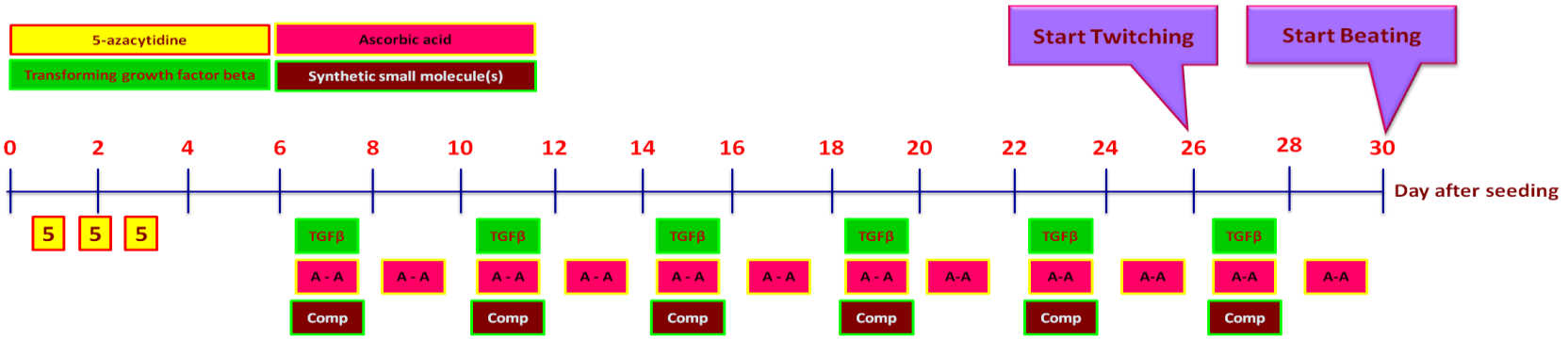
### 5.3.3 Cytotoxicity tests

Cells were treated with 5-Aza or a small molecule for seven days and medium changed every 2-3 day. Cell death was measured at day-1, day-3 and day-7 using "LIVE/DEAD®Cytotoxicity Assay Kit", following the manufacturer's instructions. The condition with the least cytotoxicity from each small molecule was selected for further cardiomyogenic differentiation of P2-CDCs.

### 5.3.4 Cardiomyogenic differentiation of P2-CDCs

Seven different cardiomyogenic differentiation protocols were performed by culturing P2-CDCs on FN-coated plates with media changes as shown in Figure 5.2B, using 5-Aza (5μM) AA (0.1μM), TGF-β (1ng/ml), WY14643 (10μM), CP775146 (1μM), dichloroacetate (10μM), butyrate (1mM), and 4-compounds (including WY14643, CP775146, dichloroacetate, and butyrate with corresponding concentrations) for a total of 30 days treatment (Figure 5.3A). Following differentiation protocols the cells from some of the samples were enzymatically digested and frozen in liquid nitrogen for further molecular analysis (qRT-PCR and Western blot), some were fixed with PFA for immunocytochemistry study and confocal imaging, some live cells stained with MitoTracker, and the rest were kept alive to perform functional metabolic studies using radiolabelled isotopes.

**A.**




**B.**

| No | Type of Conditions | Number of days with their corresponding treatments | | | | | | | |
|---|---|---|---|---|---|---|---|---|---|
| | | 1 | 2 | 3 | 4 | 5 | 6 | 7 ..... 20 ..... 15 .....20..... 30 | |
| 1 | Baseline | | | | | | | | |
| 2 | TGFβ | CDM-1 | | | | | | CDM-2 + AA + TGFβ | |
| 3 | 5-azA + TGFβ | CDM-1 + 5-Aza | | | CDM-1 | | | CDM-2 + AA + TGFβ | |
| 4 | 5-azA + TGFβ + WY-14643 | | | | | | | CDM-2 + AA + TGFβ + WY-14643 | |
| 5 | 5-azA + TGFβ + CP-775146 | | | | | | | CDM-2 + AA + TGFβ + CP-775146 | |
| 6 | 5-azA + TGF + Dichloroacetate | | | | | | | CDM-2 + AA + TGFβ + Dichloroacetate | |
| 7 | 5-azA + TGFβ + Butyrate | | | | | | | CDM-2 + AA + TGFβ + Butyrate | |
| 8 | 5-azA + TGFβ + 4 Compounds | | | | | | | CDM-2 + AA + TGFβ + WY-14643 + CP-775146 + Dichloroacetate + Butyrate | |

***Figure 5.3 Cardiomyogenic differentiation protocols. A. Timeline of cardiomyogenic differentiation procedures.*** *The blue line indicates the number of days after plating. For the first three consecutive days, in all cases apart from Baseline and TGFβ alone, 5 μM 5-Aza (yellow boxes) was added to the culture medium, CDM-1, followed by CDM-1 alone for a further four days. From day-7 forward cells were supplied with CDM-2 containing ascorbic acid (pink boxes), and TGFβ (1ng/ml) added every two days, plus one or more of the small molecule(s) (brown boxes) added twice a week until day-30. The medium was refreshed when is needed.* ***B. Cardiomyogenic differentiation plan.*** *Cardiomyogenic differentiation protocol with specific medium and small molecule(s). Abbreviations: CDM-1 and 2: cardiomyogenic differentiation medium-1 and 2.*

### 5.3.5 Real-time quantitative RT-PCR

The level of gene expression of three different cell markers for cardiac (cTNNT2, MYBPC3, MYH6, MYH7), endothelial (KDR, Cdh5, VEGFa, VEGFb), and smooth muscle (Cnn1, MYH11) cells, as well as calcium transporters (SERCA2A, PLN) and metabolic (MCAT, ACADM, CPT1B, CD36, GLUT1, GLUT4, PPARα, PDK1, PDK4) markers were investigated in controls and differentiated P2-CDCs using qRT-PCR. All qRT-PCR data were normalized to Actb and B2M as the reference genes and baseline as calibrator.

### 5.3.6 Determination of glycolytic flux

A trace of [5-$^{3}$H]glucose (1.48 MBq/mmol) was added to controls and small molecule induced cardiomyogenic differentiated P2-CDCs for 72 hours. Samples were taken at different intervals (1-, 4-, 6-, 8-, 24-, 48-, and 72-hours) and run through prepared Dowex resin ion exchange columns in order to separate $^{3}$H-glucose from $^{3}H_2O$ (Chapter 2, Figure 2.1) and the radioactivity was measured using a liquid scintillation counting machine (See section 2.12).

### 5.3.7 Determination of substrates oxidation rates

The $^{14}CO_2$-capture technique based on the Collins method [224] (Chapter 2, Figure 2.2) was used to determine the oxidative level of different substrates in controls and small molecule induced cardiomyogenic differentiated P2-CDCs including 10 mM glucose containing 21 MBq/mmol D-U-$^{14}$C-glucose and 2 mM palmitate containing 10.27 Mβq/mmol U-$^{14}$C-palmitate (See section 2.13).

### 5.3.8 Calculation of ATP production

Adenosine triphosphate produced through the glycolysis, and oxidative metabolism was calculated based on glycolytic flux and different individual substrate oxidation levels (See section 2.14).

### 5.3.9 Western blot

Whole cell lysates from powdered frozen control and differentiated cells were used to measure protein levels of glucose metabolism (Glut1, Glut4, PDK1, and PDK4), fatty acid metabolism (MCAD, UCP3, CD36) and mitochondrial proteins (αKGDH, citrate synthase) by western blotting.

### 5.3.10 Confocal imaging

Controls and WY-14643+TGFβ induced cardiomyocyte differentiated P2-CDCs cells on coverslips were fixed with PFA, immunolabelled with primary then secondary antibodies for cardiac-specific markers (cTnnT2, MHC, MLC, CX43, and Titin) and scanned using an Inverted Olympus FV1000 Confocal system. In addition, MitoTracker probe was used to stain the mitochondria in these cells and visualised by confocal microscope imaging (Chapter 2.10.2).

## 5.4 Results

### 5.4.1 Cell viability and cytotoxicity

P2-CDCs created through ColIV/HD were seeded into FN pre-coated 96-well plates at a cell density of 10,000 cells/cm$^2$ overnight. The next day cells were treated with different synthetic molecules at two concentrations (Figure 5.4). Treated cells were subjected to cytotoxicity tests on day-1, day-3, and day-7. The results indicated that relative to the culture in CEM, cardiomyogenic differentiation medium-1 (CDM-1) containing 5µM 5-Aza had a high level of toxicity at day-1 ($p < 0.0001$). This was reduced slightly at day-3 ($p = 0.0003$), and by the day-7, when there was no 5-Aza present in the medium, the percentage of dead cells did not differ from that in CEM cultured cells. Treatment with the various compounds at two different concentrations (low and high) caused moderate cytotoxicity in both concentrations at day-3, however by day-7 the % of dead cells did not differ from that in the CEM baseline. Therefore, the highest concentrations of compounds were used for further differentiations (Table 5.1).

| Synthetic Compounds | Concentration (µM) |
|---|---|
| **WY-14643 (PPARα Agonist - 1 )** | **10 or 100*** |
| **CP-775146 (PPARα Agonist - 2 )** | **1 or 10*** |
| **Sodium Dichloroacetate (DCA)** | **10 or 100*** |
| **Sodium Butyrate** | **1 or 10*** |

***Table 5.1 The list of small molecules used for cardiomyogenic differentiation.*** *The two different concentration of each compound were at cytotoxicity tests. *selected candidate concentration.*

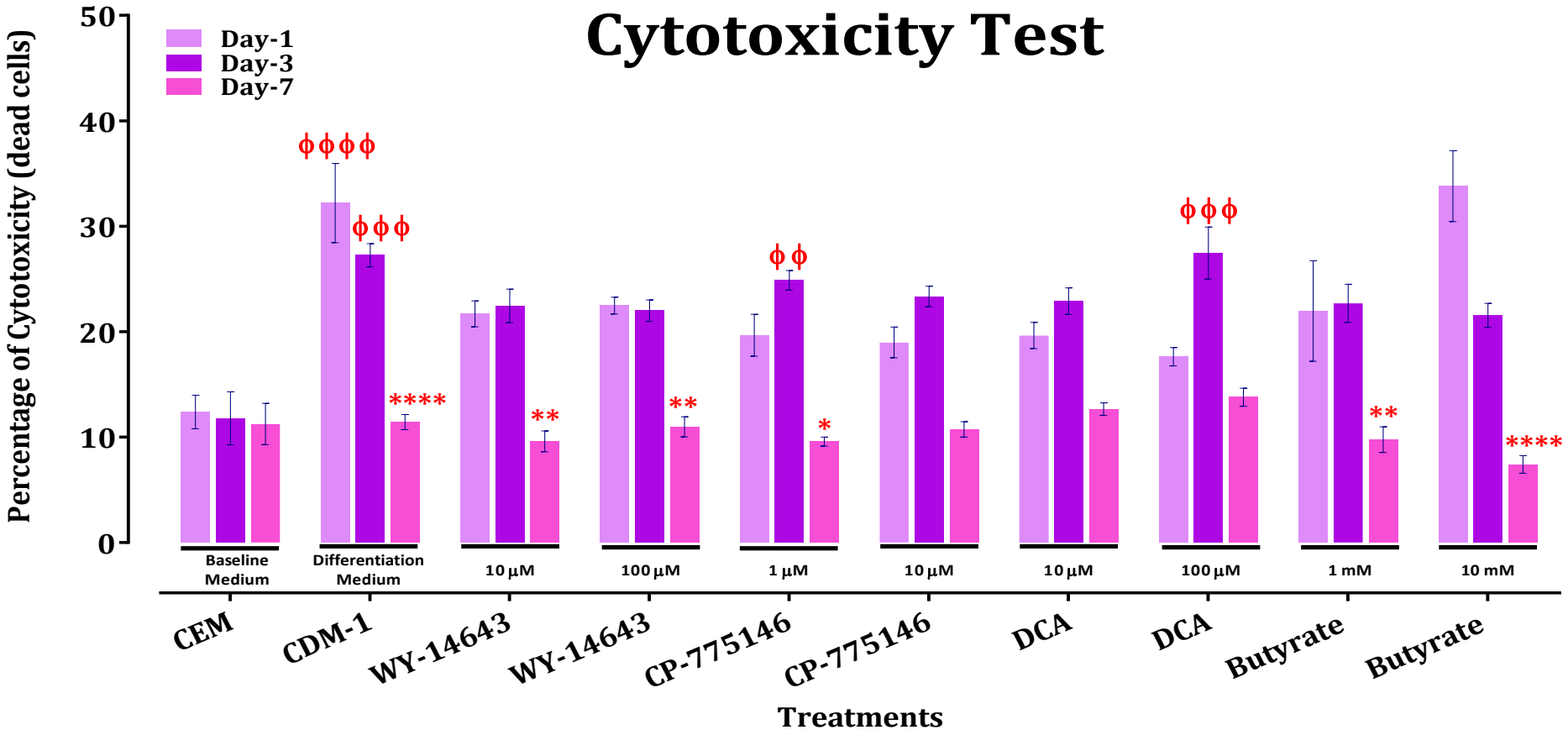



***Figure 5.4 The cytotoxicity test of compounds treated CDCs.*** *Passage 2 CDCs were cultured on fibronectin pre-coated 96-well plates overnight then treated with different drugs for 1-day, 3-days and 7-days and cytotoxicity was assessed using the Live/Dead assay kit. Abbreviations: CDM-1: Cardiomyogenic Differentiation Medium-1; CEM: Complete Explant Medium; DCA: Dichloroacetate. Data are presented as mean ± SEM (n=5) and were analysed using a two-way ANOVA with Tukey post hoc test. *day-7 treatment vs. day-1 treatment; φ compound treatments vs. CEM culture. *or φ: $p < 0.05$; ** or φφ: $p < 0.01$; *** or φφφ: $p < 0.0003$; **** or φφφφ: $p < 0.0001$.*

## 5.4.2 Morphological differences

After 30 days of treating CDCs with differentiation media containing TGFβ plus one or more small molecule(s), an emergence of different cell morphologies was noticed. 5-Aza differentiated cells cultured on either FN or ColIV were attached to the plate firmly as a monolayer with different sizes and shapes (Figure 5.5, I). However, after 30 days of differentiation, a majority of the treated cells started to aggregate and form 3D structures with two elongated arms attached to the side of the dish and a large bulbous body in the middle (Figure 5.5, II - VIII).

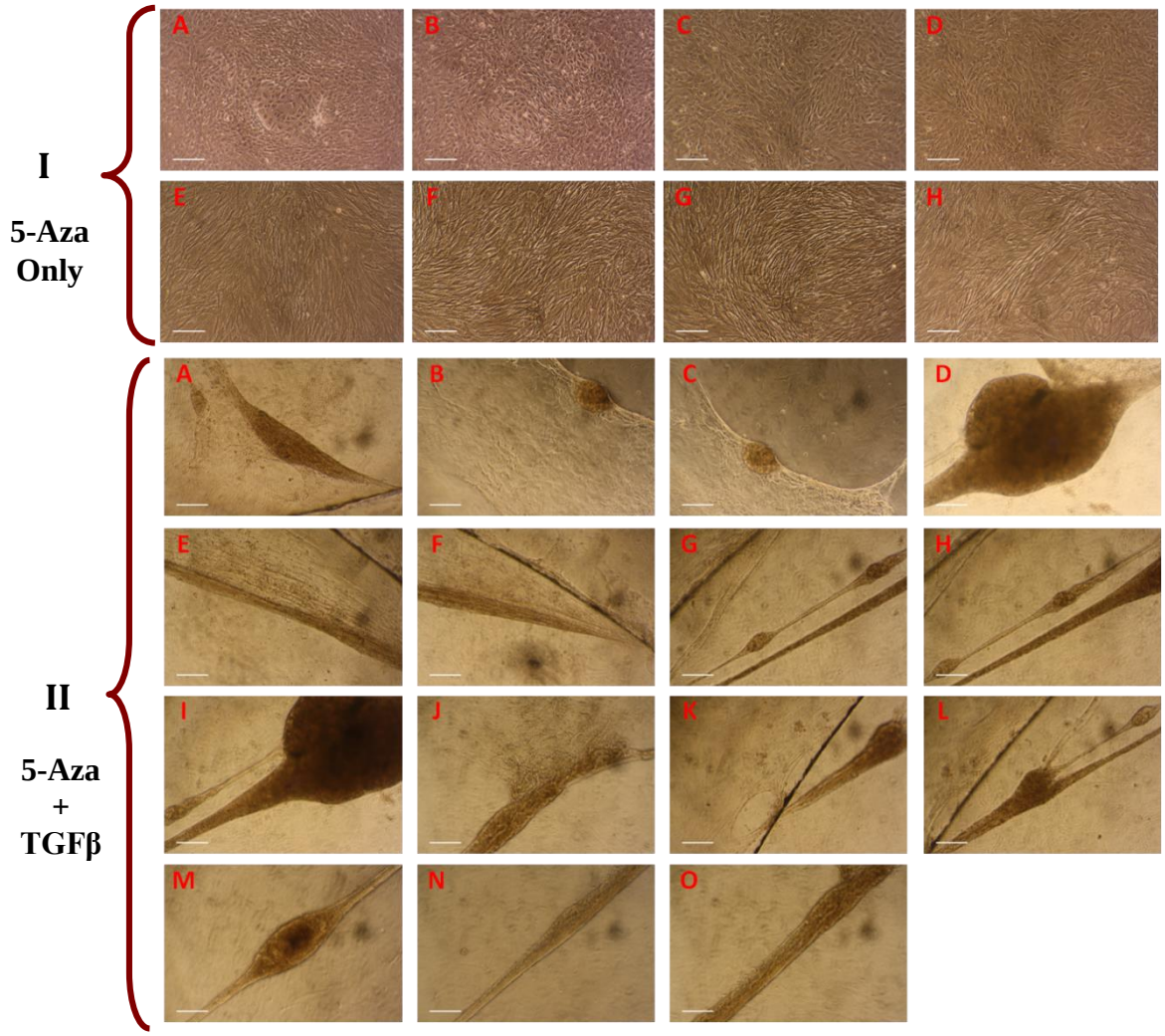
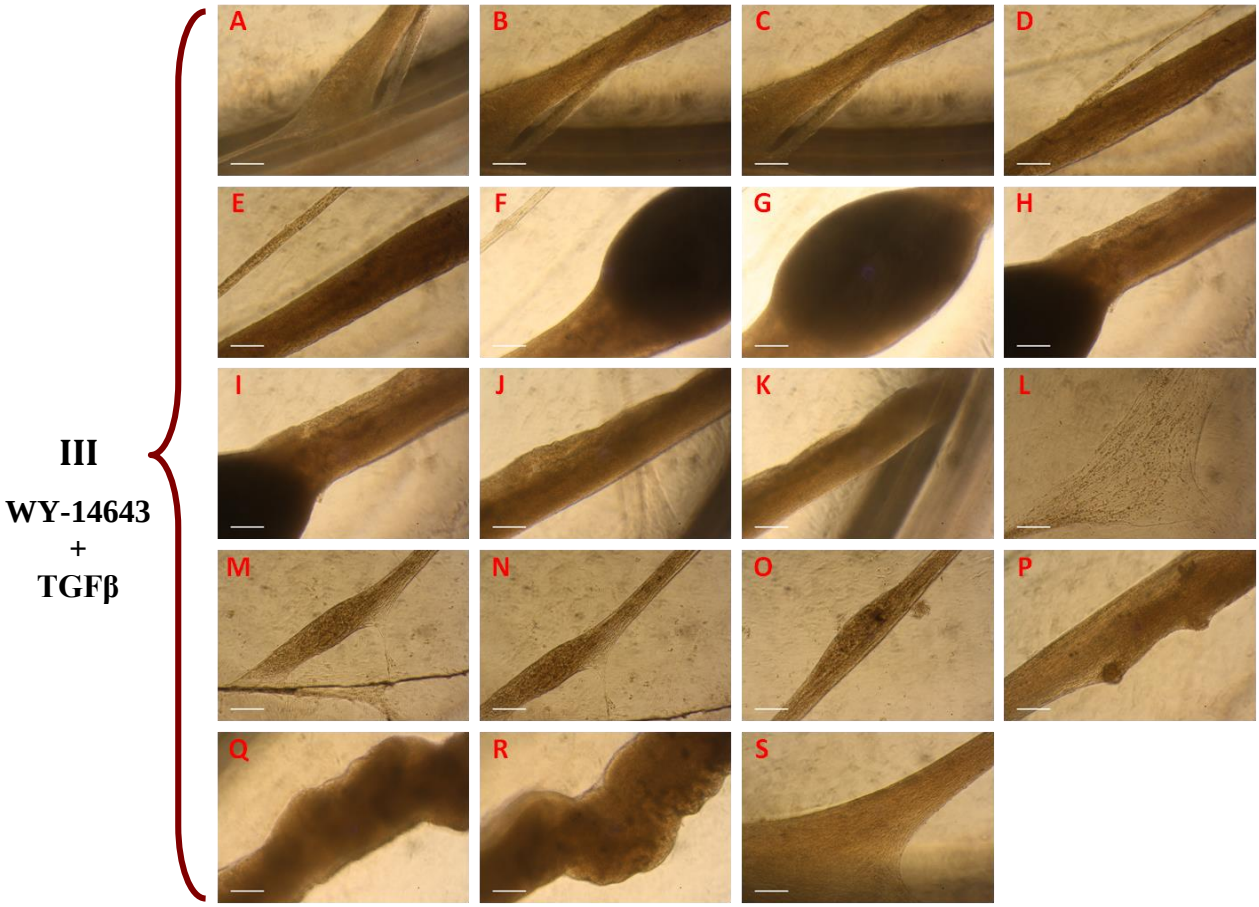
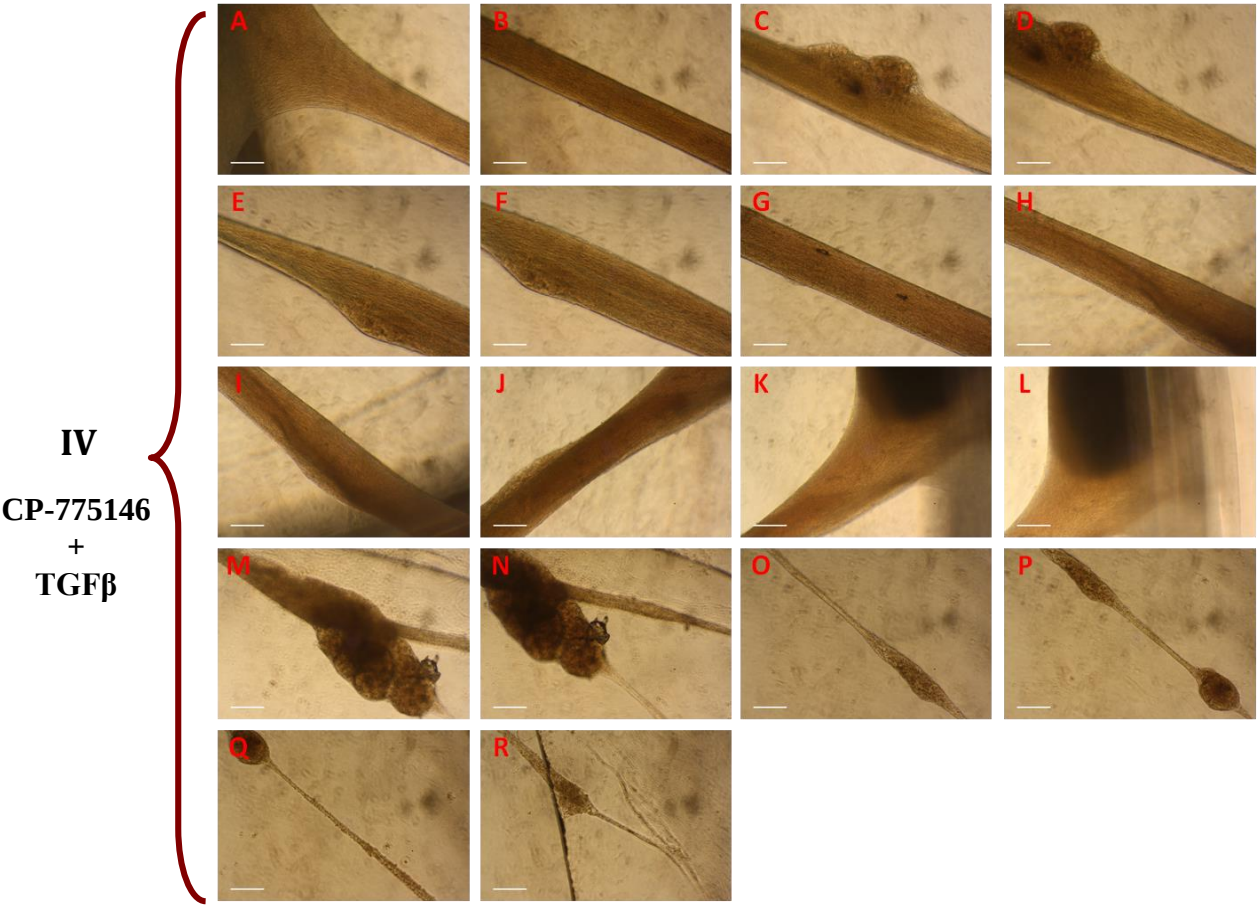
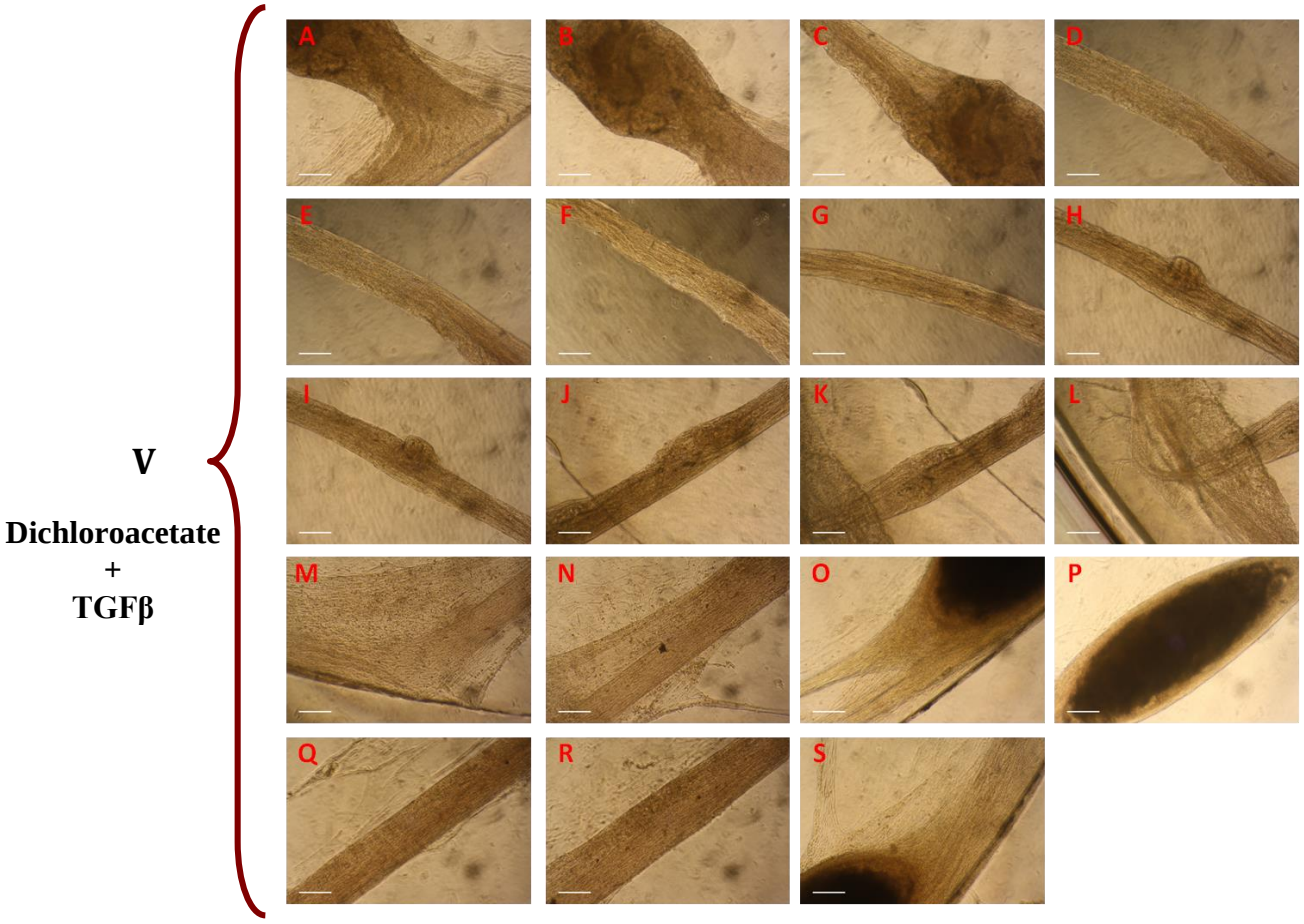
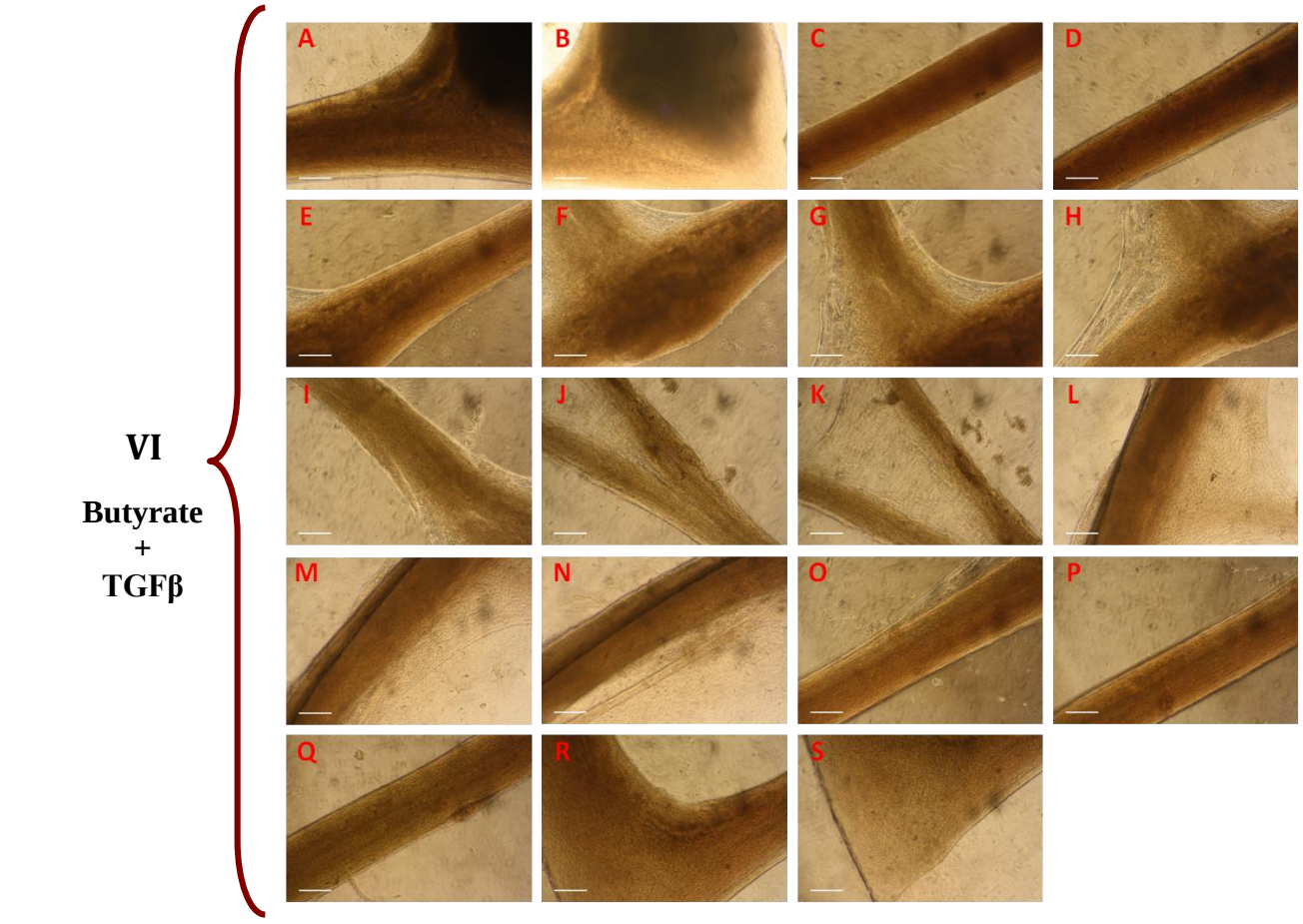



***Figure 5.5 Representative micrographs of cardiomyogenic differentiated P2-CDCs.*** *Cell morphology of P2-CDCs treated with CDM-1 plus 5-Aza (**I.**) for 3-weeks on FN (**A**-**D**) or ColIV (**E**-**H**) coated plates. Cell morphologies of 30-days differentiated P2-CDCs with 5-Aza +TGFβ (**II**, **A**-**O**), WY-14643 +TGFβ (**III**, **A**-**S**), CP-775146 +TGFβ (**IV**, **A**-**R**), dichloroacetate +TGFβ (**V**, **A**-**S**), butyrate +TGFβ (**VI**, **A**-**S**), 4-Compounds +TGFβ (**VII**, **A**-**R**), and TGFβ only (**VIII**, **A**-**Q**). Scale bar = 200 µM.*


III
WY-14643
+
TGFβ
A
B
C
D
E
F
G
H
I
J
K
L
M
N
O
P
Q
R
S

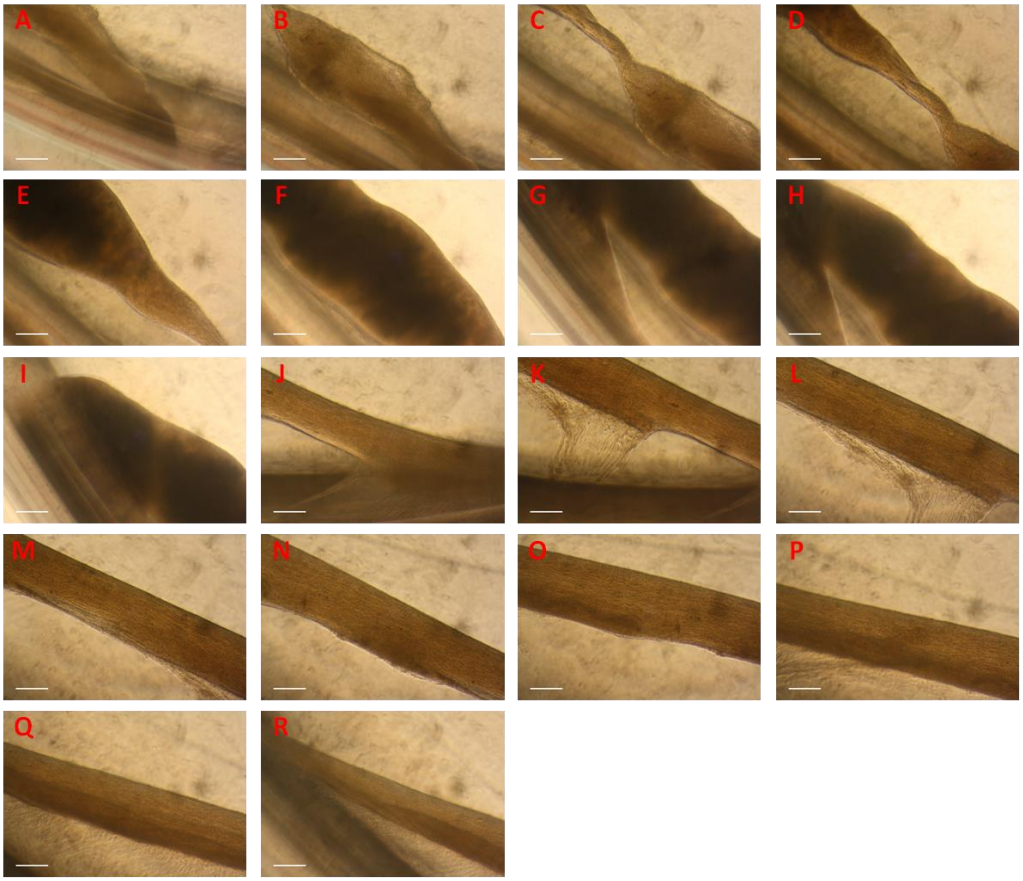

IV
CP-775146
+
TGFβ
A
B
C
D
E
F
G
H
I
J
K
L
M
N
O
P
Q
R


V
Dichloroacetate
+
TGFβ
A
B
C
D
E
F
G
H
I
J
K
L
M
N
O
P
Q
R
S


VI
Butyrate
+
TGFβ
A
B
C
D
E
F
G
H
I
J
K
L
M
N
O
P
Q
R
S

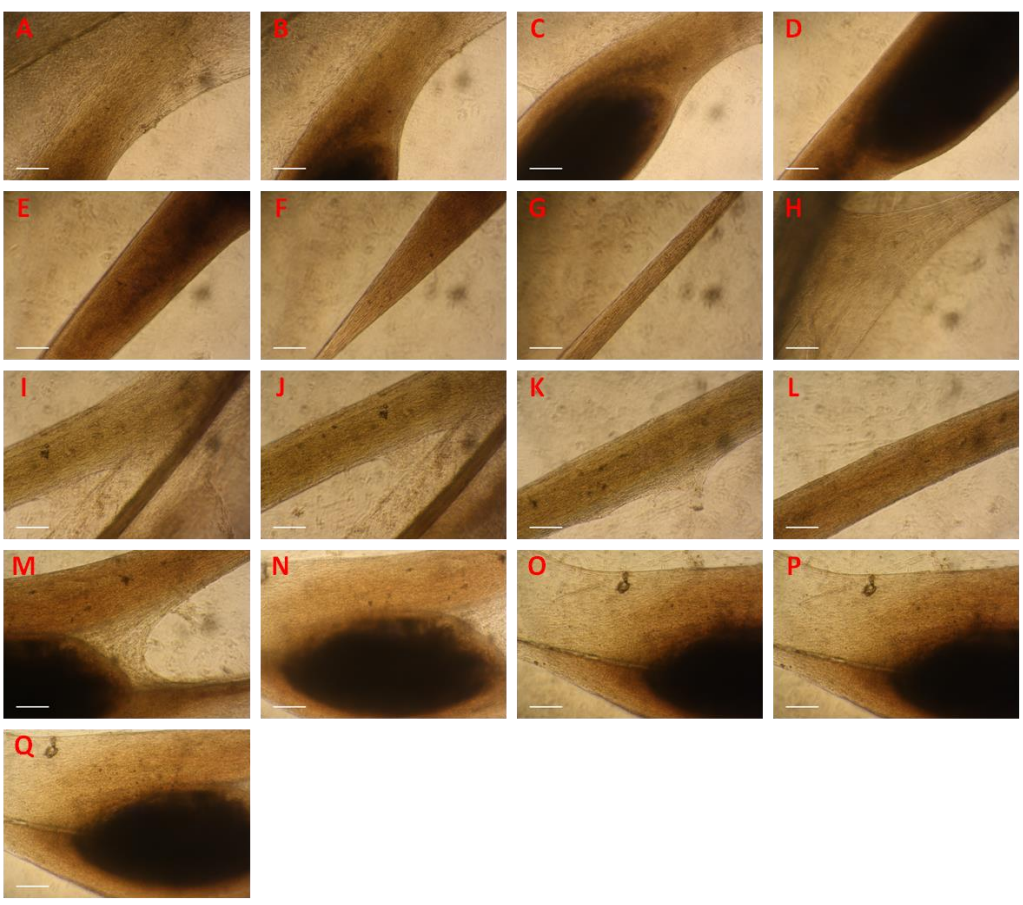
**VII**

**4-Compounds**
**+**
**TGFβ**




**VIII**

**TGFβ only**



## 5.4.3 *In Vitro* Cellular Metabolism

### 5.4.3.1 Glycolytic flux

To determine, for the first time, the level of glycolytic flux in control and 30-days small molecule(s) treated P2-CDCs, $^{3}$H-glucose was added into the cell culture medium, and sample medium was collected at different intervals (1-, 4-, 6-, 8-, 24-, 48-, and 72-hours).

The rate of glycolytic flux in WY-14643 treated P2-CDCs was significantly reduced compared to the three controls including baseline, at 8- and 24-hours ($p < 0.0001$ and $p = 0.0005$ respectively); TGFβ at 8-, 24-, 48-hours ($p < 0.0001$), and 72-hours ($p = 0.0008$); and 5-Aza at 8- and 48-hours ($p < 0.0001$ and $p = 0.0008$ respectively) (Figure 5.6). Likewise, 4-compound treatment significantly reduced the glycolytic rate compared with all three controls at 8-hours ($p < 0.0001$) and with TGFβ at 72-hours ($p = 0.0009$, Figure 5.6).

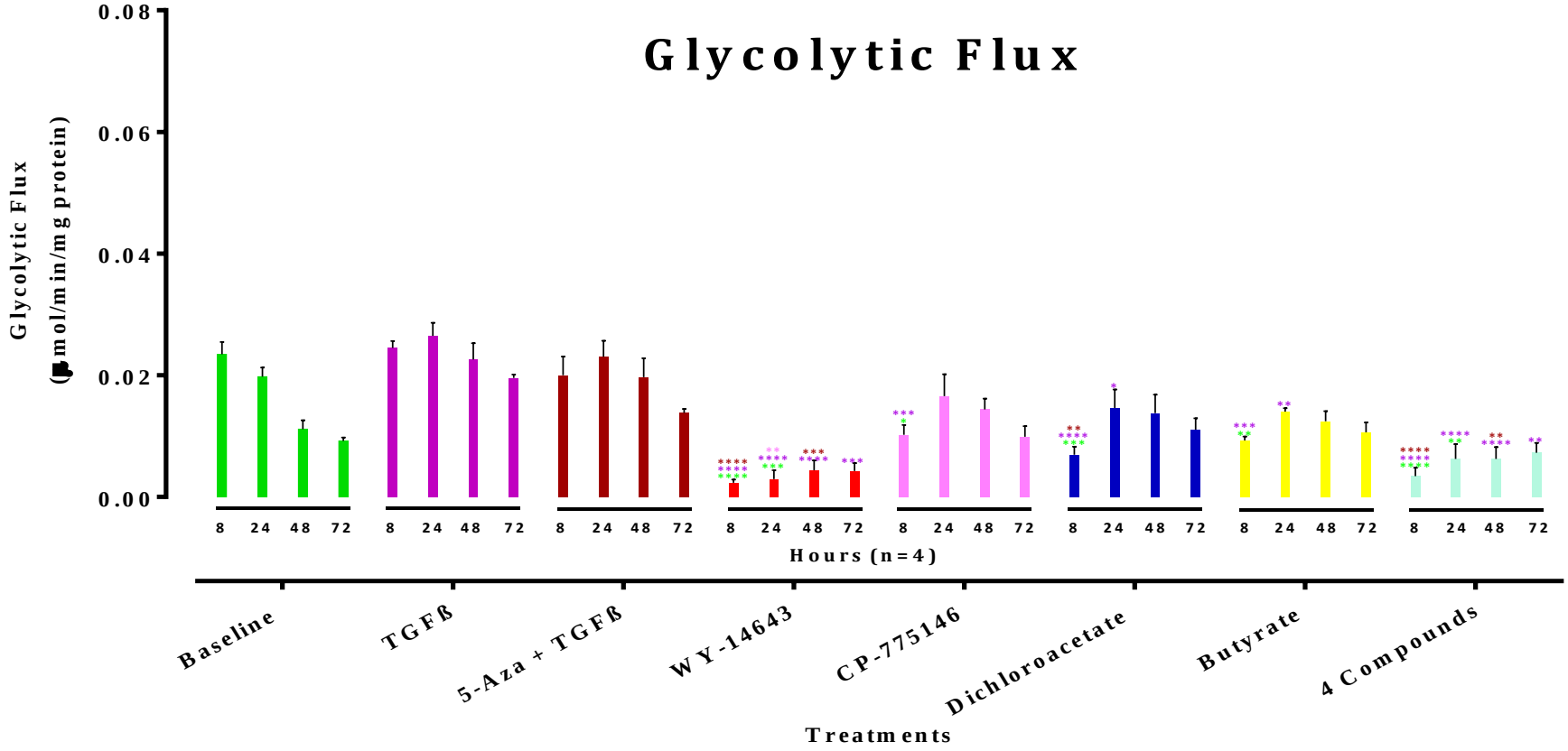



***Figure 5.6 The rate of glycolytic flux in controls and 30-days small molecule treated P2-CDCs.*** *The level of glycolytic flux was assessed by adding [5-$^{3}$H] glucose in the culture medium controls (baseline, TGFβ, and 5-Aza + TGFβ) and 30-days small molecule treated P2-CDCs. The sample mediums were collected at different intervals (8, 24, 48, and 72 hours), then the $^{3}H_2O$, glycolysis by-product, was analysed. Abbreviations: P2-CDCs: Passage 2-Cardiosphere-Derived Cells; 5-Aza: 5-azacytidine; TGFβ: Transforming growth factor beta; 4-compounds: WY-14643 + CP-775146 + dichloroacetate + Butyrate. Data are presented as mean ± SEM (n=3) and were analysed using a two-way ANOVA with Tukey post hoc test. Multicolour stars indicate multiple comparisons with every other condition. *: p < 0.01; **: p < 0.001; ***: p < 0.004; ****: p < 0.0001.*

### 5.4.3.2 Oxidative metabolism

To determine the level of the cellular oxidation and decarboxylation reactions of respiratory substrates in control and 30-days small molecule(s) treated P2-CDCs, $^{14}$C-radiolabelled glucose and palmitate were added individually into the cell culture medium and assessed for the level of oxidation using multiwell $^{14}CO_2$ capture technique over 4-hours (Chapter 2, Figure 2.2). Furthermore, the level of ATP production was calculated as before (Section 4.4.3). Glucose oxidation was highest in WY-14643 treated cells then butyrate and finally cells treated with CP-775146 or 4-compounds, relative to the controls and other experimental conditions ($p < 0.01$, Figure 5.7). Likewise, the highest palmitate oxidation was in the WY-14643 treated cells, followed by the 4-compounds treated P2-CDCs relative to the controls and other experimental conditions ($p < 0.0001$, Figure 5.8).

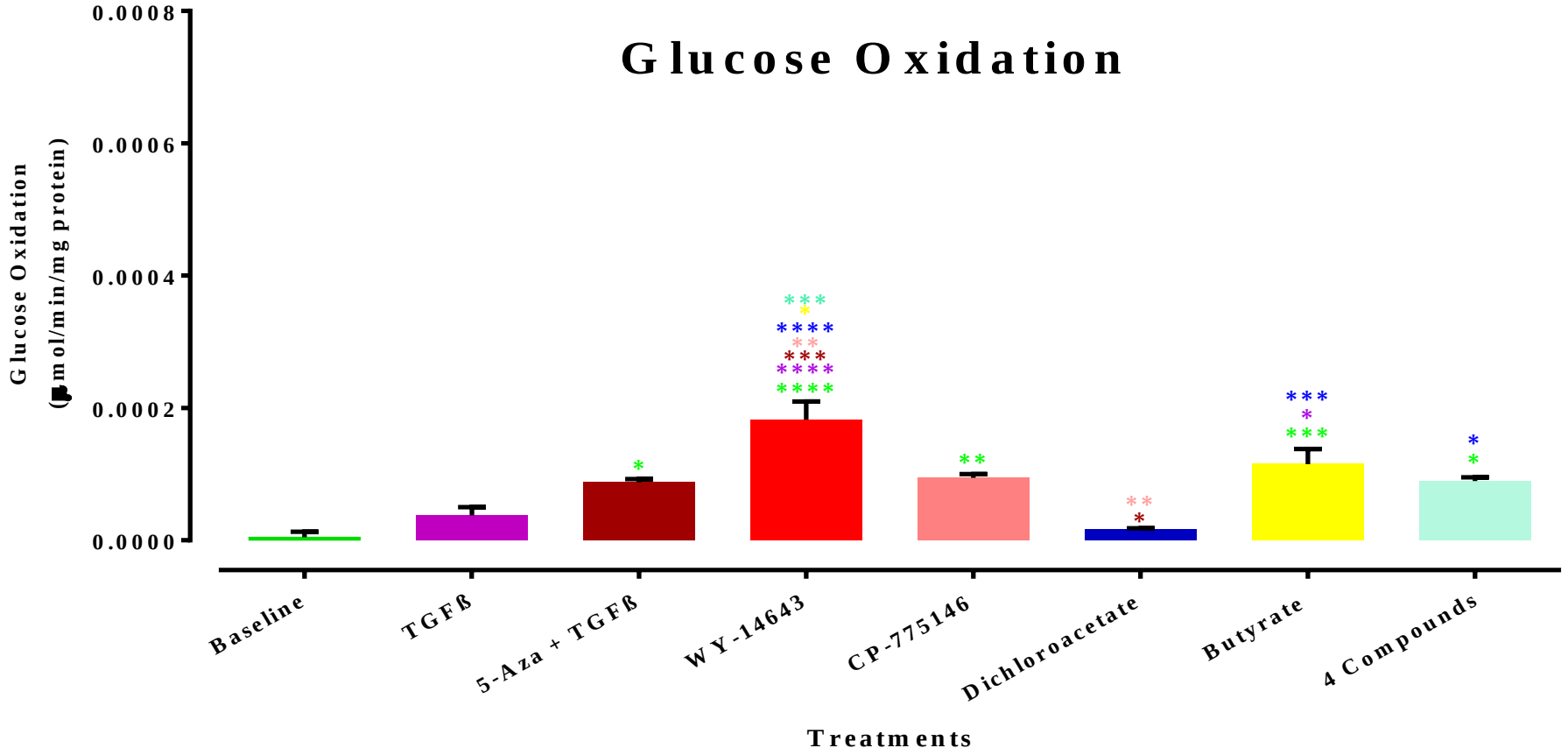



***Figure 5.7 The rate of oxidative glucose in control and cardiomyogenic differentiated P2-CSCs.*** *The level of glucose oxidation was assessed in control and 30-days small molecule(s) treated P2-CDCs using radiolabelled isotope, $^{14}$C-glucose and $^{14}CO_2$-capture technique. Abbreviations: P2-CDCs: Passage 2-Cardiosphere-Derived Cells; 5-Aza: 5-Azacytidine; TGFβ: Transforming growth factor beta; 4-compounds: WY-14643 + CP-775146 + dichloroacetate + Butyrate. Data are presented as mean ± SEM (n=3) and were analysed using a one-way ANOVA with Tukey post hoc test. Multicolour stars indicate multiple comparisons with every other condition. *: p < 0.01; **: p < 0.001; ***: p < 0.004; ****: p < 0.0001.*

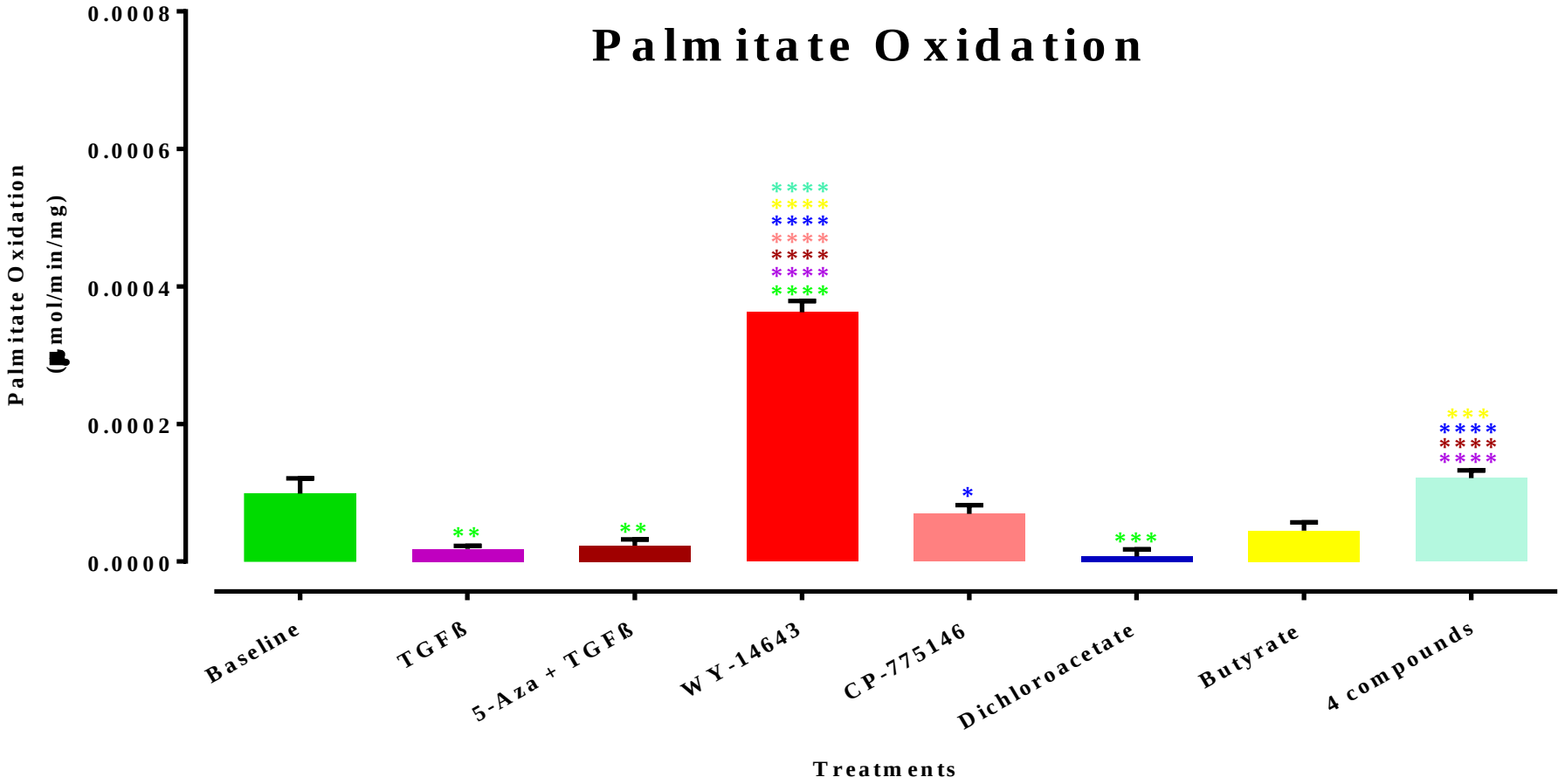



***Figure 5.8 The rate of oxidative palmitate in control and cardiomyogenic differentiated P2-CSCs.*** *The level of palmitate oxidation was assessed in control and 30-days small molecule(s) treated P2-CDCs using radiolabelled isotope, $^{14}$C-palmitate $^{14}CO_2$-capture technique. Abbreviations: P2-CDCs: Passage 2-Cardiosphere-Derived Cells; 5-Aza: 5-azacytidine; TGFβ: Transforming growth factor beta; 4-compounds: WY-14643 + CP-775146 + dichloroacetate + Butyrate. Data are presented as mean ± SEM (n=3) and were analysed using a one-way ANOVA with Tukey post hoc test. Multicolour stars indicate multiple comparisons with every other condition. *: p < 0.01; **: p < 0.001; ***: p < 0.004; ****: p < 0.0001.*

#### 5.4.3.3 Adenosine triphosphate (ATP) production in both glycolysis and oxidative metabolism

Different substrates produce different levels of adenosine triphosphate (ATP) depending on the metabolic pathway (See Chapter 4, Table 4.1). The ATP level produced in glycolysis, as well as oxidative metabolism, were calculated based on the glycolytic flux and oxidation levels. The results from the ATP calculations revealed glycolysis is the major source of energy production in undifferentiated, proliferating cells, P2-CDCs, as well as individually treated 5-Aza and TGF-β cells ($p < 0.0001$, Figure 5.9). However, the ATP production from glycolysis was reduced in compound treated cells, particularly those treated with TGF-β+WY-14643 ($p < 0.0001$, Figure 5.9). Furthermore, the ATP calculations revealed the oxidation of both fatty acid (palmitate) and carbohydrate (glucose), as the major source of energy production in compound treated cells particularly in those treated with TGF-β+WY-14643 in comparison to other differentiated cells with ($p < 0.0001$, Figure 5.9).

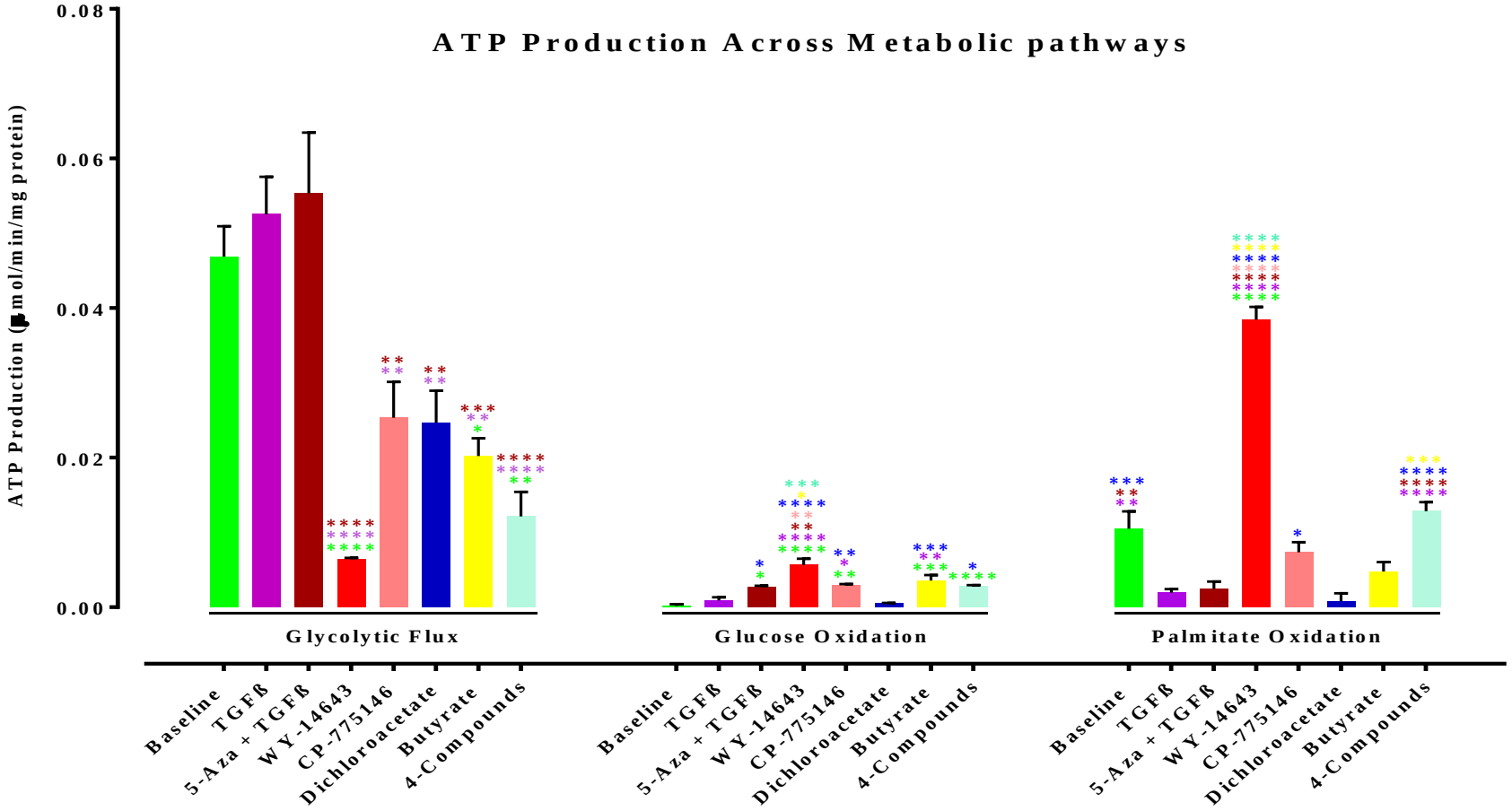



***Figure 5.9 ATP production during glycolysis and oxidative metabolism.*** *The level of ATP production was calculated based on the glycolysis and glucose and palmitate oxidation levels as 1 mole of glucose produce 2 moles of ATP during glycolysis, but 33 moles of ATP during glucose oxidation and 1 mole of palmitate produce 106 moles of ATP during palmitate oxidation. Data are presented as mean ± SEM (n=3) and were analysed using a one-way ANOVA with Tukey post hoc test. Multicolour stars indicate multiple comparisons with every other condition. *: p < 0.01; **: p < 0.001; ***: p < 0.004; ****: p < 0.0001.*

### 5.4.4 Molecular profile of cardiomyogenic differentiated P2-CDCs

Genotypic characterization of the differentiated P2-CDCs was assessed using quantitative real-time PCR (qRT-PCR) by looking at genes for proteins that are present in the heart including cardiomyocytes (cTnnT2, Mybpc3, Myh6, Myh7) (Figure 5.10), smooth muscle (Cnn1, Myh11) (Figure 5.11), and endothelial (KDR, Cdh5, VEGFa, VEGFb) (Figure 5.12) cells; calcium ($Ca^{2+}$) handling genes of sarcoplasmic reticulum (Serca2a, PLN) (Figure 5.13); and genes involved in metabolic pathways including glycolysis (Figure 5.14), fatty acid transporter genes (Figure 5.15), and fatty acid metabolism (Figure 5.16). All qRT-PCR data were normalized to Actb and B2M as the reference genes.

#### 5.4.4.1 Molecular profile of cardiomyocyte markers

qRT-PCR showed that all compounds significantly increased the mRNA expression of cardiac troponin T (cTnnT2) in comparison with baseline, TGFβ, and 5-Aza conditions ($p < 0.0001$, Figure 5.10A). However, myosin-binding protein C (MYBPC3) expression was only increased in cells treated with TGFβ, relative to the rest of the conditions ($p < 0.01$, Figure 5.10B). In contrast, the expression level of MYH7 that encodes for the myosin heavy chain beta isoform (slow twitch) protein, an early stage of myosin heavy chain during embryonic development, showed an ~10-fold increase in WY-14743 and butyrate-treated cells compared to the controls and other treatments ($p < 0.0001$, Figure 5.10C). On the other hand, MYH6, which encodes for myosin heavy chain, α isoform (MHCα) protein, the late stage of myosin heavy chain development, was increased by treatment with butyrate, WY-14743, TGFβ or 5-Aza in comparison to the controls and other treatments ($p < 0.01$, Figure 5.10D).

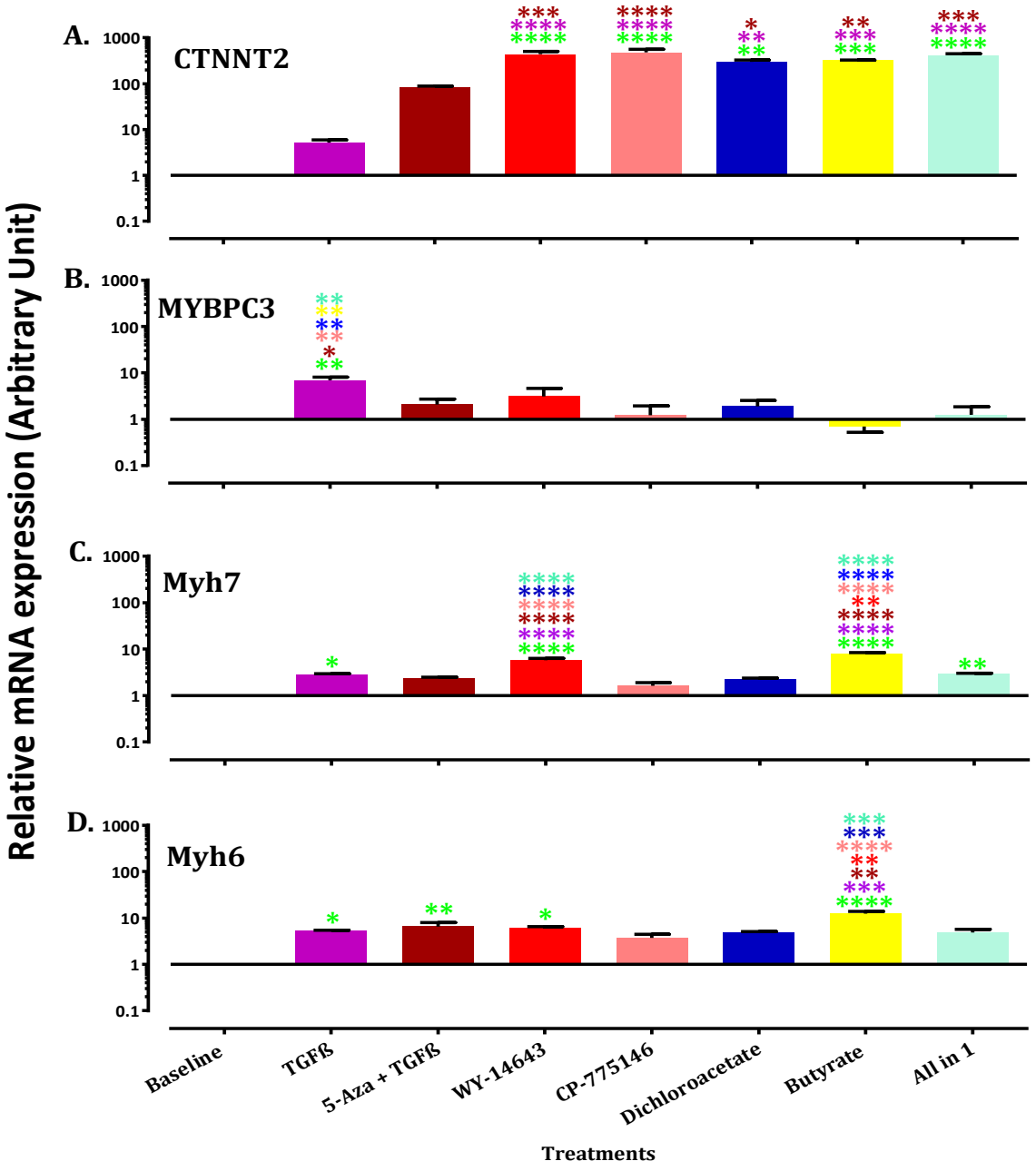



***Figure 5.10 The relative mRNA expression of cardiomyocyte-specific genes in controls and cardiomyogenic differentiated P2-CDCs (n=3).*** *The level of mRNA expression of cardiac-specific genes including cTnnT2 (A.), MYBPC3 (B.), MYH7 (C.), and MYH6 (D.) was assessed in control and 30-days small molecule(s) treated P2-CDCs using qRT-PCR. The mRNA expression was normalized both to the geometric mean of Actb and β2M (housekeeping genes) and P2-CDCs (calibrator). Abbreviations: P2-CDCs = Passage 2 Cardiosphere-Derived Cells. Data are presented as mean ± SEM (n=3) and were analysed using a one-way ANOVA with Tukey post hoc test. Multicolour stars indicate multiple comparisons with every other condition. *: $p < 0.01$; **: $p < 0.001$; ***: $p < 0.004$; ****: $p < 0.0001$.*

### 5.4.4.2 Molecular profile of smooth muscle cell markers

qRT-PCR results revealed low levels of mRNA expression of the smooth muscle cell markers MYH11, which encodes for the myosin-11 protein, and Cnn1, that encodes for calponin 1, in controls; which were significantly decreased in compound treated P2-CDCs (Figure 5.11).

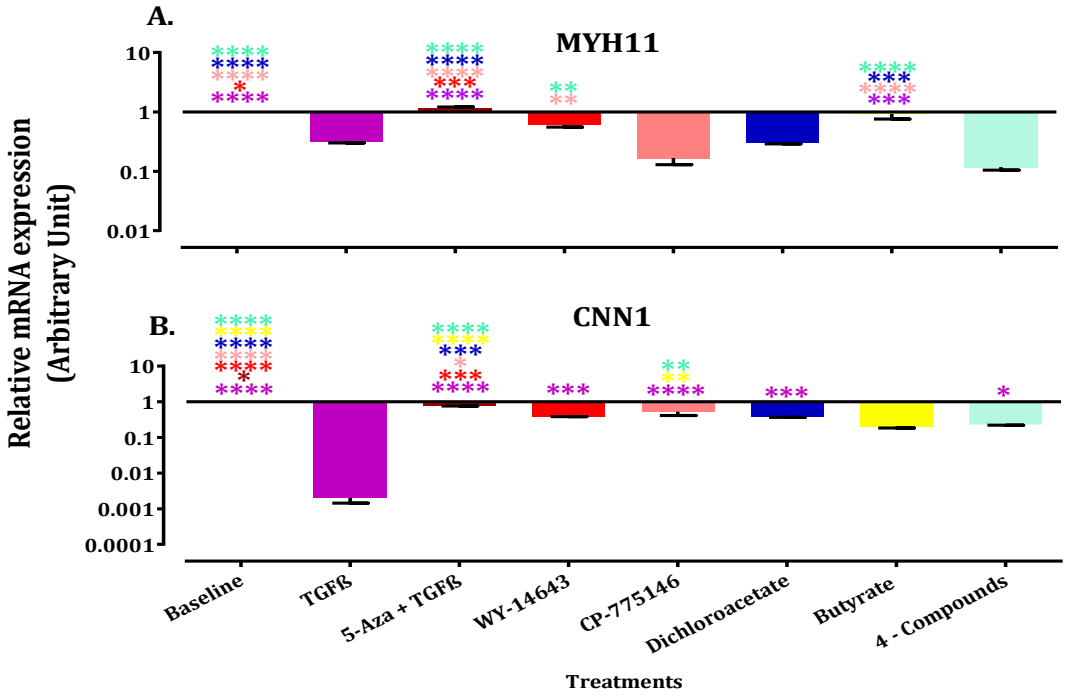



***Figure 5.11 The relative mRNA expression of specific genes of smooth muscle cells in controls and cardiomyogenic differentiated P2-CDCs (n=3).*** *The level of mRNA expression of smooth muscle cell marker genes including MYH11 (A.), and CNN1 (B.) was assessed in control and 30-days small molecule(s) treated P2-CDCs using qRT-PCR. The mRNA expression was normalized both to the geometric mean of Actb and β2M (housekeeping genes) and P2-CDCs (calibrator). Abbreviations: P2-CDCs = Passage 2 Cardiosphere-Derived Cells. Data are presented as mean ± SEM (n=3) and were analysed using a one-way ANOVA with Tukey post hoc test. Multicolour stars indicate multiple comparisons with every other condition. *: $p < 0.01$; **: $p < 0.001$; ***: $p < 0.004$; ****: $p < 0.0001$.*

### 5.4.4.3 Molecular profile of endothelial cell markers

The results from qRT-PCR revealed no significant differences in endothelial cell marker, KDR, which encodes for kinase insert domain receptor known as the vascular endothelial growth factor receptor 2 (VEGFR-2) and Fetal liver kinase 1 (KLF1) protein in controls and treated cells (Figure 5.12A.). However, there was increased expression of other endothelial cell marker genes including CDH5, that encodes for cadherin 5, type 2 or vascular endothelial-cadherin protein, which was increased in TGFβ treated cells ($p < 0.01$); VEGFa, which encodes for vascular endothelial growth factor A protein, which was slightly increased in 4-compound treated cells but reduced significantly in other compound treated cells ($p < 0.0001$); and VEGFb, that encodes for vascular endothelial growth factor B protein, which was increased in 4 compounds treated cells ($p < 0.0001$) as well as in cells treated with TGFβ, 5-Aza or DCA in comparison to the baseline ($p < 0.001$) (Figure 5.12B-D).

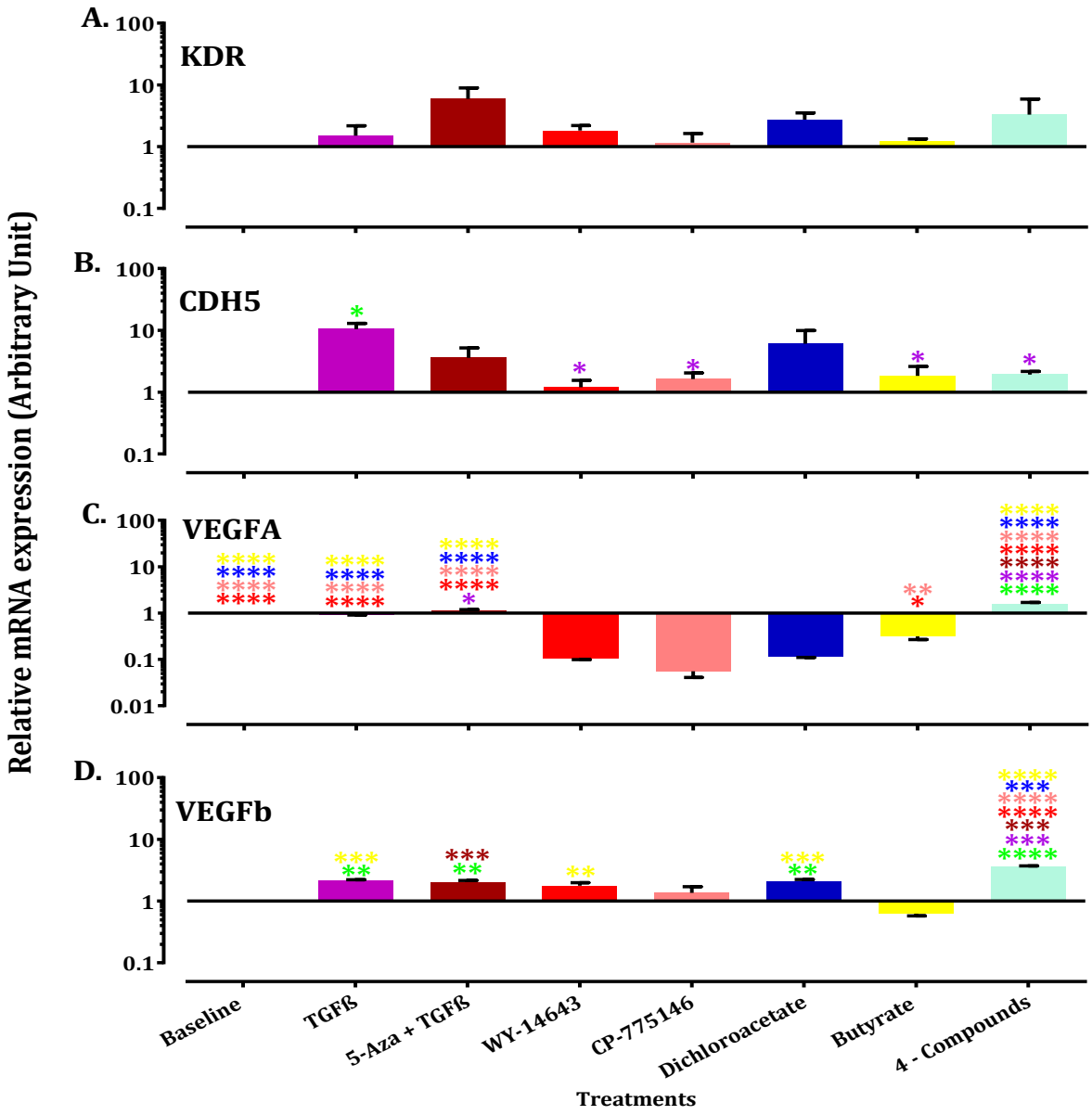



***Figure 5.12 The relative mRNA expression of specific genes of endothelial cell in controls and cardiomyogenic differentiated P2-CDCs (n=3).*** *The level of mRNA expression of endothelial cell marker genes including MYH11 (A.), and CNN1 (B.) was assessed in control and 30-days small molecule(s) treated P2-CDCs using qRT-PCR. The mRNA expression was normalized both to the geometric mean of Actb and β2M (housekeeping genes) and P2-CDCs (calibrator). Abbreviations: P2-CDCs = Passage 2 Cardiosphere-Derived Cells. Data are presented as mean ± SEM (n=3) and were analysed using a one-way ANOVA with Tukey post hoc test. Multicolour stars indicate multiple comparisons with every other condition. *: $p < 0.01$; **: $p < 0.001$; ***: $p < 0.004$; ****: $p < 0.0001$.*

### 5.4.4.4 Molecular profile of calcium handling genes

Here the qRT-PCR results revealed that, in comparison to the controls and cardiomyogenic differentiated P2-CDCs, WY-14643 caused the greatest increase in expression (~10 fold) of SERCA2a, the calcium $Ca^{2+}$ ATPase, which help to transfer $Ca^{2+}$ from the cytosol of the cell to the lumen of the sarcoplasmic reticulum at the expense of ATP hydrolysis during muscle relaxation ($p < 0.0001$, Figure 5.13A). However, the level of SERCA2a was reduced significantly in all other conditions in comparison to the P2-CDC. Nevertheless, the level of phospholamban (PLN) mRNA expression, which normally inhibits SERCA, was significantly lower in WY-14643 treated cells in comparison to other compounds treated cells (CP-775146, Dichloroacetate, butyrate and TGFβ) ($p < 0.01$, Figure 5.13B).

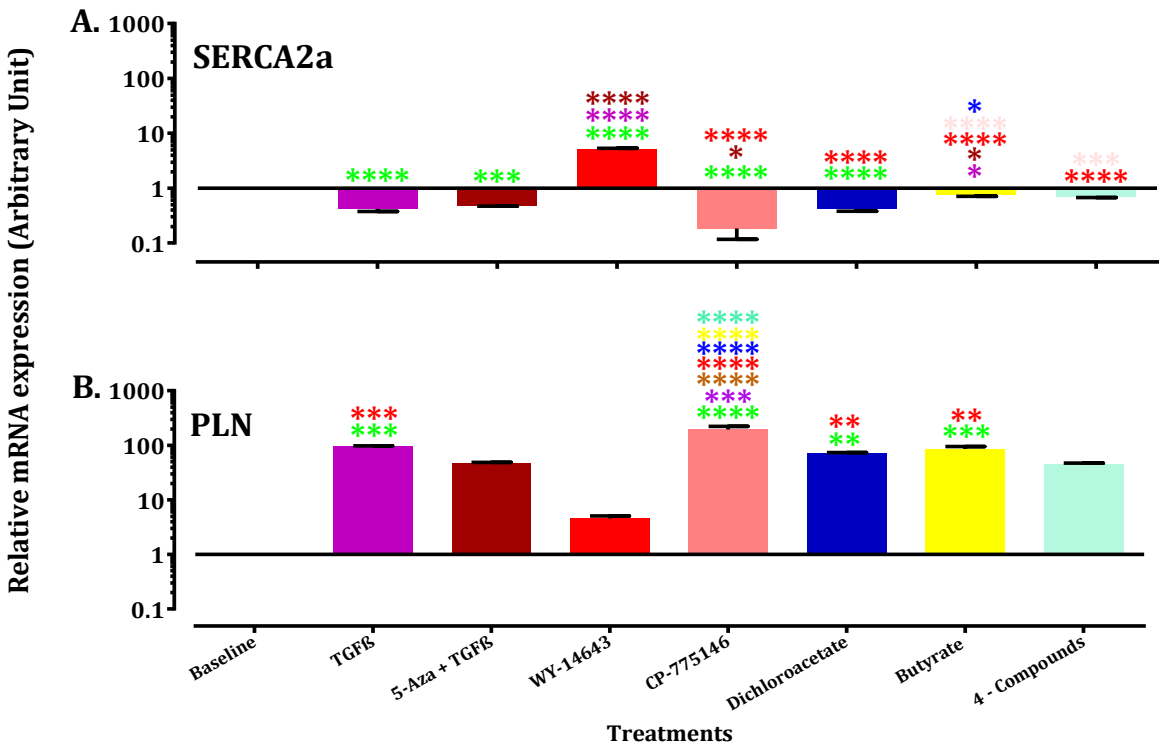



***Figure 5.13 The relative mRNA expression of specific calcium handling genes in control and cardiomyogenic differentiated P2-CDCs (n=3).*** *The level of mRNA expression of SERCA2a (**A.**) and PLN (**B.**) genes was assessed in control and 30-days small molecule(s) treated P2-CDCs using qRT-PCR. The mRNA expression was normalized both to the geometric mean of Actb and β2M (housekeeping genes) and P2-CDCs (calibrator). Abbreviations: P2-CDCs = Passage 2 Cardiosphere-Derived Cells. Data are presented as mean ± SEM (n=3) and were analysed using a one-way ANOVA with Tukey post hoc test. Multicolour stars indicate multiple comparisons with every other condition. *: $p < 0.01$; **: $p < 0.001$; ***: $p < 0.004$; ****: $p < 0.0001$.*

### 5.4.4.5 Molecular profile of glucose metabolism

The results from qRT-PCR for genes involved in the glycolysis pathway showed that glucose transporter 1 (GLUT1) gene expression was reduced significantly (~ 100 fold) in all conditions of compound differentiated cells in comparison to the baseline ($p < 0.0001$) (Figure 5.14A). Whereas, the opposite was observed for glucose transporter 4 (GLUT4), which showed the high level of expression in treated cells relative to the baseline ( $p < 0.01$, Figure 5.14B).

mRNA expression of pyruvate dehydrogenase kinase 1 (PDK1), which negatively regulates glucose oxidation, was increased over 100 fold, in 30-days treated TGFβ, 5-Aza and 4-Compounds relative to the baseline and other treated cells ($p < 0.0001$, Figure 5.14C). Similarly, PDK4 mRNA level was increased in TGFβ-treated cells by 100 fold in comparison to the baseline and other treated cells ($p < 0.0001$, Figure 5.14D).

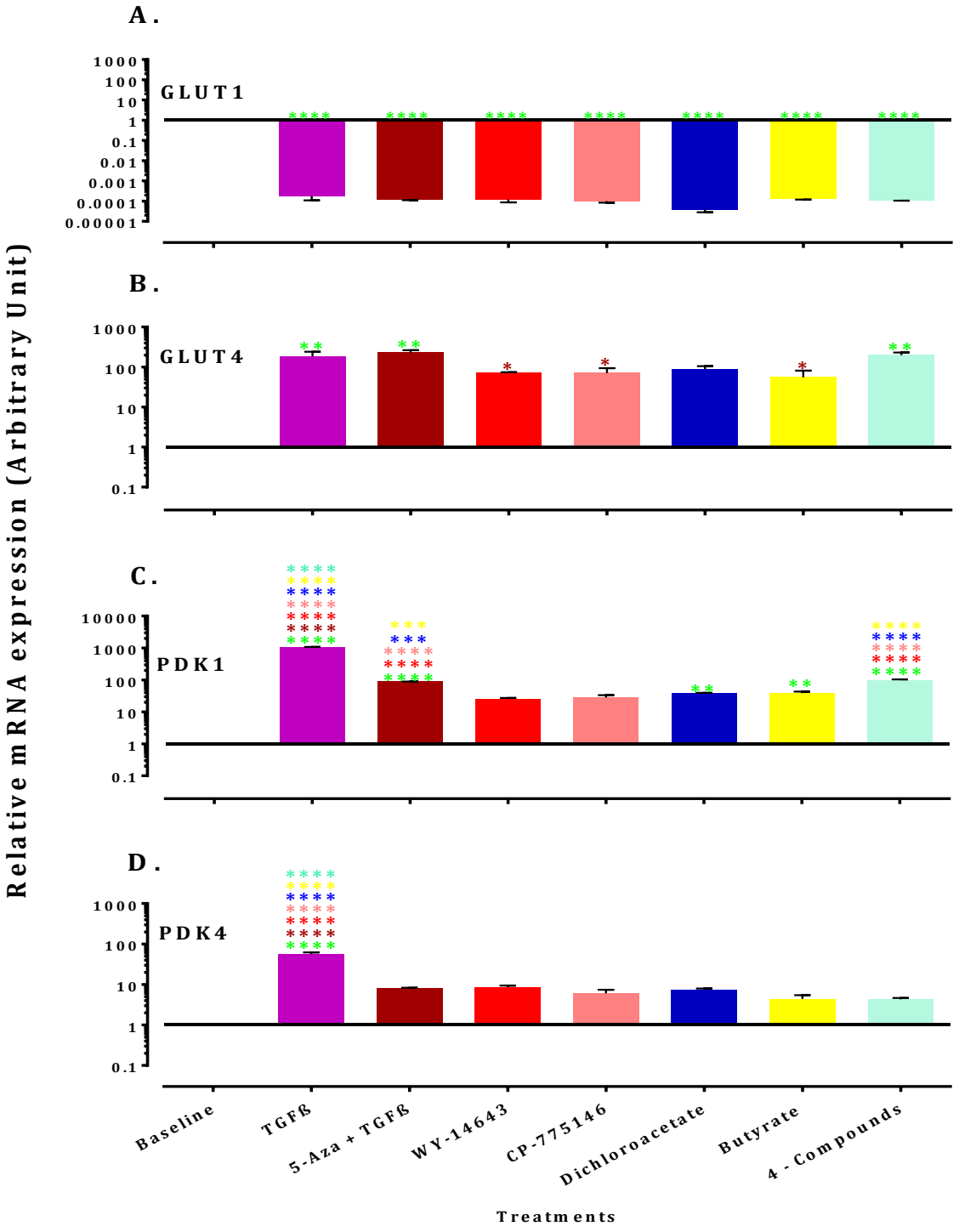



**Figure 5.14** ***The relative mRNA expression of genes involved in glucose metabolism.*** *Control and 30-days treated P2-CDCs (n=3) were used to assess the molecular profile of glycolytic flux including GLUT 1(**A.**), GLUT4 (**B.**), PDK1 (**C.**) and PDK4 (**D.**). The mRNA expression was normalized both to the geometric mean of Actb and β2M as reference genes and P2-CDCs as calibrator. Abbreviations: Glut1 and 4: glucose transporter-1 and 4; PDK1 and 4: pyruvate dehydrogenase kinase, isozyme 1 and 4; P2-CDCs: Passage 2-Cardiosphere-Derived Cells. Data are presented as mean ± SEM (n=3) and were analysed using a one-way ANOVA with Tukey post hoc test; Multicolour stars indicate multiple comparisons between groups;* *: $p < 0.01$; **: $p < 0.001$; ****: $p < 0.0001$.

### 5.4.4.6 Molecular profile of fatty acid transporters

The results from mRNA expression of fatty acid transporters revealed that all 30-days treated cells (except TGFβ) demonstrated increased expression of the cluster of differentiation 36 (CD36) in comparison to the baseline (Figure 5.15A). In addition, the mRNA expression level of the carnitine palmitoyltransferase 1B (CPT1B) was increased in WY-14643 treated cells in comparison to the baseline and other treatments ($p < 0.0001$, Figure 5.15B).

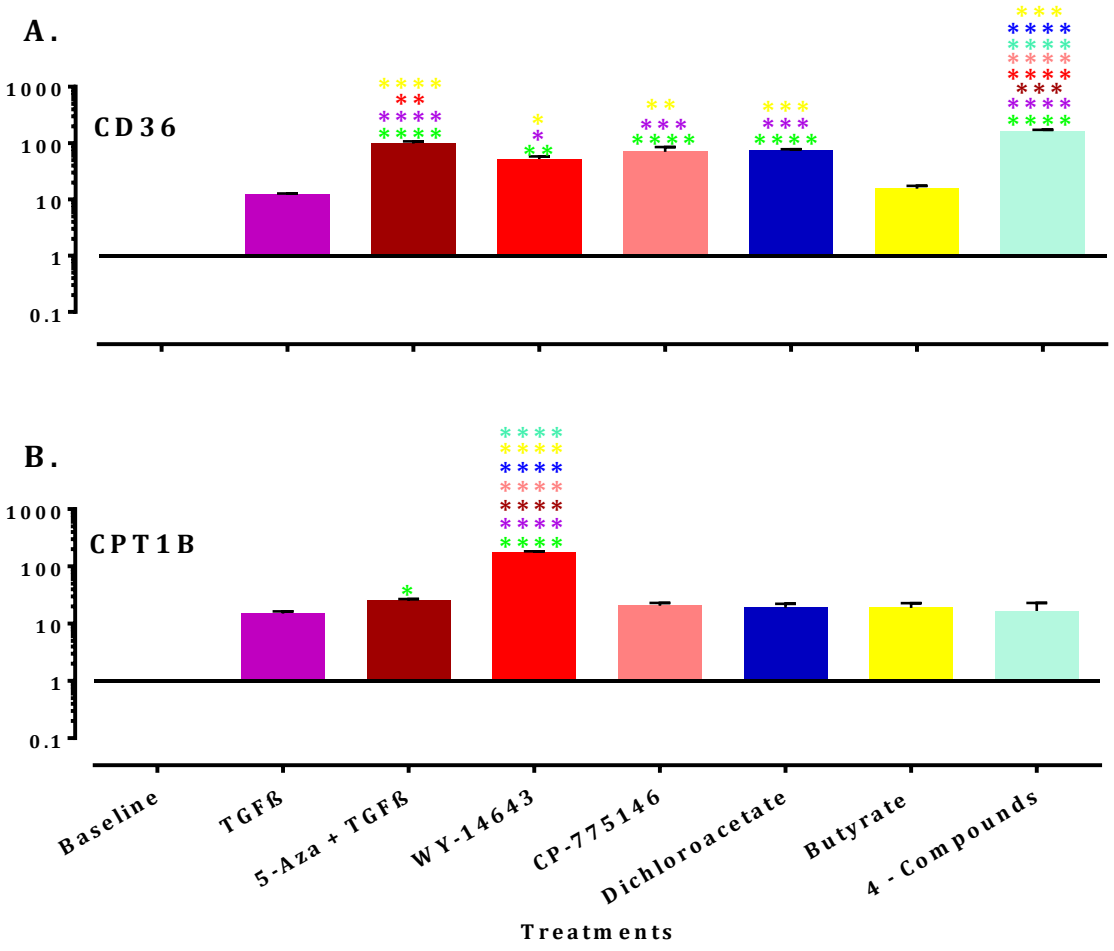



**Figure 5.15** ***The relative mRNA expression of genes involved in the fatty acid transporter.*** *Control and 30-days treated P2-CDCs (n=3) were used to assess the molecular profile of fatty acid transporter genes including CD36 (**A.**) and CPT1B (**B.**). The mRNA expression was normalized both to the geometric mean of Actb and β2M as reference genes and P2-CDCs as calibrator. Abbreviations: CD36: Cluster of differentiation 36; CPT1B: carnitine palmitoyltransferase I; P2-CDCs: Passage 2-Cardiosphere-Derived Cells. Data are presented as mean ± SEM (n=3) and were analysed using a one-way ANOVA with Tukey post hoc test; Multicolour stars indicate multiple comparisons between groups;* *: $p < 0.01$; **: $p < 0.001$; ****: $p < 0.0001$.

### 5.4.4.7 Molecular profile of fatty acid metabolism

The qRT-PCR results for genes involved in fatty acid metabolism showed increased expression of PPARα (~10 fold) in all 30-days small molecule treated P2-CDCs except those treated with CP-775146, in comparison to the baseline with the highest expression in WY-14643 treated cells ($p < 0.0001$) (Figure 5.16A). In addition, MCAD mRNA expression was increased in all treated CDCs (~ 10 fold) in comparison to the baseline ($p < 0.0001$) having the highest expression after treatment with WY-14643 or 4-compounds ($p < 0.0001$) (Figure 5.16B). Furthermore, qRT-PCR results demonstrated significantly increased ACADM expression in WY-14643-treated cells of over 100 fold ($p < 0.0001$) (Figure 5.16C).

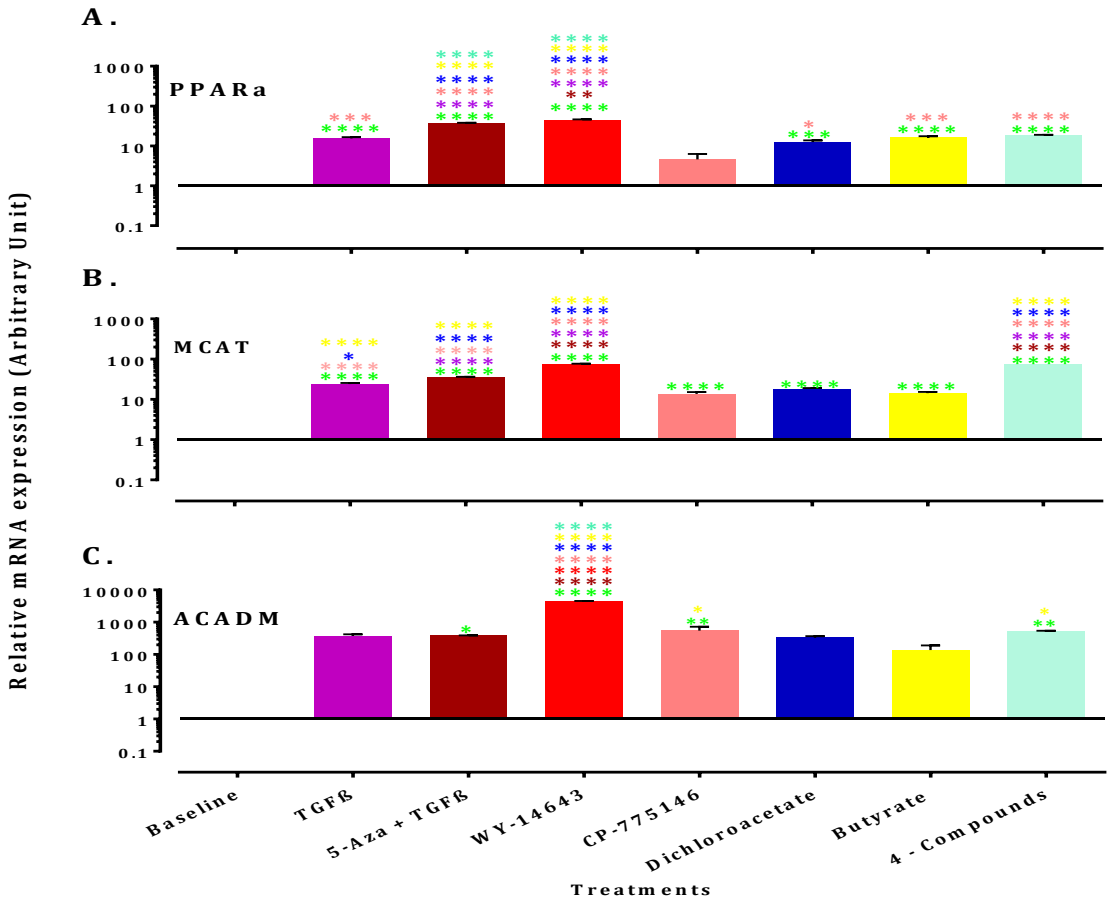



**Figure 5.16** ***The relative mRNA expression of genes involved in fatty acid metabolism.*** *Control and 30-days treated P2-CDCs (n=3) were used to assess the molecular profile of fatty acid metabolism genes including PPARα (**A.**), MCAT (**B.**) and ACADM (**C.**). The mRNA expression was normalized both to the geometric mean of Actb and β2M as reference genes and P2-CDCs as calibrator. Abbreviations: PPARα: peroxisome proliferator-activated receptor alpha, MCAT: malonyl-CoA-acyl carrier protein transacylase; ACADM: Acyl-Coenzyme A dehydrogenase; P2-CDCs: Passage 2-Cardiosphere-Derived Cells. Data are presented as mean ±SEM (n=3) and performed one-way ANOVA with Tukey post hoc test; Multicolour stars indicate multiple comparisons between groups;* *: $p < 0.01$; **: $p < 0.001$; ****: $p < 0.0001$.

## 5.4.5 Molecular profile of proteins involves in metabolic pathways

To validate and support the aforementioned metabolic studies, Western blotting of whole cell lysates from baseline and small molecule(s) treated CDCs with synthetic small molecule(s) was used to quantify the levels of proteins involve in glucose metabolism (Glut1, Glut4, PDK1, PDK4), fatty acid metabolism (MCAD, CD36 and UCP3) and mitochondrial proteins (αKGDH, CISY) (Figures 5.17).

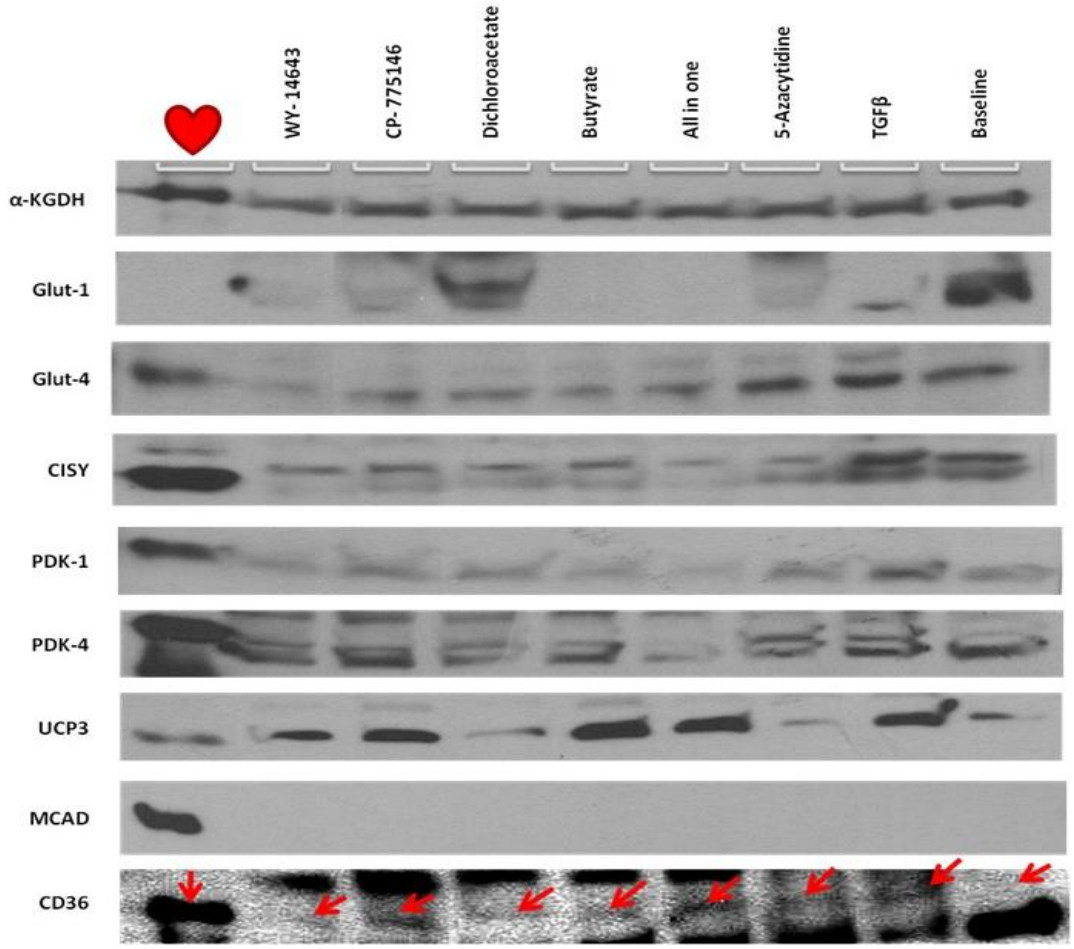



***Figure 5.17 Immunoblotting gels showing control and 30-days small molecule treated P2-CDCs expressed proteins involved in glycolysis, citric acid cycle, and fatty acid metabolism.*** *Control and 30-days small molecule treated P2-CDCs were used to assess the protein level of glucose metabolism (Glut1, Glut4, PDK 1 and PDK4), citric acid cycle (CISY and αKGDH), and fatty acid transporter (CD36) and fatty acid metabolism (MCAD, and UCP3). Adult rat heart lysates were used as positive controls. Abbreviations: αKGDH: Alpha-Ketoglutarate Dehydrogenase; CD36: Cluster of differentiation 36; CISY: Citrate synthase; Glut1 and 4: Glucose transporter 1 and 4; PDK1 and 4: Pyruvate dehydrogenase lipoamide kinase 1 and 4; MCAD: Medium-chain acyl-coenzyme A dehydrogenase; UCP3: uncoupling protein 3.*

#### 5.4.5.1 Molecular profile of protein expression of glucose metabolism

Analysis of the expression of proteins involve in the glucose metabolism pathway revealed a significant reduction of GLUT1 protein level in all differentiated CDCs comparing to the baseline ($p < 0.001$) whereas the GLUT4 and PDK1 protein levels were significantly higher in TGFβ treated cells in comparison to the small molecule treated cells ($p < 0.01$). However, there were no differences in PDK4 level between control and treated cells (Figure 5.18).

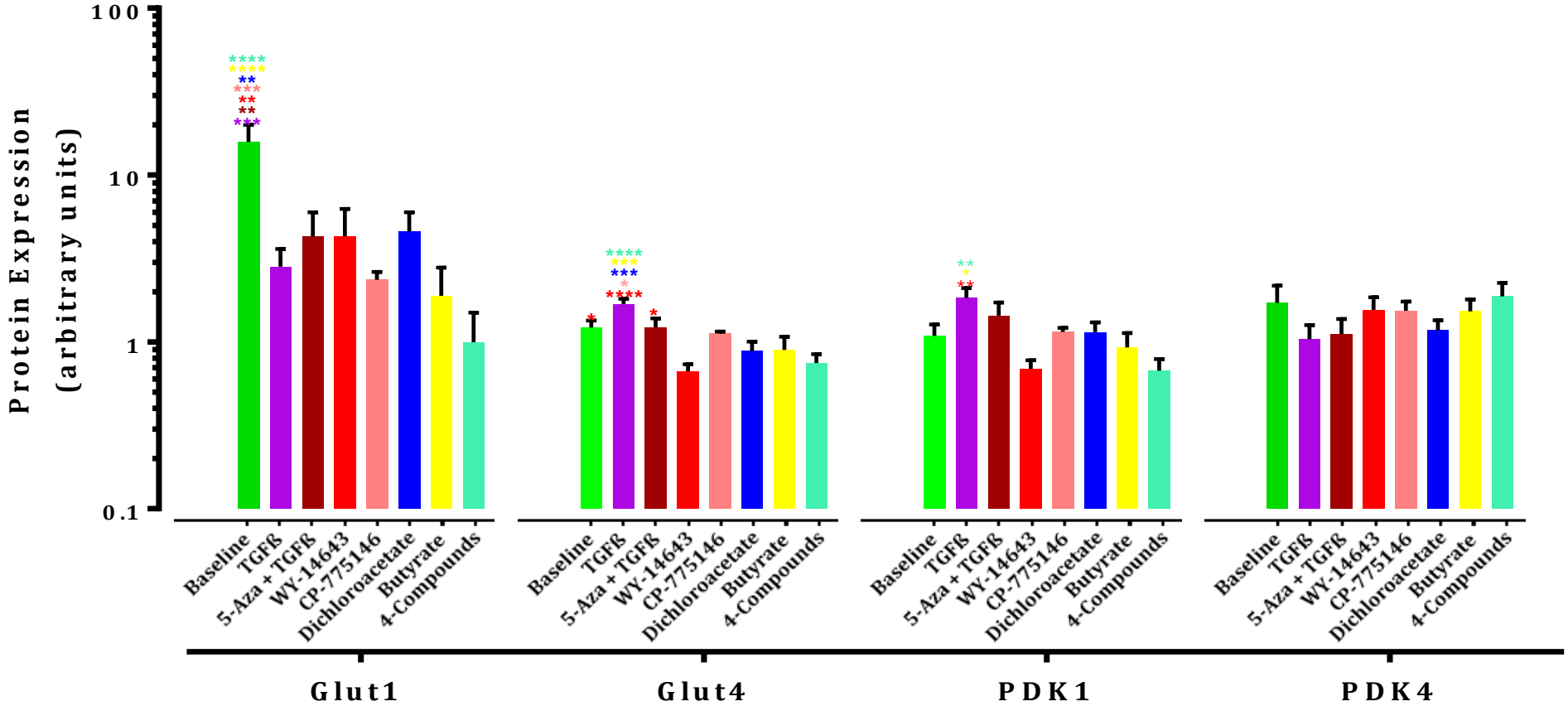



***Figure 5.18 The relative expression of proteins involved in glucose metabolism.*** *Control and 30-days small molecule treated P2-CDCs cultured on FN were lysed to assess the molecular profile of proteins involved in glucose metabolism including Glut1 and Glut4, PDK1 and PDK4. Abbreviations: FN: Fibronectin substrate; Glut1 and 4: Glucose transporter 1 and 4; PDK1 and 4: Pyruvate dehydrogenase lipoamide kinase 1 and 4. Multicolour stars indicate multiple comparisons with every other condition. *: $p < 0.01$; **: $p < 0.001$; ***: $p < 0.004$; ****: $p < 0.0001$.*

### 5.4.5.2 Molecular profile of mitochondrial and fatty acid transport proteins

Analysis of the expression of proteins in the TCA cycle revealed an increased level of CISY protein in baseline and TGFβ-treated cells in comparison to the small molecule(s) treated cells. However, there were no significant differences in protein expression of αKGDH (TCA cycle) and the fatty acid transporter, CD36, between the baseline and other treated cells. Nevertheless, mitochondrial uncoupling protein 3 (UCP3) protein level was higher in CP-775146, butyrate, and 4-Compounds treated cells compared to the baseline and other treated cells ($p < 0.001$, Figure 5.19).

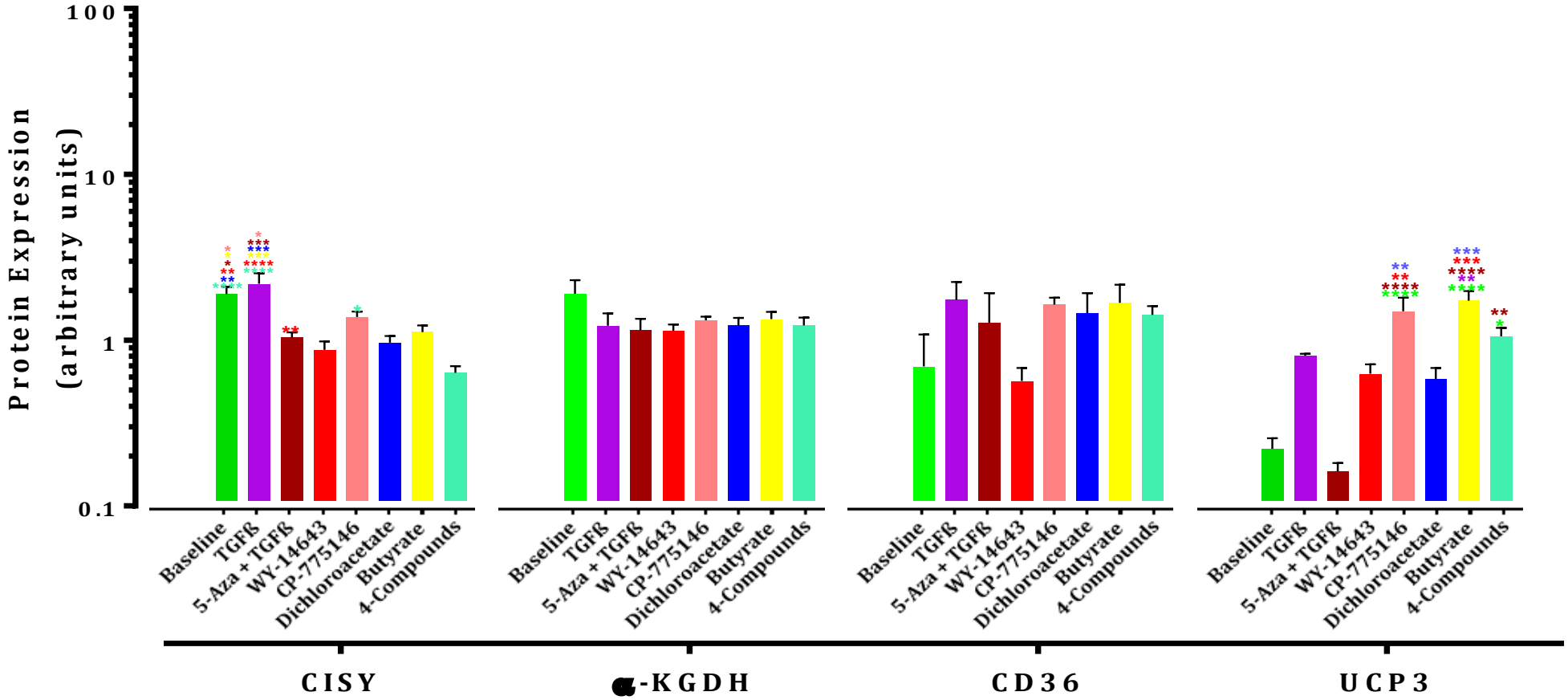



***Figure 5.19 The relative expression of proteins involved in the citric acid cycle and fatty acid metabolism.*** *Control and 30-days small molecule treated P2-CDCs cultured on FN were lysed to assess the molecular profile of the citric acid cycle proteins CISY and αKGDH, and proteins involved in fatty acid metabolism CD36, MCAD, and UCP3. Abbreviations: αKGDH: Alpha-Ketoglutarate Dehydrogenase; CD36: Cluster of differentiation 36; CISY: Citrate synthase; UCP3: uncoupling protein 3. Multicolour stars indicate multiple comparisons with every other condition. *: p < 0.01; **: p < 0.001; ***: p < 0.004; ****: p < 0.0001.*

### 5.4.6 Immunophenotypic characterisation of WY-14643+TGFβ treated cells

Phenotypic characterization of differentiated P2-CDCs grown on glass coverslips and treated with WY-14643+TGFβ for 30-days was assessed using immunocytochemistry with confocal microscopy to localize mature cardiac marker(s) including Titin (Figure 5.22), cardiac troponin T (cTnnT2) (Figure 5.23 and 5.25), myosin heavy chain (MHC) (Figure 5.24), myosin light chain (MLC) (Figure 5.23 and 5.24), and connexin 43 (CX43) (Figure 5.25). Negative controls for WY-14643+TGFβ differentiated cells (secondary antibody only, Figure 5.20) and positive controls (neonatal rat heart cells courtesy of Prof Zaccolo's group, Figure 5.21) confirmed the integrity of secondary and primary antibodies respectively. Moreover, mitochondrial staining showed a high fluorescent intensity, indicative of mitochondrial $\Delta\psi m$, of the differentiated CDCs (Figure 5.27) as seen with that from beating neonatal rat heart cells (Figure 5.26).

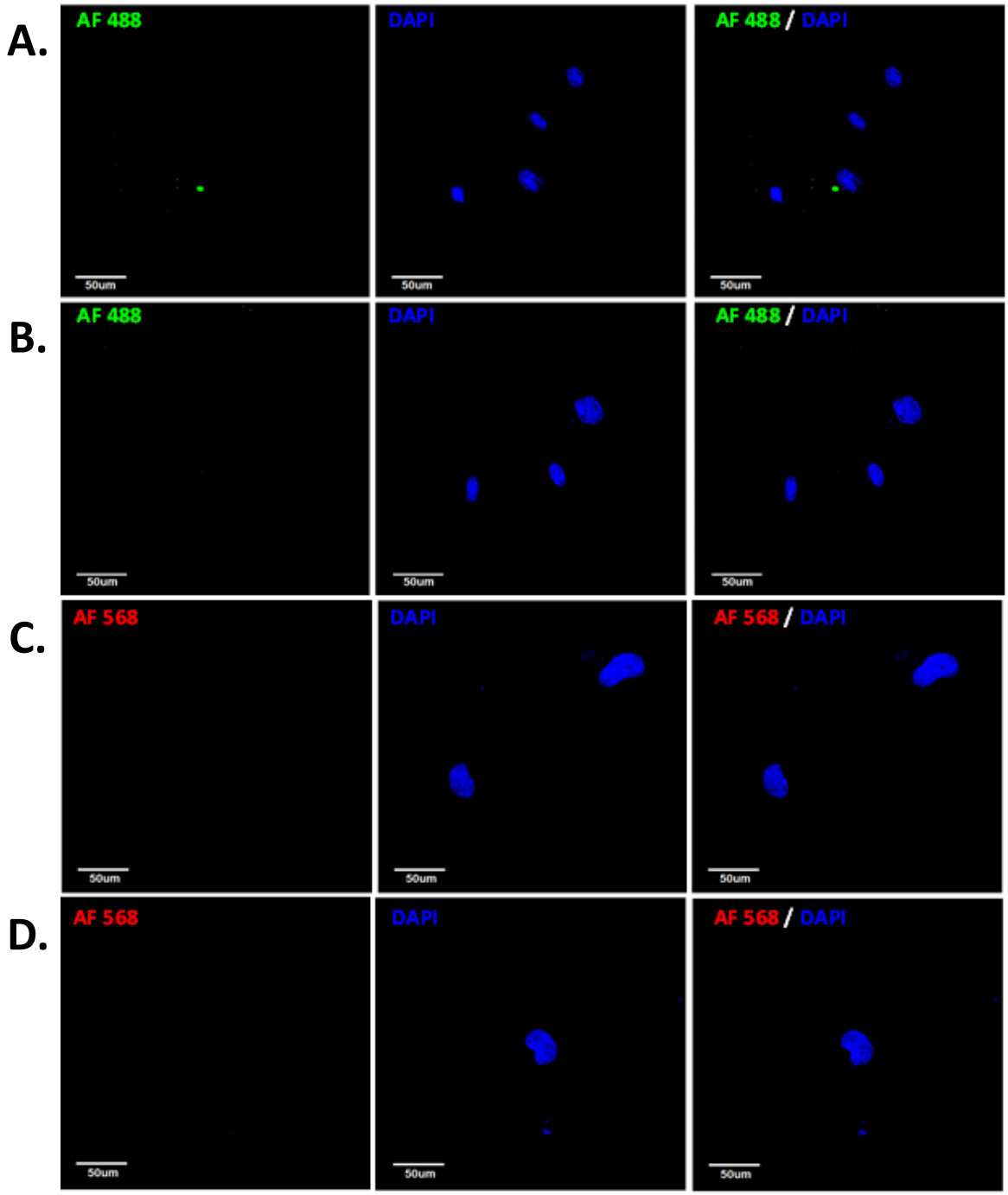



***Figure 5.20 Representative confocal images of negative controls on WY-14643+TGFβ differentiated cells.*** *Differentiated P2-CDCs with WY-14643+TGFβ for 30-days, fixed with PFA, blocked and stained with secondary antibodies only,* ***A.*** *Fluor 488 Donkey anti-Mouse (D@M);* ***B.*** *Alexa Fluor 488 Donkey anti-Rabbit (D@R);* ***C.*** *and* ***D.*** *Alexa Fluor 568 Goat anti-Rabbit (G@Rb). Nuclei were stained with DAPI (blue). Abbreviations: P2-CDCs: Passage 2 Cardiosphere-Derived Cells, transforming growth factor-beta (TGF-β), DAPI: 4', 6-diamidino-2-phenylindole. Scale bar 50 µm.*

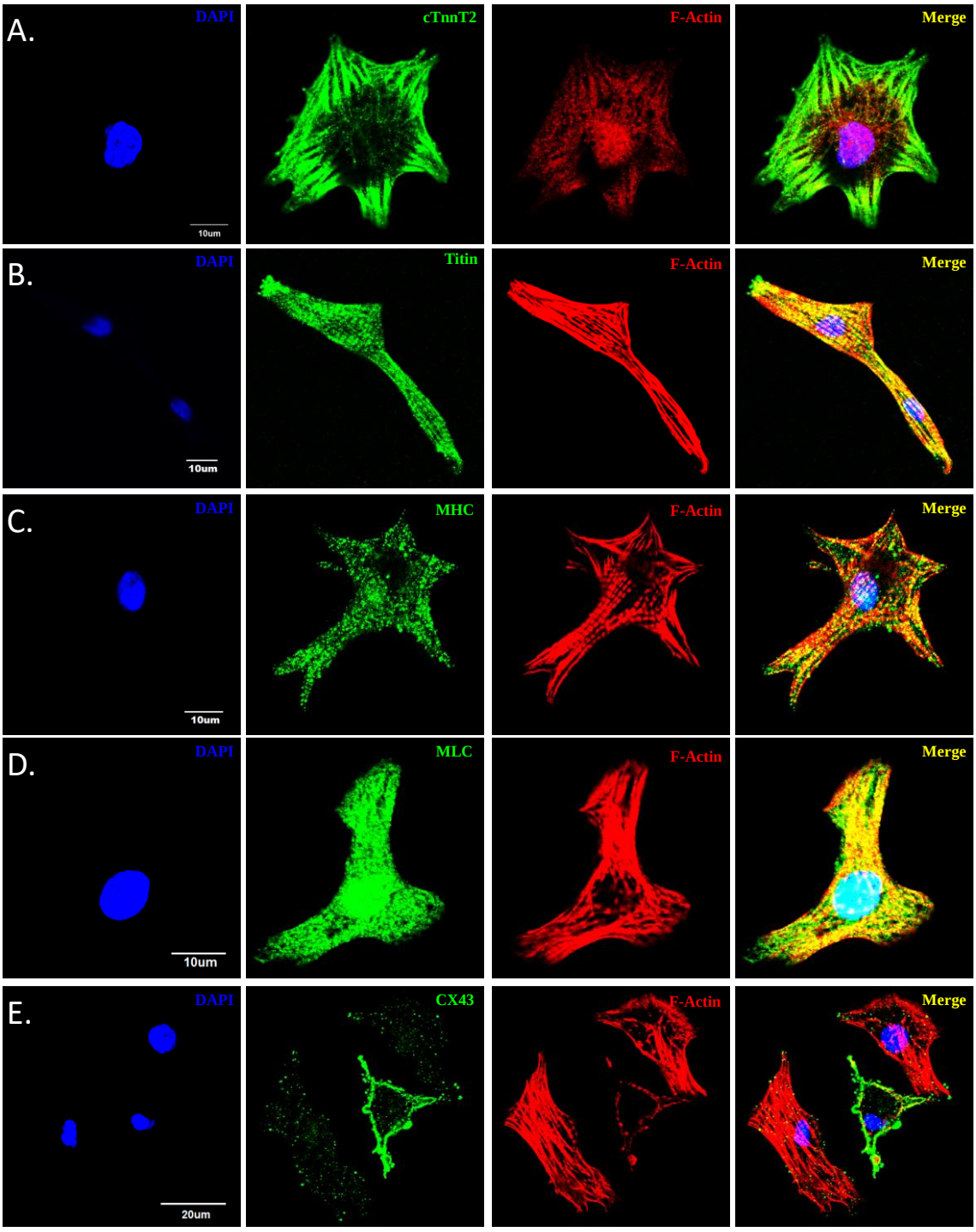



***Figure 5.21 Representative confocal images of positive controls on neonatal rat heart cells.*** *Enzymatically isolated cells from neonatal rat heart and cultured on coverslips for 24 hours were fixed, permeabilized, blocked, stained and visualized by confocal microscopy for cardiac-specific cell markers including* ***A.*** *cardiac troponin T2 (cTnnT2) (green),* ***B.*** *Titin (green),* ***C.*** *myosin heavy chain (MHC) (green),* ***D.*** *myosin light chain (MLC) (green),* ***E.*** *Connexin 43 (CX43) (green) and filamentous actin (F-Actin) (red). Abbreviations: DAPI: 4', 6-diamidino-2-phenylindole. Scale bar 10 µm and 20 µm.*

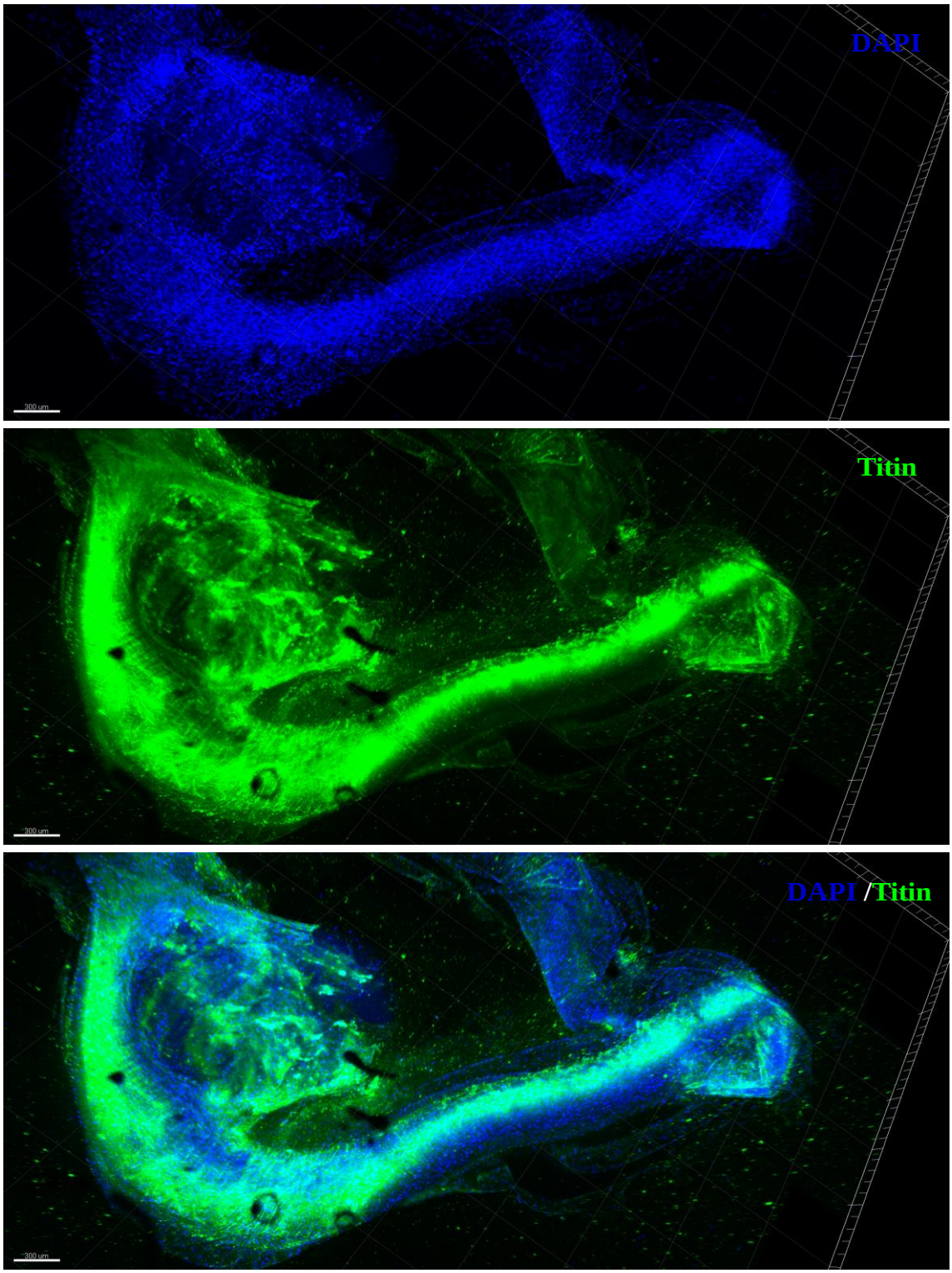



***Figure 5.22 Immunophenotyping of WY-14643+TGFβ differentiated cells.*** *Representative confocal images of immunostained WY-14643+TGFβ treated P2-CDCs for 30-days demonstrated the expression of the cardiac specific protein Titin (green). Nuclei were stained with DAPI (blue). Abbreviations: P2-CDCs: Passage 2 Cardiosphere-Derived Cells, DAPI: 4', 6-diamidino-2-phenylindole. Scale bar: 1000 μm.*

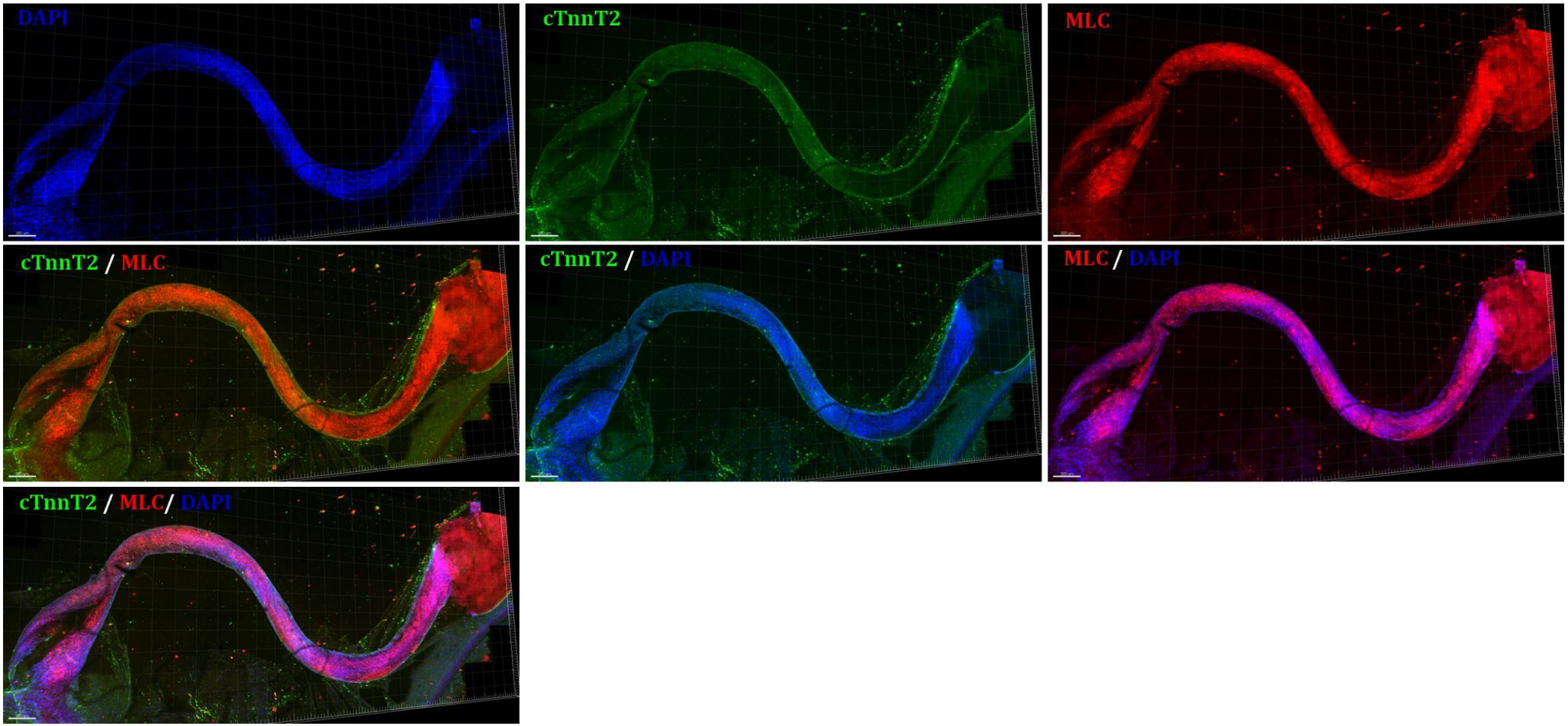



***Figure 5.23 Immunophenotyping of WY-14643+TGFβ differentiated cells.*** *Representative confocal images of immunostained WY-14643+TGFβ treated P2-CDCs for 30-days demonstrated the expression of the cardiac specific proteins cTnnT2 (green) and MLC (red). Nuclei were stained with DAPI (blue). Abbreviations: P2-CDCs = Passage 2 Cardiosphere-Derived Cells, DAPI = 4', 6-diamidino-2-phenylindole; cTnnT2: cardiac troponin T2; MLC: myosin light chain. Scale bar = 300 µm.*

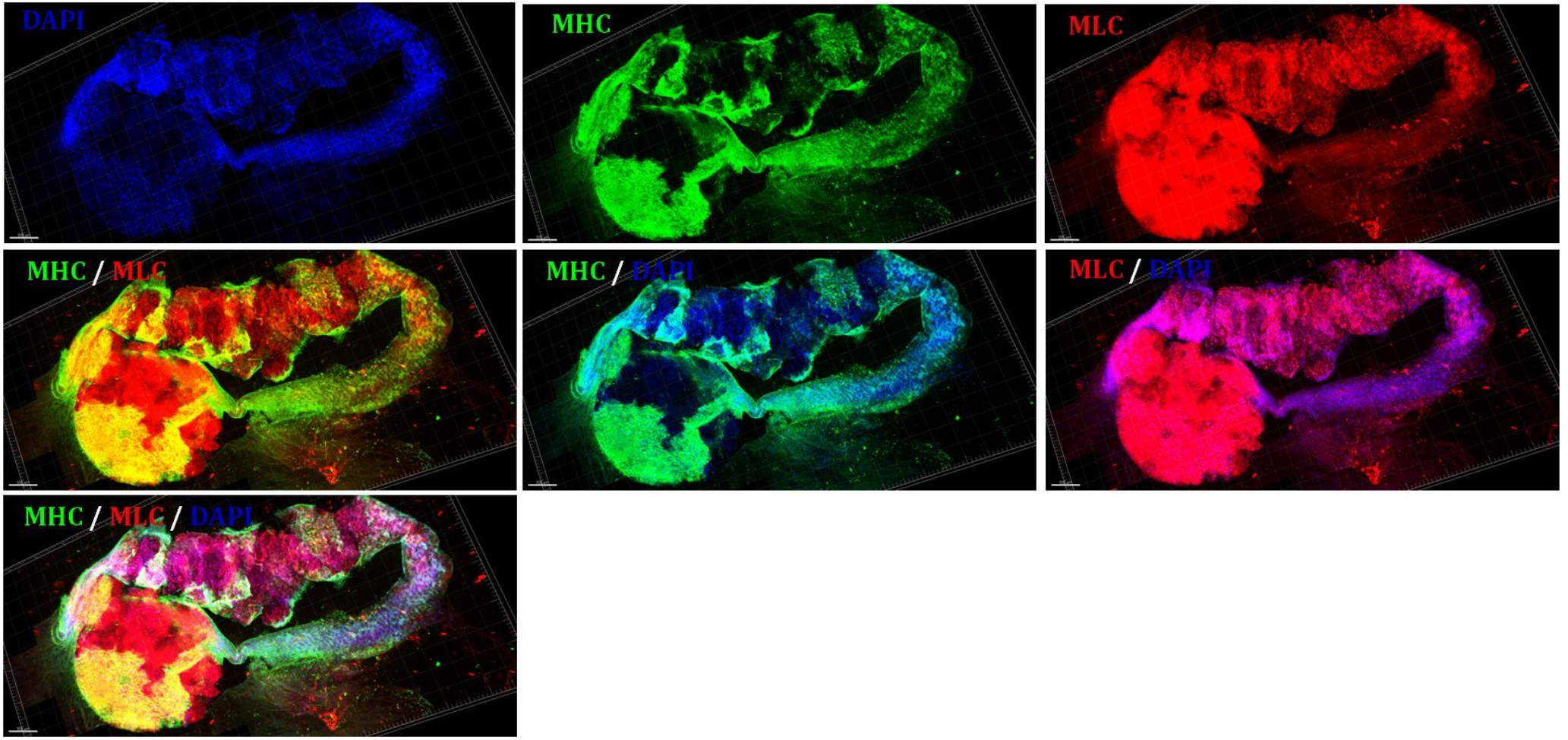



***Figure 5.24 Immunophenotyping of WY-14643+TGFβ differentiated cells.*** *Representative confocal images of immunostained WY-14643+TGFβ treated P2-CDCs for 30-days demonstrated the expression of the cardiac specific cell proteins MHC (green) and MLC (red). Nuclei were stained with DAPI (blue). Abbreviations: P2-CDCs = Passage 2 Cardiosphere-Derived Cells, DAPI = 4', 6-diamidino-2-phenylindole; MHC: myosin heavy chain; MLC: myosin light chain. Scale bar = 300 µm.*

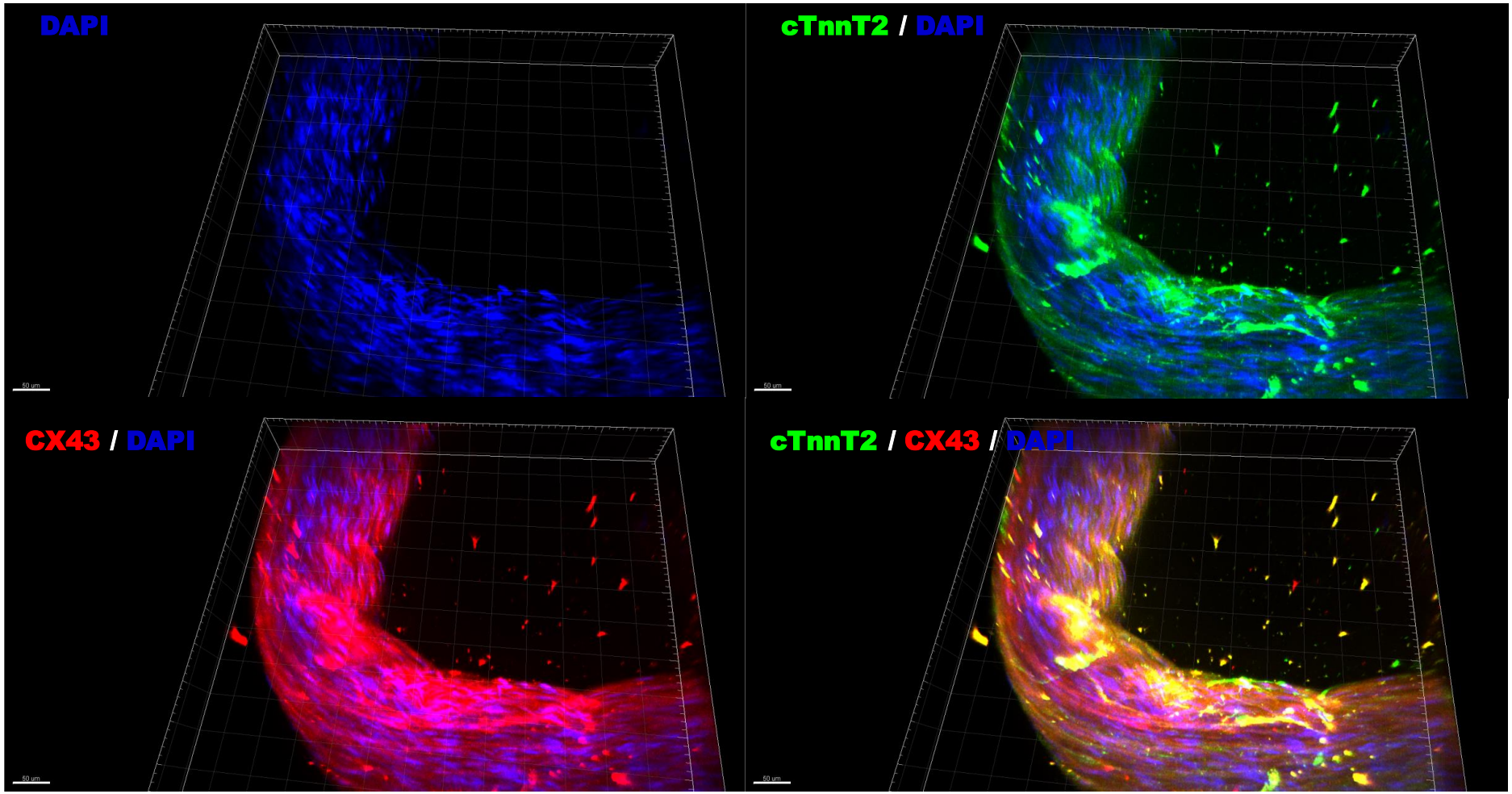



***Figure 5.25 Immunophenotyping of WY-14643+TGFβ differentiated cells.*** *Representative confocal images of immunostained WY-14643+TGFβ treated P2-CDCs for 30-days demonstrated the expression of the cardiac specific cell proteins cardiac troponin T2 (cTnnT2) (green) and connexin 43 (CX43) (red). Nuclei were stained with DAPI (blue). Abbreviations: P2-CDCs = Passage 2 Cardiosphere-Derived Cells, DAPI = 4', 6-diamidino-2-phenylindole. Scale bar = 50 µm.*

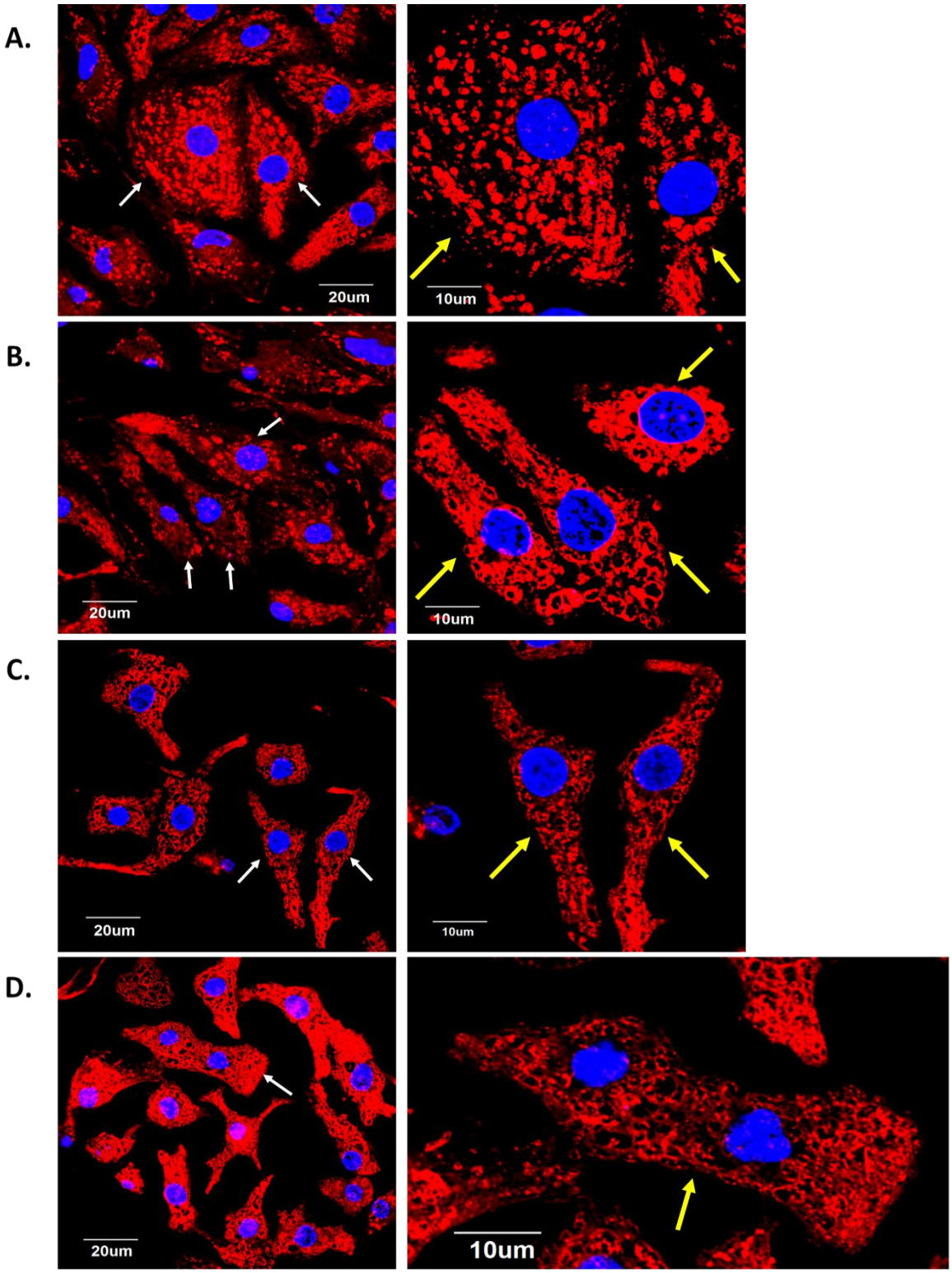



***Figure 5.26 Mitochondria membrane potential (Δψm) in neonatal rat heart cells.*** *Enzymatically isolated cells from neonatal rat heart and cultured on coverslips for 24 hours were incubated with MitoTracker® Red CMXRos reagent (100 nM) at 37°C for 20 min, fixed with PFA and visualized by confocal microscopy. Selected individual cells (white arrows) were zoomed in (indicated by yellow arrows). The visible light absorption maximum of Mito Tracker Red CMXRos is 579 nm, and the emission maximum occurs at 599 nm. Nuclei were stained with blue-fluorescent DAPI. Abbreviations: DAPI = 4', 6-diamidino-2-phenylindole. Scale bars are 10 µm and 20 µm.*

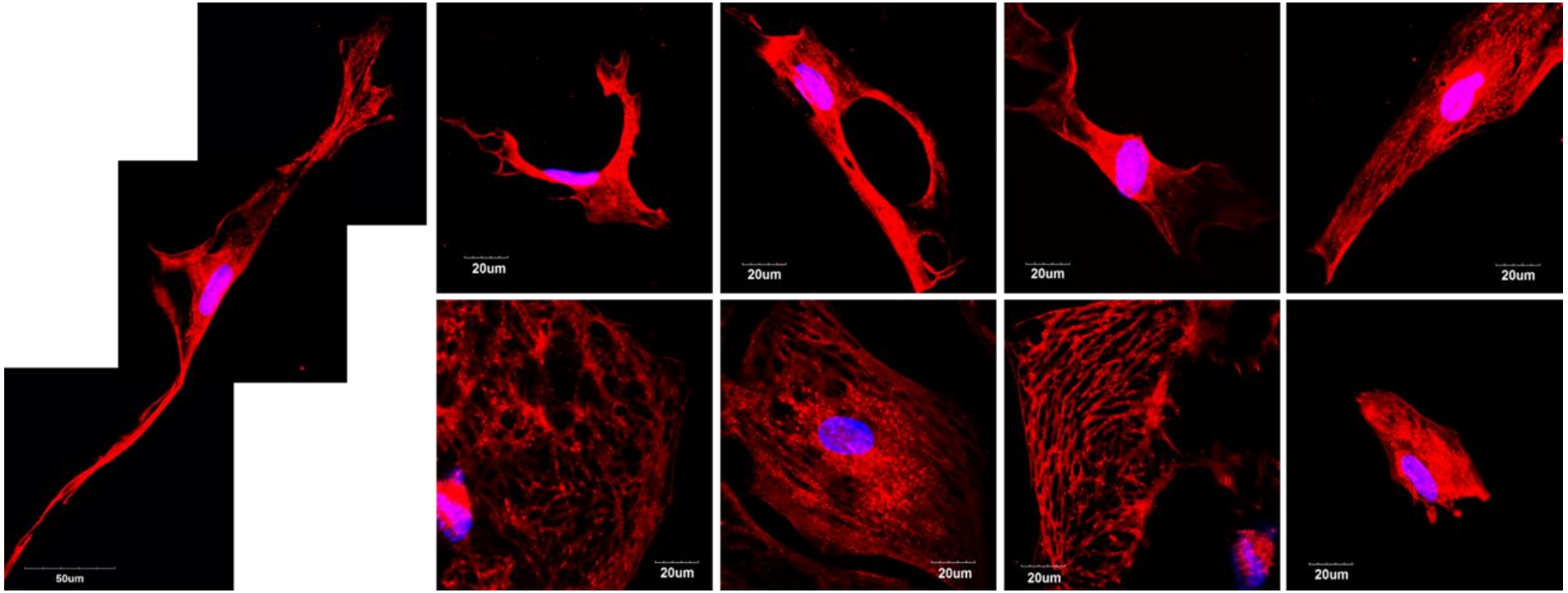



***Figure 5.27 Mitochondria membrane potential (Δψm) in cardiomyogenic differentiated CDCs with WY-14643+TGFβ.*** *Differentiated CDCs cultured on coverslips for 30 days were incubated with MitoTracker® Red CMXRos reagent (0.05 ng/µl in serum free DMEM) at 37°C for 20 min, fixed with PFA and visualized by confocal microscopy. The visible light absorption maximum of Mito Tracker Red CMXRos is 579 nm, and the emission maximum occurs at 599 nm. Nuclei were stained with blue-fluorescent DAPI. Abbreviations: P2-CDCs = Passage 2 Cardiosphere-Derived Cells, DAPI = 4', 6-diamidino-2-phenylindole. Scale bars are 20 µm and 50 µm.*

## 5.5 Discussion

The aims of the work described in this chapter were to create P2-CDCs through ColIV/HD technique and differentiate them on FN in gelatine coated dishes using TGF-β and different small molecule(s) followed by examining substrate utilisation through glycolysis and OXPHOS of glucose and palmitate. Furthermore, the molecular profile of gene and protein expression levels involved in each pathway were assessed.

***Cardiac Stem/Progenitor cells, P2-CDCs, were successfully differentiated into beating cardiomyocyte cells using TGF-β +WY-14643***

In the current study, 5-weeks old rat cardiac stem/progenitor cells, P2-CDCs, have been successfully differentiated into beating cardiomyocytes after treatment with WY-14643+TGF-β2 for 30 days. The differentiated cardiomyocyte cells expressed significant levels of cardiac-specific genes and proteins as well as metabolic changes from glycolytic metabolism to fatty acid oxidation or mitochondrial OXPHOS.

***Differentiated CDCs with TGF-β had remarkable morphological changes***

Following cardiomyogenic differentiation of CDCs with TGF-β either with or without the presence of small molecule(s), the cells experienced morphological changes. For the first three days of differentiation, there was a significantly high level of cell death due to cytotoxicity of 5-Azacytidine during its incorporation into the DNA and RNA[320, 321]. However, following TGF-β treatment the cell population reached 100% confluency. The cells then started to form circular patterns followed by aggregation to 3D structures with a large globular body in the middle and two elongated arms, which attached to the side of the dish and held the entire 3D structure. These morphological changes may be similar to those seen in other studies[165-167, 318] where TGF-β treatment also increased cell population up to 100% confluency and cells started to a form circular pattern[318]. The 3D structure of CDCs in this study may be due to the several different types of ECM proteins that are produced and secreted by the cells in culture. This can be supported by other studies that report that, in many cell

types, TGF-β increases expression of ECM proteins including fibronectin; collagen I, III, V, VI; proteoglycans; tenascin; osteonectin; osteopontin, and thrombospondin as well as upregulating integrin receptors for collagen, fibronectin, laminin and vitronectin[170, 171]. Moreover, TGF-β increases expression of collagen[172] in cardiac fibroblasts and decreases expression of collagenase and transin in stimulated cardiomyocytes and cardiac fibroblasts[164, 171].

***Effect of TGF-β on cardiomyogenic differentiation***

Hitherto *in vitro* cardiomyogenic differentiation of cardiac stem/progenitor cells was most successful through co-culture with neonatal cardiomyocytes[106, 138]. It is possible that cardiomyocyte co-culture effects on differentiation are mediated by TGF-β, which is secreted by neonatal cardiomyocytes [164] as it is involved in cardiac differentiation of ESCs[165, 166] and hCMPCs with up to 100% efficiency[167]. Furthermore, TGF-β is usually secreted by neonatal as well as adult cardiomyocyte cells, induces expression of contractile protein genes which are up-regulated in hypertrophy[168] and maintains the beating rate of cells[169]. Moreover, TGF-β induces its expression in cardiomyocyte and fibroblasts cells[164]. Both mRNA and protein TGF-β expression increased following ischemic injury and a decrease in cardiac damage following ischemia-reperfusion in the rat was observed when TGF-β was exogenously administered. Differentiation with TGF-β and 5-azacytidine resulted in upregulation of cardiac markers. However, these cells showed that they are still immature and metabolically rely mostly on glycolysis instead of mitochondrial OXPHOS. Hence, we tried to use small molecules to change the metabolism of CDCs from glycolytic to the mitochondrial OXPHOS.

***Effect of PPARα on cardiac metabolism***

We investigated whether progenitors expanded on plastic are able to fully differentiate and whether maturation can be stimulated in vitro by upregulation of fatty acid oxidation. We tested the synthetic fibrate WY-14643[322] and showed that the differentiated cells had increased the level of gene expression of the fatty acid transporters in the cells, CD36, and the mitochondria, CPT1b; and oxidation enzymes MCAT and ACADM and protein expression of mitochondrial uncoupling protein 3, UCP3.

***Proliferating undifferentiated P2-CDCs had high glycolytic flux***

Adult cardiac stem/progenitor cells in the stem cell niche are predominantly quiescent. When stimulated to migrate and replace damaged myocytes, the cells need to increase mitochondrial numbers and fatty acid metabolism. Cardiac progenitor cells expanded in vitro also need to upregulate mitochondrial numbers and TCA cycle metabolism, to generate energy for proliferation. Hitherto there have been a limited number of studies into the metabolism of adult cardiac stem/progenitor cells.

Recent studies have shown that glutamine regulates cardiac progenitor cell metabolism and proliferation[306]. Moreover, bone marrow and adipose-derived stem cells cultured under hypoxia, like cancer cells, metabolise glutamine to maintain cell proliferation[323]. Nevertheless, other studies found that glutamine is not a major source of energy in bone marrow stromal cells[324] as we found with cardiac stem/progenitor cells (Chapter 4, Figure 4.6). In comparison to normal cells, proliferating tumour cells, which are in a great need of ATP, generate energy by aerobic glycolysis, known as the Warburg effect[205]. These cells, regardless of the availability of oxygen, metabolise tenfold more glucose to lactate in a given time[205, 206] without any sign of oxidative impairment[207]. Glycolysis outpaces the pyruvate oxidation, and the cells eliminate excess pyruvate into lactate[208]. In agreement with the aforementioned studies, our findings show that proliferating undifferentiated cardiac stem/progenitor cells, P2-CDCs, have a high level of glycolytic flux which may provide the intermediates needed for biosynthetic pathways such as ribose sugars for nucleotides, glycerol and citrate for lipids, nonessential amino acids, and NADPH (through the oxidative pentose phosphate pathway)[208].

***Differentiated P2-CDCs treated with TGF-β +WY-14643 had significantly decreased glycolytic flux and increased glucose and palmitate oxidation***

Several studies have shown that when ESCs differentiate, they acquire a more oxidized state, as the glycolytic flux in these cells decreases considerably, Thr-Gly metabolism is extinguished and mitochondrial OXPHOS fuelled by glucose and fatty acids increases[204, 214, 325]. In agreement with

these findings, in the current study, the differentiated P2-CDCs treated with WY-14643+TGF-β2 for 30 days showed decreased glycolytic flux with significantly increased glucose and palmitate (fatty acid) oxidation.

Decreased glycolysis and increased glucose oxidation were further supported with gene and protein analysis. In agreement with other studies on cardiomyogenic differentiation[266, 267], the differentiated cells had decreased GLUT1 expression and switched to the high-affinity and insulin-sensitive transporter GLUT4. Furthermore, the gene expression level of PDK1[269 271, 272] and PDK4, which inactivate PDH, was lower in differentiated cells with synthetic compounds when compared to those treated with TGF-β2. This may explain that differentiated cells with lowered PKDs expression have shifted the pyruvate metabolism from glycolysis and lactate production to glucose oxidation in mitochondria. Surprisingly, pyruvate oxidation was not increased in DCA-treated cells despite the known inhibiting PDKs by DCA, possibly due to off-targeting effects of DCA in another part of the cells.

The mechanism of cellular fatty acid uptake (FA) remains controversial as it may be either via passive diffusion or mediated by transporter proteins. Studies on artificial phospholipid bilayers suggest the mechanism is likely to be a passive diffusion as the rate of FA flip-flop across the bilayer was extremely fast[326]. Other studies on the kinetics of long-chain fatty acid (LCFA) uptake from the heart and skeletal muscle using isolated vesicles revealed that LCFA uptake in these tissues is mainly via a protein-mediated mechanism, involving fatty acid translocase (FAT/CD36) and plasma membrane-bound fatty acid binding protein (FABPpm)[327]. The results of the current study of fatty acid oxidation may suggest the involvement of the latter scenarios as the results demonstrated significant increases in both FA transporter genes and proteins (CD36 and CPT1) as well as increased $^{14}$C-palmitate oxidation.

***Differentiated P2-CDCs treated with TGF-β +WY-14643 had a significant increase in cardiomyocyte lineage, contractile and calcium handling genes***

There are changes in gene expression patterns in the initial stages of heart development (stage I. cardiac crest; stage II. cardiac tube; and stage III. cardiac loop). For instance, in mouse embryos (E8) most of the genes that encode for contractile proteins including heavy-chain myosin (MHC), light-chain myosin (MLC), actin, and the troponin-tropomyosin complex are expressed at stage II of heart development, the primitive cardiac tube, which composed of two layers of myocardium and endocardium[323]. The current study demonstrated that the differentiated P2-CDCs treated with WY-14643+TGF-β2 are likely to be at stage II of heart development (Cardiac tube) since the differentiated cells expressed high levels of both genes and proteins involved in contractile activity including MHC, MLC, cTnnt2, and Titin as well as myosin heavy chain beta (MHC-β) or Myh7, which is expressed in over 90% of ventricular cardiomyocytes, suggesting they may be forming ventricular myocytes.

At stage II of heart development (cardiac tube), cardiac contraction is regulated by changes in the intracellular concentration of calcium ions ($Ca^{2+}$) through the SERCA, which pumps $Ca^{2+}$ from the cytosol into the endoplasmic reticulum (ER). SERCA is controlled by phospholamban (PLN), for which expression is opposed to that observed for SERCA2a, which has greater expression in the atrioventricular canal, ventricle, and outflow tract but is lower in the inflow tract[323]. In agreement with these studies, in the current study, the differentiated P2-CDCs treated with WY-14643+TGF-β2 expressed the high level of SERCA2a but less PLN, suggesting they may be forming ventricular myocytes.

In the mammalian heart, the major cardiac gap junction protein, connexin 43 (CX43) mediates the propagation of the cardiac impulse, by quickly transmitting changes through the membrane potential[323]. The current study showed that the differentiated P2-CDCs treated with WY-14643+TGF-β2 expressed high levels of CX43 proteins allowing propagation of the observed twitch

***Differentiated P2-CDCs treated with WY-14643+TGF-β increased mitochondrial membrane potential activity***

The aforementioned results showed metabolic changes from glycolytic metabolism into a more efficiently producing higher energy system, using fatty acid oxidation, in differentiated CDCs treated

with TGF-β+WY-14643. Further studies by mitochondrial confocal imaging revealed that these differentiated cells have a similar fluorescent intensity of the MitoTracker probe, indicative of the same level of mitochondrial Δψm, and of mitochondrial networks to those on beating neonatal rat heart cells. This may suggest the higher ATP production of these cells in comparison to control P2-CDCs.

## 5.6 Conclusion

In summary, the major focus of this work was to induce cardiomyogenic differentiation of glycolytic P2-CDCs into mature cardiomyocytes by increasing mitochondrial OXPHOS using various small molecule(s). Successfully, for the first time, rat P2-CDCs started to have a slow twitch and slow beating when treated with specific differentiation medium containing TGFβ and the PPARα agonist, WY-14643, for 30 days. Furthermore, the differentiated cells demonstrated remarkable morphological changes forming 3D tissue-like structures, as well as increased expression of cardiac-specific genes and proteins, and fundamentally switching from glycolytic metabolism into more energy producing, OXPHOS, which suggesting they may be forming ventricular myocytes.

# CHAPTER 6

# General Discussion

# General Discussion

Although studies have shown that endogenous cardiac progenitors, that have been expanded *in vitro* are able to upregulate cardiac proteins such as troponin I and myosin heavy-chain[100, 110, 152], differentiation to beating cardiomyocytes can mostly be achieved *via* co-culture with neonatal myocytes[152, 163]. Nevertheless, undifferentiated CDCs, administered to the infarcted rat heart, significantly improved ejection fraction by 9% measured *in vivo* using MRI[110]. However, in no studies has the energetics of the differentiated donor cells been assessed and it is yet to be determined whether prolonged expansion in culture impairs the potential of progenitor cells to differentiate to mature cardiomyocytes. Hence, measuring substrate utilisation and energetics, to characterise and optimise differentiation were the main objectives of the studies in this thesis.

### *Isolated CDCs from ColIV/HD technique provided higher cell numbers as they proliferate faster*

In chapter 3, *in vitro* isolation and expansion of CDCs was performed by culturing explants on either FN or ColIV, followed by stem/progenitor cell enrichment through the generation of cardiospheres either on P-D-L coated plates or hanging drops. In the currently published protocol, 1.7 ± 0.4 million CDCs were produced from 21.0 ± 1.9 mg specimens within 60 days[152]. However, here in this study using only the atria and apex of adult rat hearts, we obtained 118.6 ± 62 million cells per 168.67 mg specimen within 46 ± 5 days when cultured through ColIV/HD technique. Thus, the number of obtained cells from this technique (703,000 cells/mg tissue) was 10-fold higher than FN/PDL (66,231 cells/mg tissue) and 9-fold higher than published protocol (80,952 cells/mg tissue) in a shorter time period. This higher quantity of CDCs from the ColIV/HD technique was partly due to an increased proliferation rate compared to the CDC number produced using the FN/PDL technique. ColIV-mediated signalling has been shown to induce proliferation through intracellular signalling molecules in active forms of focal adhesion kinase (FAK) and mitogen-activated protein kinase 1/2 (MAPK 1/2)[229].

### *P2-CDCs isolated from adult rat were cardiac lineage committed*

Characterization of P2-CDCs suggested that the CDCs were a heterogeneous cell population containing both progenitors and cells committed towards cardiac lineage. Despite studies that suggested that murine CSCs and CDCs are not a source of stem cells but rather cardiac fibroblasts and $CD45^+$ hematopoietic cells[230], here in this study, we have shown that CDCs express stemness markers such as Oct4, Nanog, CD90, and c-Kit, although the latter was only at a low level. In addition, P2-CDCs have shown commitment to cardiac lineage, by expression of a relatively low level of the cardiac transcription factor, Nkx-2.5, and cardiac-specific proteins, cTnnT2, Titin, cMHC, and endothelial cell marker, vwf.

### *An immature cardiac phenotype was obtained from cardiomyogenic differentiation of P2-CDCs cultured on FN and treated with 5-Aza+AA*

Unlike a study that suggested that murine CSCs and CDCs have no cardiomyogenic potential[230], similar to other studies we were able to differentiate CDCs into an immature cardiac phenotype[174-183, 185, 186, 188-192, 232-234]. Cardiomyogenic differentiation of P2-CDCs using different conditions revealed that cells cultured at higher densities (10,000 cells / $cm^2$) on FN, and treated with 5-Aza + AA for 14 days, differentiated more compared to the cells differentiated on ColIV. *In vitro* studies have suggested that confluence cell density induced commitment to terminal differentiation by decreasing proliferation and increasing early differentiation markers[236, 237]. Likewise, here in this study, the results showed that cells differentiated better in confluent CDCs compared to non-confluent CDCs both on FN or ColIV. Studies have shown that FN-induced differentiation through the integrin-mediated activation of MEK/ERK and by a significant increase in FN receptor, integrin-β5 (ITGB5)[252, 254, 255]. Likewise, in this study differentiated CDCs cultured on FN demonstrated a significant increase in cardiac troponin T2 (cTnnT2), and PPARα gene expression in comparison to those differentiated on ColIV. Moreover, immunocytochemistry staining on differentiated cells on FN demonstrated localized proteins for cTnnT2, cTnnI, MyHC, and titin.

### *Control P2-CDCs either on FN or ColIV possess glycolytic metabolism*

Despite being resident in the heart, which derives most its energy needs from the oxidation of fatty acids[256], cardiac stem/progenitor cells are assumed to be glycolytic. Here for the first time, we investigated in vitro substrate and energy metabolism of isolated cardiac stem/progenitor cells before and after 3-weeks of cardiomyogenic differentiation. The rate of glycolysis was considerably higher in control P2-CDCs cultured on ColIV compared to those on FN. This was further supported by increased lactate production and significantly higher GLUT1 expression in control CDCs on ColIV at both gene and protein level compared to cells cultured on FN.

### *Differentiated P2-CDCs using 5-Aza, decreased glycolytic flux but increased oxidative metabolism*

The transition of cardiac stem/progenitor cells, which mainly use glycolysis for their energy need, into beating cardiomyocytes, which mostly use oxidative phosphorylation, requires a change in the energetic infrastructure of metabolism from glycolysis to oxidative phosphorylation[214, 257]. The results here showed that differentiated CDCs had decreased glycolytic flux and lactate production as well as decreased the GLUT1 mRNA expression. Differentiated CDCs cultured on FN demonstrated a higher level of glucose and palmitate oxidation level in comparison to those cells differentiated on ColIV. This was also supported by a switch from GLUT1 to the high-affinity and insulin-sensitive GLUT4 and increased fatty acid transporter genes (CD36 and CPT1), and genes involved in fatty acid metabolism (PPARα, MCAD, and ACADM). The oxidation of glucose, glutamine, and palmitate was low in control P2-CDCs cultured on either FN or ColIV. Surprisingly, control P2-CDCs cultured on either FN or ColIV had high acetoacetate (ACA) and pyruvate oxidation, which decreased after differentiation with 5-Aza. This high level of ACA oxidation in control cells may be aimed to reduce the high level of ROS production seen during proliferation and to aid cell survival and maintenance in an undifferentiated state[292], as ACA oxidation has a low level of ROS production[290, 291]. When the CDCs differentiated, the ACA oxidation was reduced, as the differentiated cells had begun to switch to fatty acid oxidation. In addition, reduced pyruvate

oxidation in differentiated CDCs may be due to the high level of the PDH inhibitors PDK1 and PDK4.

### *P2-CDCs were successfully differentiated into beating cardiomyocytes when treated with TGF-β +WY-14643*

TGFβ has been shown to induce cardiac differentiation of ESCs[165, 166], hCMPCs[167] and is thought to be part of the signalling to induce CDC differentiation through co-culture with neonatal cardiomyocytes[106, 138] as it induces expression of contractile protein genes[168, 169]. In chapter 5, adult rat cardiac stem/progenitor cells, P2-CDCs, were successfully differentiated into beating cardiomyocytes after treatment with TGF-β2 together with the PPARα agonist, WY-14643, for 30 days. The differentiated cells demonstrated an increased level of cardiac-specific genes and proteins as well as metabolic changes from glycolysis to more oxidative metabolism especially fatty acid oxidation.

### *Scaffold-free 3D structure of P2-CDCs when treated with TGF-β +WY-14643*

In previous CDC differentiations, in chapter 3 and 4, the differentiated cells were attached firmly to the bottom of the plates, whereas here, following TGF-β treatment, the cells had a 3D structure. Similar to other studies[165-167, 318], here TGF-β treated cells reached 100% confluency and started to form circular patterns followed by aggregation into 3D structures. Aggregated cells contained a large globular body in the middle and two elongated arms, which attached to the side of the dish and held the entire 3D structure. This 3D structure may be due to the excess extracellular matrix (ECM) produced by cells as TGF-β increases expression of extracellular matrix proteins as well as upregulating integrin receptors to bind to the ECM[170-172].

### *Differentiated P2-CDCs using TGF-β +WY-14643 had a significant increase in cardiomyocyte lineage, contractile and calcium handling genes*

Differentiation of the P2-CDCs using TGF-β+WY-14643 resulted in a significantly high level of specific mRNA expression in cardiac muscle cells including cTnnT2, MYH7, MYH6, and

SERCA2a, as well as a lower level of PLN expression. In contrast, these differentiated cells did not express endothelial (KDR, CDH5, VEGFa, and VEGFb) or smooth muscle (MYH11 and CNN1) markers. This was also supported by immunocytochemistry showing localization of cardiac proteins (cTnnT2, MHC, MLC, Titin) and the gap junction protein, connexin 43 (CX43).

### *Differentiated P2-CDCs using TGF-β+WY-14643 had significantly decreased glycolytic flux and increased glucose and palmitate oxidation*

Adult cardiac stem/progenitor cells in the stem cell niche are predominantly quiescent. When stimulated to migrate and replace damaged myocytes, the cells need to increase mitochondrial numbers and fatty acid metabolism. Cardiac progenitor cells expanded in vitro also need to upregulate mitochondrial numbers and TCA cycle metabolism, to generate energy for proliferation. Studies have shown that when ESCs differentiate, they acquire a more oxidized state, hence, the glycolytic flux in these cells decreases considerably and mitochondrial OXPHOS fuelled by glucose and fatty acids increases[204, 214, 325]. Likewise, the successfully differentiated P2-CDCs using TGF-β+WY-14643 demonstrated a significantly lower level of glycolytic flux and increased mitochondrial OXPHOS fuelled by glucose and palmitate.

### *Fatty acid oxidation became TGF-β+WY-14643 the main source of ATP production in differentiated P2-CDCs with TGF-β+WY-14643 than glucose oxidation and glycolysis*

Calculated adenosine triphosphate (ATP) level produced during glycolysis and oxidative metabolism revealed that for successfully differentiated P2-CDCs using TGF-β+WY-14643, the largest source of their energy came from palmitate followed by glucose oxidation, and glycolytic flux.

### *WY-14643+TGF-β differentiated CDCs had similar fluorescent intensity of mitochondrial Δψm to neonatal rat heart cells*

Mitochondria oxidize dietary hydrogen such as carbohydrates and fatty acids with $O_2$ to generate heat and ATP. Electrons donated from NADH and $FADH_{2'}$ produced during glycolysis, fatty acid oxidation and in the Krebs cycle, to complex I and III of the electron transport chain (ETC), flow

down a redox gradient to complex IV and finally to $O_2$ to form $H_2O$ (respiration). When electrons flow down the ETC, $H^+$ from complex I, III, and IV is pumped out of the mitochondrial matrix, creating a very negative potential, Δψm (>-240 mV)[328]. The stored energy in Δψm is used to synthesize ATP, as protons flow back into the matrix through a proton channel in complex V, ADP and Pi are bound, forming ATP (oxidative phosphorylation), and then matrix ATP is exchanged for cytosolic ADP[328]. Hence, mitochondria are the most negatively charged organelles in the cell.

Here in this study, MitoTracker staining suggested that the mitochondrial Δψm of these differentiated cells was increased since the intensity of staining seen with WY-14643+TGF-β treated cells was greater than that of the control and 5-Aza differentiated P2-CDCs and similar to that of beating neonatal rat heart cells

### *Study limitation and future work*

Although the optimized protocol used here to isolated endogenous cardiac progenitor cells resulted in a great cell yield with higher proliferation rate using ColIV/HD, and better cardiomyogenic differentiation using the FN/PDL culture technique, the effect of the FN and/or ColIV on specific integrin(s) involved, and their molecular signalling pathways, has not been studied. Furthermore, the cardiomyogenic differentiation protocol using WY-14346+TGFβ may have induced an increase in the mitochondrial Δψm, but the mitochondrial mass and oxygen consumption were not studied to demonstrate the ratio of mitochondrial Δψm to mitochondrial mass and an increased level of oxygen consumption. Moreover, the control P2-CDCs demonstrated high level of pyruvate oxidation compare to glucose oxidation. Also, although the cardiomyogenic differentiation protocol via WY-14346+TGFβ resulted in scaffold-free 3D tissue with slow beating cells, this has not been tested *in vivo*. Future research will focus on first: *in vitro* isolation and expansion of CDCs using both FN/PDL and ColIV/HD techniques, followed by characterizing particular integrin(s) and their signalling pathways. Second: cardiomyogenic differentiation of CDCs using WY-14346+TGFβ and measurement of oxygen consumption level, the ratio of mitochondrial mass to mitochondrial Δψm using MitoTracker green and red respectively as well as studying the regulatory factors on glucose

oxidation. Finally, *in vivo* functional study by administration of cardiomyogenic differentiated CDCs via WY-14346+TGFβ by suturing 3D tissue-like cells onto the infarcted heart and monitoring heart function using MRI analysis.

### *Conclusion*

In summary, the work in this thesis has shown that isolated and expanded cardiac stem/progenitor cells, P2-CDCs, are a heterogeneous cell population of both stem/progenitor and early committed cardiac lineage. P2-CDCs were shown to proliferate highly on ColIV and produced most of their energy needs from glycolysis, with a high level of lactate production. P2-CDCs were immaturely differentiated into cardiac lineage when cultured on FN and treated with 5-Aza for 2-weeks without beating. These immature cardiac cells had reduced glycolytic flux and lactate production, with increased OXPHOS. Therefore, we induced further cardiac differentiation by stimulating fatty acid oxidation using small molecule(s). Consequently, for the first time, P2-CDCs were successfully differentiated into beating cardiomyocytes, when cultured on FN+gelatine coated plates and treated with TGFβ+WY-14643 for 30-days. These differentiated cells were shown to have increased calcium handling genes, cardiac-specific genes, and proteins, as well as switching from glycolysis into more efficiently producing higher energy system, fatty acid oxidation, suggesting they may be forming outflow tract or ventricular myocytes.

# References

1. World Health Organisation W. The 10 leading causes of death in the world, . 2012; http://www.who.int/mediacentre/factsheets/fs310/en/index2.html Media centre, Fact sheet 310.
2. Hellermann JP, Jacobsen SJ, Gersh BJ, Rodeheffer RJ, Reeder GS, Roger VL. Heart failure after myocardial infarction: A review. *American Journal of Medicine*. 2002;113:324-330
3. Lange RA, Hillis LD. Perspective: Reperfusion therapy in acute myocardial infarction. *N. Engl. J. Med.* 2002;346:954-955
4. Keeley EC, Hillis LD. Primary pci for myocardial infarction with st-segment elevation. *N. Engl. J. Med.* 2007;356:47-54
5. McCarthy PM. Surgical therapies for post-myocardial infarction patients. *Am. J. Cardiol.* 2008;102:42G-46G
6. Frangogiannis NG, Smith CW, Entman ML. The inflammatory response in myocardial infarction. *Cardiovascular Research*. 2002;53:31-47
7. Hofstra L, Liem IH, Dumont EA, Boersma HH, van Heerde WL, Doevendans PA, DeMuinck E, Wellens HJJ, Kemerink GJ, Reutelingsperger CPM, Heidendal GA. Visualisation of cell death in vivo in patients with acute myocardial infarction. *Lancet*. 2000;356:209-212
8. Rouleau JL, De Champlain J, Klein M, Bichet D, Moye L, Packer M, Dagenais GR, Sussex B, Arnold JM. Activation of neurohumoral systems in postinfarction left ventricular dysfunction. *Journal of the American College of Cardiology*. 1993;22:390-398
9. Sutton MGS, Sharpe N. Left ventricular remodeling after myocardial infarction - pathophysiology and therapy. *Circulation*. 2000;101:2981-2988
10. Shin SH, Hung CL, Uno H, Hassanein AH, Verma A, Bourgoun M, Kober L, Ghali JK, Velazquez EJ, Califf RM, Pfeffer MA, Solomon SD, Valsartan Acute Myocardial I. Mechanical dyssynchrony after myocardial infarction in patients with left ventricular dysfunction, heart failure, or both. *Circulation*. 2010;121:1096-1103
11. Rippon HJ, Bishop AE. Embryonic stem cells. *Cell Proliferation*. 2004;37:23-34
12. Amit M, Itskovitz-Eldor J. Feeder-free culture of human embryonic stem cells. In: Klimanskaya I, Lanza R, eds. *Stem cell tools and other experimental protocols*. 2006:37-49.
13. Amit M, Carpenter MK, Inokuma MS, Chiu CP, Harris CP, Waknitz MA, Itskovitz-Eldor J, Thomson JA. Clonally derived human embryonic stem cell lines maintain pluripotency and proliferative potential for prolonged periods of culture. *Developmental Biology*. 2000;227:271-278
14. Itskovitz-Eldor J, Schuldiner M, Karsenti D, Eden A, Yanuka O, Amit M, Soreq H, Benvenisty N. Differentiation of human embryonic stem cells into embryoid bodies comprising the three embryonic germ layers. *Molecular Medicine*. 2000;6:88-95
15. Thomson JA. Embryonic stem cell lines derived from human blastocysts (vol 282, pg 1147, 1998). *Science*. 1998;282:1827-1827
16. Reubinoff BE, Pera MF, Fong CY, Trounson A, Bongso A. Embryonic stem cell lines from human blastocysts: Somatic differentiation in vitro (vol 18, pg 402, 2000). *Nature Biotechnology*. 2000;18:559-559
17. Martin GR. Isolation of a pluripotent cell-line from early mouse embryos cultured in medium conditioned by teratocarcinoma stem-cells. *Proceedings of the National Academy of Sciences of the United States of America-Biological Sciences*. 1981;78:7634-7638
18. Evans MJ, Kaufman MH. Establishment in culture of pluripotential cells from mouse embryos. *Nature*. 1981;292:154-156
19. Levenberg S, Golub JS, Amit M, Itskovitz-Eldor J, Langer R. Endothelial cells derived from human embryonic stem cells. *Proceedings of the National Academy of Sciences of the United States of America*. 2002;99:4391-4396
20. Carpenter MK, Inokuma MS, Denham J, Mujtaba T, Chiu CP, Rao MS. Enrichment of neurons and neural precursors from human embryonic stem cells. *Experimental Neurology*. 2001;172:383-397

21. Assady S, Maor G, Amit M, Itskovitz-Eldor J, Skorecki KL, Tzukerman M. Insulin production by human embryonic stem cells. *Diabetes*. 2001;50:1691-1697
22. Segev H, Fishman B, Ziskind A, Shulman M, Itskovitz-Eldor J. Differentiation of human embryonic stem cells into insulin-producing clusters. *Stem Cells*. 2004;22:265-274
23. Kehat I, Kenyagin-Karsenti D, Snir M, Segev H, Amit M, Gepstein A, Livne E, Binah O, Itskovitz-Eldor J, Gepstein L. Human embryonic stem cells can differentiate into myocytes with structural and functional properties of cardiomyocytes. *Journal of Clinical Investigation*. 2001;108:407-414
24. Hodgson DM, Behfar A, Zingman LV, Kane GC, Perez-Terzic C, Alekseev AE, Puceat M, Terzic A. Stable benefit of embryonic stem cell therapy in myocardial infarction. *American Journal of Physiology-Heart and Circulatory Physiology*. 2004;287:H471-H479
25. Gerecht Nir S, David R, Zaruba M, Franz W-M, Itskovitz-Eldor J. Human embryonic stem cells for cardiovascular repair. *Cardiovascular Research*. 2003;58:313-323
26. Nussbaum J, Minami E, Laflamme MA, Virag JAI, Ware CB, Masino A, Muskheli V, Pabon L, Reinecke H, Murry CE. Transplantation of undifferentiated murine embryonic stem cells in the heart: Teratoma formation and immune response. *Faseb Journal*. 2007;21:1345-1357
27. Draper JS, Pigott C, Thomson JA, Andrews PW. Surface antigens of human embryonic stem cells: Changes upon differentiation in culture. *Journal of Anatomy*. 2002;200:249-258
28. Orive G, Hernandez RM, Gascon AR, Igartua M, Pedraz JL. Controversies over stem cell research. *Trends in Biotechnology*. 2003;21:109-112
29. Takahashi K, Tanabe K, Ohnuki M, Narita M, Ichisaka T, Tomoda K, Yamanaka S. Induction of pluripotent stem cells from adult human fibroblasts by defined factors. *Cell*. 2007;131:861-872
30. Takahashi K, Yamanaka S. Induction of pluripotent stem cells from mouse embryonic and adult fibroblast cultures by defined factors. *Cell*. 2006;126:663-676
31. Moad M, Pal D, Hepburn AC, Williamson SC, Wilson L, Lako M, Armstrong L, Hayward SW, Franco OE, Cates JM, Fordham SE, Przyborski S, Carr-Wilkinson J, Robson CN, Heer R. A novel model of urinary tract differentiation, tissue regeneration, and disease: Reprogramming human prostate and bladder cells into induced pluripotent stem cells. *European Urology*. 2013;64:753-761
32. Okita K, Nagata N, Yamanaka S. Immunogenicity of induced pluripotent stem cells. *Circ.Res.* 2011;109:720-721
33. Mauritz C, Schwanke K, Reppel M, Neef S, Katsirntaki K, Maier LS, Nguemo F, Menke S, Haustein M, Hescheler J, Hasenfuss G, Martin U. Generation of functional murine cardiac myocytes from induced pluripotent stem cells. *Circulation*. 2008;118:507-517
34. Zhang J, Wilson GF, Soerens AG, Koonce CH, Yu J, Palecek SP, Thomson JA, Kamp TJ. Functional cardiomyocytes derived from human induced pluripotent stem cells. *Circ.Res.* 2009;104:E30-E41
35. Laurent LC, Ulitsky I, Slavin I, Tran H, Schork A, Morey R, Lynch C, Harness JV, Lee S, Barrero MJ, Ku S, Martynova M, Semechkin R, Galat V, Gottesfeld J, Belmonte JCI, Murry C, Keirstead HS, Park H-S, Schmidt U, Laslett AL, Muller F-J, Nievergelt CM, Shamir R, Loring JF. Dynamic changes in the copy number of pluripotency and cell proliferation genes in human escs and ipscs during reprogramming and time in culture. *Cell Stem Cell*.8:106-118
36. Okita K, Ichisaka T, Yamanaka S. Generation of germline-competent induced pluripotent stem cells. *Nature*. 2007;448:313-317
37. Lister R, Pelizzola M, Kida YS, Hawkins RD, Nery JR, Hon G, Antosiewicz-Bourget J, O'Malley R, Castanon R, Klugman S, Downes M, Yu R, Stewart R, Ren B, Thomson JA, Evans RM, Ecker JR. Hotspots of aberrant epigenomic reprogramming in human induced pluripotent stem cells. *Nature*. 2011;471:68-U84
38. Polo JM, Liu S, Figueroa ME, Kulalert W, Eminli S, Tan KY, Apostolou E, Stadtfeld M, Li Y, Shioda T, Natesan S, Wagers AJ, Melnick A, Evans T, Hochedlinger K. Cell type of origin

influences the molecular and functional properties of mouse induced pluripotent stem cells. *Nature Biotechnology*. 2010;28:848-U130
39. Kim K, Doi A, Wen B, Ng K, Zhao R, Cahan P, Kim J, Aryee MJ, Ji H, Ehrlich LIR, Yabuuchi A, Takeuchi A, Cunniff KC, Hongguang H, McKinney-Freeman S, Naveiras O, Yoon TJ, Irizarry RA, Jung N, Seita J, Hanna J, Murakami P, Jaenisch R, Weissleder R, Orkin SH, Weissman IL, Feinberg AP, Daley GQ. Epigenetic memory in induced pluripotent stem cells. *Nature*. 2010;467:285-U260
40. Panopoulos AD, Ruiz S, Izpisua Belmonte JC. Ipscs: Induced back to controversy. *Cell Stem Cell*. 2011;8:347-348
41. Li LH, Xie T. Stem cell niche: Structure and function. *Annual review of cell and developmental biology*. 2005:605-631.
42. Urbanek K, Cesselli D, Rota M, Nascimbene A, De Angelis A, Hosoda T, Bearzi C, Boni A, Bolli R, Kajstura J, Anversa P, Leri A. Stem cell niches in the adult mouse heart. *Proceedings of the National Academy of Sciences of the United States of America*. 2006;103:9226-9231
43. National Institutes of Health TDIH. What are adult stem cells? Http://stemcells.Nih.Gov/info/basics/pages/basics4.Aspx.
44. Poulsom R, Alison MR, Forbes SJ, Wright NA. Adult stem cell plasticity. *Journal of Pathology*. 2002;197:441-456
45. Forbes SJ, Vig P, Poulsom R, Wright NA, Alison MR. Adult stem cell plasticity: New pathways of tissue regeneration become visible. *Clinical Science*. 2002;103:355-369
46. Friedens.Aj, Piatetzk, II, Petrakov.Kv. Osteogenesis in transplants of bone marrow cells. *Journal of Embryology and Experimental Morphology*. 1966;16:381-&
47. Friedens.Aj, Chailakh.Rk, Lalykina KS. Development of fibroblast colonies in monolayer cultures of guinea-pig bone marrow and spleen cells. *Cell and Tissue Kinetics*. 1970;3:393-&
48. Owen M. Marrow stromal stem cells. *Journal of cell science. Supplement*. 1988;10:63-76
49. Jackson KA, Majka SM, Wang H, Pocius J, Hartley CJ, Majesky MW, Entman ML, Michael LH, Hirschi KK, Goodell MA. Regeneration of ischemic cardiac muscle and vascular endothelium by adult hematopoietic stem cells. *Circulation*. 2001;104:II.289-II.289
50. Orlic D, Kajstura J, Chimenti S, Jakoniuk I, Anderson SM, Li BS, Pickel J, McKay R, Nadal-Ginard B, Bodine DM, Leri A, Anversa P. Bone marrow cells regenerate infarcted myocardium. *Nature*. 2001;410:701-705
51. Fisher SA, Zhang H, Doree C, Mathur A, Martin-Rendon E. Stem cell treatment for acute myocardial infarction. *The Cochrane database of systematic reviews*. 2015;9:CD006536-CD006536
52. Lunde K, Solheim S, Aakhus S, Arnesen H, Abdelnoor M, Egeland T, Endresen K, Ilebekk A, Mangschau A, Fjeld JG, Smith HJ, Taraldsrud E, Grogaard HK, Bjornerheim R, Brekke M, Mueller C, Hopp E, Ragnarsson A, Brinchmann JE, Forfang K. Intracoronary injection of mononuclear bone marrow cells in acute myocardial infarction. *N. Engl. J. Med.* 2006;355:1199-1209
53. Schaechinger V, Erbs S, Elsaesser A, Haberbosch W, Hambrecht R, Hoelschermann H, Yu J, Corti R, Mathey DG, Hamm CW, Sueselbeck T, Assmus B, Tonn T, Dimmeler S, Zeiher AM, Investigators R-A. Intracoronary bone marrow-derived progenitor cells in acute myocardial infarction. *N. Engl. J. Med.* 2006;355:1210-1221
54. Adler ED, Maddox TM. Cell therapy for cardiac disease: Where do we go from here? *Nat Clin Pract Cardiovasc Med*. 2007;4:2-3
55. Abdel-Latif A, Bolli R, Tleyjeh IM, Montori VM, Perin EC, Hornung CA, Zuba-Surma EK, Al-Mallah M, Dawn B. Adult bone marrow-derived cells for cardiac repair - a systematic review and meta-analysis. *Archives of Internal Medicine*. 2007;167:989-997
56. Xaymardan M, Cimini M, Fazel S, Weisel RD, Lu W-Y, Martin U, Harvey RP, Li R-K. C-kit function is necessary for in vitro myogenic differentiation of bone marrow hematopoietic cells. *Stem Cells*. 2009;27:1911-1920

57. Chien KR, Domian IJ, Parker KK. Cardiogenesis and the complex biology of regenerative cardiovascular medicine. *Science*. 2008;322:1494-1497
58. Meirelles LDS, Chagastelles PC, Nardi NB. Mesenchymal stem cells reside in virtually all post-natal organs and tissues. *J. Cell Sci.* 2006;119:2204-2213
59. Horwitz EM, Le Blanc K, Dominici M, Mueller I, Slaper-Cortenbach I, Marini FC, Deans RJ, Krause DS, Keating A. Clarification of the nomenclature for msc: The international society for cellular therapy position statement. *Cytotherapy*. 2005;7:393-395
60. Pittenger MF, Martin BJ. Mesenchymal stem cells and their potential as cardiac therapeutics. *Circ.Res.* 2004;95:9-20
61. Cho KJ, Trzaska KA, Greco SJ, McArdle J, Wang FS, Ye JH, Rameshwar P. Neurons derived from human mesenchymal stem cells show synaptic transmission and can be induced to produce the neurotransmitter substance p by interleukin-1 alpha. *Stem Cells*. 2005;23:383-391
62. Rojas M, Xu JG, Woods CR, Mora AL, Spears W, Roman J, Brigham KL. Bone marrow-derived mesenchymal stem cells in repair of the injured lung. *American Journal of Respiratory Cell and Molecular Biology*. 2005;33:145-152
63. Toma C, Pittenger MF, Cahill KS, Byrne BJ, Kessler PD. Human mesenchymal stem cells differentiate to a cardiomyocyte phenotype in the adult murine heart. *Circulation*. 2002;105:93-98
64. Makkar RR, Price MJ, Lill M, Frantzen M, Takizawa K, Kleisli T, Zheng J, Kar S, McClelan R, Miyamota T, Bick-Forrester J, Fishbein MC, Shah PK, Forrester JS, Sharifi B, Chen PS, Qayyum M. Intramyocardial injection of allogenic bone marrow-derived mesenchymal stem cells without immunosuppression preserves cardiac function in a porcine model of myocardial infarction. *Journal of Cardiovascular Pharmacology and Therapeutics*. 2005;10:225-233
65. Nagaya N, Fujii T, Iwase T, Ohgushi H, Itoh T, Uematsu M, Yamagishi M, Mori H, Kangawa K, Kitamura S. Intravenous administration of mesenchymal stem cells improves cardiac function in rats with acute myocardial infarction through angiogenesis and myogenesis. *American Journal of Physiology-Heart and Circulatory Physiology*. 2004;287:H2670-H2676
66. Shake JG, Gruber PJ, Baumgartner WA, Senechal G, Meyers J, Redmond JM, Pittenger MF, Martin BJ. Mesenchymal stem cell implantation in a swine myocardial infarct model: Engraftment and functional effects. *Annals of Thoracic Surgery*. 2002;73:1919-1925
67. Williams AR, Hare JM. Mesenchymal stem cells biology, pathophysiology, translational findings, and therapeutic implications for cardiac disease. *Circ.Res.* 2011;109:923-940
68. Hare JM, Fishman JE, Gerstenblith G, Velazquez DLD, Zambrano JP, Suncion VY, Tracy M, Ghersin E, Johnston PV, Brinker JA, Breton E, Davis-Sproul J, Schulman IH, Byrnes J, Mendizabal AM, Lowery MH, Rouy D, Altman P, Foo CWP, Ruiz P, Amador A, Da Silva J, McNiece IK, Heldman AW. Comparison of allogeneic vs autologous bone marrow-derived mesenchymal stem cells delivered by transendocardial injection in patients with ischemic cardiomyopathy the poseidon randomized trial. *Jama-Journal of the American Medical Association*. 2012;308:2369-2379
69. Behfar A, Yamada S, Crespo-Diaz R, Nesbitt JJ, Rowe LA, Perez-Terzic C, Gaussin V, Homsy C, Bartunek J, Terzic A. Guided cardiopoiesis enhances therapeutic benefit of bone marrow human mesenchymal stem cells in chronic myocardial infarction. *Journal of the American College of Cardiology*. 2010;56:721-734
70. Bartunek J, Behfar A, Dolatabadi D, Vanderheyden M, Ostojic M, Dens J, El Nakadi B, Banovic M, Beleslin B, Vrolix M, Legrand V, Vrints C, Vanoverschelde JL, Crespo-Diaz R, Homsy C, Tendera M, Waldman S, Wijns W, Terzic A. Cardiopoietic stem cell therapy in heart failure. *Journal of the American College of Cardiology*. 2013;61:2329-2338
71. Carr CA, Stuckey DJ, Tatton L, Tyler DJ, Hale SJM, Sweeney D, Schneider JE, Martin-Rendon E, Radda GK, Harding SE, Watt SM, Clarke K. Bone marrow-derived stromal cells home to

and remain in the infarcted rat heart but fail to improve function: An in vivo cine-mri study. *American Journal of Physiology-Heart and Circulatory Physiology*. 2008;295:H533-H542
72. Luttun A, Carmeliet G, Carmeliet P. Vascular progenitors: From biology to treatment. *Trends in Cardiovascular Medicine*. 2002;12:88-96
73. Hager G, Holnthoner W, Wolbank S, Husa A-M, Godthardt K, Redl H, Gabriel C. Three specific antigens to isolate endothelial progenitor cells from human liposuction material. *Cytotherapy*. 2013;15:1426-1435
74. Peichev M, Naiyer AJ, Pereira D, Zhu ZP, Lane WJ, Williams M, Oz MC, Hicklin DJ, Witte L, Moore MAS, Rafii S. Expression of vegfr-2 and ac133 by circulating human cd34(+) cells identifies a population of functional endothelial precursors. *Blood*. 2000;95:952-958
75. Ye L, Poh K-K. Enhancing endothelial progenitor cell for clinical use. *World journal of stem cells*. 2015;7:894-898
76. Yeh ETH, Zhang S, Wu HD, Korbling M, Willerson JT, Estrov Z. Transdifferentiation of human peripheral blood cd34(+)-enriched cell population into cardiomyocytes, endothelial cells, and smooth muscle cells in vivo. *Circulation*. 2003;108:2070-2073
77. Yao Y, Sheng Z, Li Y, Fu C, Ma G, Liu N, Chao J, Chao L. Tissue kallikrein-modified human endothelial progenitor cell implantation improves cardiac function via enhanced activation of akt and increased angiogenesis. *Laboratory Investigation*. 2013;93:577-591
78. Kocher AA, Schuster MD, Szabolcs MJ, Takuma S, Burkhoff D, Wang J, Homma S, Edwards NM, Itescu S. Neovascularization of ischemic myocardium by human bone-marrow-derived angioblasts prevents cardiomyocyte apoptosis, reduces remodeling and improves cardiac function. *Nature Medicine*. 2001;7:430-436
79. Kawamoto A, Gwon HC, Iwaguro H, Yamaguchi JI, Uchida S, Masuda H, Silver M, Ma H, Kearney M, Isner JM, Asahara T. Therapeutic potential of ex vivo expanded endothelial progenitor cells for myocardial ischemia. *Circulation*. 2001;103:634-637
80. Yoder MC, Mead LE, Prater D, Krier TR, Mroueh KN, Li F, Krasich R, Temm CJ, Prchal JT, Ingram DA. Redefining endothelial progenitor cells via clonal analysis and hematopoietic stem/progenitor cell principals. *Blood*. 2007;109:1801-1809
81. Heeschen C, Lehmann R, Honold J, Assmus B, Aicher A, Walter DH, Martin H, Zeiher AM, Dimmeler S. Profoundly reduced neovascularization capacity of bone marrow mononuclear cells derived from patients with chronic ischemic heart disease. *Circulation*. 2004;109:1615-1622
82. Wu Y, Ip JE, Huang J, Zhang L, Matsushita K, Liew C-C, Pratt RE, Dzau VJ. Essential role of icam-1/cd18 in mediating epc recruitment, angiogenesis, and repair to the infarcted myocardium. *Circ.Res.* 2006;99:315-322
83. Birbrair A, Delbono O. Pericytes are essential for skeletal muscle formation. *Stem Cell Reviews and Reports*. 2015;11:547-548
84. Kadi F, Charifi N, Denis C, Lexell J, Andersen JL, Schjerling P, Olsen S, Kjaer M. The behaviour of satellite cells in response to exercise: What have we learned from human studies? *Pflugers Archiv-European Journal of Physiology*. 2005;451:319-327
85. Kadi F, Schjerling P, Andersen LL, Charifi N, Madsen JL, Christensen LR, Andersen JL. The effects of heavy resistance training and detraining on satellite cells in human skeletal muscles. *Journal of Physiology-London*. 2004;558:1005-1012
86. Siegel AL, Kuhlmann PK, Cornelison DDW. Muscle satellite cell proliferation and association: New insights from myofiber time-lapse imaging. *Skeletal Muscle*. 2011;1
87. Menasche P. Skeletal myoblasts as a therapeutic agent. *Progress in Cardiovascular Diseases*. 2007;50:7-17
88. Menasche P, Hagege AA, Vilquin JT, Desnos M, Abergel E, Pouzet B, Bel A, Sarateanu S, Scorsin M, Schwartz K, Bruneval P, Benbunan M, Marolleau JP, Duboc D. Autologous skeletal myoblast transplantation for severe postinfarction left ventricular dysfunction. *Journal of the American College of Cardiology*. 2003;41:1078-1083

89. Menasch P, Alfieri O, Janssens S, McKenna W, Reichenspurner H, Trinquart L, Vilquin JT, Marolleau JP, Seymour B, Larghero J, Lake S, Chatellier G, Solomon S, Desnos M, Hagege AA. The myoblast autologous grafting in ischemic cardiomyopathy (magic) trial - first randomized placebo-controlled study of myoblast transplantation. *Circulation*. 2008;117:1189-1200
90. Chanseaume S, Azarnoush K, Maurel A, Bellamy V, Peyrard S, Bruneval P, Hagege AA, Menasche P. Can erythropoietin improve skeletal myoblast engraftment in infarcted myocardium? *Interactive cardiovascular and thoracic surgery*. 2007;6:293-297
91. Menasche P. Skeletal myoblasts and cardiac repair. *Journal of Molecular and Cellular Cardiology*. 2008;45:545-553
92. Menasche P. Towards the second generation of skeletal myoblasts. *Cardiovascular Research*. 2008;79:355-356
93. Duckers HJ, Houtgraaf J, Hehrlein C, Schofer J, Waltenberger J, Gershlick A, Bartunek J, Nienaber C, Macaya C, Peters N, Smits P, Siminiak T, van Mieghem W, Legrand V, Serruys PW. Final results of a phase iia, randomised, open-label trial to evaluate the percutaneous intramyocardial transplantation of autologous skeletal myoblasts in congestive heart failure patients: The seismic trial. *Eurointervention*. 2011;6:805-812
94. Kucia M, Reca R, Campbell FR, Zuba-Surma E, Majka M, Ratajczak J, Ratajczak MZ. A population of very small embryonic-like (vsel) cxcr4(+)ssea-1(+)oct-4(+) stem cells identified in adult bone marrow. *Leukemia*. 2006;20:857-869
95. Zuba-Surma EK, Kucia M, Abdel-Latif A, Dawn B, Hall B, Singh R, Lillard JW, Jr., Ratajczak MZ. Morphological characterization of very small embryonic-like stem cells (vsels) by imagestream system analysis. *Journal of Cellular and Molecular Medicine*. 2008;12:292-303
96. Zuba-Surma EK, Kucia M, Wu W, Klich I, Lillard JW, Jr., Ratajczak J, Ratajczak MZ. Very small embryonic-like stem cells are present in adult murine organs: Imagestream-based morphological analysis and distribution studies. *Cytometry Part A*. 2008;73A:1116-1127
97. Kucia M, Ratajczak MZ. A hypothesis for an embryonic origin of pluripotent oct-4 stem cells in adult bone marrow and other tissues. *Xenotransplantation*. 2007;14:442-443
98. Kucia M, Wu W, Ratajczak MZ. Bone marrow-derived very small embryonic-like stem cells: Their developmental origin and biological significance. *Developmental Dynamics*. 2007;236:3309-3320
99. Zuba-Surma EK, Guo Y, Taher H, Sanganalmath SK, Hunt G, Vincent RJ, Kucia M, Abdel-Latif A, Tang X-L, Ratajczak MZ, Dawn B, Bolli R. Transplantation of expanded bone marrow-derived very small embryonic-like stem cells (vsel-scs) improves left ventricular function and remodelling after myocardial infarction. *Journal of Cellular and Molecular Medicine*. 2011;15:1319-1328
100. Beltrami AP, Barlucchi L, Torella D, Baker M, Limana F, Chimenti S, Kasahara H, Rota M, Musso E, Urbanek K, Leri A, Kajstura J, Nadal-Ginard B, Anversa P. Adult cardiac stem cells are multipotent and support myocardial regeneration. *Cell*. 2003;114:763-776
101. Quaini F, Urbanek K, Beltrami AP, Finato N, Beltrami CA, Nadal-Ginard B, Kajstura J, Leri A, Anversa P. Chimerism of the transplanted heart. *N. Engl. J. Med.* 2002;346:5-15
102. Oh H, Bradfute SB, Gallardo TD, Nakamura T, Gaussin V, Mishina Y, Pocius J, Michael LH, Behringer RR, Garry DJ, Entman ML, Schneider MD. Cardiac progenitor cells from adult myocardium: Homing, differentiation, and fusion after infarction. *Proceedings of the National Academy of Sciences of the United States of America*. 2003;100:12313-12318
103. Matsuura K, Nagai T, Nishigaki N, Oyama T, Nishi J, Wada H, Sano M, Toko H, Akazawa H, Sato T, Nakaya H, Kasanuki H, Komuro I. Adult cardiac sca-1-positive cells differentiate into beating cardiomyocytes. *Journal of Biological Chemistry*. 2004;279:11384-11391
104. Pfister O, Oikonomopoulos A, Sereti KI, Liao RL. Isolation of resident cardiac progenitor cells by hoechst 33342 staining. In: Lee RJ, ed. *Stem cells for myocardial regeneration: Methods and protocols*. Totowa: Humana Press Inc; 2010:53-63.

105. Laugwitz KL, Moretti A, Lam J, Gruber P, Chen Y, Woodard S, Lin LZ, Cai CL, Lu MM, Reth M, Platoshyn O, Yuan JXJ, Evans S, Chien KR. Postnatal isl1(+) cardioblasts enter fully differentiated cardiomyocyte lineages (vol 433, pg 647, 2005). *Nature*. 2007;446:934-934
106. Messina E, De Angelis L, Frati G, Morrone S, Chimenti S, Fiordaliso F, Salio M, Battaglia M, Latronico MVG, Coletta M, Vivarelli E, Frati L, Cossu G, Giacomello A. Isolation and expansion of adult cardiac stem cells from human and murine heart. *Circ.Res.* 2004;95:911-921
107. Li TS, Suzuki R, Ueda K, Murata T, Hamano K. Analysis of the origin and population dynamics of cardiac progenitor cells in a donor heart model. *Stem Cells*. 2007;25:911-917
108. Pfister O, Mouquet F, Jain M, Summer R, Helmes M, Fine A, Colucci WS, Liao R. Cd31(-) but not cd31(+) cardiac side population cells exhibit functional cardiomyogenic differentiation. *Circ.Res.* 2005;97:52-61
109. Gaetani R, Doevendans PA, Metz CHG, Alblas J, Messina E, Giacomello A, Sluijtera JPG. Cardiac tissue engineering using tissue printing technology and human cardiac progenitor cells. *Biomaterials*. 2012;33:1782-1790
110. Carr CA, Stuckey DJ, Tan JJ, Tan SC, Gomes RSM, Camelliti P, Messina E, Giacomello A, Ellison GM, Clarke K. Cardiosphere-derived cells improve function in the infarcted rat heart for at least 16 weeks - an mri study. *PLoS One*. 2011;6
111. Oyama T, Nagai T, Wada H, Naito AT, Matsuura K, Iwanaga K, Takahashi T, Goto M, Mikami Y, Yasuda N, Akazawa H, Uezumi A, Takeda S, Komuro I. Cardiac side population cells have a potential to migrate and differentiate into cardiomyocytes in vitro and in vivo. *Journal of Cell Biology*. 2007;176:329-341
112. Chong JJH, Chandrakanthan V, Xaymardan M, Asli NS, Li J, Ahmed I, Heffernan C, Menon MK, Scarlett CJ, Rashidianfar A, Biben C, Zoellner H, Colvin EK, Pimanda JE, Biankin AV, Zhou B, Pu WT, Prall OWJ, Harvey RP. Adult cardiac-resident msc-like stem cells with a proepicardial origin. *Cell Stem Cell*. 2011;9:527-540
113. Hierlihy AM, Seale P, Lobe CG, Rudnicki MA, Megeney LA. The post-natal heart contains a myocardial stem cell population. *FEBS Lett.* 2002;530:239-243
114. Martin CM, Meeson AP, Robertson SM, Hawke TJ, Richardson JA, Bates S, Goetsch SC, Gallardo TD, Garry DJ. Persistent expression of the atp-binding cassette transporter, abcg2, identifies cardiac sp cells in the developing and adult heart. *Developmental Biology*. 2004;265:262-275
115. Oyama T, Nagai T, Wada H, Naito AT, Matsuura K, Iwanaga K, Takahashi T, Goto M, Mikami Y, Yasuda N, Akazawa H, Uezumi A, Takeda Si, Komuro I. Cardiac side population cells have a potential to migrate and differentiate into cardiomyocytes in vitro and in vivo. *Journal of Cell Biology*. 2007;176:329-341
116. Holmes C, Stanford WL. Concise review: Stem cell antigen-1: Expression, function, and enigma. *Stem Cells*. 2007;25:1339-1347
117. Blackburn EH. Structure and function of telomeres. *Nature*. 1991;350:569-573
118. Wu KJ, Grandori C, Amacker M, Simon-Vermot N, Polack A, Lingner J, Dalla-Favera R. Direct activation of tert transcription by c-myc. *Nature Genetics*. 1999;21:220-224
119. Allsopp RC, Cheshier S, Weissman IL. Telomere shortening accompanies increased cell cycle activity during serial transplantation of hematopoietic stem cells. *Journal of Experimental Medicine*. 2001;193:917-924
120. Coussens M, Davy P, Brown L, Foster C, Andrews WH, Nagata M, Allsopp R. Rnai screen for telomerase reverse transcriptase transcriptional regulators identifies hif1 alpha as critical for telomerase function in murine embryonic stem cells. *Proceedings of the National Academy of Sciences of the United States of America*. 2010;107:13842-13847
121. Wang X, Hu Q, Nakamura Y, Lee J, Zhang G, From AHL, Zhang J. The role of the sca-1(+)/cd31(-) cardiac progenitor cell population in postinfarction left ventricular remodeling. *Stem Cells*. 2006;24:1779-1788

122. Noseda M, Harada M, McSweeney S, Leja T, Belian E, Stuckey DJ, Paiva MSA, Habib J, Macaulay I, de Smith AJ, al-Beidh F, Sampson R, Lumbers RT, Rao P, Harding SE, Blakemore AIF, Jacobsen SE, Barahona M, Schneider MD. Pdgfr alpha demarcates the cardiogenic clonogenic sca1(+) stem/progenitor cell in adult murine myocardium. *Nature Communications*. 2015;6
123. Barile L, Messina E, Giacomello A, Marban E. Endogenous cardiac stem cells. *Progress in Cardiovascular Diseases*. 2007;50:31-48
124. Besmer P, Murphy JE, George PC, Qiu F, Bergold PJ, Lederman L, Snyder HW, Brodeur D, Zuckerman EE, Hardy WD. A new acute transforming feline retrovirus and relationship of its oncogene v-kit with the protein-kinase gene family *Nature*. 1986;320:415-421
125. Miettinen M, Lasota J. Kit (cd117): A review on expression in normal and neoplastic tissues, and mutations and their clinicopathologic correlation. *Applied Immunohistochemistry & Molecular Morphology*. 2005;13:205-220
126. Ronnstrand L. Signal transduction via the stem cell factor receptor/c-kit. *Cellular and Molecular Life Sciences*. 2004;61:2535-2548
127. Edling CE, Hallberg B. C-kit - a hematopoietic cell essential receptor tyrosine kinase. *International Journal of Biochemistry & Cell Biology*. 2007;39:1995-1998
128. Soonpaa MH, Field LJ. Survey of studies examining mammalian cardiomyocyte DNA synthesis. *Circ.Res.* 1998;83:15-26
129. Anversa P, Sussman MA, Bolli R. Molecular genetic advances in cardiovascular medicine - focus on the myocyte. *Circulation*. 2004;109:2832-2838
130. Miyamoto S, Kawaguchi N, Ellison GM, Matsuoka R, Shin'oka T, Kurosawa H. Characterization of long-term cultured c-kit(+) cardiac stem cells derived from adult rat hearts. *Stem Cells and Development*. 2010;19:105-116
131. Tang XL, Rokosh G, Sanganalmath SK, Yuan FP, Sato H, Mu JY, Dai SJ, Li CX, Chen N, Peng Y, Dawn B, Hunt G, Leri A, Kajstura J, Tiwari S, Shirk G, Anversa P, Bolli R. Intracoronary administration of cardiac progenitor cells alleviates left ventricular dysfunction in rats with a 30-day-old infarction. *Circulation*. 2010;121:293-U235
132. Bolli R, Chugh AR, D'Amario D, Loughran JH, Stoddard MF, Ikram S, Beache GM, Wagner SG, Leri A, Hosoda T, Sanada F, Elmore JB, Goichberg P, Cappetta D, Solankhi NK, Fahsah I, Rokosh DG, Slaughter MS, Kajstura J, Anversa P. Cardiac stem cells in patients with ischaemic cardiomyopathy (scipio): Initial results of a randomised phase 1 trial. *Lancet*. 2011;378:1847-1857
133. Kajstura J, Rota M, Cappetta D, Ogorek B, Arranto C, Bai Y, Ferreira-Martins J, Signore S, Sanada F, Matsuda A, Kostyla J, Caballero M-V, Fiorini C, D'Alessandro DA, Michler RE, del Monte F, Hosoda T, Perrella MA, Leri A, Buchholz BA, Loscalzo J, Anversa P. Cardiomyogenesis in the aging and failing human heart. *Circulation*. 2012;126:1869-U1238
134. Kajstura J, Rota M, Cappetta D, Ogorek B, Arranto C, Bai Y, Ferreira-Martins J, Signore S, Sanada F, Matsuda A, Kostyla J, Caballero M-V, Fiorini C, D'Alessandro DA, Michler RE, del Monte F, Hosoda T, Perrella MA, Leri A, Buchholz BA, Loscalzo J, Anversa P. Cardiomyogenesis in the aging and failing human heart (vol 126, pg 1869, 2012). *Circulation*. 2014;129:E466-E466
135. Karlsson O, Thor S, Norberg T, Ohlsson H, Edlund T. Insulin gene enhancer binding-protein isl-1 is a member of a novel class of proteins containing both a homodomain and a cys-his domain. *Nature*. 1990;344:879-882
136. Cai CL, Liang XQ, Shi YQ, Chu PH, Pfaff SL, Chen J, Evans S. Isl1 identifies a cardiac progenitor population that proliferates prior to differentiation and contributes a majority of cells to the heart. *Developmental Cell*. 2003;5:877-889
137. Rochais F, Mesbah K, Kelly RG. Signaling pathways controlling second heart field development. *Circ.Res.* 2009;104:933-942

138. Laugwitz KL, Moretti A, Lam J, Gruber P, Chen YH, Woodard S, Lin LZ, Cai CL, Lu MM, Reth M, Platoshyn O, Yuan JXJ, Evans S, Chien KR. Postnatal isl1+cardioblasts enter fully differentiated cardiomyocyte lineages. *Nature*. 2005;433:647-653
139. Moretti A, Caron L, Nakano A, Lam JT, Bernshausen A, Chen Y, Qyang Y, Bu L, Sasaki M, Martin-Puig S, Sun Y, Evans SM, Laugwitz K-L, Chien KR. Multipotent embryonic isl1(+) progenitor cells lead to cardiac, smooth muscle, and endothelial cell diversification. *Cell*. 2006;127:1151-1165
140. Bu L, Jiang X, Martin-Puig S, Caron L, Zhu S, Shao Y, Roberts DJ, Huang PL, Domian IJ, Chien KR. Human isl1 heart progenitors generate diverse multipotent cardiovascular cell lineages. *Nature*. 2009;460:113-U130
141. Bu L, Jiang X, Martin-Puig S, Caron L, Zhu SJ, Shao Y, Roberts DJ, Huang PL, Domian IJ, Chien KR. Human isl1 heart progenitors generate diverse multipotent cardiovascular cell lineages. *Nature*. 2009;460:113-U130
142. Moretti A, Caron L, Nakano A, Lam JT, Bernshausen A, Chen YH, Qyang YB, Bu L, Sasaki M, Martin-Puig S, Sun YF, Evans SM, Laugwitz KL, Chien KR. Multipotent embryonic isl1(+) progenitor cells lead to cardiac, smooth muscle, and endothelial cell diversification. *Cell*. 2006;127:1151-1165
143. Sun Y, Liang X, Najafi N, Cass M, Lin L, Cai C-L, Chen J, Evans SM. Islet 1 is expressed in distinct cardiovascular lineages, including pacemaker and coronary vascular cells. *Developmental Biology*. 2007;304:286-296
144. Serradifalco C, Catanese P, Rizzuto L, Cappello F, Puleio R, Barresi V, Nunnari CM, Zummo G, Di Felice V. Embryonic and foetal islet-1 positive cells in human hearts are also positive to c-kit. *European Journal of Histochemistry*. 2011;55:229-234
145. Reese DE, Mikawa T, Bader DM. Development of the coronary vessel system. *Circ.Res.* 2002;91:761-768
146. Limana F, Zacheo A, Mocini D, Mangoni A, Borsellino G, Diamantini A, De Mori R, Battistini L, Vigna E, Santini M, Loiaconi V, Pompilio G, Germani A, Capogrossi MC. Identification of myocardial and vascular precursor cells in human and mouse epicardium. *Circ.Res.* 2007;101:1255-1265
147. Lepilina A, Coon AN, Kikuchi K, Holdway JE, Roberts RW, Burns CG, Poss KD. A dynamic epicardial injury response supports progenitor cell activity during zebrafish heart regeneration. *Cell*. 2006;127:607-619
148. van Tuyn J, Atsma DE, Winter EM, van der Velde-van Dijke I, Pijnappels DA, Bax NAM, Knaan-Shanzer S, Gittenberger-de Groot AC, Poelmann RE, van der Laarse A, van der Wall EE, Schalij MJ, de Vries AAF. Epicardial cells of human adults can undergo an epithelial-to-mesenchymal transition and obtain characteristics of smooth muscle cells in vitro. *Stem Cells*. 2007;25:271-278
149. Smart N, Risebro CA, Melville AAD, Moses K, Schwartz RJ, Chien KR, Riley PR. Thymosin beta 4 induces adult epicardial progenitor mobilization and neovascularization. *Nature*. 2007;445:177-182
150. Riley PR, Smart N. Thymosin beta 4 induces epicardium-derived neovascularization in the adult heart. *Biochemical Society Transactions*. 2009;37:1218-1220
151. Smart N, Bollini S, Dube KN, Vieira JM, Zhou B, Davidson S, Yellon D, Riegler J, Price AN, Lythgoe MF, Pu WT, Riley PR. De novo cardiomyocytes from within the activated adult heart after injury. *Nature*. 2011;474:640-U117
152. Smith RR, Barile L, Cho HC, Leppo MK, Hare JM, Messina E, Giacomello A, Abraham MR, Marban E. Regenerative potential of cardiosphere-derived cells expanded from percutaneous endomyocardial biopsy specimens. *Circulation*. 2007;115:896-908
153. Davis DR, Zhang Y, Smith RR, Cheng K, Terrovitis J, Malliaras K, Li T-S, White A, Makkar R, Marban E. Validation of the cardiosphere method to culture cardiac progenitor cells from myocardial tissue. *PLoS One*. 2009;4

154. Makkar RR, Smith RR, Cheng K, Malliaras K, Thomson LEJ, Berman D, Czer LSC, Marban L, Mendizabal A, Johnston PV, Russell SD, Schuleri KH, Lardo AC, Gerstenblith G, Marban E. Intracoronary cardiosphere-derived cells for heart regeneration after myocardial infarction (caduceus): A prospective, randomised phase 1 trial. *Lancet*. 2012;379:895-904
155. Li TS, Cheng K, Malliaras K, Smith RR, Zhang YQ, Sun BM, Matsushita N, Blusztajn A, Terrovitis J, Kusuoka H, Marban L, Marban E. Direct comparison of different stem cell types and subpopulations reveals superior paracrine potency and myocardial repair efficacy with cardiosphere-derived cells. *Journal of the American College of Cardiology*. 2012;59:942-953
156. Taylor DA, Zenovich AG. Cardiovascular cell therapy and endogenous repair. *Diabetes Obesity & Metabolism*. 2008;10:5-15
157. Hsiao L-C, Perbellini F, Gomes RSM, Tan JJ, Vieira S, Faggian G, Clarke K, Carr CA. Murine cardiosphere-derived cells are impaired by age but not by cardiac dystrophic dysfunction. *Stem Cells and Development*. 2014;23:1027-1036
158. Heng BC, Haider HK, Sim EKW, Cao T, Ng SC. Strategies for directing the differentiation of stem cells into the cardiomyogenic lineage in vitro. *Cardiovascular Research*. 2004;62:34-42
159. Condorelli G, Borello U, De Angelis L, Latronico M, Sirabella D, Coletta M, Galli R, Balconi G, Follenzi A, Frati G, De Angelis MGC, Gioglio L, Amuchastegui S, Adorini L, Naldini L, Vescovi A, Dejana E, Cossu G. Cardiomyocytes induce endothelial cells to trans-differentiate into cardiac muscle: Implications for myocardium regeneration. *Proceedings of the National Academy of Sciences of the United States of America*. 2001;98:10733-10738
160. Badorff C, Brandes RP, Popp R, Rupp S, Urbich C, Aicher A, Fleming I, Busse R, Zeiher A, Dimmeler S. Transdifferentiation of blood-derived human adult endothelial progenitor cells into functionally active cardiomyocytes. *Circulation*. 2003;107:1024-1032
161. Iijima Y, Nagai T, Mizukami M, Matsuura K, Ogura T, Wada H, Toko H, Akazawa H, Takano H, Nakaya H, Komuro I. Beating is necessary for transdifferentiation of skeletal muscle-derived cells into cardiomyocytes. *Faseb Journal*. 2003;17:1361-+
162. Choi YS, Dusting GJ, Stubbs S, Arunothayaraj S, Han XL, Collas P, Morrison WA, Dilley RJ. Differentiation of human adipose-derived stem cells into beating cardiomyocytes. *Journal of Cellular and Molecular Medicine*. 2010;14:878-889
163. Tan SC GR, Yeoh KK, Ambrose L, Schofield CJ, Davies KE, Clarke K, Carr CA. Preconditioning of cardiosphere-derived cells under hypoxia or with prolyl-4-hydroxylase inhibitors. *Cell Transplant*. 2015
164. Flanders KC, Holder MG, Winokur TS. Autoinduction of messenger-rna and protein expression for transforming growth factor-beta-s in cultured cardiac-cells. *Journal of Molecular and Cellular Cardiology*. 1995;27:805-812
165. Slager HG, Vaninzen W, Freund E, Vandeneijndenvanraaij AJM, Mummery CL. Transforming growth-factor-beta in the early mouse embryo - implications for the regulation of muscle formation and implantation *Developmental Genetics*. 1993;14:212-224
166. Behfar A, Zingman LV, Hodgson DM, Rauzier JM, Kane GC, Terzic A, Puceat M. Stem cell differentiation requires a paracrine pathway in the heart. *Faseb Journal*. 2002;16:1558-1566
167. Goumans M-J, de Boer TP, Smits AM, van Laake LW, van Vliet P, Metz CHG, Korfage TH, Kats KP, Hochstenbach R, Pasterkamp G, Verhaar MC, van der Heyden MAG, de Kleijn D, Mummery CL, van Veen TAB, Sluijter JPG, Doevendans PA. Tgf-beta1 induces efficient differentiation of human cardiomyocyte progenitor cells into functional cardiomyocytes in vitro. *Stem cell research*. 2007;1:138-149
168. Parker TG, Chow KL, Schwartz RJ, Schneider MD. Differential regulation of skeletal alpha-actin transcription in cardiac-muscle by 2 fibroblast growth-factors. *Proceedings of the National Academy of Sciences of the United States of America*. 1990;87:7066-7070
169. Roberts AB, Roche NS, Winokur TS, Burmester JK, Sporn MB. Role of transforming growth-factor-beta in maintenance of function of cultured neonatal cardiac myocytes - autocrine

action and reversal of damaging effect of interleukin-1. *Journal of Clinical Investigation*. 1992;90:2056-2062
170. Roberts A.B.; Sporn M.B. The transforming growth factor-βs. *In M. B. Sporn and A. B. Roberts. eds Hand- book of Experimental Phtmnacology, Peptide Growth Factor's and their Receptors. Vol. 95, part 1. Springer-Verlag, Heidelberg, 419-472.* 1990
171. Massague J. The transforming growth-factor-beta family. *Annual Review of Cell Biology*. 1990;6:597-641
172. Eghbali M, Tomek R, Sukhatme VP, Woods C, Bhambi B. Differential-effects of transforming growth factor-beta-1 and phorbol-myristate acetate on cardiac fibroblasts-regulation of fibrillar collagen messenger-rnas and expression of early transciption factors. *Circ.Res.* 1991;69:483-490
173. Smits AM, van Vliet P, Metz CH, Korfage T, Sluijter JPG, Doevendans PA, Goumans M-J. Human cardiomyocyte progenitor cells differentiate into functional mature cardiomyocytes: An in vitro model for studying human cardiac physiology and pathophysiology. *Nat. Protoc.* 2009;4:232-243
174. Ye JQ, Boyle A, Shih H, Sievers RE, Zhang Y, Prasad M, Su H, Zhou Y, Grossman W, Bernstein HS, Yeghiazarians Y. Sca-1(+) cardiosphere-derived cells are enriched for isl1-expressing cardiac precursors and improve cardiac function after myocardial injury. *PLoS One*. 2012;7
175. Qian Q, Qian H, Zhang X, Zhu W, Yan YM, Ye SQ, Peng XJ, Li W, Xu Z, Sun LY, Xu WR. 5-azacytidine induces cardiac differentiation of human umbilical cord-derived mesenchymal stem cells by activating extracellular regulated kinase. *Stem Cells and Development*. 2012;21:67-75
176. Antonitsis P, Ioannidou-Papagiannaki E, Kaidoglou A, Papakonstantinou C. In vitro cardiomyogenic differentiation of adult human bone marrow mesenchymal stem cells. The role of 5-azacytidine. *Interactive cardiovascular and thoracic surgery*. 2007;6:593-597
177. Xu WR, Zhang XR, Qian H, Zhu W, Sun XC, Hu J, Zhou H, Chen YC. Mesenchymal stem cells from adult human bone marrow differentiate into a cardiomyocyte phenotype in vitro. *Experimental Biology and Medicine*. 2004;229:623-631
178. Makino S, Fukuda K, Miyoshi S, Konishi F, Kodama H, Pan J, Sano M, Takahashi T, Hori S, Abe H, Hata J, Umezawa A, Ogawa S. Cardiomyocytes can be generated from marrow stromal cells in vitro. *Journal of Clinical Investigation*. 1999;103:697-705
179. Moscoso I, Centeno A, Lopez E, Rodriguez-Barbosa JI, Santamarina I, Filgueira P, Sanchez MJ, Dominguez-Perles R, Penuelas-Rivas GP, Domenech N. Differentiation "in vitro" of primary and immortalized porcine mesenchymal stem cells into cardiomyocytes for cell transplantation. *Transplantation Proceedings*. 2005;37:481-482
180. Wan Safwani WKZ, Makpol S, Sathapan S, Chua KH. 5-azacytidine is insufficient for cardiogenesis in human adipose-derived stem cells. *Journal of negative results in biomedicine*. 2012;11:3
181. Issa J-PJ, Kantarjian HM, Kirkpatrick P. Azacitidine. *Nat Rev Drug Discov*. 2005;4:275-276
182. Issa JPJ. DNA methylation as a therapeutic target in cancer. *Clinical Cancer Research*. 2007;13:1634-1637
183. Santos NC, Prieto MJE, MornaGomes A, Betbeder D, Castanho M. Structural characterization (shape and dimensions) and stability of polysaccharide/lipid nanoparticles. *Biopolymers*. 1997;41:511-520
184. HDAC Inhibitors Base www.hdacis.com
185. Bridges K, Levenson R, Housman D, Cantley L. Calcium regulates the commitment of murine erythroleukemia-cells to terminal erythroid-differentiation *Journal of Cell Biology*. 1981;90:542-544
186. Mariadason JM. Hdacs and hdac inhibitors in colon cancer. *Epigenetics*. 2008;3:28-37
187. Alcarraz-Vizan G, Boren J, Lee WNP, Cascante M. Histone deacetylase inhibition results in a common metabolic profile associated with ht29 differentiation. *Metabolomics*. 2010;6:229-237

188. Nakamura T, Sano M, Songyang Z, Schneider MD. A wnt- and beta-catenin-dependent pathway for mammalian cardiac myogenesis. *Proceedings of the National Academy of Sciences of the United States of America*. 2003;100:5834-5839
189. Jasmin, Spray DC, de Carvalho ACC, Mendez-Otero R. Chemical induction of cardiac differentiation in p19 embryonal carcinoma stem cells. *Stem Cells and Development*. 2010;19:403-411
190. Gong J, Gu H-y, Wang X, Liang Y, Sun T, Liu P-j, Wang Y, Yan J-c, Jiao Z-j. Src kinase family inhibitor pp2 promotes dmso-induced cardiac differentiation of p19 cells and inhibits proliferation. *International Journal of Cardiology*.
191. Darling D, Tavassoli M, Linskens MHK, Farzaneh F. Dmso induced modulation of c-myc steady-state rna levels in a variety of different cell-lines. *Oncogene*. 1989;4:175-179
192. Srinivas S, Sironmani TA, Shanmugam G. Dimethyl-sulfoxide inhibits the expression of early growth-response genes and arrests fibroblasts at quiescence. *Experimental Cell Research*. 1991;196:279-286
193. Ashrafian H, Frenneaux MP, Opie LH. Metabolic mechanisms in heart failure. *Circulation*. 2007;116:434-448
194. Opie LH. Heart physiology: from cell to circulation. .
195. Stanley WC, Recchia FA, Lopaschuk GD. Myocardial substrate metabolism in the normal and failing heart. *Physiological Reviews*. 2005;85:1093-1129
196. Wisneski JA, Gertz EW, Neese RA, Mayr M. Myocardial metabolism of free fatty acids. Studies with 14c-labeled substrates in humans. *Journal of Clinical Investigation*. 1987;79:359-366
197. Taegtmeyer H. Switching metabolic genes to build a better heart. *Circulation*. 2002;106:2043-2045
198. Lopaschuk GD. Advantages and limitations of experimental techniques used to measure cardiac energy metabolism. *Journal of Nuclear Cardiology*. 1997;4:316-328
199. Neely JR, Rovetto MJ, Oram JF. Myocardial utilization of carbohydrate and lipids. *Progress in Cardiovascular Diseases*. 1972;15:289-329
200. van der Vusse GJ, van Bilsen M, Glatz JFC. Cardiac fatty acid uptake and transport in health and disease. *Cardiovascular Research*. 2000;45:279-293
201. Salway J. Metabolism at a glance. *Blackwell* ed1999; 2nd edition
202. Taegtmeyer H, Golfman L, Sharma S, Razeghi P, Van Arsdall M. Linking gene expression to function: Metabolic flexibility in the normal and diseased heart. In: Sideman S, Beyar R, eds. *Cardiac engineering: From genes and cells to structure and function*. 2004:202-213.
203. Eaton S. Control of mitochondrial beta-oxidation flux. *Progress in Lipid Research*. 2002;41:197-239
204. Shyh-Chang N, Daley GQ, Cantley LC. Stem cell metabolism in tissue development and aging. *Development (Cambridge, England)*. 2013;140:2535-2547
205. Warburg O. (1925). Uber den Stoffwechsel der Carcinomzelle. Klin. Wochenschr. 4, 534–536.
206. Keilin D. The History of Cell Respiration and Cytochrome (Cambridge Univ. Press, Cambridge, 1970).
207. Moreno-Sánchez R, Rodríguez-Enríquez S, Marín-Hernández A, Saavedra E. Energy metabolism in tumor cells. *FEBS Journal*. 2007;274:1393-1418
208. DeBerardinis RJ, Lum JJ, Hatzivassiliou G, Thompson CB. The biology of cancer: Metabolic reprogramming fuels cell growth and proliferation. *Cell Metabolism*. 2008;7:11-20
209. Warburg O. Origin of cancer cells *Science*. 1956;123:309-314
210. Guppy M, Greiner E, Brand K. The role of the crabtree effect and an endogenous fuel in the energy metabolism of resting and proliferating thymocytes. *European Journal of Biochemistry*. 1993;212:95-99
211. Pfeiffer T, Schuster S, Bonhoeffer S. Cooperation and competition in the evolution of atp-producing pathways. *Science*. 2001;292:504-507

212. Pantaleon M, Kaye PL. Glucose transporters in preimplantation development. *Reviews of Reproduction*. 1998;3:77-81
213. Leese HJ, Barton AM. Pyruvate and glucose-uptake by mouse ova and preimplantation embryos. *Journal of Reproduction and Fertility*. 1984;72:9-13
214. Chung S, Dzeja PP, Faustino RS, Perez-Terzic C, Behfar A, Terzic A. Mitochondrial oxidative metabolism is required for the cardiac differentiation of stem cells. *Nat Clin Pract Cardiovasc Med*. 2007;4 Suppl 1:S60-67
215. Klimmeck D, Hansson J, Raffel S, Vakhrushev SY, Trumpp A, Krijgsveld J. Proteomic cornerstones of hematopoietic stem cell differentiation: Distinct signatures of multipotent progenitors and myeloid committed cells. *Molecular & Cellular Proteomics*. 2012;11:286-302
216. Kirby ML, Waldo KL. Molecular embryogenesis of the heart. *Pediatric and Developmental Pathology*. 2002;5:516-543
217. Foley A, Mercola M. Heart induction: Embryology to cardiomyocyte regeneration. *Trends in Cardiovascular Medicine*. 2004;14:121-125
218. Dzeja PP, Terzic A. Phosphotransfer networks and cellular energetics. *Journal of Experimental Biology*. 2003;206:2039-2047
219. Naya FJ, Black BL, Wu H, Bassel-Duby R, Richardson JA, Hill JA, Olson EN. Mitochondrial deficiency and cardiac sudden death in mice lacking the mef2a transcription factor. *Nature Medicine*. 2002;8:1303-1309
220. Behfar A, Hodgson DM, Zingman LV, Perez-Terzic C, Yamada S, Kane GC, Alekseev AE, Puceat M, Terzic A. Administration of allogenic stem cells dosed to secure cardiogenesis and sustained infarct repair. In: Ourednik J, Ourednik V, Sakaguchi DS, NilsenHamilton M, eds. *Stem cell biology: Development and plasticity*. 2005:189-198.
221. Menard C, Hagege AA, Agbulut O, Barro M, Morichetti MC, Brasselet C, Bel A, Messas E, Bissery A, Bruneval P, Desnos M, Puceat M, Menasche P. Transplantation of cardiac-committed mouse embryonic stem cells to infarcted sheep myocardium: A preclinical study. *Lancet*. 2005;366:1005-1012
222. Tan J.J. Cardiosphere-derived stem cell culture, characterisation and labelling for in vivo testing in the infarcted heart. 2011
223. Tan SC, Carr CA, Yeoh KK, Schofield CJ, Davies KE, Clarke K. Identification of valid housekeeping genes for quantitative rt-pcr analysis of cardiosphere-derived cells preconditioned under hypoxia or with prolyl-4-hydroxylase inhibitors. *Mol. Biol. Rep.* 2012;39:4857-4867
224. Collins CL, Bode BP, Souba WW, Abcouwer SF. Multiwell (co2)-c-14-capture assay for evaluation of substrate oxidation rates of cells in culture. *Biotechniques*. 1998;24:803-808
225. Urbanek K, Quaini F, Tasca G, Torella D, Castaldo C, Nadal-Ginard B, Leri A, Kajstura J, Quaini E, Anversa P. Intense myocyte formation from cardiac stem cells in human cardiac hypertrophy. *Proceedings of the National Academy of Sciences of the United States of America*. 2003;100:10440-10445
226. Jun Jie Tan - DPhil Thesis 2011
227. Tan J-J, Carr CA, Stuckey DJ, Ellison GM, Messina E, Giacomello A, Clarke K. Isolation and expansion of cardiosphere-derived stem cells. *Current protocols in stem cell biology*. John Wiley & Sons, Inc.; 2007.
228. Izadpanah R, Kaushal D, Kriedt C, Tsien F, Patel B, Dufour J, Bunnell BA. Long-term in vitro expansion alters the biology of adult mesenchymal stem cells. *Cancer Research*. 2008;68:4229-4238
229. Anbalagan M, Rao AJ. Collagen iv-mediated signalling is involved in progenitor leydig cell proliferation. *Reproductive Biomedicine Online*. 2004;9:391-403
230. Andersen DC, Andersen P, Schneider M, Jensen HB, Sheikh SP. Murine "cardiospheres'' are not a source of stem cells with cardiomyogenic potential. *Stem Cells*. 2009;27:1571-1581

231. Cheng K, Ibrahim A, Hensley MT, Shen D, Sun B, Middleton R, Liu W, Smith RR, Marbán E. Relative roles of cd90 and c-kit to the regenerative efficacy of cardiosphere-derived cells in humans and in a mouse model of myocardial infarction. *Journal of the American Heart Association: Cardiovascular and Cerebrovascular Disease*. 2014;3:e001260
232. Ye N-S, Zhang R-L, Zhao Y-F, Feng X, Wang Y-M, Luo G-A. Effect of 5-azacytidine on the protein expression of porcine bone marrow mesenchymal stem cells in vitro. *Genomics Proteomics & Bioinformatics*. 2006;4:18-25
233. Komashko VM, Farnham PJ. 5-azacytidine treatment reorganizes genomic histone modification patterns. *Epigenetics*. 2010;5
234. Alcarraz-Vizan G, Boren J, Lee W-NP, Cascante M. Histone deacetylase inhibition results in a common metabolic profile associated with ht29 differentiation. *Metabolomics*. 2010;6:229-237
235. HDAC Inhibitors Base www.hdacis.com
236. Chowdhury SR, Muneyuki Y, Takezawa Y, Kino-oka M, Saito A, Sawa Y, Taya M. Growth and differentiation potentials in confluent state of culture of human skeletal muscle myoblasts. *Journal of Bioscience and Bioengineering*. 2010;109:310-313
237. Poumay Y, Pittelkow MR. Cell-density and culture factors regulate keratinocyte commitment to differentiation and expression of suprabasal k1/k10 keratins *Journal of Investigative Dermatology*. 1995;104:271-276
238. Watt FM, Hogan BLM. Out of eden: Stem cells and their niches. *Science*. 2000;287:1427-1430
239. Trappmann B, Gautrot JE, Connelly JT, Strange DGT, Li Y, Oyen ML, Stuart MAC, Boehm H, Li BJ, Vogel V, Spatz JP, Watt FM, Huck WTS. Extracellular-matrix tethering regulates stem-cell fate (vol 11, pg 642, 2012). *Nature Materials*. 2012;11:742-742
240. Quesenberry PJ, Becker PS. Stem cell homing: Rolling, crawling, and nesting. *Proceedings of the National Academy of Sciences of the United States of America*. 1998;95:15155-15157
241. Peifer M. Signal transduction - neither straight nor narrow. *Nature*. 1999;400:213-215
242. Hall PA, Watt FM. Stem-cells - the generation and maintenance of cellular diversity *Development*. 1989;106:619-633
243. Morrison SJ, Shah NM, Anderson DJ. Regulatory mechanisms in stem cell biology. *Cell*. 1997;88:287-298
244. Macfelda K, Kapeller B, Wilbacher I, Losert UM. Behavior of cardiomyocytes and skeletal muscle cells on different extracellular matrix components - relevance for cardiac tissue engineering. *Artificial Organs*. 2007;31:4-12
245. Corda S, Samuel JL, Rappaport L. Extracellular matrix and growth factors during heart growth. *Heart failure reviews*. 2000;5:119-130
246. Hanson KP, Jung JP, Tran QA, Hsu S-PP, Iida R, Ajeti V, Campagnola PJ, Eliceiri KW, Squirrell JM, Lyons GE, Ogle BM. Spatial and temporal analysis of extracellular matrix proteins in the developing murine heart: A blueprint for regeneration. *Tissue Engineering Part A*. 2013;19:1132-1143
247. Shim JH, Kang HH, Lee TR, Shin DW. Enrichment and characterization of human dermal stem/progenitor cells using collagen type iv. *Journal of Dermatological Science*. 2012;67:202-205
248. Shim JH, Lee TR, Shin DW. Novel in vitro culture condition improves the stemness of human dermal stem/progenitor cells. *Molecules and Cells*. 2013;36:556-563
249. Dontu G, Abdallah WM, Foley JM, Jackson KW, Clarke MF, Kawamura MJ, Wicha MS. In vitro propagation and transcriptional profiling of human mammary stem/progenitor cells. *Genes Dev.* 2003;17:1253-1270
250. Ohlund D, Franklin O, Lundberg E, Lundin C, Sund M. Type iv collagen stimulates pancreatic cancer cell proliferation, migration, and inhibits apoptosis through an autocrine loop. *Bmc Cancer*. 2013;13

251. Poschl E, Schlotzer-Schrehardt U, Brachvogel B, Saito K, Ninomiya Y, Mayer U. Collagen iv is essential for basement membrane stability but dispensable for initiation of its assembly during early development. *Development*. 2004;131:1619-1628
252. Sa S, Wong L, McCloskey KE. Combinatorial fibronectin and laminin signaling promote highly efficient cardiac differentiation of human embryonic stem cells. *BioResearch Open Access*. 2014;3:150-161
253. Xiao Q, Jiang Y, Liu Q, Yue J, Liu C, Zhao X, Qiao Y, Ji H, Chen J, Ge G. Minor type iv collagen α5 chain promotes cancer progression through discoidin domain receptor-1. *PLoS Genetics*. 2015;11:e1005249
254. Bentzinger CF, Wang YX, von Maltzahn J, Soleimani VD, Yin H, Rudnicki MA, Rudnicki A. Fibronectin regulates wnt7a signaling and satellite cell expansion. *Cell Stem Cell*. 2013;12:75-87
255. Cheng P, Andersen P, Hassel D, Kaynak BL, Limphong P, Juergensen L, Kwon C, Srivastava D. Fibronectin mediates mesendodermal cell fate decisions. *Development (Cambridge, England)*. 2013;140:2587-2596
256. Taegtmeyer H, Wilson CR, Razeghi P, Sharma S. Metabolic energetics and genetics in the heart. In: Sideman S, Beyar R, Landesberg A, eds. *Communicative cardiac cell*. New York: New York Acad Sciences; 2005:208-218.
257. Chung S, Arrell DK, Faustino RS, Terzic A, Dzeja PP. Glycolytic network restructuring integral to the energetics of embryonic stem cell cardiac differentiation. *Journal of Molecular and Cellular Cardiology*. 2010;48:725-734
258. Onay-Besikci A. Radioactive measurements as an indicator of metabolic fluxes in myocytes. *The Open Chemical and Biomedical Methods Journal,*. 2010;3:128-131
259. Liu B, ElAlaouiTalibi Z, Clanachan AS, Schulz R, Lopaschuk GD. Uncoupling of contractile function from mitochondrial tca cycle activity and mvo(2) during reperfusion of ischemic hearts. *American Journal of Physiology-Heart and Circulatory Physiology*. 1996;270:H72-H80
260. Lopaschuk GD, Spafford MA, Davies NJ, Wall SR. Glucose and palmitate oxidation in isolated working rat hearts reperfused after a period of transient global-ischemia. *Circ.Res.* 1990;66:546-553
261. Wisneski JA, Stanley WC, Neese RA, Gertz EW. Effects of acute hyperglycemia on myocardial glycolytic activity in humans. *Journal of Clinical Investigation*. 1990;85:1648-1656
262. Saddik M, Lopaschuk GD. Myocardial triglyceride turnover and contribution to energy substrate utilization in isolated working rat hearts. *Journal of Biological Chemistry*. 1991;266:8162-8170
263. Benzi RH, Lerch R. Dissociation between contractile function and oxidative-metabolism in postischemic myocardium - attenuation by ruthenium red administrered during reperfusion. *Circ.Res.* 1992;71:567-576
264. Renstrom B, Liedtke AJ, Nellis SH, Whitesell LF, Caby DA, Eggleston AM. Mechanisms of substrate preference for oxidative-metabolism during early myocardial reperfusion. *American Journal of Physiology*. 1990;259:H317-H323
265. Wood IS, Trayhurn P. Glucose transporters (glut and sglt): Expanded families of sugar transport proteins. *British Journal of Nutrition*. 2003;89:3-9
266. Guilletdeniau I, Leturque A, Girard J. Expression and cellular-localization of glucose transporters (glut1, glut3, glut4) during differentiation of myogenic cells isolated from rat fetuses. *J. Cell Sci.* 1994;107:487-496
267. Charron MJ, Brosius FC, Alper SL, Lodish HF. A glucose-transport protein expressed predominately in insulin-responsive tissues. *Proceedings of the National Academy of Sciences of the United States of America*. 1989;86:2535-2539
268. Yeaman SJ, Hutcheson ET, Roche TE, Pettit FH, Brown JR, Reed LJ, Watson DC, Dixon GH. Sites of phosphorylation on pyruvate-dehydrogenase from bovine kidney and heart. *Biochemistry*. 1978;17:2364-2370

269. Bowker-Kinley MM, Davis WI, Wu PF, Harris RA, Popov KM. Evidence for existence of tissue-specific regulation of the mammalian pyruvate dehydrogenase complex. *Biochemical Journal*. 1998;329:191-196
270. Huang BL, Wu PF, Bowker-Kinley MM, Harris RA. Regulation of pyruvate dehydrogenase kinase expression by peroxisome proliferator-activated receptor-alpha ligands, glucocorticoids, and insulin. *Diabetes*. 2002;51:276-283
271. Gudi R, Bowkerkinley MM, Kedishvili NY, Zhao Y, Popov KM. Diversity of the pyruvate-dehydrogenase kinase gene family in humans. *Journal of Biological Chemistry*. 1995;270:28989-28994
272. Marchington DR, Kerbey AL, Jones AE, Randle PJ. Insulin reverses effects of starvation on the activity of pyruvate-dehydrogenase kinase in cultured-hepatocytes. *Biochemical Journal*. 1987;246:233-236
273. Lopaschuk GD, Ussher JR, Folmes CDL, Jaswal JS, Stanley WC. Myocardial fatty acid metabolism in health and disease. *Physiological Reviews*. 2010;90:207-258
274. Lopaschuk GD, Belke DD, Gamble J, Itoi T, Schonekess BO. Regulation of fatty-acid oxidation in the mammalian heart in health and disease. *Biochimica Et Biophysica Acta-Lipids and Lipid Metabolism*. 1994;1213:263-276
275. Goodwin GW, Taylor CS, Taegtmeyer H. Regulation of energy metabolism of the heart during acute increase in heart work. *Journal of Biological Chemistry*. 1998;273:29530-29539
276. Paulson DJ, Ward KM, Shug AL. Malonyl coa inhibition of carnitine palmityltransferase in rat-heart mitochondria. *FEBS Lett.* 1984;176:381-384
277. Hafstad AD, Khalid AM, Hagve M, Lund T, Larsen TS, Severson DL, Clarke K, Berge RK, Aasum E. Cardiac peroxisome proliferator-activated receptor-alpha activation causes increased fatty acid oxidation, reducing efficiency and post-ischaemic functional loss. *Cardiovascular Research*. 2009;83:519-526
278. Motojima K, Passilly P, Peters JM, Gonzalez FJ, Latruffe N. Expression of putative fatty acid transporter genes are regulated by peroxisome proliferator-activated receptor alpha and gamma activators in a tissue- and inducer-specific manner. *Journal of Biological Chemistry*. 1998;273:16710-16714
279. van der Lee K, Vork MM, De Vries JE, Willemsen PHM, Glatz JFC, Reneman RS, Van der Vusse GJ, Van Bilsen M. Long-chain fatty acid-induced changes in gene expression in neonatal cardiac myocytes. *Journal of Lipid Research*. 2000;41:41-47
280. van Bilsen M, van der Vusse GJ, Gilde AJ, Lindhout M, van der Lee K. Peroxisome proliferator-activated receptors: Lipid binding proteins controling gene expression. *Molecular and Cellular Biochemistry*. 2002;239:131-138
281. Djouadi F, Brandt JM, Weinheimer CJ, Leone TC, Gonzalez FJ, Kelly DP. The role of the peroxisome proliferator-activated receptor alpha (ppar alpha) in the control of cardiac lipid metabolism. *Prostaglandins Leukotrienes and Essential Fatty Acids*. 1999;60:339-343
282. Brandt JM, Djouadi F, Kelly DP. Fatty acids activate transcription of the muscle carnitine palmitoyltransferase i gene in cardiac myocytes via the peroxisome proliferator-activated receptor alpha. *Journal of Biological Chemistry*. 1998;273:23786-23792
283. Gulick T, Cresci S, Caira T, Moore DD, Kelly DP. The peroxisome proliferator-activated receptor regulates mitochondrial fatty-acid oxidative enzyme gene-expression. *Proceedings of the National Academy of Sciences of the United States of America*. 1994;91:11012-11016
284. Young ME, Patil S, Ying J, Depre C, Ahuja HS, Shipley GL, Stepkowski SM, Davies PJA, Taegtmeyer H. Uncoupling protein 3 transcription is regulated by peroxisome proliferator-activated receptor alpha in the adult rodent heart. *Faseb Journal*. 2001;15:833-845
285. Murray AJ, Anderson RE, Watson GC, Radda GK, Clarke K. Uncoupling proteins in human heart. *Lancet*. 2004;364:1786-1788
286. Sugden MC, Bulmer K, Gibbons GF, Holness MJ. Role of peroxisome proliferator-activated receptor-alpha in the mechanism underlying changes in renal pyruvate dehydrogenase

kinase isoform 4 protein expression in starvation and after refeeding. *Archives of Biochemistry and Biophysics*. 2001;395:246-252
287. Hopkins TA, Sugden MC, Holness MJ, Kozak R, Dyck JRB, Lopaschuk GD. Control of cardiac pyruvate dehydrogenase activity in peroxisome proliferator-activated receptor-alpha transgenic mice. *American Journal of Physiology-Heart and Circulatory Physiology*. 2003;285:H270-H276
288. Zhang L, Joshi AK, Smith S. Cloning, expression, characterization, and interaction of two components of a human mitochondrial fatty acid synthase - malonyltransferase and acyl carrier protein. *Journal of Biological Chemistry*. 2003;278:40067-40074
289. Owen OE, Felig P, Morgan AP, Wahren J, Cahill GF. Liver and kidney metabolism during prolonged starvation *Journal of Clinical Investigation*. 1969;48:574-&
290. Fukao T, Lopaschuk GD, Mitchell GA. Pathways and control of ketone body metabolism: On the fringe of lipid biochemistry. *Prostaglandins Leukotrienes and Essential Fatty Acids*. 2004;70:243-251
291. Maalouf M, Rho JM, Mattson MP. The neuroprotective properties of calorie restriction, the ketogenic diet, and ketone bodies. *Brain Research Reviews*. 2009;59:293-315
292. Suda T, Takubo K, Semenza GL. Metabolic regulation of hematopoietic stem cells in the hypoxic niche. *Cell Stem Cell*. 2011;9:298-310
293. Musa-Veloso K, Likhodii SS, Rarama E, Benoit S, Liu YMC, Chartrand D, Curtis R, Carmant L, Lortie A, Comeau FJE, Cunnane SC. Breath acetone predicts plasma ketone bodies in children with epilepsy on a ketogenic diet. *Nutrition*. 2006;22:1-8
294. Kashiwaya Y, Bergman C, Lee J-H, Wan R, King MT, Mughal MR, Okun E, Clarke K, Mattson MP, Veech RL. A ketone ester diet exhibits anxiolytic and cognition-sparing properties, and lessens amyloid and tau pathologies in a mouse model of alzheimer's disease. *Neurobiology of Aging*. 2013;34:1530-1539
295. Laeger T, Metges CC, Kuhla B. Role of beta-hydroxybutyric acid in the central regulation of energy balance. *Appetite*. 2010;54:450-455
296. Paoli A, Rubini A, Volek JS, Grimaldi KA. Beyond weight loss: A review of the therapeutic uses of very-low-carbohydrate (ketogenic) diets (vol 67, pg 789, 2013). *European Journal of Clinical Nutrition*. 2014;68:641-641
297. Paoli A, Bianco A, Damiani E, Bosco G. Ketogenic diet in neuromuscular and neurodegenerative diseases. *BioMed research international*. 2014;2014:474296-474296
298. Brinster RL, Troike DE. Requirements for blastocyst development in vitro. *Journal of animal science*. 1979;49 Suppl 2:26-34
299. Gunstone FD, John L. Harwood, and Albert J. Dijkstra. The lipid handbook with cd-rom. . *3rd ed. Boca Raton: CRC Press,* . 2007
300. Fillmore N, Huqi A, Jaswal JS, Mori J, Paulin R, Haromy A, Onay-Besikci A, Ionescu L, Thebaud B, Michelakis E, Lopaschuk GD. Effect of fatty acids on human bone marrow mesenchymal stem cell energy metabolism and survival. *PLoS One*. 2015;10
301. Mookerjee SA, Goncalves RLS, Gerencser AA, Nicholls DG, Brand MD. The contributions of respiration and glycolysis to extracellular acid production. *Biochimica Et Biophysica Acta-Bioenergetics*. 2015;1847:171-181
302. Yeh L-CC, Ford JJ, Lee JC, Adamo ML. Palmitate attenuates osteoblast differentiation of fetal rat calvarial cells. *Biochem. Biophys. Res. Commun.* 2014;450:777-781
303. Otten JJ, et al. Dietary reference intakes: The essential guide to nutrient requirements, published by the institute of medicine's food and nutrition board, currently available online at http://fnic.Nal.Usda.Gov/dietary-guidance/dietary-reference-intakes/dri-reports.
304. Brosnan JT. Interorgan amino acid transport and its regulation. *Journal of Nutrition*. 2003;133:2068S-2072S
305. Aledo JC. Glutamine breakdown in rapidly dividing cells: Waste or investment? *Bioessays*. 2004;26:778-785

306. Salabei JK, Lorkiewicz PK, Holden CR, Li Q, Hong KU, Bolli R, Bhatnagar A, Hill BG. Glutamine regulates cardiac progenitor cell metabolism and proliferation. *Stem Cells*. 2015;33:2613-2627
307. Buckman JF, Hernandez H, Kress GJ, Votyakova TV, Pal S, Reynolds IJ. Mitotracker labeling in primary neuronal and astrocytic cultures: Influence of mitochondrial membrane potential and oxidants. *Journal of Neuroscience Methods*. 2001;104:165-176
308. Ehrenberg B, Montana V, Wei MD, Wuskell JP, Loew LM. Membrane-potential can be determined in individual cells from the nernstian distribution of cationic dyes. *Biophysical Journal*. 1988;53:785-794
309. Nicholls DG, Ward MW. Mitochondrial membrane potential and neuronal glutamate excitotoxicity: Mortality and millivolts. *Trends in Neurosciences*. 2000;23:166-174
310. Lemasters JJ, Ramshesh VK. Imaging of mitochondnial polarization and depolarization with cationic fluorophores. In: Pon LA, Schon EA, eds. *Mitochondria, 2nd edition*. 2007:283-+.
311. Johnson LV, Walsh ML, Bockus BJ, Chen LB. Monitoring of relative mitochondrial-membrane potential in living cells by fluorescence microscopy. *Journal of Cell Biology*. 1981;88:526-535
312. Taegtmeyer H, Wilson CR, Razeghi P, Sharma S. Metabolic energetics and genetics in the heart. *Ann N Y Acad Sci*. 2005;1047:208-218
313. Chung S, Arrell DK, Faustino RS, Terzic A, Dzeja PP. Glycolytic network restructuring integral to the energetics of embryonic stem cell cardiac differentiation. *J Mol Cell Cardiol*.
314. Blouin J-M, Penot G, Collinet M, Nacfer M, Forest C, Laurent-Puig P, Coumoul X, Barouki R, Benelli C, Bortoli S. Butyrate elicits a metabolic switch in human colon cancer cells by targeting the pyruvate dehydrogenase complex. *International Journal of Cancer*. 2011;128:2591-2601
315. Stacpoole PW. The pharmacology of dichloroacetate *Metabolism-Clinical and Experimental*. 1989;38:1124-1144
316. Bonnet S, Archer SL, Allalunis-Turner J, Haromy A, Beaulieu C, Thompson R, Lee CT, Lopaschuk GD, Puttagunta L, Bonnet S, Harry G, Hashimoto K, Porter CJ, Andrade MA, Thebaud B, Michelakis ED. A mitochondria-k+ channel axis is suppressed in cancer and its normalization promotes apoptosis and inhibits cancer growth. *Cancer Cell*. 2007;11:37-51
317. Zhu S, Li W, Zhou H, Wei W, Ambasudhan R, Lin T, Kim J, Zhang K, Ding S. Reprogramming of human primary somatic cells by oct4 and chemical compounds. *Cell Stem Cell*. 2010;7:651-655
318. Smits AM, van Vliet P, Metz CH, Korfage T, Sluijter JPG, Doevendans PA, Goumans MJ. Human cardiomyocyte progenitor cells differentiate into functional mature cardiomyocytes: An in vitro model for studying human cardiac physiology and pathophysiology. *Nat. Protoc.* 2009;4:232-243
319. Perbellini F. Adipose and cardiac progenitor cells for regenerative medicine.,. *DPhil Thesis* 2014
320. Dapp MJ, Clouser CL, Patterson S, Mansky LM. 5-azacytidine can induce lethal mutagenesis in human immunodeficiency virus type 1. *Journal of Virology*. 2009;83:11950-11958
321. Diamantopoulos PT, Michael M, Benopoulou O, Bazanis E, Tzeletas G, Meletis J, Vayopoulos G, Viniou N-A. Antiretroviral activity of 5-azacytidine during treatment of a htlv-1 positive myelodysplastic syndrome with autoimmune manifestations. *Virology Journal*. 2012;9
322. Murray AJ, Panagia M, Hauton D, Gibbons GF, Clarke K. Plasma free fatty acids and peroxisome proliferator-activated receptor alpha in the control of myocardial uncoupling protein levels. *Diabetes*. 2005;54:3496-3502
323. Franco D, Dominguez J, de Castro MD, Aranega A. Regulation of myocardial gene expression during heart development. *Revista Espanola De Cardiologia*. 2002;55:167-184
324. van Berlo JH, Kanisicak O, Maillet M, Vagnozzi RJ, Karch J, Lin S-CJ, Middleton RC, Marban E, Molkentin JD. C-kit(+) cells minimally contribute cardiomyocytes to the heart. *Nature*. 2014;509:337-+

325. Laflamme MA, Murry CE. Heart regeneration. *Nature*. 2011;473:326-335
326. Kamp F, Westerhoff HV, Hamilton JA. Movement of fatty-acids, fatty-acid analogs, and bile-acids across phospholipid-bilayers - kinetics of fatty acid-mediated proton movement across small unilamellar vesicles *Biochemistry*. 1993;32:11074-11086
327. Luiken J, Turcotte LP, Bonen A. Protein-mediated palmitate uptake and expression of fatty acid transport proteins in heart giant vesicles. *Journal of Lipid Research*. 1999;40:1007-1016
328. Michelakis ED. Mitochondrial medicine - a new era in medicine opens new windows and brings new challenges. *Circulation*. 2008;117:2431-2434

# Appendixes

# Appendix 1 - Medium compositions

| Medium | Composition | | Manufacturer |
|---|---|---|---|
| Complete explant medium (CEM) | 500 ml Iscove's Modified Dulbecco's Medium (IMDM) | | Invitrogen |
| | 20% (v/v) Fetal Bovine Serum (FBS) | | BioSera |
| | 1 x Antibiotic Antimycotic Solution (added from 100x solution which contains 10,000 U/ml Penicillin, 10 mg/ml Streptomycin and 25 µg/ml Amphotericin B, and solubilised in citrate buffer; recommended 10ml/L) | | Sigma |
| | 5 ml L-Glutamine Solution (0.2mM) | | Sigma |
| | | | |
| Medium Supplement (MS) | 500 ml Dulbecco's Modified Eagle's Medium and Ham's F-12 (DMEM/F12) | | Invitrogen |
| | 5 ml Antibiotic Antimycotic Solution (100x) | | Sigma |
| | 5 ml L-Glutamine Solution (0.2mM) | | Sigma |
| | | | |
| Cardiosphere growth medium (CGM) | 35% Complete Explant Medium (CEM) | | Invitrogen |
| | 7% Fetal Bovine Serum (FBS) | | BioSera |
| | 65% MS | | Invitrogen |
| | Growth Factors | B27 (2%) | Invitrogen |
| | | Cardiotrophin (25 ng/ml) | Invitrogen |
| | | Human Recombinant Epidermal Growth Factor (EGF) (10 ng/ml) | Peprotech |
| | | Human Recombinant Fibroblast Growth Factor (FGF) (20 ng/ml) | Promega |
| | | Thrombin from human plasma (25 µg/ml) | Sigma |

| Medium | Composition | Manufacturer |
|---|---|---|
| Cardiomyogenic differentiation medium-1 (CDM-1) | 240 ml Iscove's Modified Dulbecco's Medium (IMDM) | Gibco, Life technology |
| | 240 ml Dulbecco's Modified Eagle's Medium and Ham's F-12 (DMEM/F12) | Gibco, Life technology |
| | 10 ml Fetal Bovine Serum (FBS) | BioSera |
| | 5 ml Antibiotic Antimycotic Solution (100x) | Sigma |
| | 5 ml L-Glutamine Solution (0.2mM) | Sigma |
| | 5 ml Insulin-Transferrin-selenium (ITS) | Invitrogen |
| | | |
| Cardiomyogenic differentiation medium-2 (CDM-2) | 235 ml Iscove's Modified Dulbecco's Medium (IMDM) | Gibco, Life technology |
| | 235 ml Ham's F12 Nutrient Mixture with GlutaMAX-I | Gibco, Life technology |
| | 10 ml Horse Serum (HS) | Invitrogen |
| | 5 ml Antibiotic Antimycotic Solution (100x) | Sigma |
| | 5 ml L-Glutamine Solution (0.2mM) | Sigma |
| | 5 ml Insulin-Transferrin-selenium (ITS) | Invitrogen |
| | 5 ml MEM non essential amino acid | Invitrogen |

# Appendix 2 - Synthetic small molecules and concentrations

| Synthetic Compounds | Concentration (µM) |
|---|---|
| WY-14643 (PPARα Agonist - 1 ) | 10 or 100* |
| CP-775146 (PPARα Agonist - 2 ) | 1 or 10* |
| Sodium Dichloroacetate (DCA) | 10 or 100* |
| Sodium Butyrate | 1 or 10* |

*: Selected Concentration

# Appendix 3 - Designed 20 primer sequences

| Cardiac Muscle Specific Genes | | | | | | | |
|---|---|---|---|---|---|---|---|
| **1** | **TnnT2** | | | | | | |
| Forward | GCTCTTCATGCCCAACTTG | | | Reverse | TGCCTTTCCTTCTCTCGTTC | | |
| TM(°C) | GC(%) | Hairpin | | TM(°C) | GC(%) | Hairpin | Amplicon Length |
| 61.1 | 52.6 | 0 | | 61.8 | 50 | 0 | 243 |
| **2** | **Mybpc3** | | | | | | |
| Forward | AGTGGTTTAAGGGCAAGTGG | | | Reverse | GTCGGAAAGCTGATCTGAGG | | |
| TM(°C) | GC(%) | Hairpin | | TM(°C) | GC(%) | Hairpin | Amplicon Length |
| 62.4 | 50 | 0 | | 61.9 | 55 | 0 | 249 |
| **3** | **Myh7 (Slow Twitch)** | | | | | | |
| Forward | CCTCCCAAGTTCGACAAGATC | | | Reverse | GATAGGCGTTGTCAGAGATGG | | |
| TM(°C) | GC(%) | Hairpin | | TM(°C) | GC(%) | Hairpin | Amplicon Length |
| 62.2 | 52.4 | 0 | | 62 | 52.4 | 0 | 247 |
| **4** | **Myh6 (Fast Isoform)** | | | | | | |
| Forward | CCAGAACACCAGCCTCATC | | | Reverse | GGTCCTTGATGGTCTGCTC | | |
| TM(°C) | GC(%) | Hairpin | | TM(°C) | GC(%) | Hairpin | Amplicon Length |
| 62 | 57.9 | 0 | | 61.7 | 57.9 | -0.37 | 224 |

| Smooth Muscle Specific Genes | | | | | | | |
|---|---|---|---|---|---|---|---|
| **5** | **Cnn1 (Calponin-1)** | | | | | | |
| Forward | CGGAGATTTGAGCCTGAGAAG | | | Reverse | GTAGACTGATAGTTGCCTGATCC | | |
| TM(°C) | GC(%) | Hairpin | | TM(°C) | GC(%) | Hairpin | Amplicon Length |
| 62.2 | 52.4 | 0 | | 61.8 | 47.8 | -0.13 | 172 |
| **6** | **Myl6** | | | | | | |
| Forward | GTGGAGGTTCTGGACTTTGAG | | | Reverse | CTTCCTCTGTCATATTCTCGCC | | |
| TM(°C) | GC(%) | Hairpin | | TM(°C) | GC(%) | Hairpin | Amplicon Length |
| 62.1 | 52.4 | 0 | | 62 | 50 | 0 | 187 |
| **7** | **Myh11** | | | | | | |
| Forward | GAGCAGTACAAGGAGCAGG | | | Reverse | CAATAACTCTACGGCCTCCAG | | |
| TM(°C) | GC(%) | Hairpin | | TM(°C) | GC(%) | Hairpin | Amplicon Length |
| 61.7 | 57.9 | -0.34 | | 61.7 | 52.4 | 0 | 250 |

| Endothelial Specific Genes | | | | | | | |
|---|---|---|---|---|---|---|---|
| 8 | KDR (Flk-1) | | | | | | |
| Forward | CTCTGTGGTTCTGCGTGG | | Reverse | TGGGAACTGTGAGTGTCTTG | | | |
| TM(°C) | GC(%) | Hairpin | TM(°C) | GC(%) | Hairpin | Amplicon Length | |
| 62.2 | 61.1 | 0 | 61.7 | 50 | -0.23 | 246 | |
| 9 | Cdh5 (VE-Cadherin) | | | | | | |
| Forward | CGCAAGACCAGTGACAGAG | | Reverse | CTTTAGGTTCGTAGGGCTGG | | | |
| TM(°C) | GC(%) | Hairpin | TM(°C) | GC(%) | Hairpin | Amplicon Length | |
| 62.1 | 57.9 | -0.02 | 61.7 | 55 | -0.21 | 232 | |
| 10 | VEGFb | | | | | | |
| Forward | CCCTGTGTCCCAGTTTGATG | | Reverse | AGGATCTGCATTCGGACTTG | | | |
| TM(°C) | GC(%) | Hairpin | TM(°C) | GC(%) | Hairpin | Amplicon Length | |
| 62.6 | 55 | 0 | 61.9 | 50 | 0 | 243 | |
| 11 | VEGFa | | | | | | |
| Forward | AGCAGAAAGCCCATGAAGTG | | Reverse | CTTTGGTGAGGTTTGATCCG | | | |
| TM(°C) | GC(%) | Hairpin | TM(°C) | GC(%) | Hairpin | Amplicon Length | |
| 62.8 | 50 | -0.83 | 60.8 | 50 | 0 | 241 | |

| Metabolic Marker Genes | | | | | | | |
|---|---|---|---|---|---|---|---|
| 12 | CD36 | | | | | | |
| Forward | TGACGTGCAAAACCCAGAG | | Reverse | AGACAGTGAAGGCTCAAAGATG | | | |
| TM(°C) | GC(%) | Hairpin | TM(°C) | GC(%) | Hairpin | Amplicon Length | |
| 62.6 | 52.6 | 0 | 62.4 | 45.5 | 0 | 178 | |
| 13 | CPT1b | | | | | | |
| Forward | CAAGGTTTGGCTCTATGAGGG | | Reverse | AGTGAGAGTCTTCGTCCAGG | | | |
| TM(°C) | GC(%) | Hairpin | TM(°C) | GC(%) | Hairpin | Amplicon Length | |
| 62.4 | 52.4 | -0.24 | 62.6 | 55 | 0 | 248 | |
| 14 | Acadm (Malonyl-CoA dehydrogenase) | | | | | | |
| Forward | CTGGGAACTTTTGATGCGTG | | Reverse | TCACCCTTCTTCTCTGCTTTG | | | |
| TM(°C) | GC(%) | Hairpin | TM(°C) | GC(%) | Hairpin | Amplicon Length | |
| 61.6 | 50 | 0 | 62.1 | 47.6 | 0 | 245 | |
| 15 | Mcat (Malonyl-CoA acyltransferase) (MCAD) | | | | | | |
| Forward | TTTGCAGCCCTTGTGTTTG | | Reverse | CAGTCAGGAAAGAGGTAGTTGG | | | |
| TM(°C) | GC(%) | Hairpin | TM(°C) | GC(%) | Hairpin | Amplicon Length | |
| 61.8 | 47.4 | 0 | 61.9 | 50 | 0 | 236 | |

| 16 | PDK-1 | | | | | | |
|---|---|---|---|---|---|---|---|
| Forward | GGACAAGAGTGCTGAGGATG | | Reverse | AAGAGTGCTGGTTGAGTAGC | | | |
| TM(°C) | GC(%) | Hairpin | TM(°C) | GC(%) | Hairpin | Amplicon Length | |
| 62 | 55 | -0.13 | 61.8 | 50 | -0.33 | 224 | |

| 17 | PDK-4 | | | | | | |
|---|---|---|---|---|---|---|---|
| Forward | CTACTCGGATGCTCATGAACC | | Reverse | TGGTGAAGGTGTGAAGGAAC | | | |
| TM(°C) | GC(%) | Hairpin | TM(°C) | GC(%) | Hairpin | Amplicon Length | |
| 62 | 52.4 | 0 | 62 | 50 | 0 | 247 | |

| 18 | PPARα | | | | | | |
|---|---|---|---|---|---|---|---|
| Forward | AGTACTGCCGTTTCCACAAG | | Reverse | CTTTCCTGCGAGTATGACCC | | | |
| TM(°C) | GC(%) | Hairpin | TM(°C) | GC(%) | Hairpin | Amplicon Length | |
| 62.3 | 50 | 0 | 62 | 55 | 0 | 236 | |

| 19 | GLUT-1 | | | | | | |
|---|---|---|---|---|---|---|---|
| Forward | GCAGTTTGGCTATAACACCG | | Reverse | AGACACAAAGGCCAACAGG | | | |
| TM(°C) | GC(%) | Hairpin | TM(°C) | GC(%) | Hairpin | Amplicon Length | |
| 61.1 | 50 | 0 | 62.4 | 52.6 | 0 | 247 | |

| 20 | GLUT-4 | | | | | | |
|---|---|---|---|---|---|---|---|
| Forward | CATCGTCATTGGCATTCTGG | | Reverse | CATCAGACACATCAGCCCAG | | | |
| TM(°C) | GC(%) | Hairpin | TM(°C) | GC(%) | Hairpin | Amplicon Length | |
| 61.3 | 50 | 0 | 62.3 | 55 | 0 | 230 | |

# Appendix 4 – Primary and secondary antibodies used for flow cytometry

| Primary antibody | Manufacturer | Dilution | Secondary antibody (dilution) | Manufacturer |
|---|---|---|---|---|
| Oct-04 | Abcam Ab27985 | 5 µg/ml | AF488 Donkey anti goat (1:500) | Invitrogen A11055 |
| Nanog | Abcam Ab106465 | 20 µg/ml | AF488 Donkey anti rabbit (1:500) | Invitrogen A21206 |
| C-kit | Santa Cruz sc-5535 | 1 in 100 | AF488 Donkey anti rabbit (1:500) | Invitrogen A21206 |
| CD90 | BD Bioscience 554892 | 1 in 100 | AF488 Donkey anti mouse (1:1000) | Invitrogen A21202 |
| Nkx-2.5 | Santa Cruz sc-8697 | 1 in 50 | AF488 Donkey anti goat (1:500) | Invitrogen A11055 |
| Titin | Sigma T9030 | 1 in 1000 | AF488 Donkey anti mouse (1:1000) | Invitrogen A21202 |
| cTnnT2 | Abcam Ab10214 | 1 in 200 | AF488 Donkey anti mouse (1:1000) | Invitrogen A21202 |
| MHC | Abcam Ab15 | 1 in 200 | AF488 Donkey anti mouse (1:1000) | Invitrogen A21202 |
| vwf | Abcam Ab6994 | 1 in 1000 | AF488 Donkey anti rabbit (1:1000) | Invitrogen A21206 |

# Appendix 5 - Primary and secondary antibodies and probes used for immunocytochemistry

| Primary antibody | Manufacturer | Dilution | Seconday antibody (dilution) | Manufacturer |
|---|---|---|---|---|
| Cardiac Troponin I | Santa Cruz SC-15368 | 1 in 100 | AF488 Donkey anti rabbit (1:1000) | Invitrogen A21206 |
| Cardiac Troponin $T_2$ | Abcam Ab10214 | 1 in 200 | AF488 Donkey anti mouse (1:1000) | Invitrogen A21202 |
| Titin | Sigma Aldrich T9030 | 1 in 1000 | AF488 Donkey anti mouse (1:1000) | Invitrogen A21202 |
| α-Sarcomeric Actin | Sigma A2172 | 1 in 500 | AF488 Donkey anti mouse (1:1000) | Invitrogen A21202 |
| Myosin heavy chain | Abcam Ab15 | 1 in 200 | AF488 Donkey anti mouse (1:1000) | Invitrogen A21202 |
| Myosin light chain | Abcam Ab92721 | 1 in 250 | AF568 Goat anti rabbit (1:500) | Invitrogen A21206 |
| Connexin 43 | Abcam Ab194928 | 1 in 100 | AF568 Goat anti rabbit (1:500) | Invitrogen A21206 |

| Molecular Probes | Manufacturer | Dilution or Concentration |
|---|---|---|
| Filamentous Actin (Rhodamine Phalloidin) | Invitrogen R415 | 1 in 40 |
| MitoTracker® Red CMXRos | ThermoFisher SCIENIFIC M7512 | 100 nM |

# Appendix 6 - Fluorochromes and corresponding laser used for confocal microscopy

| Fluorochromes | Peak excitation wavelength | Peak emission wavelength |
|---|---|---|
| Alexa Fluor 488 | 499 | 519 |
| Alexa Fluor 568 | 579 | 603 |
| DAPI | 345 | 455 |
| MitoTracker® Red | 579 | 599 |
| Rhodamine Phalloidin | 579 | 599 |

# Appendix 7 – Buffer Compositions

| Buffer | Composition | Manufacturer |
|---|---|---|
| **Lysis Buffer** | 75 mM Trizma-Hydrochloride Reagent Grade (pH6.8) | Sigma (T3253) |
| | 3.8% Sodium Dodecyl Sulfate (w/v) | Fluka Biochemika (71729) |
| | 4 M urea | Sigma (U5128) |
| | 20% Glycerol (v/v) | Fisher Scientific (G/0900/17) |
| | 0.1% Triton X-100 (v/v) | Sigma (93420) |
| | Protease Inhibitor Cocktail tablets (1 in 10 ml Lysis Buffer) | Roch, Germany (11836153001) |
| **Laemmli Loading Buffer** | 187.5 mM Trizma-Hydrochloride Reagent Grade (pH6.8) | Sigma (T3253) |
| | 6% Sodium Dodecyl Sulfate (w/v) | Fluka Biochemika (71729) |
| | 4 M urea | Sigma (U5128) |
| | 30% Glycerol (v/v) | Fisher Scientific (G/0900/17) |
| | 0.003% Brilliant Blue R (w/v) | Sigma (B0149) |
| | pH 6.8 | |
| **TBS - Tween** | 0.9% Sodium chloride (NaCl) (w/v) | Sigma (S9625) |
| | 10 mM Trizma®-Base | Sigma (T1503) |
| | 0.05% Tween®20 (v/v) | Sigma, USA (P7949) |
| | pH 7.4 | |
| **SDS-Transfer Buffer** | 48 mM Trizma®-Base | Sigma (T1503) |
| | 30 mM Glycine | Sigma (G8898) |
| | 0.0375% Sodium Dodecyl Sulfate (w/v) | Fluka Biochemika (71729) |
| | 20% Methanol (v/v) | Sigma |

# Appendix 8 - Primary and secondary antibodies used for immunoblotting

| Primary antibody | | | | Secondary antibody | | |
|---|---|---|---|---|---|---|
| Primary antibody | Protein size (KD) | Dilution | Source | Secondary antibody | Dilution | Manufacturer |
| GLUT-1 | 50 | 1 in 4000 | Abcam (ab652) | Goat anti-rabbit | 1 in 2000 | Santa Cruz |
| Polyclonal rabbit anti GLUT-4 | 55 | 1 in 4000 | A gift from Prof. G. Holman, University of Bath, Uk | Goat anti-rabbit | 1 in 2000 | Santa Cruz |
| PDK-1 | 50 | 1 in 1000 | A gift from Prof. Mary Sugden, Queen Mary,University of London, Uk | Goat anti-rabbit | 1 in 2000 | Santa Cruz |
| PDK-4 | 50 | 1 in 1000 | A gift from Prof. Mary Sugden, Queen Mary,University of London, Uk | Goat anti-rabbit | 1 in 2000 | Santa Cruz |
| CISY | 50 | 1 in 1000 | Alpha Diagnostic (CISY11-S) | Goat anti-rabbit | 1 in 2000 | Santa Cruz |
| α-KGDH | 113 | 1 in 1000 | Santa Cruz | Donkey anti-goat | 1 in 2000 | Santa Cruz |
| MCAD | 45 | 1 in 500 | Alpha Diagnostic | Donkey anti-goat | 1 in 2000 | Santa Cruz |
| CD36 | 75 | 1 in 1000 | NOVUS Biologicals (NB400-144SS) | Goat anti-rabbit | 1 in 2000 | Santa Cruz |